REPORT NO.
UCB/EERC-97/12
December 1997

EARTHQUAKE ENGINEERING RESEARCH CENTER

NEW DESIGN AND ANALYSIS PROCEDURES FOR INTERMEDIATE HINGES IN MULTIPLE-FRAME BRIDGES

by

REGINALD DESROCHES
GREGORY L. FENVES

A report on research sponsored by the California Department of Transportation under Contract RTA-59A131

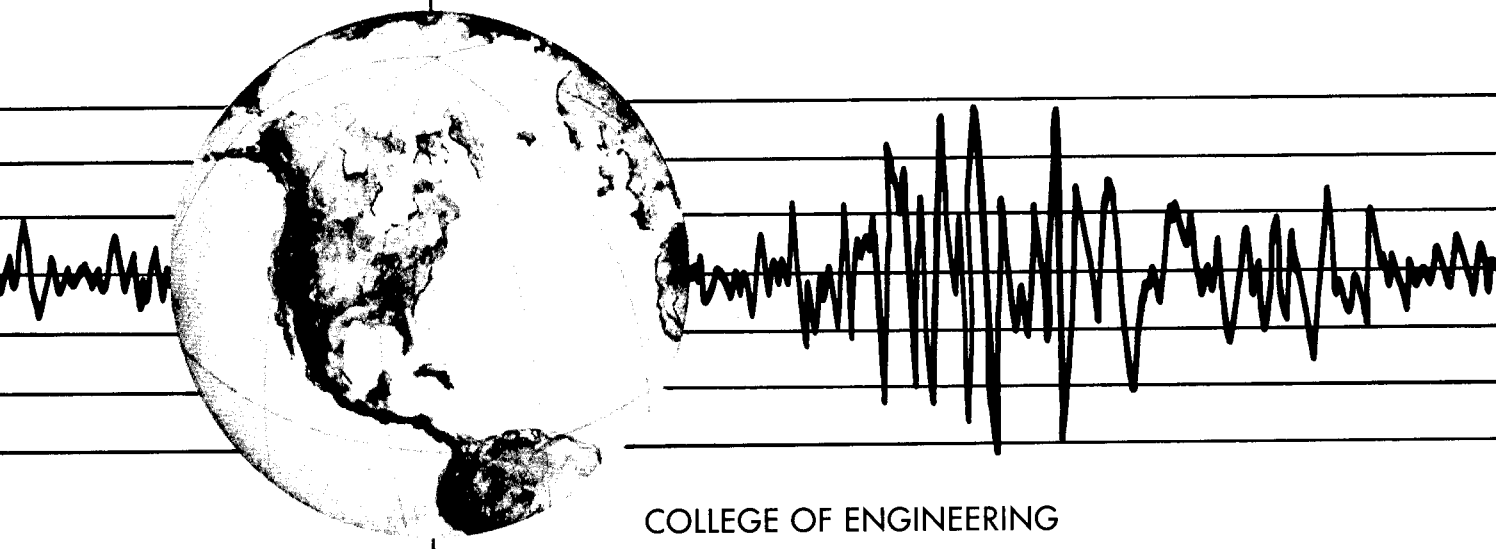

COLLEGE OF ENGINEERING

UNIVERSITY OF CALIFORNIA AT BERKELEY

For sale by the National Technical Information Service, U.S. Department of Commerce, Springfield, Virginia 22161

See back of report for up to date listing of EERC reports.

DISCLAIMER

Technical Report Documentation Page

1. Report No.	2. Government Accession No.	3. Recipient's Catalog No.
UCB/EERC-97/12		

4. Title and Subtitle	5. Report Date
New Design and Analysis Procedures for Intermediate Hinges in Multiple-Frame Bridges	December 1997
	6. Performing Organization Code: UCB/ENG-7915
	8. Performing Organization Report No.: UCB/EERC-97/12

PB99-136301

7. Author's	
Reginald DesRoches and Gregory L. Fenves	

9. Performing Organization Name and Address	10. Work Unit No. (TRAIS)
Earthquake Engineering Research Center University of California, Berkeley	11. Contract or Grant No.: 59A131
	13. Type of Report and Period Covered: Final Report 1995-1998
12. Sponsoring Agency Name and Address California Department of Transportation (Caltrans) Engineering Service Center 1801 30th Street - MS #9 Sacramento, CA 95816	14. Sponsoring Agency Code: 59-185-910137

15. Supplementary Notes

16. Abstract

During an earthquake adjacent bridge frames can vibrate out-of-phase exceeding the range of support provided by the hinge seat, leading to collapse. The collapse of bridges in recent earthquakes due to hinge unseating emphasized the importance of providing an adequate number of hinge restrainers to limit the relative displacement between hinges. Current restrainer design procedures do not account for controlling factors in the response of multiple-frame bridges.

Multiple-step and single-step restrainer design procedures based on a linearized numerical model are developed. Parameter studies show that the procedures work well in limiting the relative hinge displacement to a target displacement for a wide range of parameters. The required number of restrainers decreases as the frame period ratio increases and as the frame ductility increases. The new procedures are recommended except for cases with highly out-of-phase frames and large skew (greater than 30 degrees). For these cases, a nonlinear analysis may be needed to adequately capture the response.

Recommendations are made for hinge seat widths for new bridges. The recommendations are based on a modal analysis of the frames adjacent to the hinge. The recommended hinge seat width correlates well with nonlinear time history analysis.

17. Key Words	18. Distribution Statement
Restrainers, Multiple-frame, Bridges, Hinges, Pounding, Hinge seats	No restrictions. This document is available to the public through the National Technical Information Service, Springfield, Virginia 22161

19. Security Classif. (of this report)	20. Security Classif. (of this page)	21. No. of Pages	22. Price
Unclassified	Unclassified	196	

New Design and Analysis Procedures for Intermediate Hinges in Multiple-Frame Bridges

by

Reginald DesRoches
and
Gregory L. Fenves

A report on research sponsored by the California Department of Transportation under Contract RTA-59A131

UCB/EERC-97/12
Earthquake Engineering Research Center
College of Engineering
University of California, Berkeley

December, 1997

Abstract

During an earthquake adjacent bridge frames can vibrate out-of-phase, exceeding the range of support provided by the hinge seat, leading to collapse. The collapse of bridges in recent earthquakes due to hinge unseating emphasized the importance of providing an adequate number of hinge restrainers to limit the relative displacement between hinges. Current restrainer design procedures are not adequate because they do not account for controlling factors in the response of multiple-frame bridges.

A nonlinear numerical model representing the longitudinal earthquake response of two frames connected at a hinge is developed. The model has nonlinear force-displacement relationships for the frames, and nonlinear elements accounting for tension-only restrainers and friction. Pounding is accounted for directly in the equations of motion. A parameter study shows that the response of the hinge is governed by the frame period ratio, the target ductility demand of the frames, and the stiffness of the hinge restrainers.

A multiple-step design procedure based on a linearized numerical model, is developed. The procedure accounts for the phasing between frames with a modal analysis. Yielding of frames is linearized by using a substitute structure method, and optimization theory is used to obtain the restrainer stiffness. Parameter studies show that the procedure works well in limiting the relative hinge displacement for a wide range of parameters. The required number of restrainers decreases as the frame period ratio and the frame target ductility increase. A simplified single-step restrainer design procedure for hinge restrainers is also developed. The single-step design procedure is based on a non-dimensional value of the restrainer stiffness which is determined by performing a large parameter study. The results from the single-step procedure are generally more conservative compared with the multiple-step procedure.

Comparisons with current restrainer design procedures show that the new multiple-step and single-step procedures are more accurate than current procedures for designing hinge restrainers.

Pounding of frames and engaging of restrainers produce forces and displacements significantly different than what is typically assumed in design. Pounding typically

increases the demand on stiffer frames and decreases the demand on the most flexible frames. Although estimates from bounding models generally report the maximum elastic forces, they do not bound frame ductilities.

Acknowledgements

The findings conclusions, and recommendations expressed in this report were developed as part of the research project entitled, "Earthquake Response of Multiple-Frame Freeway Structures", Task 1 of the Coordinated Structural Analysis and Design Program at the University of California at Berkeley. This project was funded by the California Department of Transportation under Contract No. 59A131. The work was conducted under the overall direction of James Roberts, Director, Engineering Service Center. the authors are especially appreciative of his leadership and support in the conduction of this research. The authors thank Dr. Brian Maroney and Mr. Tim Leahy of Caltrans for assistance on this project.

Additional funding was provided by the National Center for Earthquake Engineering at the State University of New York at Buffalo. This study is part of Task 106-F-3.1 of the NCEER Highway Project, funded by the Federal Highway Administration.

This report is substantially based on the dissertation by Reginald DesRoches, which was submitted to fulfill the doctoral degree requirements at the University of California, Berkeley.

Contents

List of Figures

List of Tables

Nomenclature

Symbols

$\mathbf{1}$	Influence Vector
$\mathbf{a}$	Transformation Vector for Relative Hinge Displacement
B_i	Frame Bent i
$\mathbf{C}$	System Damping Matrix
D_{eq}	Relative Hinge Displacement
D_{eq_o}	Relative Hinge Displacement without Restrainers
D_r	Maximum Permissible Restrainer Displacement
D_y	Yield Length of Restrainers
$\tilde{D}_y$	Yield Displacement of Frames
e	Coefficient of Restitution
E	Modulus of Elasticity
$\mathbf{F}$	Total Restoring Force
F_f	Friction Force
F_y	Restrainer Yield Strength
g_p	Hinge Gap
H_i	Intermediate Hinge i
H_r	Design Horizontal Force and Linkage
$\mathbf{K}$	System Stiffness Matrix
K_h	Design Horizontal Acceleration Coefficient
K_i	Frame Stiffness
$K_{eff_{mod}}$	Effective Modified Frame Stiffness
K_{mod}	Modified Frame Stiffness
K_p	Load Reversal Stiffness for Q-Hyst Model
K_q	Unloading Stiffness for Q-Hyst Model
K_r	Restrainer Stiffness
$\tilde{K}_r$	Normalized Restrainer Stiffness
K_s	Largest Frame Stiffness (Used in Caltrans Procedure)
$\mathbf{K}_T$	Tangent Stiffness Matrix
L	Span Length in Multi-Span Bridge
L_r	Length of Restrainers
N	Design Hinge Seat Width

$N_{available}$	Available Hinge Seat Width
N_r	Number of Cable Restrainers
m_i	Frame Mass
$\mathbf{m}$	System Mass Matrix
$\mathbf{r}$	Residual Load
$\mathbf{P}$	Effective Earthquake Load
R_d	Vertical Reaction Due to Dead Load and Support
R_y	Yield Force of Frames
$\tilde{R}_i$	Normalized Force-Deformation Relationship
S	Skew of Hinge
s	Restrainer Slack
S_a	Pseudo-Acceleration Response Spectrum
$\tilde{T}$	Modified Input Period Ratio
T_{eff}	Effective Period
t_f	Duration of Ground Shaking
T_g	Characteristic Site Period
T_i	Individual Frame Period
T_{mi}	Modal Period
v_i'	Frame Velocity after Impact
v_i	Frame Velocity before Impact
V_H	Shear Force at a Hinge
x_i	Frame i Displacement
$\tilde{u_g}$	Normalized Free-Field Ground Displacement

α	Frame Mass Ratio (m_1/m_2)
α_s	Strain Hardening Ratio
β_{in}	Frame Frequency Ratio
ϵ	Error Tolerance
η	Frame Yield Strength Ratio
$\tilde{\eta}$	η_1/η_2
κ	Frame Stiffness Ratio (K_r/K_{mod})
μ	Target Design Ductility
$\tilde{\mu}$	Direction Cosines for Pricipal Direction of Ground Motion
μ_f	Coefficient of Friction
ω	Frequency
ω_{eff}	Effect Frequency
ϕ	Mode Shape
ρ_{in}	Cross-Correlation Coefficient for Complete Quadratic Modal Combination Rule
ξ_i	Modal Damping Ratios
ξ_{eff}	Effective Modal Damping Ratios

Acronyms

AASHTO	American Association of State Highway Transportation Officials
Caltrans	California Department of Transportation
CQC	Complete Quadratic Combination Rule
EPD	Epicentral Distance
MATLAB	MATrix LABoratory
PGA	Peak Ground Acceleration
PGV	Peak Ground Velocity
PGD	Peak Ground Displacement
SRSS	Square Root of the Sum of the Squares

Units of Measure

cm	centimeter
ft	feet
in	inches
kips	kipopounds
kN	kilo-Newton
ksi	kips per square inch
m	meter
mm	millimeter
MN	Mega-Newton
MPa	Mega-Pascal
N	Newton
Pa	Pascal
psi	pounds per square inch
rad	radians
Hz	Hertz (cycles per second)

Chapter 1

Introduction

1.1 Problem Description

A typical multiple-frame bridge, shown schematically in figure 1.1, is composed of frames, intermediate hinges (expansion joints), and abutments. The frames provide support for gravity and lateral loads of the superstructure. Intermediate hinges are used to allow for thermal expansion without developing forces in the columns, and to facilitate construction and post-tensioning of the superstructure. The abutments support gravity loads for end frames, and provide for transfer of seismic forces to the footing and soil.

During an earthquake, adjacent bridge frames can vibrate out-of-phase due to their different dynamic characteristics and variations in the ground motion, as illustrated in figure 1.2. The out-of-phase motion leads to two problems. First, when the displacement between the frames exceeds the range of support provided by the hinge seat, the supported span can unseat. The collapse of bridges in recent earthquakes have occurred because of this phenomenon (Moehle, 1995; Saiidi et al., 1993). Second, when the distance between the frames decreases (eventually reaching zero) pounding of frames occurs. The impact force developed can result in local damage and crushing of concrete. More importantly, the impact can increase displacements in frames beyond what is typically assumed in design. Pounding of frames produces large impact forces which can increase hinge opening, resulting in a greater possibility of unseating.

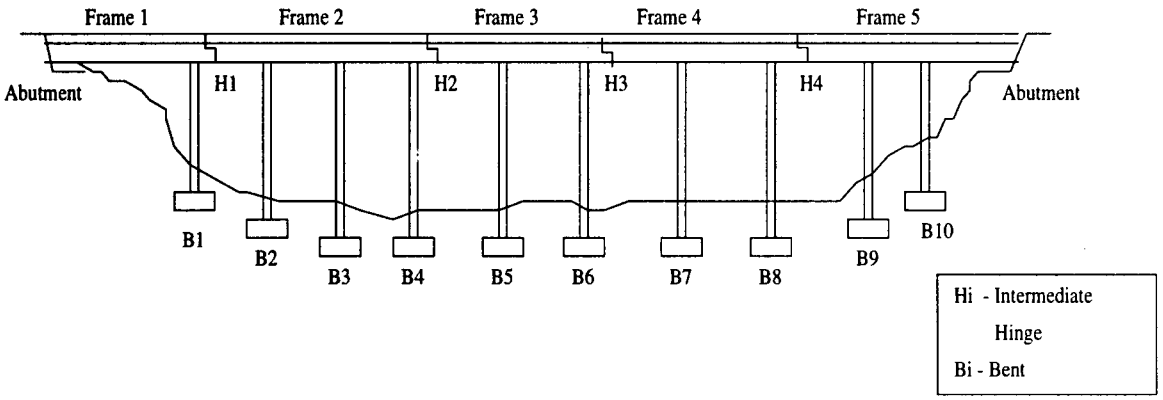

Figure 1.1: Typical Multiple-Frame Bridge.

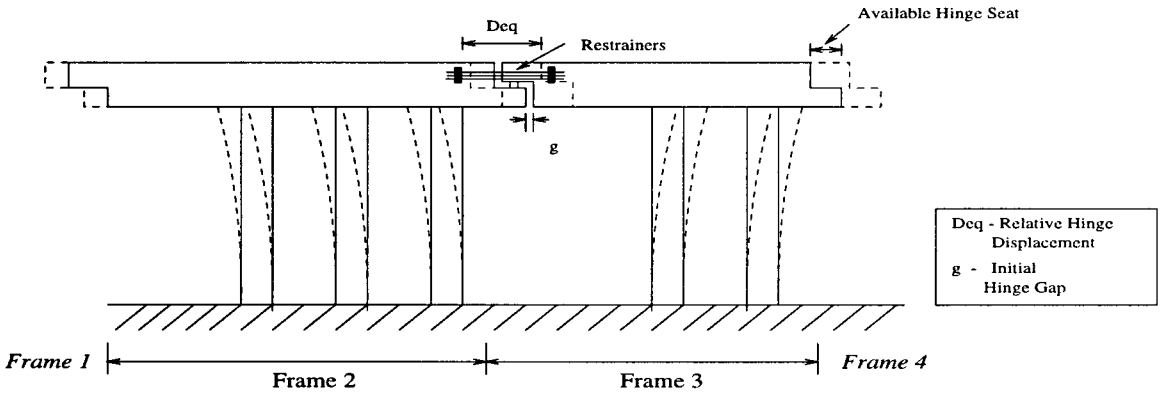

Figure 1.2: Interaction of Frames Subjected to Earthquake Loads.

The 1971 San Fernando earthquake showed that bridges are vulnerable to collapse due to unseating at hinges (Jennings, 1971). To prevent unseating, the California Department of Transportation (Caltrans) initiated a retrofit scheme, which consisted of tying spans together with cable restrainers at their hinges. Caltrans uses an equivalent static procedure to determine the required number of restrainers to limit the hinge displacements to a prescribed value. The procedure considers only the frame on either side of the intermediate hinge which has the smallest displacement. Restrainers are provided until the frame displacement is less than a prescribed value for a given design load. Studies have shown that the procedure is unconservative for cases where frames are out-of-phase, and very conservative for cases where frames are in phase (Yang et al., 1994).

Recent earthquakes have provided an opportunity to study the performance of hinge restrainers. Reconnaissance reports following the 1989 Loma Prieta earthquake found several cases where restrainers failed (Saiidi et al., 1993). During the 1994 Northridge earthquake, several bridges which had been retrofitted with cable restrainers collapsed due to unseating at the hinges (Moehle, 1995). During the 1995 Kobe earthquake, over 60% of all bridge structures in the Kobe area were damaged, costing approximately 10 billion US dollars to repair (Comartin et al., 1995). In general modern bridges performed better than older ones. However, a major problem was excessive movement at the hinges due to bearing and restrainer failure.

Another problem associated with intermediate hinges in multiple frame bridges is pounding. Pounding of frames at hinges can significantly increase forces and inelastic ductility demands on stiff frames. There were several instances during the 1994 Northridge earthquake where pounding caused damage in bridges (Moehle, 1995). Current design procedures may not adequately represent the distribution of forces and deformations in long, multiple-frame bridges.

1.2 Objectives of Research

The goal of this study is to investigate the factors affecting the response of intermediate hinges in long multiple-frame bridges subjected to longitudinal input motion. Current design procedures are evaluated, and new design procedures which better ac-

count for the dynamic characteristics of bridges are developed. The effects of torsion of the deck and skew hinges are not investigated in this study, although extensions of the new methodology to account for these effects are possible.

The specific objectives of the research are:

- Develop a numerical model to investigate the response of multiple-frame bridges subjected to earthquake ground motion, focusing on the longitudinal response of the frames and the hinges.
- Examine the effects of various dynamic characteristics on the inelastic earthquake response of multiple-frame bridges.
- Develop design procedures for hinge restrainers.
- Through parameter studies and case studies, determine the efficacy of the proposed design procedure.
- Study the effectiveness of linear bounding models for estimating the forces and ductility demands in multiple-frame bridges.

1.3 Outline of Report

This report is organized into 10 chapters with the following contents. Chapter 2 summarizes the history of hinge restrainers as a retrofit measure for bridges. Typical restrainer configurations in the US and Japan are discussed. A literature review focuses on past studies as well as recent developments on hinge restrainers. Current procedures for hinge restrainers and restrainer performance in recent earthquakes are summarized.

Chapter 3 presents the models used to analyze the earthquake response of multiple-frame bridges. The hinge model used in the analysis and solution strategies is discussed.

Chapter 4 presents the results of a parameter study that examines the effects of important non-dimensional parameters on the earthquake response of the intermediate hinge.

Chapter 5 presents the theoretical basis for the proposed design procedure. The proposed procedure is an iterative multiple-step procedure which determines the required number of restrainers to limit the hinge opening to a prescribed value. The procedure is verified by parameter studies and case studies.

Chapter 6 presents the theory and background for a single-step design procedure. The single-step design procedure is an approximate method for predicting the required number of restrainers to limit hinge opening to a prescribed value. The procedure is verified by parameter studies and case studies.

Chapter 7 compares the new design procedure for hinge restrainers with current restrainer design procedures, including the Caltrans, AASHTO, Trochalakis, and capacity design procedures.

Chapter 8 studies the effect of frame pounding and restrainer pulling on the distribution of the ductility demands in bridge frames. In addition, the efficacy of linear bounding models is investigated.

Chapter 9 presents the design recommendations for hinge restrainers and hinge seat widths.

Chapter 10 presents the conclusions of the study and discusses possible extensions.

Chapter 2

Summary of Hinge Restrainer Behavior and Design Procedures

2.1 Typical Configurations of Restrainer Devices

Typical restrainer cables used in California are 3/4-inch (19 mm) diameter and 0.22 square inch (143 mm^2) steel cables as shown in Figure 2.1. They are made of 6x19 strands, galvanized with a wire strand core, a right regular lay, and made of improved plow steel. The cables have a yield strength of 39.1 kips (174 kN), which coincides with a yield stress of 176 ksi (1210 MPa). The initial modulus of elasticity is 10,000 ksi (69,000 MPa). The post yield strength of the cables increases to an ultimate of about 53 kips (235 kN) per cable. The commonly used twenty foot long 3/4-inch (19 mm) cables will stretch approximately 4.22 inches (107 mm) at yield and 10.5 inches (267 mm) at ultimate. The force-deformation relationship for a typical restrainer cable is shown in Figure 2.2.

The restrainer system is composed of cables, swagged fittings, studs, nuts, and turnbuckles - all which should be 25% stronger than the cables (Caltrans, 1990). The connection between the cables and supporting elements is key to the performance of the restrainer system. Although restrainer systems are designed to fail in the cables, studies have shown that the restrainer hardware and adjacent reinforced concrete box girder sections are the weak links in the restrainer system (Selna et al., 1989). When tested to failure, the typical restrainer system experienced a loss of resistance due to

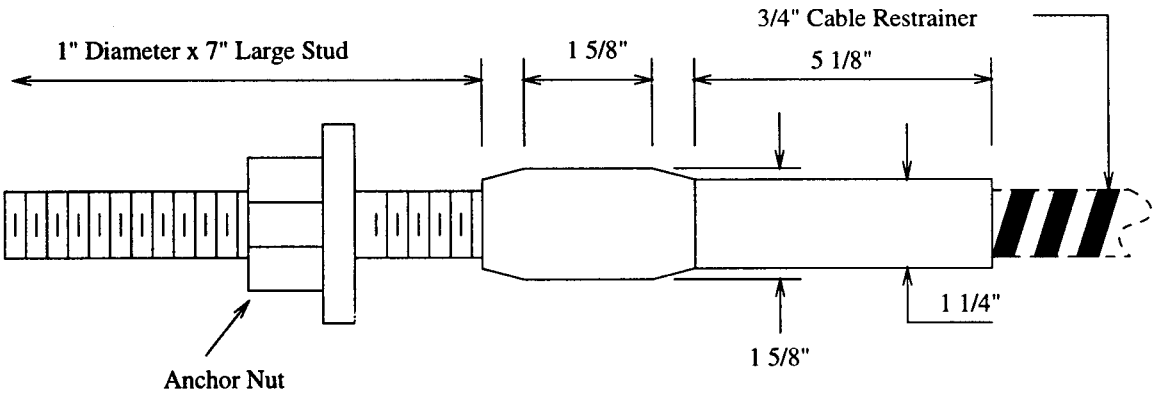

Figure 2.1: Typical Cable Restrainer and Swagged Fitting.

a reinforced concrete punching shear failure in the seat side of the hinge diaphragm.

2.1.1 Configuration of Restrainer Devices for Bridges with Adequate Hinge Seat

There are many different types and methods of installment for intermediate hinge restrainers. The most common configuration for older retrofits of concrete T- and box girder bridges with adequate hinge seat widths is the Type C-1 restrainer unit shown in Figure 2.3. Type C-1 has 5 cables wrapped around two 90 degree bends on the drum and threaded through holes in the hinge diaphragms. At the location of bending around the drum, the combination of contact stresses and shear stresses adversely effect the maximum elongation of the restrainer cables. Studies show that the ultimate strain in the cable is reduced 2.5 times compared to a straight cable (Selna et al., 1989). Bolsters are provided on either side of the hinge to distribute the restrainer force into the superstructure. The restrainer units are bolted to metal plates on the other side of the hinge to distribute the restrainer force into the superstructure. The nuts are tightened and then backed off a number of turns depending on the ambient temperature. This allows for thermal expansion without putting restrainers into tension. Typically the weak link in the Type C-1 installation is failure in the hinge diaphragm.

Modern retrofits of concrete T- and box girder bridges with adequate hinge seat widths use a restrainer configuration known as Type I restrainer retrofit. In the Type

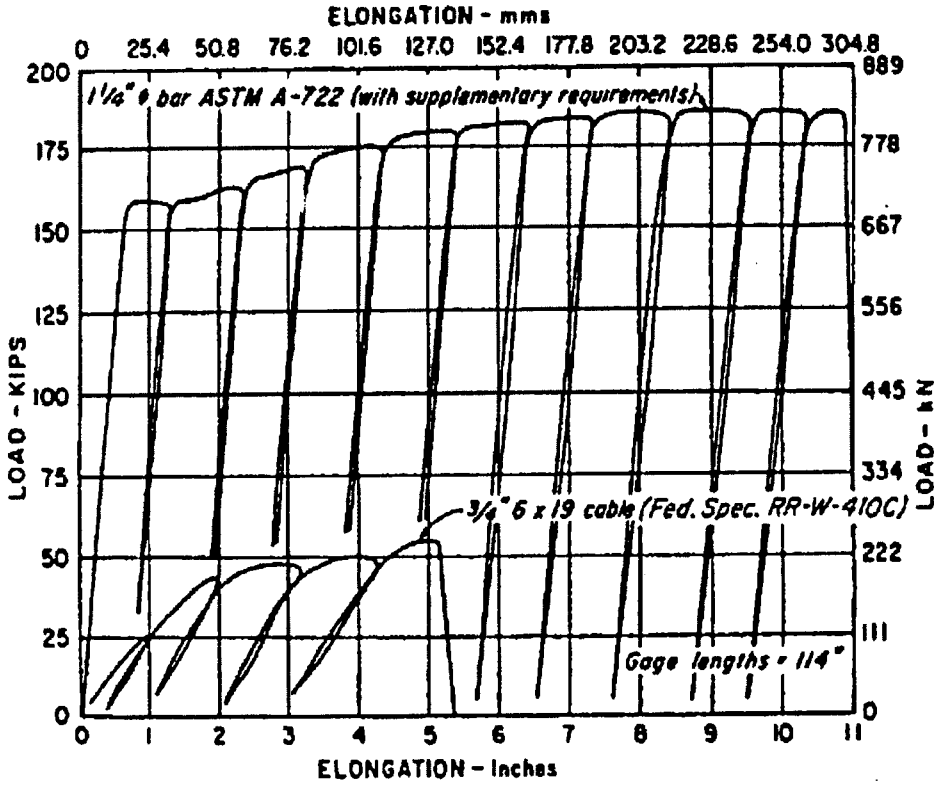

Figure 35

Figure 2.2: Load Deformation Relationship for Restrainers (Caltrans, 1990).

I retrofit, cable restrainers a threaded through a 6 in. (150 mm) hole cored on the top part of the hinge. Bolsters are provided on one side of the hinge to distribute the restrainer force into the superstructure. The restrainer units are bolted to metal plates on the other side of the hinge. The Type I retrofit is shown in Figure 2.4.

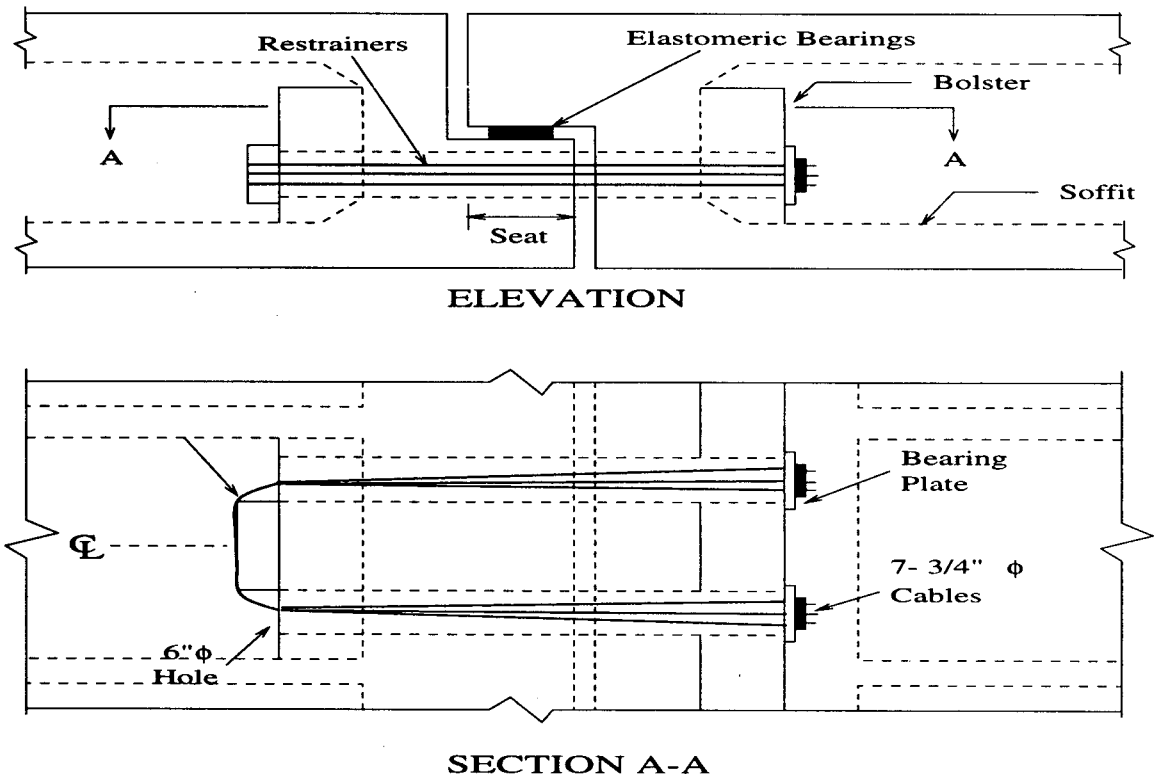

Figure 2.3: Older Hinge Restrainer Retrofit Scheme : Type C1 Restrainer Unit.

2.1.2 Configuration of Restrainer Devices for Bridges with Inadequate Hinge Seat

For concrete box girder bridges with inadequate hinge seats, Caltrans uses pipe extenders in conjunction with restrainers. A hole is bored through the hinge and an 8 inch (203 mm) double strong pipe is inserted in the hole. A new bolster anchors the pipe at one end. Cable restrainers are then placed below the pipe as shown in Figure 2.5. An adequate number of extenders are added to the hinge to support the superstructure if it becomes unseated during the earthquake. A more modern design places the cable restrainers inside the pipe to limit coring of the diaphragm as shown in Figure 2.6.

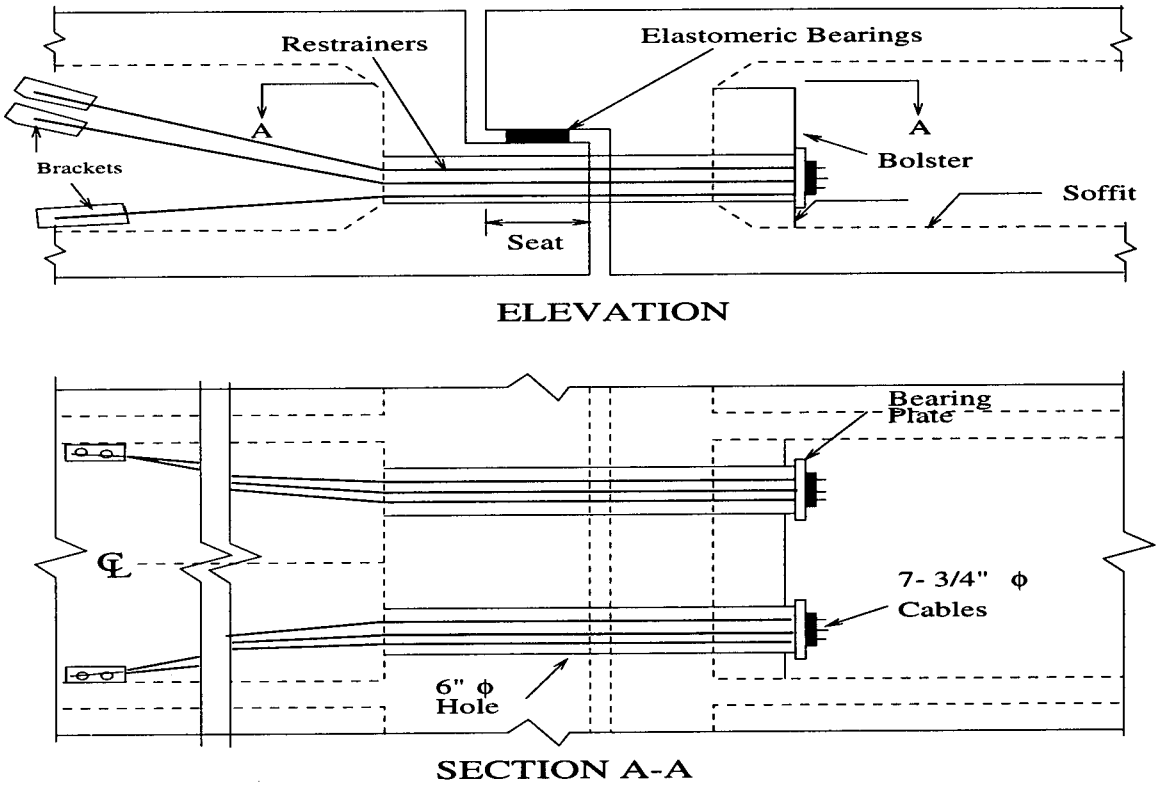

Figure 2.4: Modern Hinge Restrainer Retrofit Scheme : Type 1 Restrainer Unit.

2.1.3 Restrainer Configurations for Steel and Precast Girder Bridges

For steel and precast girder bridge retrofits there are a variety of restrainer configurations. If the columns can handle the force, restrainers are wrapped around the girders and bent cap, as shown in Figure 2.7 to provide additional restraint to the superstructure. If the columns are thought to be vulnerable, however, the steel girders are tied together with cable restrainers or steel plates and the force is resisted at the abutments.

2.1.4 Japanese Falling-off Prevention Devices

Typical Japanese construction does not use the flexible cable restrainers as in the United States. Instead, "falling-off prevention" devices are used which do not allow relative displacement between spans. They include devices that connect a girder and

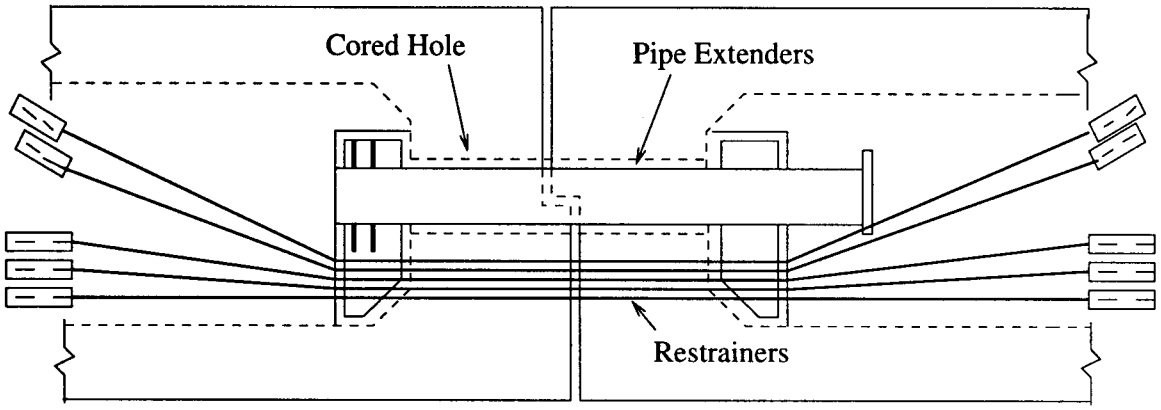

ELEVATION

Figure 2.5: Pipe Extender Configuration for Inadequate Hinge Seats for Older Configuration.

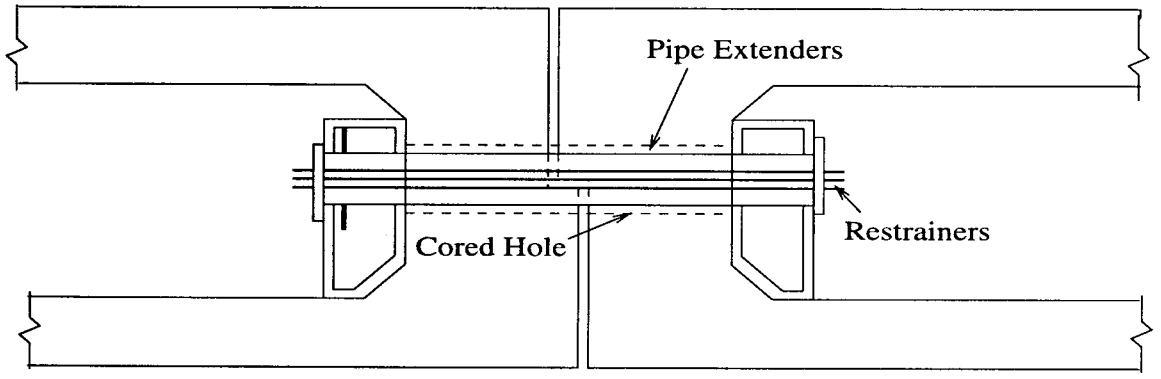

ELEVATION

Figure 2.6: Pipe Extender Configuration for Inadequate Hinge Seats : Modern Configuration.

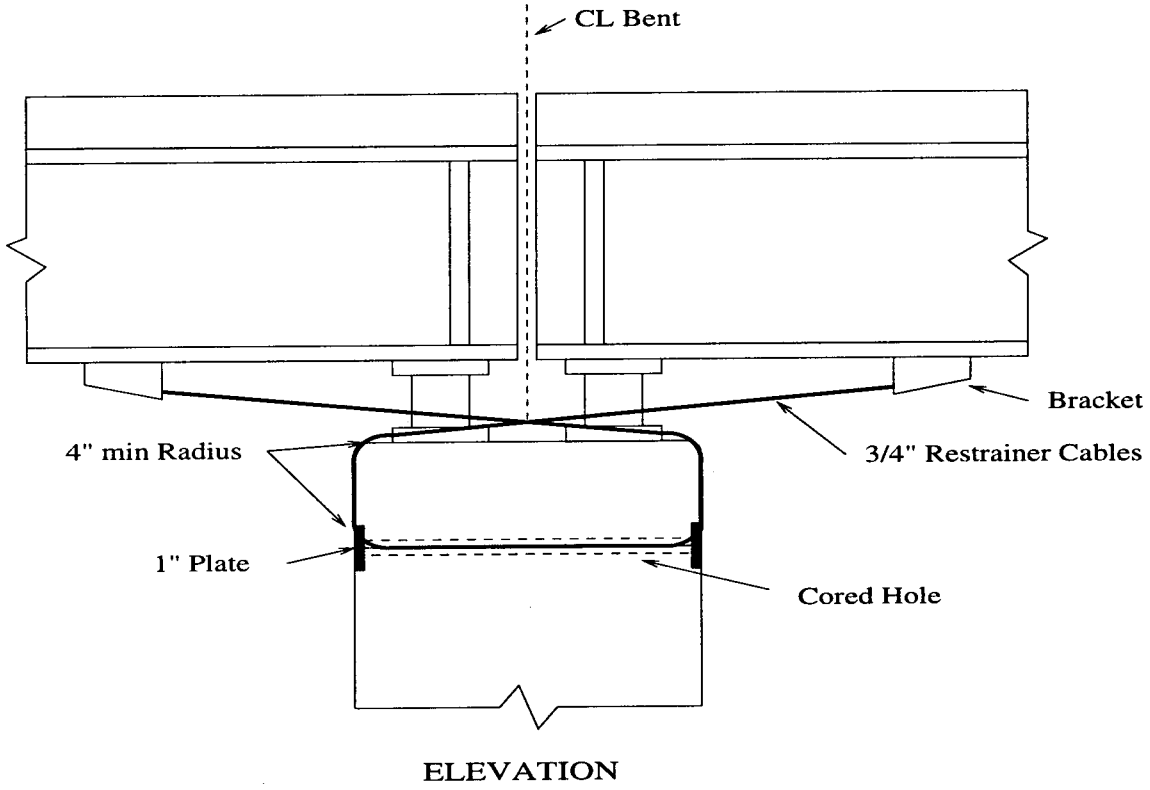

Figure 2.7: Typical Restrainer Configuration for Steel Bridges

substructure, devices to provide a protrudor into a girder or substructure, and devices to connect two girders. Figure 2.8 illustrates the types of devices employed in Japan (Yashinsky, 1995).

2.2 Restrainer Performance in Past Earthquakes

Recent earthquakes in the US and Japan have provided an opportunity to study the performance of hinge restrainers. The ideal performance of restrainers is one capable of resisting appropriate forces, restricting movement of bridge frames, and restoring the bridge frames to their relative pre-earthquake positions. A common cause of damage and collapse in three recent earthquakes is large hinge displacements which led to unseating at the hinges. This section briefly summarizes the performance of hinge restrainers in multiple frame bridges in the Loma Prieta, Northridge, and Kobe earthquakes.

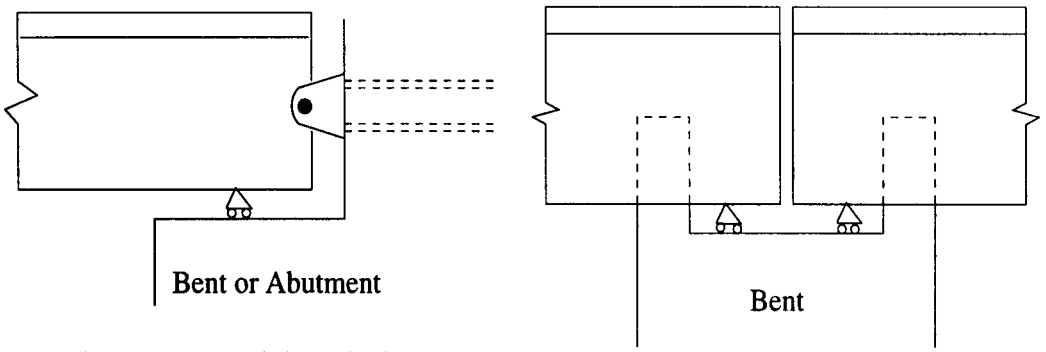

(a) Device to connect a girder and substructure (b) Device to provide a protrudor into a girder or substructure

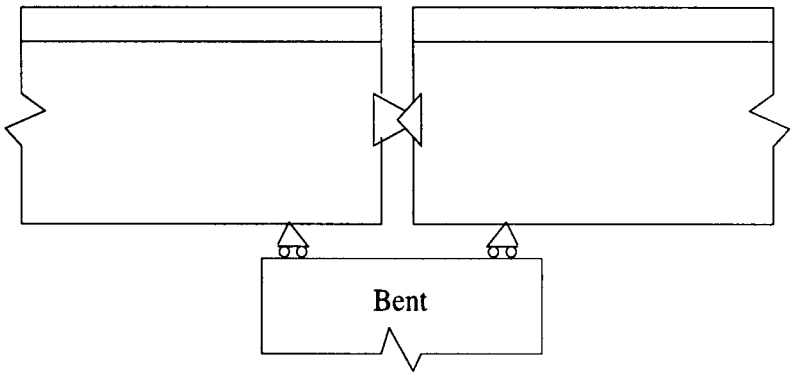

(c) Device to Connect two Girders

Figure 2.8: Japanese Displacement Restriction Devices

2.2.1 Loma Prieta, 1989

The Caltrans Maintenance Division reported that 23 bridges which had hinge restrainers suffered damage during the Loma Prieta earthquake. Field observations indicated that restrainers were activated in many instances, but failed in only two cases (Saiidi et al., 1993). The Richardson Bay Bridge and Separation is a 21-span bridge built in 1957 and retrofitted with cable restrainers in 1973. Failure of the restrainer and the connection devices was observed at the hinges. In addition the diaghragm cracked where the restrainers were connected. The Oakland Overcrossing (West Grand Avenue Viaduct) is a steel girder bridge built in 1937 and retrofitted in 1976. The retrofit consisted of longitudinal restrainers at each joint connected by steel brackets to the bottom girder flange or web. Failure of the restrainers and connection devices was also observed at the hinges. Yielding of restrainers occurred

in the China Basin Viaduct and the Route 92/101 Separation. In addition, excessive crack opening in the soffit of the superstructure was observed. It is believed that the restrainer forces in the superstructure reduced the flexural strength and helped open the flexural cracks that were developed by the gravity loads. There were several other bridges in which restrainers were engaged but did not yield or sustain damage.

2.2.2 Northridge, 1994

The epicentral region contained several bridges which had been retrofitted with hinge restrainers, and most of the bridges performed well. However, in some cases, hinge restrainers did not perform adequately. The Gavin Canyon Undercrossing is a concrete box-girder bridge which had been retrofitted in 1974 with restrainer cables and diaphragm bolsters across the in-span hinges. The heavily skewed bridge collapsed due to unseating. The end frames in the bridge were vulnerable to in-plane torsional response because of the eccentricity of the centers of mass and stiffness. The restrainer cables provided minimal restraint to transverse displacement at the hinge. Based on the observed damage, it is difficult to determine whether restrainers failed before or after loss of seat support. (Moehle, 1995; Priestley et al., 1994). The Interstate 5/State Road 14 Interchange and the South Connector Overcrossing are concrete box-girder bridges located approximately 12 km from the epicenter. It had also been retrofitted with cable restrainers following the 1971 San Fernando earthquake. Although the collapse of a frame was caused by shear failure in columns, spans in other frames that did not collapse were barely supported on hinge seats. Other structures in the interchange showed evidence of hinge and restrainer damage. The older C-1-type restrainers had been grouted during installation. The grouting led to large strains in the cable outside the grouted segment and premature fracture. Several bridges had evidence of pounding at the hinges.

2.2.3 Hyogo-Ken Nanbu (Kobe), 1995

The Hanshin Expressway, which is the major traffic artery through the city of Kobe, sustained extensive damage in the Kobe earthquake. Inadequate seat widths and insufficient restrainers ("falling-off prevention devices") caused many spans to

fall off their bearings and bents (Comartin et al., 1995). The eastern portion of the Hanshin Expressway is nearly normal to the strike-slip fault which produced primarily longitudinal movement due to the fault normal near source effect of the earthquake. The Harbor Freeway also sustained significant damage. In particular, almost every expansion joint along the freeway was damaged. Many hinge restrainers sustained damage and failure.

2.3 Current Restrainer and Hinge Seat Width Design Procedures

In this section, current procedures for hinge restrainers and hinge seat widths are reviewed. In the United States these procedures include the Caltrans Static Procedure, the AASHTO (American Association of State Highway and Transportation Officials) procedure. There are also recommended procedures for bridges in the Japanese and New Zealand codes.

2.3.1 Caltrans Design Procedures

After the San Fernando earthquake, Caltrans' policy was to design hinge restrainers to yield at a force equal to 25% of the weight of the lighter adjacent frame. Later this force was increased to 35%. Years later, Caltrans recommended performing a multi-modal dynamic analysis to determine the number of restrainer required to limit hinge displacement (Yashinsky, 1992). Caltrans currently uses an equivalent static procedure to design hinge restrainers for multiple frame bridges (Caltrans, 1990). The procedure simplifies the problem by replacing the coupled two degree-of-freedom system representing the longitudinal behavior of two adjacent frames with two uncoupled single degree-of-freedom systems as shown in Figure 2.9. The frame with the smaller displacement is assumed to control the response. Restrainers are provided to this frame until the frame displacement, D_{eq}, is less than the maximum permissible restrainer displacement, D_r. The maximum permissible restrainer displacement is usually taken as the yield displacement plus the restrainer slack. Since the function of restrainers is to avoid excessive relative movement at hinges, restrainers should be

designed to avoid yielding even under the maximum credible earthquake.

The principal shortcoming of the Caltrans procedure is with the estimate of the relative hinge displacement. The procedure uses the smallest displacement of the two frames, which can lead to an unconservative estimate of the relative hinge displacement. For example, in the case of a very stiff frame next to a very flexible frame, the relative hinge displacement predicted by the Caltrans procedure would be very small. The more flexible frame response, however, will likely dominate relative hinge displacement. In addition, since the procedure only considers only one frame, it cannot represent the in-phase response of frames with similar dynamic characteristics.

The effect of the Caltrans procedure based on independent single degree of freedom systems may be interpreted with the aid of a displacement response spectrum (Figure 2.9). The initial period of the of the frame, T_o, corresponds to a frame displacement of D_{eq_0}. The period of a single frame is modified by the addition of restrainers until the restrained period, T_r, corresponds to a frame displacement of D_r. Figure 2.10 shows a plot of the relative hinge displacement based on the Caltrans produce, and the relative hinge displacement based on a nonlinear elastic time history analysis of two frames with the properties shown. The relative hinge displacement is shown as a function of the frame period ratio, T_1/T_2, where T_1 and T_2 represent the Frame 1 and Frame 2 periods. For this plot Frame 2 period is held constant at a period of 1.0 sec, and Frame 1 period is varied from 0.30 sec to 1.00 sec. The frames are subjected to the 1940 El Centro S00E earthquake, scaled by a factor of two (PGA=0.70). The Caltrans procedure underestimates the hinge opening for small frame period ratios and overestimates the hinge opening for frame period ratios near unity. For low frame period ratios, the response is controlled by the more flexible frame. However, the Caltrans procedure only considers the response of the frame with the smallest displacement. For frame period ratios approaching unity, the hinge opening approaches zero due to in-phase motion of the frames. Since the Caltrans procedure only considers one frame, it does not account for the in-phase motion of the frames.

Considering design procedures for hinge seat widths, the Caltrans design procedure is based on the following empirical expression :

$$N = 12 + .03L + .08H(1 + \frac{S^2}{8000}),\ N > 30 \text{ inches}$$

$$N = 300 + 2.5L + 6.7H(1 + \frac{S^2}{8000}),\ N > 760 \text{ mm}$$

where N=hinge seat (inches, mm), L=frame length (feet, meters), H=average height of two adjacent frames (feet,meters), and S=skew of support (degrees). The factor $.03L$, corresponding to a strain of 0.0025, accounts for the movement of the hinge due to thermal expansion of the deck. The factor $.08H$ accounts for displacement of the hinge due to displacement of the column associated with an approximate drift ratio of 0.66 percent. The factor, $\frac{S^2}{8000}$, is a multiplier to account for the skew of the hinge. The values of $\frac{S^2}{8000}$ range from 0 for a skew of zero to 1.0 for a skew of 90 degrees.

2.3.2 American Association of State Highway and Transportation Officials (AASHTO) Specification

The AASHTO code specifies providing a positive horizontal linkagee between adjacent frames of the superstructure (AASHTO, 1992). The linkage between frames should be designed for a minimum force equal to the acceleration coefficient times the weight of the lighter of the two adjoining spans. The acceleration coefficient is the design peak ground acceleration divided by the acceleration value of gravity. Linkages may be provided by ties, cables, or dampers. However, there are no specifications or guidelines for the use of dampers in the current specifications. The AASHTO specification has similar shortcomings as the Caltrans procedure. The relative force required is based only on one frame. The restraining force required is actually a function of the relative displacement between frames and the relative period of the frames. The AASHTO procedure does not address either of the issues.

The hinge seat width requirement is based on the following empirical expression :

$$N = 12 + .03L + .12H, \text{ inches}$$

$$N = 300 + 2.5L + 10H, \text{ mm}$$

where the parameters have similar definitions to those for the Caltrans procedure. The AASHTO procedure increases the component of displacement due to drift by 50 percent corresponding to a value of 1 percent drift. In addition, there are no modifications for skew angle.

2.3.3 Japanese Bridge Specifications

Falling-off prevention devices are designed for a horizontal load, H_R, which is twice the regular seismic force (Takahashi, 1990). The devices include metal plates which connect the substructure to the superstructure, devices that protrude into the path of the superstructures, and devices that connect superstructures together. The regular seismic force is the design horizontal acceleration, based on a design spectrum, multiplied by the vertical reaction due to the dead load as shown below:

$$H_R \geq 2.0 * K_h * R_d$$

Where K_h=design horizontal acceleration coefficient, and R_d=vertical reaction due to dead load. This procedure is very similar to the AASHTO requirements. The required restrainer force in the Japanese code is only a function of the peak acceleration and reaction at the intermediate hinge. The hinge seat width requirement for Japanese bridges is similar to the AASHTO and Caltrans specifications. The hinge seats are designed according to the following:

$$N = 28 + .024L, \text{ (in) for } L \leq 328\ ft$$
$$N = 32 + .019L, \text{ (in) for } L > 328\ ft$$

$$N = 710 + 2.0L, \text{ (mm) for } L \leq 100\ meters$$
$$N = 810 + 1.6L, \text{ (mm) for } L > 100\ meters$$

where N=hinge seat width (inches,mm), and L=frame length (feet,meters). The code only accounts for hinge displacement due to thermal expansion. However, the minimum hinge seat width is considerably greater than the Caltrans and AASHTO recommendations.

2.3.4 New Zealand Bridge Specification

The New Zealand Bridge Specification allows two types of devices to limit hinge displacement: tight linkages and loose linkages (New Zealand Transit, 1990). A tight linkage is used where relative horizontal movement is not intended to occur under service loads or seismic loads. The specification requires that a tight linkage

be designed to have a strength equal to the load developed under design seismic conditions.

Loose linkages are used where relative horizontal movement between elements of the bridge is intended to occur under earthquake conditions. The elements of a loose linkage between a span and its supports are designed to have a strength equal to at least 0.20 times the dead load of the smaller of the adjacent spans. In the case of a short length (suspended span) between two longer lengths, the strength is based on the longer length. This procedure is similar to the AASHTO and Japanese procedures, except that the acceleration coefficient is always assumed to be 0.20, as opposed to a value based on a design spectrum, or seismic coefficient.

Hinge seat widths depend on the restraint for the hinge. For a no linkage system, the following recommendations apply:

$$N = 4 + .079E, N > 16 \text{ in}$$

$$N = 100 + .079E, N > 410 \text{ mm}$$

where E=relative movement between span and support under design condition (inches, mm); earthquake + shortening effects + $\frac{1}{3}$(temperature effects). For a loose linkage system, the hinge seat recommendation is

$$N = 4 + .059E', N > 12 \text{ in}$$

$$N = 100 + .059E', N > 300 \text{ mm}$$

where E'=equivalent relative movement at which the loose linkage operates.

For tight linkage systems, hinge seat widths are designed at a minimum of 7.85 inches (200 mm). On short skew bridges, overlap requirements should be increased by up to 25%. If frame movements due to earthquake loading may be out-of-phase, the earthquake components of the overlap requirements may be based on the SRSS modal combination rule of the displacements of the frames.

This procedure is much better than previous procedures because it accounts for dynamic characteristics of frames. The modal analysis of the displacements due to the earthquake loading will represent the response of frames for a wide range of

frame properties. However, since the SSRS rule is used to combine the modes, the reduction in the required number of restrainers due to in-phase motion of frames as the period ratio approaches unity is not represented correctly. In addition, the procedure accounts for hinge displacements due to temperature and shortening effects. However, it is not clear in the code how values for these effects are determined.

2.4 Review of Previous Studies on Hinge Restrainers

2.4.1 Experimental Studies

An evaluation of the strength, stiffness, and cyclic load-deflection behavior of a full-scale section of an intermediate hinge with longitudinal cable restrainers was determined from an experimental test apparatus as shown in Figure 2.11 (Selna et al., 1989). A representative portion of a reinforced concrete box girder bridge which included the hinge was constructed and tests were performed to determine the force-deformation relationship of a reinforced concrete box girder with a hinge. The specimen was 4 ft (1.2 m) high, 10 ft (3.1 m) wide, and 19 ft (5.8 m) long.

Tension forces were exerted by hydraulic actuators through the specimen. This created tensile forces in the restrainer cables and supported (ledge) side of the specimen. When tested to failure, the type C-1 installation experienced a loss of resistance due to shear failure of anchorage in the (supporting) seat side of the hinge diaphragm. The strength of the restrainer components (bolster, bearing plates, drum) at failure was slightly greater than the design yield strength of the cables. The conclusions from the study were that although failure may occur in the box girder, restrainers strengthen the seismic resistance of bridge structures. Suggested improvements for type C-1 installation were (1) increasing the radius of the bend on the drum so that the strength and ultimate strain of the cable is increased, and (2) the bolster strength should be increased to reduce the likelihood of shear failure. Modern restrainer retrofits do not wrap cables around a drum, as was shown in Figure 2.4, thus eliminating the problem with stress concentrations around the drum.

2.4.2 Performance Evaluations and Case Studies

A significant number of bridges which had been retrofit with cable restrainers were subjected to strong ground excitations during the Loma Prieta earthquake. Following the earthquake, researchers from the University of Nevada, Reno selected four bridges to model and performed nonlinear analysis (Saiidi et al., 1993). The bridges were selected based on the damage they experienced, number of hinges, type of superstructure, and skew angle. With the exception of a few cases, the restrainers did not fail or cause damage to bolsters. The study concluded that the effectiveness of restrainers depends on many factors including the intensity and frequency content of the ground motion, foundation flexibility, and flexibility of substructure. For bridges with a relatively stiff substructure in the longitudinal direction, restrainers did not play a significant role. Because of the sensitivity of the relative displacements at the hinges to many parameters, it was concluded that nonlinear time history analysis is necessary for obtaining reliable estimates of the required number of restrainers to limit hinge displacements to a prescribed value.

Singh and Fenves (1994) studied the effect of hinge restrainers on viaducts subjected to uniform and non-uniform ground motion. Using a two-dimensional model of a typical two-level reinforced concrete viaduct with two-column bents, the response of the intermediate hinges was studied. They found that a large number of hinge restrainers may be needed in cases where viaducts are subjected to non-uniform motion. Additionally, intermediate hinges should be designed with seat widths in excess of 30 inches (762 mm).

2.4.3 Analytical Studies

Several parameter studies on the effect of hinge restrainers on the response of multiple-frame bridges have been performed (Saiidi et al., 1996). Using the example bridge from the Caltrans Design Manual (Caltrans, 1990), the investigators performed a parameter study to determine the effects of changing the cross-sectional area of restrainers and the restrainer gap on the response of bridges. The response quantities of interest were the relative hinge displacement, restrainer stresses, and abutment forces. The study showed that the restrainer stiffness required to limit the hinge displacement

is sensitive to the small variations in the maximum relative hinge displacement. This point is addressed later in the study. It was found that the maximum relative hinge displacement may occur for the case of zero gap or nonzero restrainer gap, depending on the number of restrainers. The design of restrainers, therefore, should consider several possible gap lengths.

Recent studies have focused on broader parameter studies using simplified models (Yang et al., 1994). The authors performed a parameter study to investigate the influence of bridge characteristics and analytical methods on the predicted response of intermediate hinges. A simplified two degree-of-freedom model was used to represent the longitudinal earthquake response of two frames in a bridge. A nonlinear element which accounts for the tension-only restrainers and compression-only contact was used at the hinge. The parameters studied include the frame stiffness ratio (K_1/K_2), the frame mass ratio (m_1/m_2), the stiffness of restrainers (K_r), earthquake intensity (peak ground acceleration), gap width, friction force, and frame yield strength. The analytical methods investigated included elastic time history, inelastic time history, and the response spectrum analysis. The study concluded that the Caltrans equivalent static design procedure does not adequately predict the relative hinge displacement. For frames with large stiffness ratios, the Caltrans design procedure underestimates the hinge displacements. For frames with a stiffness ratio approaching unity, the design procedure is too conservative because it does not represent the in-phase motion. The study showed that the effectiveness of restrainers in limiting the relative hinge displacement depends on the frame stiffness ratio. At low frame stiffness ratios, the restrainers have a significant influence on the response, especially when the restrainer stiffness is equal to or greater than the stiffness of the more flexible frame. The yield strength of the columns was varied to study the effects of the yield strength on the response of intermediate hinges. It was found that decreasing column yield strengths resulted in smaller relative hinge displacements. This is due to the increase in in-phase motion of yielding frames. Variations in gap width and Coulomb friction force were found to have negligible effect on the relative hinge displacements.

Researchers at the University of Washington have performed an extensive study on the effect of hinge restrainers on the maximum relative hinge displacement (Trocha-

lakis et al., 1997). The study is similar to the Yang study, however, the model included the effect of abutments. The goals of the study were to identify the factors that affect the relative hinge displacement, evaluate the current restrainer design methods, and develop a new design procedure for hinge restrainers. The effect of frame stiffness was studied by holding the stiffness of one frame constant while varying the stiffness of an adjacent frame. As the frame stiffness ratio increased, the maximum relative hinge displacement increased. The effects of abutment stiffness were studied by multiplying the abutment stiffness and strength by factors of 0.0 and 2.0. Changing the abutment properties did not significantly affect the maximum relative hinge displacement. The most significant difference is obtained at a frame period ratio of unity. Without abutments, frames with a period ratio of unity have zero relative hinge displacement. With abutments, however, frames with the same period would no longer vibrate in-phase because of impact with the abutments and therefore larger hinge displacements would be obtained. For out-of-phase frames, the difference in hinge displacement without abutments and with twice the abutment stiffness is less than 10 percent. The effect of restrainer gap, Coulomb friction, and frame weight were negligible in reducing relative hinge displacement. Since this study did not explicitly account for inelastic response, the results may be misleading. Both the effect of abutments and of Coulomb friction may be underestimated depending on the level of inelastic response. The force transmitted to the abutments are reduced as the frames yield. Similarly, the friction force between the frames is much more effective as the frames yield.

2.4.4 Design Procedures

The parameter study by Yang (1994) lead to a proposal for a restrainer design procedure. It was recommended that the hinge displacement should be estimated as the absolute maximum displacement of the two frames acting as independent nonlinear oscillators. The restrainer stiffness to limit hinge displacement is recommended to be equal to or greater than the most flexible frame. Using the absolute maximum displacement of the two frames will usually result in a conservative estimate of the relative hinge displacement. The in-phase response of frames with similiar dynamic

characteristics cannot be captured with this approach. The procedure for calculating the required restrainer stiffness is also incorrect. The calculated restrainer stiffness is based on the flexibility of only one frame. Since the restrainers are pulling the two frames together, the restrainer stiffness should be based on the sum of the flexibilities of the two frames.

Using the results from a parameter study, researchers at the University of Washington proposed a new restrainer design procedure (Trochalakis et al., 1997). The new procedure considers two uncoupled single degree-of-freedom systems. The individual frame displacements are determined from a design spectrum, and the maximum relative hinge displacement is based on an expression which accounts for the influence of frame period ratio, as follows:

$$D_{eq} = \frac{D_{ave}}{2}\frac{T_L}{T_S} \leq 2D_{ave} \tag{2.1}$$

where D_{ave} is the average frame displacement, and T_L and T_S are periods associated with the frames. The subscript L is for the longer period frame, and the subscript S is for the shorter period frame. This expression was obtained from a "best fit" of data from an extensive set of nonlinear time history analyses. The expression for relative hinge displacement is used in the Caltrans procedure to determine the required restrainer stiffness. This procedure, while providing a better estimate of the relative hinge displacement, does not accurately represent the dynamic interaction of the two frames. Since the linearization of the system is achieved by considering two independent SDOF systems, the change in the periods, mode shapes, and participation factors, are not correctly accounted for in the procedure. In addition, the procedure is based on a set model with a specific frame values (such as stiffness, yield force, etc.). Therefore variations from the parameters used in the study may provide inaccurate results.

A restrainer design procedure has been suggested based on capacity design principles (Priestley et al., 1995). The authors recommend that the maximum tensile force transferred between frames should be equal to the difference between the frame overstrength longitudinal shear capacities as follows:

$$F_R = V_{F1} - V_{F2} \tag{2.2}$$

where V_{F1} and V_{F2} are the overstrength capacities, found from the summation of the overstrength capacities of all of the columns in each frame. The stiffness is adjusted so that the yield strength of the restrainers is not attained until a relative displacement based on the difference between the absolute displacement of the frames is obtained. A free body diagram of the system is shown in Figure 2.12. It is evident from the figure that the inertial force from the masses must be considered in order to accurately determine the force of the restrainers. Ignoring the inertial forces can provide grossly inaccurate results for the restrainer force. In addition the procedure assumes that the maximum relative hinge displacement occurs while the frames vibrate in phase. This assumption is not necessarily correct because the phasing depends on the frame properties and the input motion.

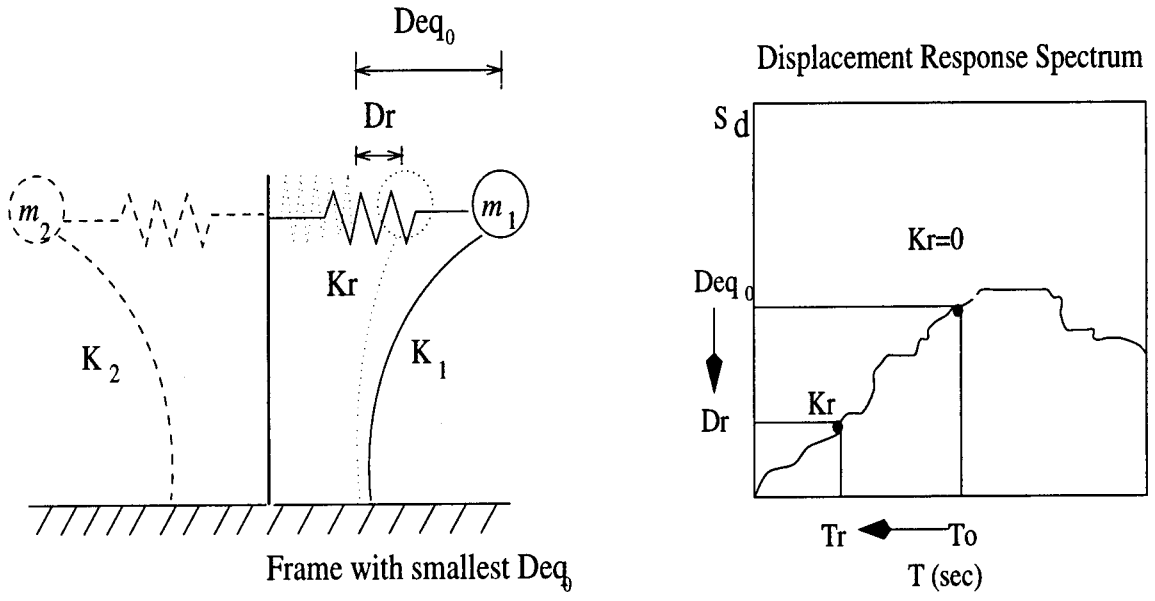

Figure 2.9: Interpretation of Caltrans Equivalent Static Procedure for Hinge Restrainers (Caltrans, 1990).

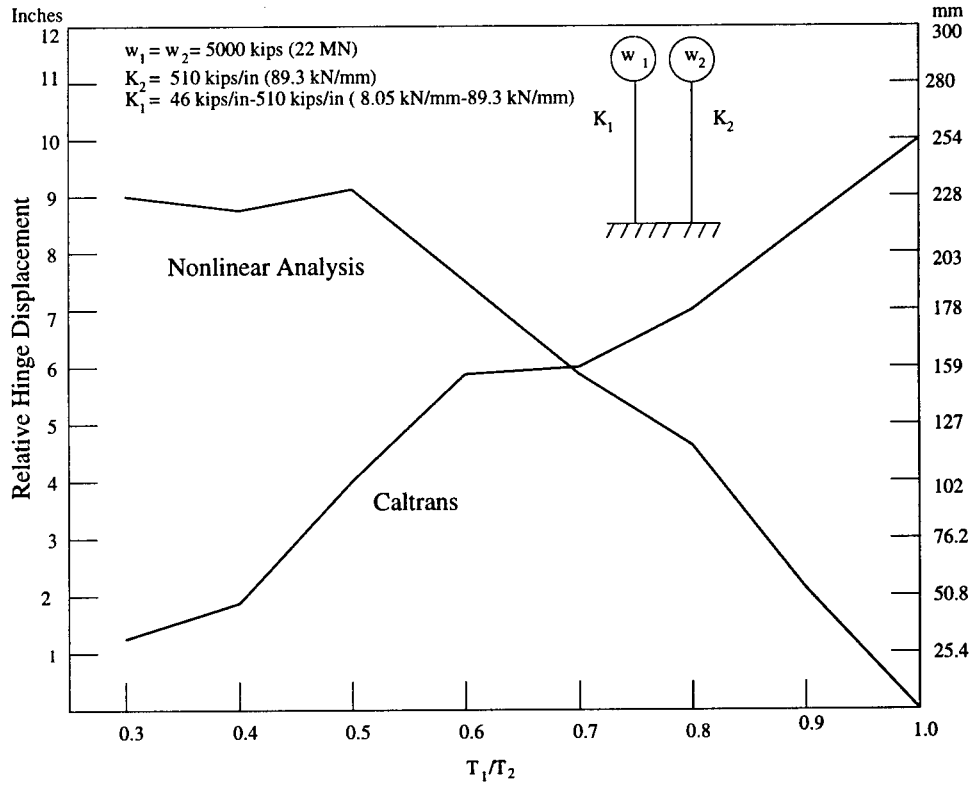

Figure 2.10: Relative Hinge Displacement Based on Nonlinear Analysis and the Caltrans Procedure.

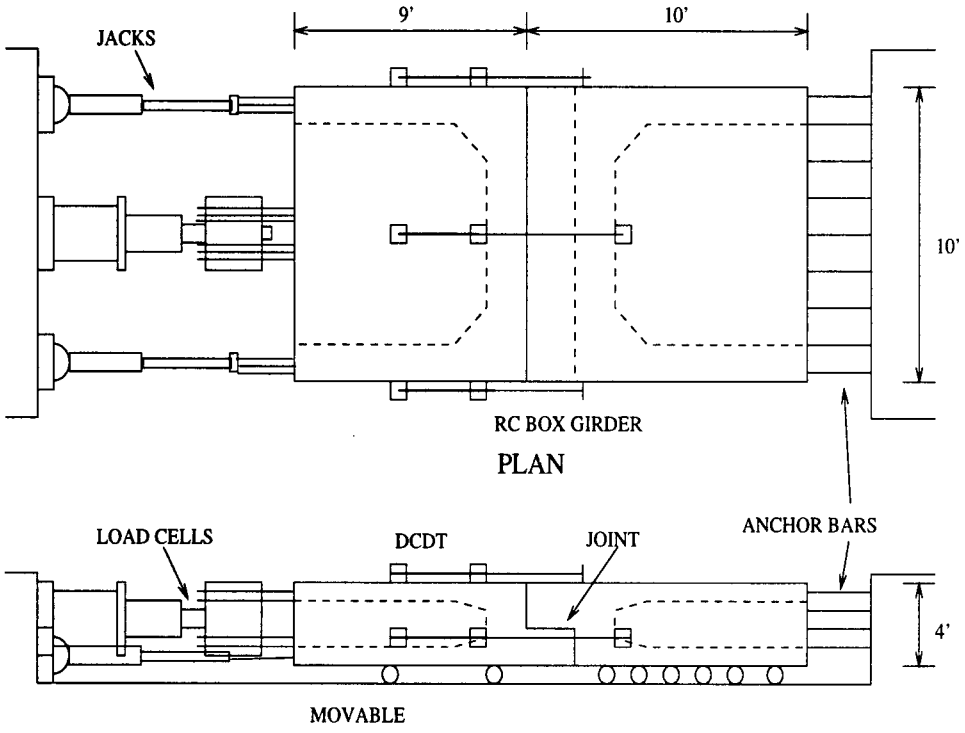

Figure 2.11: Test Specimen and Testing Arrangement for Experimental Studies on Hinge Restrainers (Selna, 1989).

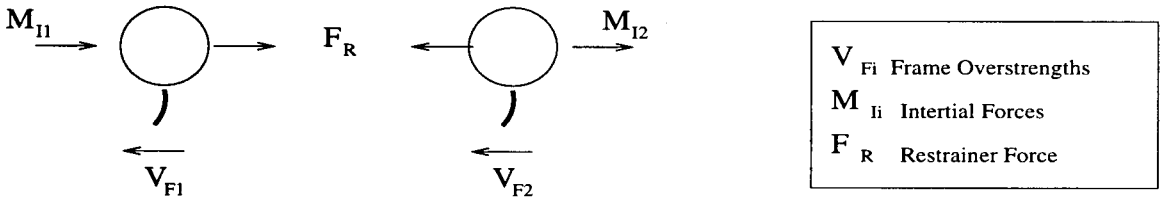

Figure 2.12: Capacity Design Procedure for Hinge Restrainers (Priestley et al., 1995)

Chapter 3

Numerical Models for Analysis of Adjacent Bridge Frames

The interaction of frames in long multiple-frame bridges includes many nonlinearities such as pounding of frames at the hinge, yielding of frames, engaging of restrainers, and friction. A nonlinear numerical model is developed to represent these effects on the longitudinal response of two adjacent frames, as shown in figure 3.1. Since the primary goal of the study is to obtain the relative hinge displacement, a more discretized model for the frames would not significantly enhance the accuracy. Each frame is modeled as a single degree-of-freedom (SDOF) oscillator with a nonlinear force-displacement relationship. The hinge model includes nonlinear elements which account for Coulomb friction, and tension-only restrainers. The effect of pounding is accounted for directly in the equations of motion.

3.1 Frame Properties

Each frame is represented as a SDOF yielding element with a mass of m_i. A Q-Hyst stiffness degrading hysteresis model represents the force-displacement relationship for the frame as shown in figure 3.2 (Saiidi and Sozen, 1979). The backbone curve used is bilinear with 5 % strain hardening. Stiffness degradation is accounted for at unloading and load reversal. The unloading stiffness at the inelastic segment of the primary curve is defined by $K_q = K\sqrt{(\tilde{D}_y/D)}$, where K is the initial elastic slope,

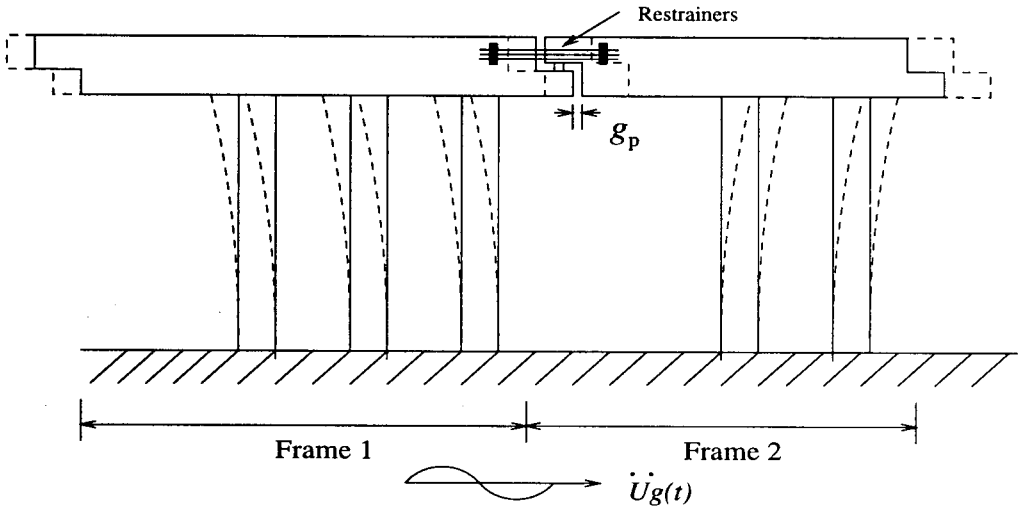

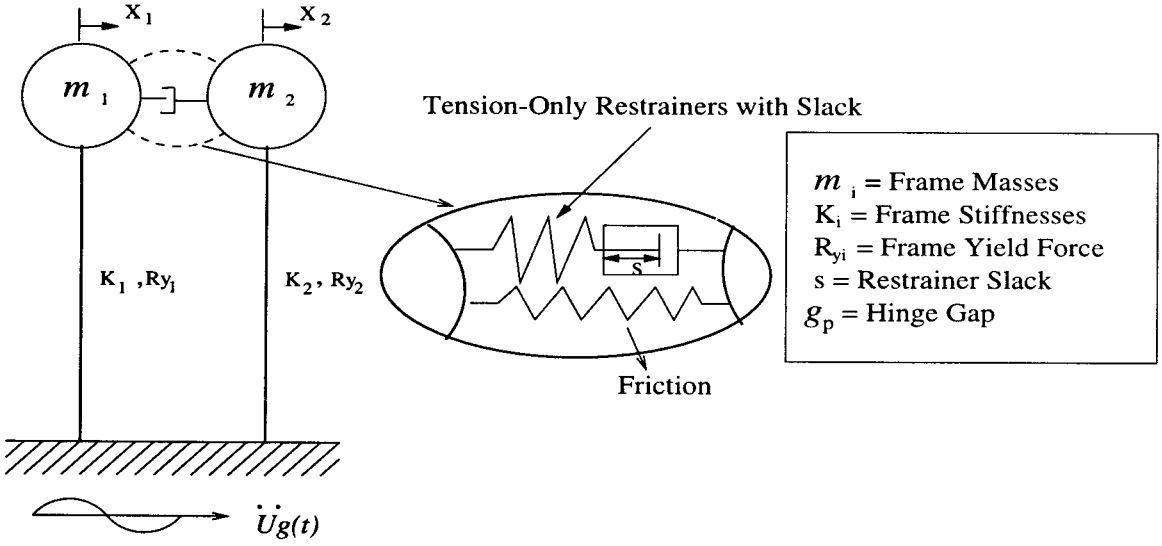

Figure 3.1: Two Degree-of-Freedom Nonlinear Model for Longitudinal Earthquake Response of Two Frames.

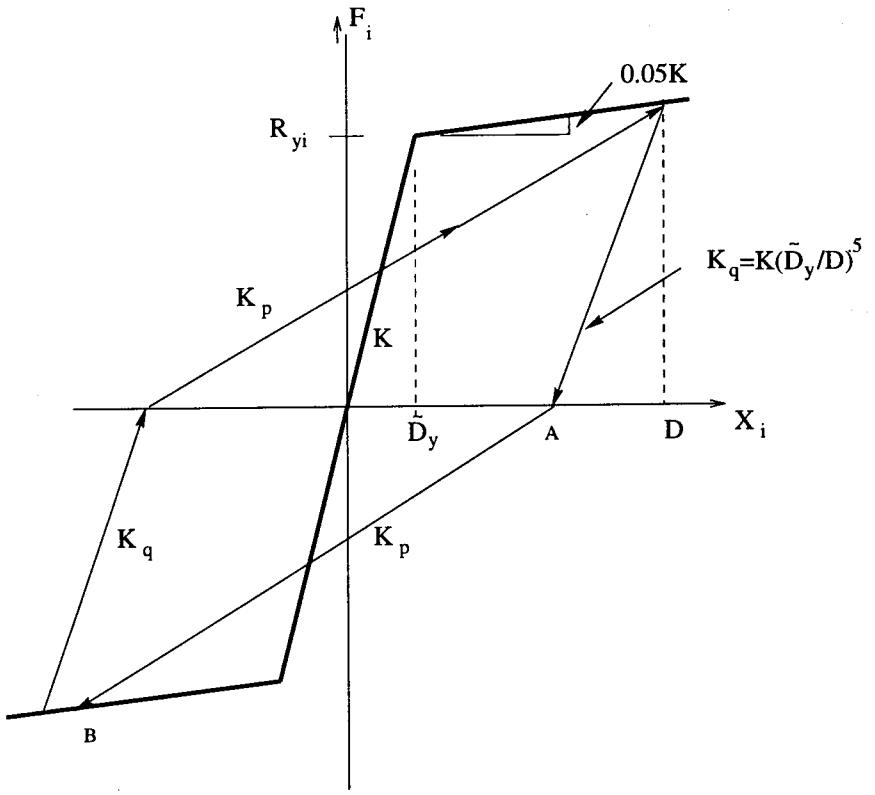

Figure 3.2: Q-Hyst Model Force-Deformation Relationship for Frame.

D is the largest absolute deformation, and $\tilde{D}_y$ is the yield deformation. The linearized K represents the stiffness of the soil-structure system, accounting for the rotational flexibility of the foundation. The stiffness at the load reversal stage, K_p, is defined by the path connecting the intersection of the latest unloading branch with the displacement axis (point A) to the largest absolute displacement (point B). The Q-Hyst model closely represents the response from a Takeda model, which is considered a realistic model for single degree-of-freedom reinforced concrete columns, as observed from experimental studies (Takeda et al., 1970). The Q-Hyst model, however, is a much simpler hysteretic model than the Takeda model. The Q-Hyst model is defined by four rules, whereas the Takeda model is defined by 16 rules.

3.2 Hinge Properties

3.2.1 Restrainers

The restrainers are modeled as a bilinear spring that only resists tensile forces. Restrainer cables have a yield strength of 39.1 kips (174 kN), which coincides with a yield stress of 176.1 ksi (1210 N/mm^2). As was previously shown in figure 2.2, restrainers have considerable post yield strength. In this study, restrainers are assumed to have a strain hardening ratio of 5 % as shown in figure 3.3(a). The number of the restrainers and hence the restrainer stiffness, K_r, is varied to study its effect on the maximum relative hinge displacement.

3.2.2 Friction

Concrete box girder superstructures are typically supported on an elastomeric bearing pad at the intermediate hinges. The effects of the elastomeric pads are negligible, and therefore not included in the study. As the frames move out-of-phase, beyond the displacement capacity, the box girder slides off the bearing and develops a frictional force. The friction force is modeled by an elasto-plastic spring with yield force equal to the friction force, as shown in figure 3.3(b). Typical two-to-three lane bridge spans have lengths of approximately 150-300 ft (46-92 m) and a weight of approximately 10 kips/ft (146 kN/m). The intermediate hinge locations are assumed to be located 1/5-1/8 across the span. Given this, the vertical shear at a hinge is 500-1000 kips (2200-4400 kN). The kinematic coefficient of friction between the bearing pads and the concrete surface is estimated to be 0.20. Therefore, the friction yield force is estimated to be 100-200 kips (445-890 kN). The friction force is varied within this range.

3.3 Governing Equations of Motion

The equations of motion for the system is expressed as:

$$\mathbf{M}\ddot{\mathbf{x}}(t) + \mathbf{C}\dot{\mathbf{x}}(t) + \mathbf{R}(\mathbf{x}(t)) + \mathbf{F}(\mathbf{x}(t)) = -\mathbf{M}\mathbf{1}\ddot{u}_g(t) \tag{3.1}$$

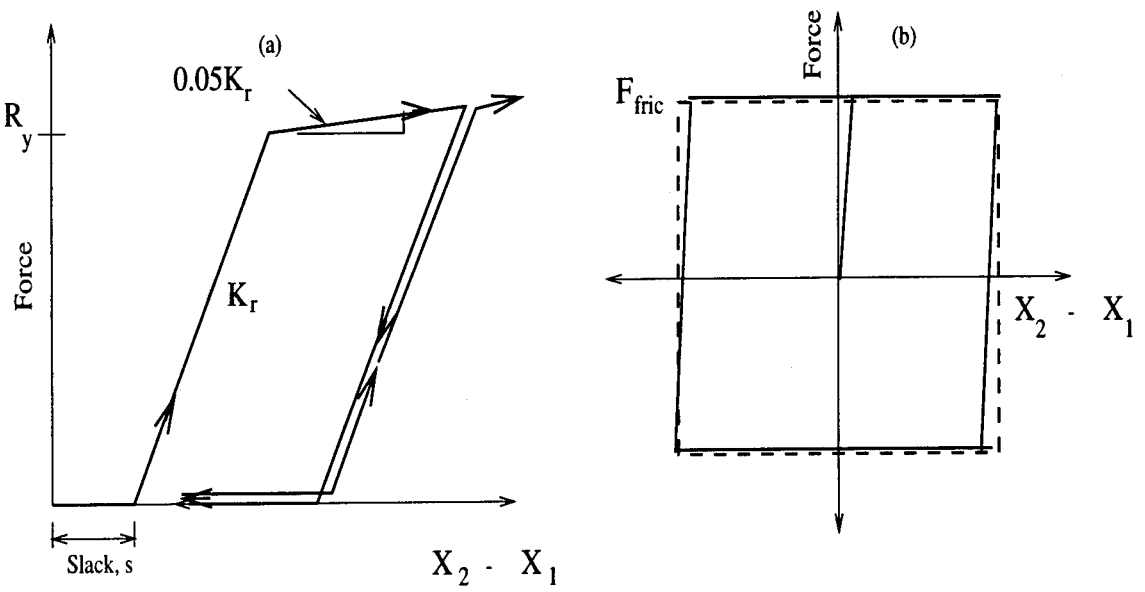

Figure 3.3: Force-Displacement Relationship for (a) Hinge Restrainers (b) Coulomb Friction.

where **M** and **C** are the mass and damping matrices, **R** is the vector of the restoring force for the frames, and **F** is the restoring force due to friction and the restrainers. The vector **1** is the influence vector, $\ddot{u}_g(t)$ is the input motion, and $\ddot{\mathbf{x}}$, $\dot{\mathbf{x}}$, and $\mathbf{x}$ are the frame acceleration, velocity, and displacement vectors, respectively. For the 2-DOF system, equation 3.1 is:

$$\begin{bmatrix} m_1 & 0 \\ 0 & m_2 \end{bmatrix} \begin{Bmatrix} \ddot{x}_1 \\ \ddot{x}_2 \end{Bmatrix} + \begin{bmatrix} c_1 & 0 \\ 0 & c_2 \end{bmatrix} \begin{Bmatrix} \dot{x}_1 \\ \dot{x}_2 \end{Bmatrix} + \begin{Bmatrix} R_1(x_1) \\ R_2(x_2) \end{Bmatrix} + \begin{Bmatrix} F_{fr}(x_2 - x_1) \\ -F_{fr}(x_2 - x_1) \end{Bmatrix} = - \begin{bmatrix} m_1 & 0 \\ 0 & m_2 \end{bmatrix} \begin{Bmatrix} 1 \\ 1 \end{Bmatrix} \ddot{u}_g \tag{3.2}$$

where $c_i = 2\omega_i \xi_i m_i$ denotes the damping coefficient, R_i is the inelastic resisting force of the frame, and F_{fr} is the inelastic force due to friction and the restrainers.

3.3.1 Numerical Solution of Governing Equations

The solution of equation 3.2 is obtained numerically using Newmark's constant acceleration method (β=1/4). For the analysis of MDOF systems, the constant average acceleration assumption has the advantage that it provides an unconditionally

stable integration procedure for linear systems (Clough and Penzien, 1993). For this method, displacement at time step $n+1$ can be written in terms of known system properties as:

$$\mathbf{u}_{n+1} = (\mathbf{K}^{\star})^{-1}\mathbf{P}^{\star}{}_{n+1} \tag{3.3}$$

where the effective stiffness and loads are defined as:

$$\mathbf{K}^{\star} = \frac{1}{\beta(\Delta t)^2}\mathbf{M} + \frac{\gamma}{\beta\Delta t}\mathbf{C} + \mathbf{K_T} \tag{3.4}$$

and

$$\mathbf{P}^{\star}{}_{n+1} = \mathbf{P}_{n+1} + \mathbf{M}(\frac{1}{\beta(\Delta t)^2}\tilde{\mathbf{u}}_n) + \mathbf{C}(\frac{\gamma}{\beta\Delta t}\tilde{\mathbf{u}}_n - \dot{\tilde{\mathbf{u}}}_n) \tag{3.5}$$

where $\mathbf{P}$ is the effective earthquake load vector and $\mathbf{K_T}$ is the tangent stiffness matrix, and

$$\dot{\tilde{\mathbf{u}}}_n = \dot{\mathbf{u}}_n + (1-\gamma)\Delta t\ddot{\mathbf{u}}_n \tag{3.6}$$

$$\tilde{\mathbf{u}}_n = \mathbf{u}_n + \dot{\mathbf{u}}_n\Delta t + 1/2(1-2\beta)(\Delta t)^2\ddot{\mathbf{u}}_n \tag{3.7}$$

The velocity and accelerations are determined from the following equations:

$$\ddot{\mathbf{u}}_{n+1} = \frac{1}{\beta}\Delta t^2(\mathbf{u}_{n+1} - \tilde{\mathbf{u}}_n) \tag{3.8}$$

and

$$\dot{\mathbf{u}}_{n+1} = \dot{\tilde{\mathbf{u}}}_n + \frac{1}{\beta}\Delta t^2(\mathbf{u}_{n+1} - \tilde{\mathbf{u}}_n) \tag{3.9}$$

Since the elements of the system are nonlinear, a solution strategy to account for changes in stiffness is needed. The Newton-Raphson iteration scheme is a well known method for the analysis of nonlinear structures. After an estimate of the displacements in a time step for the Newmark Method are obtained, equilibrium of forces is checked by calculating the residual force as follows:

$$\mathbf{r}(\mathbf{u}_{n+1}) = \mathbf{P}_{n+1} - \mathbf{F}_{n+1} - \mathbf{M}\ddot{\mathbf{u}}_{n+1} - \mathbf{C}\dot{\mathbf{u}}_{n+1} \tag{3.10}$$

where $\mathbf{F}_{n+1}$ is the total restoring force. Using a Taylor series expansion of the residual, we obtain an estimate of the $(k+1)th$ residual, where k represents the number of iterations of the Newton-Raphson procedure:

$$\mathbf{r}^{k+1}(\mathbf{u}_{n+1}) = \mathbf{r}^{k}(\mathbf{u}_{n+1}) + \frac{\partial \mathbf{r}}{\partial \mathbf{u}_{n+1}} \mid ({\mathbf{u}_{n+1}}^{k+1} - {\mathbf{u}_{n+1}}^{k}) + ...H.O.T. \tag{3.11}$$

where $H.O.T$ represents the higher order terms. Computing the gradient residual and collecting terms, the residual load is determined as

$${\mathbf{r}^{k}}_{n+1} = (\mathbf{K}^{\star})^{k}\Delta\mathbf{u} \tag{3.12}$$

or solving for the incremental displacement we obtain

$$\Delta\mathbf{u} = (\mathbf{K}^{\star k})^{-1}{\mathbf{r}^{k}}_{n+1} \tag{3.13}$$

The response is updated for the iteration as

$${\mathbf{u}_{n+1}}^{k+1} = {\mathbf{u}_{n+1}}^{k} + \Delta\mathbf{u} \tag{3.14}$$

The incremental displacement is added to the previous displacement to result in the displacement estimate at the kth step. Convergence is achieved when the norm of the residual force is less than the norm of the tolerance. The tolerance is set to $1x10^{-6}$ multiplied by the input load. The velocity and acceleration are calculated from equations 3.8 and 3.9.

3.3.2 Solution Scheme for Impact of Masses

The solution for dynamic impact of the masses must fulfill the conditions: (1) the total energy of the system is conserved for perfectly elastic impact, and (2) conservation of momentum. In the case of inelastic impact, the energy loss may be represented by a coefficient of restitution, e. The coefficient of restitution, defined as the ratio of the separation velocity to the approach velocity, is determined from (Goldsmith, 1960):

$$e = \frac{v_2' - v_1'}{v_1 - v_2} \tag{3.15}$$

where v_1, v_2 are the velocities of the two masses prior to impact, and v_1', v_2' are the velocities after impact. The values of e range from 1.0 (elastic) to 0.0 (perfectly plastic).

Previous studies show that for realistic values of e, the relative hinge displacement is not sensitive to the values of e (Athanassiadou et al., 1994). Using equation 3.15 in combination with the principle of conservation of momentum:

$$m_1 v_1' + m_2 v_2' = m_1 v_1 + m_2 v_2 \tag{3.16}$$

results in the rebound velocities after impact:

$$v_1' = v_1 - (1+e)\frac{m_2(v_1 - v_2)}{m_1 + m_2} \tag{3.17}$$

$$v_2' = v_2 + (1+e)\frac{m_1(v_1 - v_2)}{m_1 + m_2} \tag{3.18}$$

In the implementation of dynamic impact in the nonlinear solution algorithm, there are three conditions which may exist in the solution of equations of motion:

1. $x_2 - x_1 > -g_p + \epsilon$
2. $x_2 - x_1 = -g_p \pm \epsilon$
3. $x_2 - x_1 < -g_p - \epsilon$

where ϵ is the error tolerance, typically set at 0.05 in. (1.27 mm). If the first case applies, the solution proceeds using the algorithm in section 3.3.1. If the second case applies, the solution strategy is modified to account for impact as the hinge closes. Impact is assumed to occur instantly at the time of contact. If impact occurs at step t_{n+1}, the velocities are modified using equations 3.17 and 3.18. To represent the impact conditions, the solution for the next time step t_{n+2} is obtained with the modified velocities after impact. If condition 3 applies, a variable time stepping procedure is used to determine the time of impact. The procedure calculates the time when the relative displacement is $-g_p$ (within a specified tolerance). If the solution for time t_{n+1} gives that $x_2 - x_1 < -g_p - \epsilon$, the time step increment, Δt, is reduced to $\frac{\Delta t}{2}$. The solution for time t_{n+1} is re-run at the smaller time step. This is repeated until $x_2 - x_1 = -g_p \pm -\epsilon$. At that time, the velocities are modified by equations 3.17 and 3.18, and the modified velocities are used in the next time, which is performed at a time step increment of Δt. A graphical representation of the variable time step procedure is shown in figure 3.4.

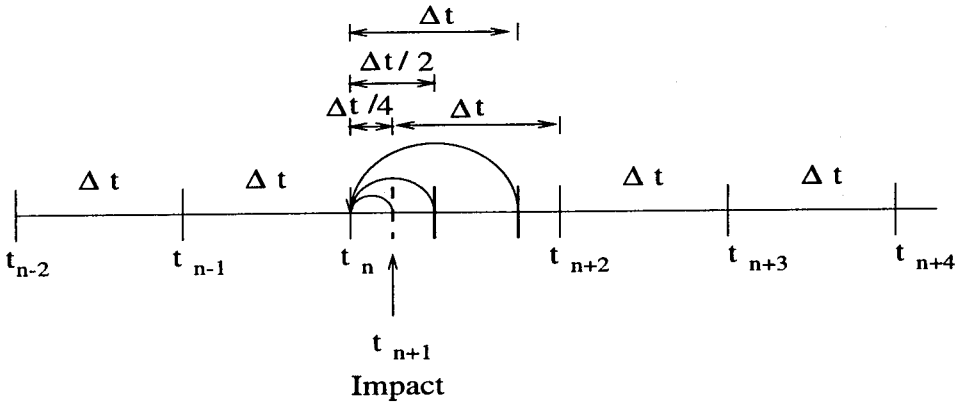

Figure 3.4: Variable Time Stepping Strategy for Numerical Solution of Pounding of Frames.

3.4 Example Cases

In this section, the response of two frames computed with the numerical algorithm in the previous section is compared with the response using DRAIN-3DX, a computer program typically used in bridge analyses (Prakash et al., 1992). DRAIN-3DX uses an event-to-event strategy for the solution of nonlinear systems. The primary difference between DRAIN-3DX and the model developed for this study is the treatment of dynamic impact (pounding). In this study, pounding is accounted for by modification of the equations of motion. Pounding is modeled in DRAIN-3DX by the use a stiff compression-only element with a gap. Although the stiffness of the compression element, $1x10^5$ kips/in ($1.75x10^4$ kN/mm), is a relatively low value compared with the axial stiffness of a typical box girder, it provides a compromise between penalizing penetration upon closing of the gap and convergence of the solution. The typical gap penetration is approximately 0.25-0.50 in. (6.4-12.7 mm).

Figure 3.5 shows a comparison between the results from an elastic two frame analysis using the procedure above and DRAIN-3DX. The frames are subjected to 1940 El Centro earthquake (S00E component), scaled by a factor of two (PGA=0.70g). Frames 1 and 2 have elastic stiffnesses of 1200 kips/in (210 kN/mm) and 510 kips/in (89.2 kN/mm), respectively. The weight of both frames is 5000 kips (22.3 MN). The frames have periods of 0.65 sec and 1.00 sec. Restrainers with a stiffness of 500 kips/in (87.5 kN/mm) and a slack of 0.50 in. (12.7 mm) are used at the hinge. The gap at

the hinge is 0.50 in. (12.7 mm). The displacement and velocity responses for the two solutions in figure 3.5 have small differences, primarily due to the representation of pounding. The pounding model used in DRAIN-3DX develops a penetration of 0.25 in. (6.4 mm), whereas the penetration allowed in the numerical procedure in the study, based on the specified tolerance, is less than 0.05 in. (1.27 mm). There are major differences in the acceleration response from the two methods. The DRAIN-3DX solution exhibits very large acceleration spikes at the times when impact occurs. At times other than impact, the two acceleration histories compare fairly well. The plot of the relative hinge displacement also shows some differences between the results from the numerical procedure and DRAIN3-DX. After impact, there are differences in peak relative displacement and phase. This is caused by the way DRAIN-3DX corrects for velocities and accelerations within a time step for very large changes in stiffness such as due to the gap element closing.

Figure 3.6 shows a comparison similar to figure 3.5, except the frames yield using a non-degrading bi-linear hysteretic model with 5% strain hardening. The strengths of the frames are selected to produce a displacement ductility of $\mu = 4$ as independent frames.

The yield force of the frames is chosen so that each frame has an independent frame ductility demand of four under the earthquake ground motion. The peak displacements of the yielding frames are slightly less than the elastic frames. However, the velocity and accelerations are significantly reduced for the yielding frames. Since the acceleration of yielding frames is limited by the yield strength of the frames, the acceleration response is reduced by approximately 50%. The relative displacements of the yielding frames is approximately 50% less than that of the elastic frames. This is due primarily to two factors. First, the effective stiffness of the frames is reduced in yielding frames, therefore making the restrainers more effective. Second, frame yielding promotes in-phase motion because of increased energy dissipation. High damping between frames reduces response between frames, providing more steady state response. The free vibration response is quickly damped out, and the resulting response is dominated by forced vibration due to the earthquake input motion. The comparisons between DRAIN3-DX and the current numerical procedure compare

much better for yielding frames than for elastic frames. Since the yielding frames are more in-phase, there is less impact. When impact does occur, the momentum transfer between the frames is reduced, since yielding frames generally have a smaller velocity and acceleration.

Figure 3.7 shows a comparison of the numerical procedure using bi-linear and Q-Hyst hysteretic models for the frames. In general, the maximum displacements are larger for the Q-Hyst hysteretic model than for the the bi-linear model. Figure 3.8 shows the force-displacement relationship corresponding to the response history in figure 3.7. For this case, the energy dissipated by the yielding frames, represented by the area under the force-deformation relation, is greater for the bi-linear model than for the Q-Hyst model, because of the pinching and degrading stiffness. Also because of the degrading stiffness, the peak frame displacements are larger than for the bilinear model. However, the inelastic model has little effect on the relative hinge displacement for this case.

Figure 3.9 shows the frame displacement responses for different values of the coefficient of restitution ($e = 0.6, 0.8, 1.0$). The value of e has little effect on the response of the frames, but a slightly greater effect on the relative displacement. A reduction in e can result in either an increase or decrease in the relative hinge displacement. Since e controls the rebound velocity, it also affects the phasing between the frames. Depending on how the phasing is affected, the hinge displacement with smaller e may either increase or decrease.

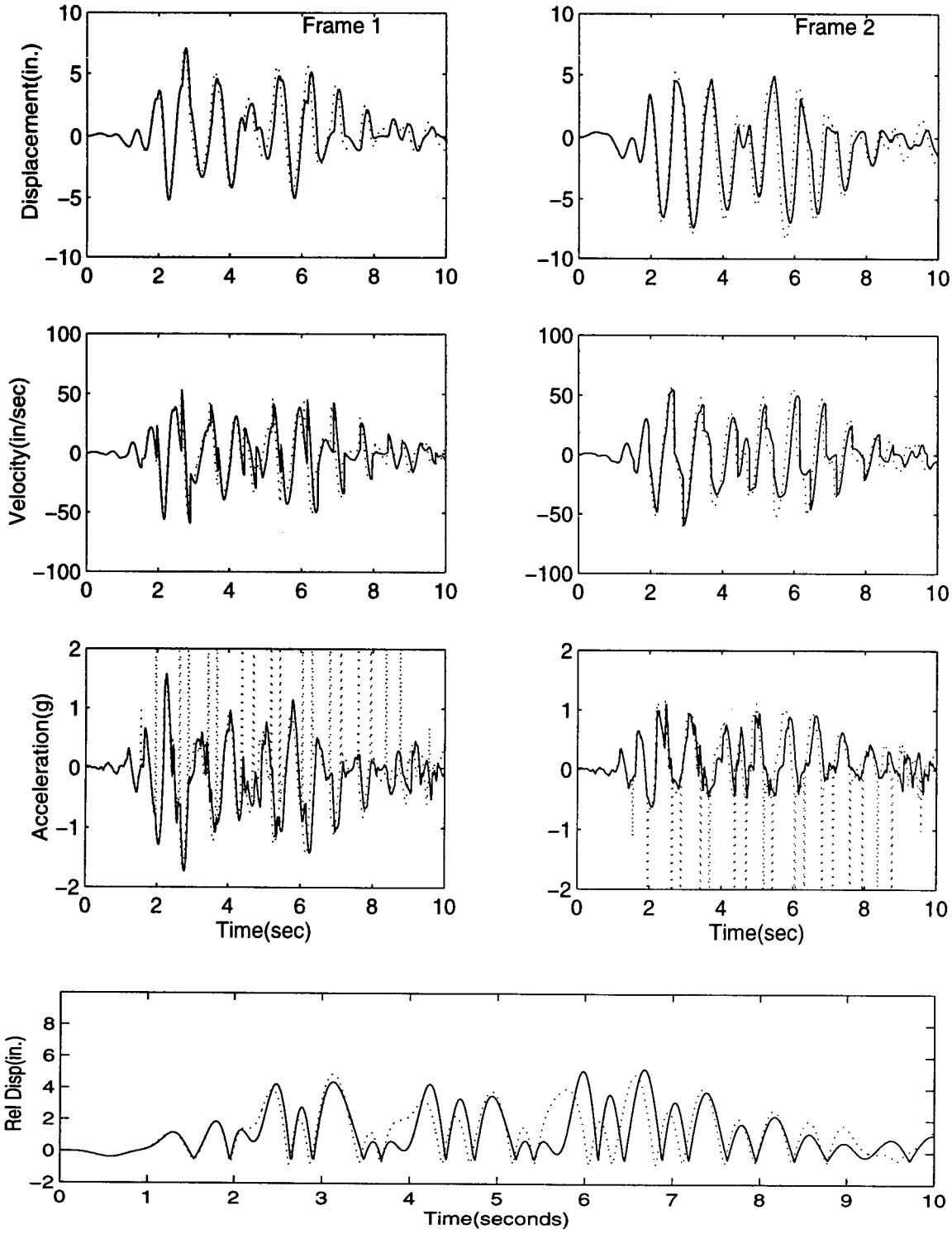

Figure 3.5: Comparison of Numerical Procedure with DRAIN3-DX for Elastic Frame Response to 1940 El Centro Earthquake (S00E Component), scaled to 0.70g (..... DRAIN3-DX), (—— Numerical Procedure).

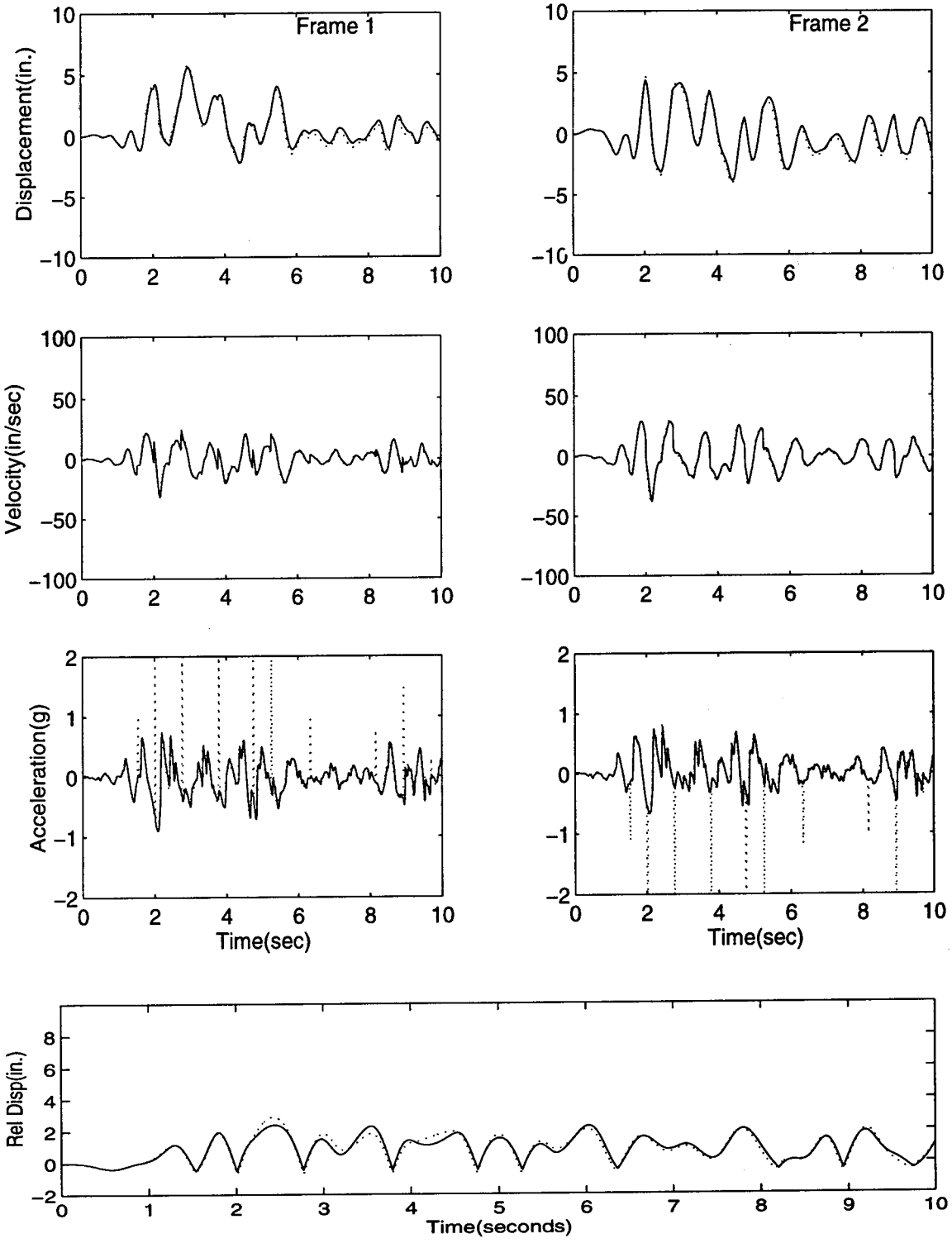

Figure 3.6: Comparison of Numerical Procedure with DRAIN3-DX for Inelastic Frame Response to 1940 El Centro Earthquake (S00E Component), Scaled to 0.70g with $\mu = 4$ (..... DRAIN3-DX) (—— Numerical Procedure).

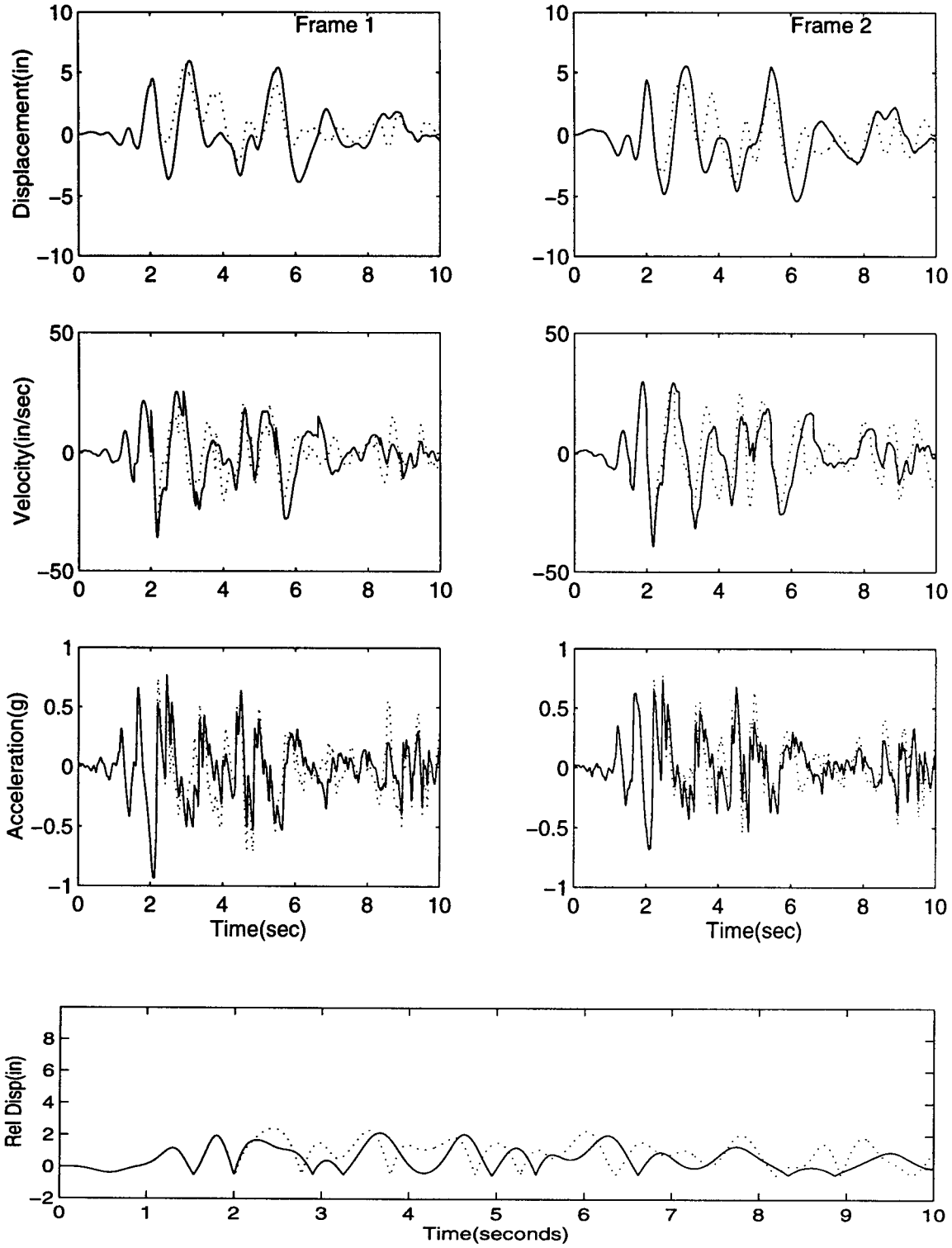

Figure 3.7: Comparison of Inelastic Frame Response to 1940 El Centro Earthquake, Scaled to 0.70g, for (Bi-Linear .....) and (Q-Hyst ———) Hysteresis Models.

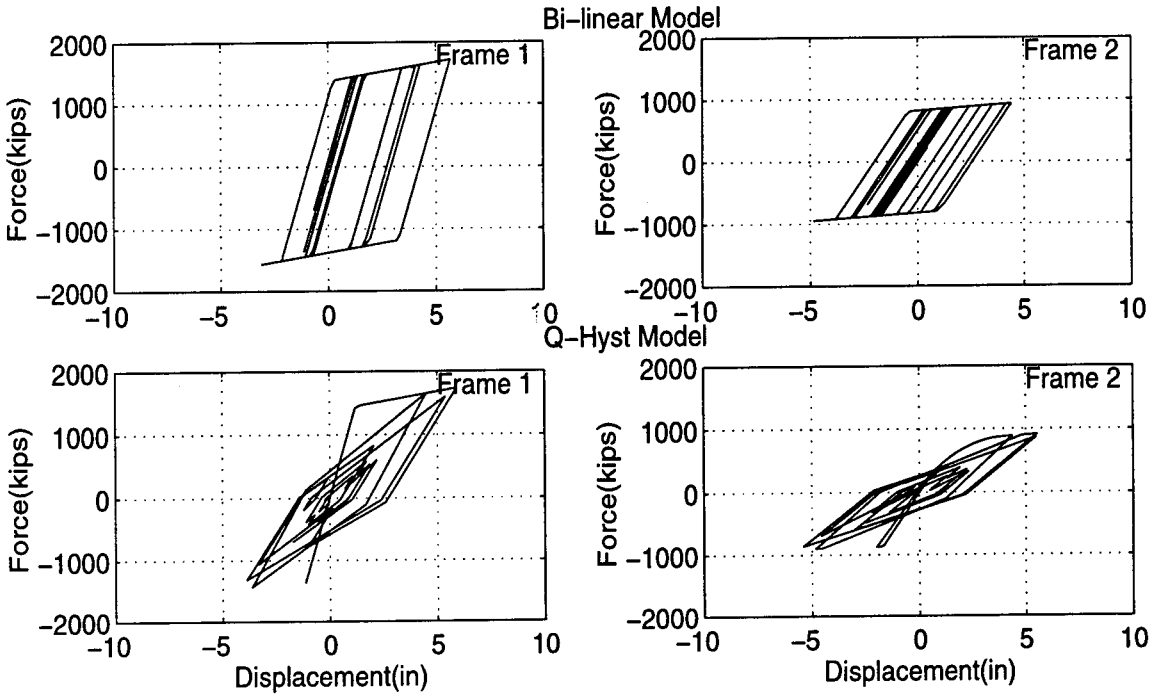

Figure 3.8: Force-Displacement Relationships for Frame Response to the 1940 El Centro Earthquake, Scaled to 0.70g, for Bi-Linear and Q-Hyst Hysteretic Models.

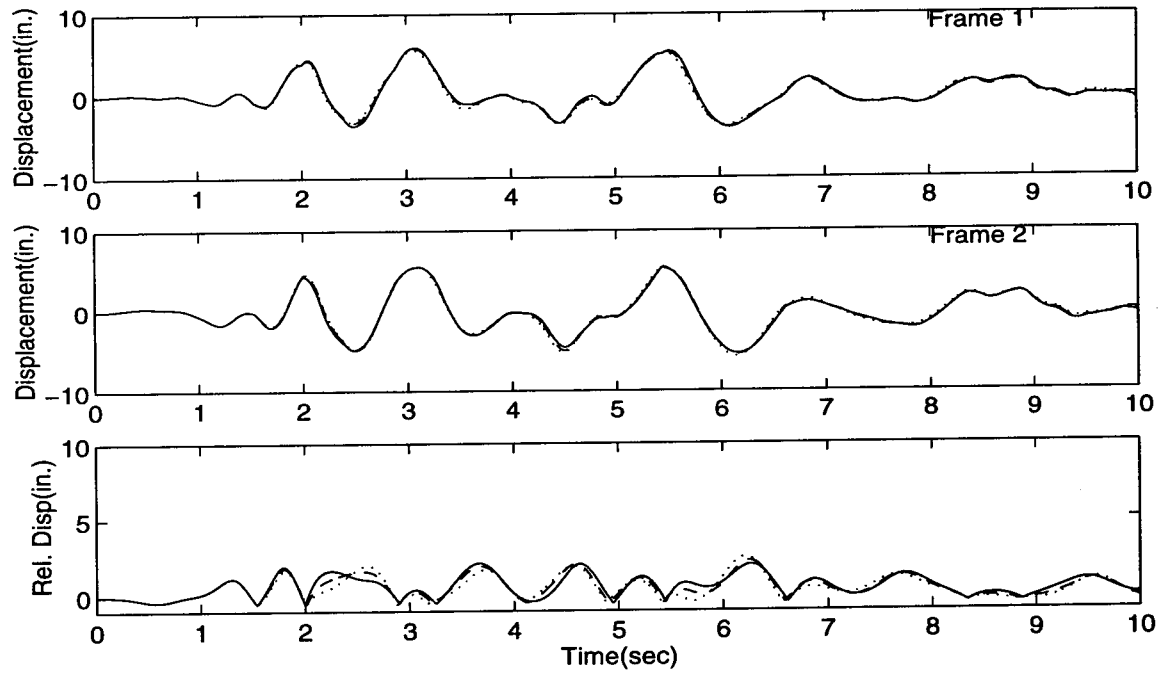

Figure 3.9: Frame Response to 1940 El Centro Earthquake, Scaled to 0.70g, for Different Values of the Coefficient of Restitution (—— $e = 1.0$), (- - - - - $e = 0.80$), (..... $e = 0.60$).

Chapter 4

Parameter Study of Factors Affecting Displacement of Intermediate Hinges

The goal of the parameter study presented in this chapter is to investigate the factors affecting the relative displacement of intermediate hinges. Recent studies have shown that the important factors affecting the hinge displacements are the frame stiffness ratio (K_1/K_2), restrainer stiffness ratio (K_r/K_2), mass ratio (m_1/m_2), earthquake loading, frame yield strength (R_y), restrainer slack (s), and compression gap (g_p) (Yang et al., 1994; Trochalakis et al., 1997). The equations of motion and responses are expressed in non-dimensionalized form in order to represent a wide range of cases.

4.1 Normalization of Equations of Motion

The equations of motion for the longitudinal response of two adjacent frames subjected to earthquake ground motion were given in equation 3.1.

For the 2-DOF system, equation 3.1 may be written as follows:

$$\begin{bmatrix} m_1 & 0 \\ 0 & m_2 \end{bmatrix} \begin{Bmatrix} \ddot{x}_1 \\ \ddot{x}_2 \end{Bmatrix} + \begin{bmatrix} c_1 & 0 \\ 0 & c_2 \end{bmatrix} \begin{Bmatrix} \dot{x}_1 \\ \dot{x}_2 \end{Bmatrix} + \begin{Bmatrix} R_1(x_1) \\ R_2(x_2) \end{Bmatrix}$$

$$+F_{fr}(x_2-x_1)\begin{Bmatrix}1\\-1\end{Bmatrix}=\begin{bmatrix}m_1&0\\0&m_2\end{bmatrix}\begin{Bmatrix}1\\1\end{Bmatrix}\ddot{u}_g(t) \tag{4.1}$$

Dividing the first and second equations by yield displacements of the frames, x_{y_1} and x_{y_2}, respectively, where $x_{y_i}=R_{y_i}/K_i$, gives

$$\begin{bmatrix}m_1&0\\0&m_2\end{bmatrix}\begin{Bmatrix}\ddot{\mu}_1\\\ddot{\mu}_2\end{Bmatrix}+\begin{bmatrix}c_1&0\\0&c_2\end{bmatrix}\begin{Bmatrix}\dot{\mu}_1\\\dot{\mu}_2\end{Bmatrix}+\begin{Bmatrix}\frac{R_1(x_1)}{x_{y_1}}\\\frac{R_2(x_2)}{x_{y_2}}\end{Bmatrix}+\begin{Bmatrix}\frac{F_{fr}(x_2-x_1)}{x_{y_1}}\\-\frac{F_{fr}(x_2-x_1)}{x_{y_2}}\end{Bmatrix}=\begin{Bmatrix}\frac{m_1}{x_{y_1}}\\\frac{m_2}{x_{y_2}}\end{Bmatrix}\ddot{u}_g(t) \tag{4.2}$$

where the quantity $\mu_i=\frac{x_i}{x_{y_i}}$ is the ductility factor for frame i. Equation 4.2 is divided by m_2, and the following terms are defined: mass ratio, $\alpha=\frac{m_1}{m_2}$; frequency ratio, $\beta=\frac{\omega_2}{\omega_1}$; normalized force-deformation relationship, $\tilde{R}_i(\mu)=\frac{R_i(x_i)}{R_{y_i}}$; frame strength ratio, $\eta_i=\frac{R_{y_i}}{m_i\ddot{u}_{gmax}}$; and normalized free-field ground acceleration, $\tilde{\ddot{u}}_g(t)=\frac{\ddot{u}_g(t)}{\ddot{u}_{gmax}}$. Applying the standard definitions, $\omega_i=\sqrt{K_i/m_i}$, and $c_i=2\xi m_i\omega_i$ with $\xi=0.05$ for all cases, equation 4.2 becomes:

$$\begin{bmatrix}\alpha&0\\0&1\end{bmatrix}\begin{Bmatrix}\ddot{\mu}_1\\\ddot{\mu}_2\end{Bmatrix}+\begin{bmatrix}2\frac{\alpha\xi_1\omega_2}{\beta}&0\\0&2\xi_2\omega_2\end{bmatrix}\begin{Bmatrix}\dot{\mu}_1\\\dot{\mu}_2\end{Bmatrix}+\begin{Bmatrix}\frac{\tilde{R}_1(\mu_1)\omega_2^2\alpha}{\beta^2}\\\tilde{R}_2(\mu_2)\omega_2^2\end{Bmatrix}+\begin{Bmatrix}\frac{1}{m_2}\frac{F_{fr}(x_2-x_1)}{x_{y_1}}\\-\frac{1}{m_2}\frac{F_{fr}(x_2-x_1)}{x_{y_2}}\end{Bmatrix}=\begin{Bmatrix}\frac{\alpha\omega_1^2}{\eta_1}\\\frac{\omega_2^2}{\eta_2}\end{Bmatrix}\tilde{\ddot{u}}_g(t) \tag{4.3}$$

At this point, it is beneficial to restate the term for the normalized force for the restrainers and friction in equation 4.3:

$$\begin{Bmatrix}\frac{1}{m_2}\frac{F_{fr}(x_2-x_1)}{x_{y_1}}\\\frac{1}{m_2}\frac{F_{fr}(x_2-x_1)}{x_{y_2}}\end{Bmatrix} \tag{4.4}$$

The force has two components,

$$F_{fr}(x_2-x_1)=F_f(x_2-x_1)+F_r(x_2-x_1) \tag{4.5}$$

where $F_f(x_2-x_1)$ is the resisting force from friction and $F_r(x_2-x_1)$ is the resisting force from the restrainers. To simplify the non-dimensionalization, the restrainers are

assumed to be nonlinear elastic (i.e., non-yielding). This simplification is justified because design procedures require restrainers to remain elastic. The restrainers are only effective in tension, and once the restrainers engage the restrainer force may be expressed as:

$$F_r(x_2 - x_1) = K_r[(x_2 - x_1) - s] \tag{4.6}$$

Substituting equation 4.6 into equation 4.4 and isolating the restrainer force in the normalization, the normalized restrainer force, $F_{r_{norm}}$, is

$$F_{r_{norm}} = \frac{K_r}{m_2 x_{y1}}[(x_2 - x_1) - s] \tag{4.7}$$

which may be expressed as:

$$F_{r_{norm}} = \frac{K_r}{K_2}{\omega_2}^2 \left[(\frac{\mu_2}{\beta\tilde{\eta}} - \mu_1) - \frac{s}{x_{y1}}\right] \tag{4.8}$$

where $\tilde{\eta} = \frac{\eta_1}{\eta_2}$ is the ratio of frame strength ratios. Equation 4.8 shows that the restrainer stiffness should be normalized by the stiffness of frame 2, K_2. However, it is recognized that both frame stiffnesses should be included in the normalization. Therefore, the numerator and denominator of equation 4.8 are multiplied by the sum of the flexibilities of the two frames, $\frac{1}{K_{mod}} = (\frac{1}{K_1} + \frac{1}{K_2})$. Equation 4.8 becomes

$$F_{r_{norm}} = \omega_2^2 \kappa (\frac{1}{1 + \frac{1}{\beta^2 \alpha}}) \left[(\frac{\mu_2}{\beta\tilde{\eta}} - \mu_1) - \frac{s}{x_{y1}}\right] \tag{4.9}$$

where $\kappa = \frac{K_r}{K_{mod}}$.

The friction force, $F_f(x_2 - x_1)$, can be expressed as:

$$F_f(x_2 - x_1) = \mu V_H \tag{4.10}$$

The friction force is a product of the coefficient of friction, μ, and the shear force at the hinge, V_H.

The factor, $\tilde{R}_i(x_i)$, is the normalized force-displacement relationship for the frames. In this study, $\tilde{R}_i(x_i)$ is based on a Q-Hyst stiffness degrading relationship. The parameters which define the Q-Hyst force-deformation relationship are the initial stiffness (K); the yield force (R_y), the strain hardening ratio (α_s), the unloading stiffness (K_q), and the load reversal stiffness (K_p).

A goal of the collapse-prevention limit state design is to ensure that the design displacement ductility for a given ground motion is less than the corresponding capacity. Therefore, there is a need to determine the lateral strength of the structure that is required in order to limit the structure displacement ductility demand to a pre-determined value. Studies have established relationships between SDOF lateral strengths and ductility demands (Miranda and Bertero, 1994). In this study, frame lateral strengths are selected to provide prescribed ductility demands for individual frames for the response to specific earthquakes.

The results of the non-dimensionalization show that the restrainer slack (s) and gap (g_p) are normalized by the frame yield displacement. However, it is recognized that the values for the restrainer slack and gap are a function of the ambient temperature. As the temperature increases and the gap decreases, the slack increases. As the temperature decreases and the gap increases, the slack decreases. However, the total value of the $g_p + s = 1$ in. (25.4 mm) remains constant in this study. The corresponding slack and gap for the various ambient temperatures are: high ($s = 1$ in. (25.4 mm), $g_p = 0$), moderate ($s = 0.5$ in. (12.7 mm), $g_p = 0.5$ in. (12.7 mm)), and low ($s = 0$, $g_p = 1$ in. (25.4 mm)).

The coefficient of restitution for pounding, e, affects the response at the hinge by modifying the rebound velocity after impact. Three values for the coefficient of restitution are investigated: e=0.60, 0.80, and 1.00.

The frequency of frame 2, ω_2, is the only parameter which is not normalized. To relate ω_2 (or T_2) to a characteristic period of the ground motion, T_2 is normalized by the predominate period of the free-field ground motion. The predominate period, T_g, is the period of the peak of the pseudo-velocity response spectrum (5% damping). The T_2/T_g ratio locates the relative position of frame 2 on the response spectrum. Based on the above normalizations, values of the parameters affecting the hinge opening displacement of the 2-DOF model are listed in Table 4.1.

The response results are plotted as a function of the frame period ratio (T_1/T_2) for four target ductilities for individual frames (μ=1,2,4,6). The 2-DOF system is subjected to synchronous free-field ground motion, with assumed 5 % viscous damping.

4.2 Earthquake Ground Motion

A database of 26 processed strong ground motion acceleration records from earthquakes of magnitude 6.0 or greater are used for the parameter study, as listed in table 4.2. The input records are selected to represent a wide range of characteristic periods (T_g), peak ground accelerations (PGA), peak ground velocities (PGV), epicentral distances (EPD), and durations (D). These factors have been shown to be important in the response of structures (Naeim et al., 1994).

4.2.1 Orientation of Ground Motion

It is desirable to transform the two components of horizontal ground motion to their principle axes (Kubo and Penzien, 1979). At sites with a large epicentral distance, the principle axes correspond with the direction to the epicenter. The principal directions are obtained from the covariance matrix for the horizontal ground acceleration components:

$$\tilde{\mu} = \frac{1}{N} \sum_{i=1}^{i=N} \hat{\mathbf{a}}_i^T \hat{\mathbf{a}}_i \tag{4.11}$$

where the vector $\hat{\mathbf{a}}$ contains the acceleration values for the two horizontal components at time step i. The eigenvectors of the 2x2 covariance matrix, $\tilde{\mu}$, are the direction cosines for the principal directions, and the eigenvalues are the mean square amplitudes of the ground acceleration in the principle directions. The ground motion in table 4.2 gives the motion along the major principal axis.

4.2.2 Ground Motion Characteristics

The ground motions selected for the study are listed in table 4.2, in order of decreasing predominate period of the ground motion (T_g). The predominate period of the ground motion is defined as the period at which the input energy of a 5% damped linear elastic system is maximum (Miranda and Bertero, 1994). Since the maximum pseudo-velocity is related to the maximum kinetic energy, the predominate period of the ground motion is estimated by the peak of the maximum pseudo-velocity response spectrum (Uang and Bertero, 1990).

Table 4.1: Parameters and Range of Values for Study

Parameter	Values
$\frac{\omega_2}{\omega_1} = \frac{T_1}{T_2}$: Frame Period Ratio	0.3, 0.4, 0.5, 0.6, 0.7, 0.8, 0.9, 1.0
$\frac{T_2}{T_g}$: Ground Motion Period Ratio	0.5, 1.0, 2.0, 4.0
$\frac{K_r}{K_{mod}}$: Restrainer Stiffness Ratio	0.0, 0.50, 1.0, 2.0
μ_i : Target Ductility Factor (Individual Frame)	1, 2, 4, 6
$\frac{m_1}{m_2}$: Frame Mass Ratio	0.5, 1, 2, 4
s : Restrainer Slack, in. (mm)	0.0, 0.5 (12.7), 1.0 (25.4)
g_p : Contact Gap, in. (mm)	0.0, 0.5 (12.7), 1.0 (25.4)
F_f: Friction Force, kips (kN)	0.0, 100 (445), 200 (890)
e: Coefficient of Restitution	0.60, 0.80, 1.0

Table 4.2 also lists the peak ground accelerations, velocities, and displacements for the records along the major axis. The largest peak ground acceleration is in the 1971 San Fernando earthquake, Pacoima Dam record. The largest velocities and displacements are found in the 1994 Northridge earthquake (Pacoima Dam - Kagel Canyon). Several near source records used in the study are: 1987 Whittier (Alhambra), 1994 Northridge (Sylmar), 1995 Kobe (Kobe), 1971 San Fernando (Pacoima Dam), 1994 Northridge (Arleta), 1979 El Centro (Bonds Corner), 1992 Cape Mendecino (Petrolia), 1989 Loma Prieta (Corralitos), and 1994 Northridge (Tarzana). For this study, the peak ground acceleration for all records is normalized to 0.70g. This coincides with typical design response spectra, which are scaled to 0.70g. This may be unrealistic for ground motions with very small peak ground accelerations, however, for consistency, all ground motions are scaled to the same value.

The response spectra for the records used are compared with the Caltrans ARS design spectra (Caltrans, 1990). The Caltrans spectra are divided into several soil types: 7D (soil depth > 150' (45.8 m) alluvium), 7C (soil depth = 80-150' (24.4-

Table 4.2: Free-Field Ground Motions in Major Principal Axis Listed in Order of Decreasing Characteristic Period, T_g.

No.	Earthquake Record	Location	Mag M_s	EPD[a] km	PGA[b] g	PGV[c] in/s (mm/s)	PGD[d] in (mm)	T_g (sec)
1	1992 Cape Mend.	Fortuna	6.9	28	0.12	11.4 (290)	0.78 (20)	2.30
2	1992 Landers	Amboy	7.5	74	0.15	7.8 (198)	1.18 (30)	2.29
3	1989 Loma Prieta	Saratoga	7.1	28	0.47	16.2 (410)	6.3 (160)	1.79
4	1987 Whittier	Alhambra	6.1	7	0.25	7.9 (200)	0.9 (22.0)	1.84
5	1992 Landers	Baker Fire	7.5	122	0.11	9.0 (229)	2.3 (59)	1.70
6	1994 Northridge	Sylmar	6.7	15	0.90	47 (1200)	12 (300)	1.60
7	1995 Kobe	Osaka	6.9	17	0.08	7.8 (198)	1.37 (35)	1.17
8	1995 Kobe	Fukushima	6.9	17	0.04	4.3 (109)	1.18 (30)	1.15
9	1971 San Fernando	Pacoima Dam	7.4	8	1.36	135 (3429)	16.9 (430)	1.13
10	1940 Imperial Val.	El Centro	6.9	12	0.35	33 (838)	10.9 (276)	1.00
11	1994 Northridge	Arleta	6.8	10	0.32	15.7 (400)	3.5 (89)	0.97
12	1995 Kobe	Kobe	6.9	5	0.85	37.0 (906)	10 (254)	0.87
13	1994 Northridge	Pico	6.8	31	0.19	55 (1400)	9.1 (230)	0.83
14	1994 Northridge	Pac. Dam (KC)	6.8	18	0.52	142 (3600)	19 (480)	0.83
15	1984 Morgan Hill	Coyote Dam	6.2	24	1.12	31.1 (791)	4.13 (105)	0.79
16	1992 Cape Mend.	Petrolia	6.9	5	0.70	37.1 (940)	12.8 (324)	0.70
17	1979 El Centro	Bonds Corner	6.6	28	0.78	18.5 (471)	6.6 (168)	0.62
18	1989 Loma Prieta	Corralitos	7.1	8	0.65	22.1 (561)	3.7 (95)	0.43
19	1980 Mammoth Lk.	HS Gym	6.5	11	0.34	6.3 (160)	1.0 (25.4)	0.43
20	1994 Northridge	LA Obrego Pk	6.7	39	0.45	12.2 (310)	1.0 (25.4)	0.39
21	1994 Northridge	Downey Co.	6.7	47	0.25	5.0 (127)	0.75 (19)	0.38
22	1994 Northridge	Tarzana	6.7	5	0.65	12.0 (305)	4.2 (107)	0.33
23	1994 Northridge	Inglewood	6.7	42	0.26	9.0 (229)	2.2 (55.9)	0.30
24	1994 Northridge	Pac. Dam (DS)	6.7	17	0.50	10.2 (258)	1.7 (43)	0.27
25	1994 Northridge	Mt. Wilson	6.7	45	0.26	3.0 (75)	0.23 (6)	0.24
26	1994 Northridge	Lake Hughes	6.7	44	0.27	4.6 (117)	2.2 (55)	0.21

[a]Epicentral Distance

[b]Peak Ground Acceleration

[c]Peak Ground Velocity

[d]Peak Ground Displacement

45.8 m) alluvium), and 7A (soil depth < 10' (3.05 m) alluvium). In figure 4.1, the records are categorized into three groups: soft soils ($T_g > 1.2$ sec), medium soils ($T_g = 0.6 - 1.2$ sec), and firm soils ($T_g < 0.5$ sec). For soft soils, the mean plus one standard deviation response spectral ordinates of the records is much higher than the Caltrans ARS design spectral for shorter periods; however, for longer periods the two show good agreement. For the medium sites ($T_g = 0.6 - 1.2$ sec) the mean plus one standard deviation of the records closely matches with the ARS spectrum for the entire period range. For firm soils, the mean plus one standard deviation response spectral ordinates is slightly larger than the ARS spectrum for the shorter periods and slightly smaller for longer periods.

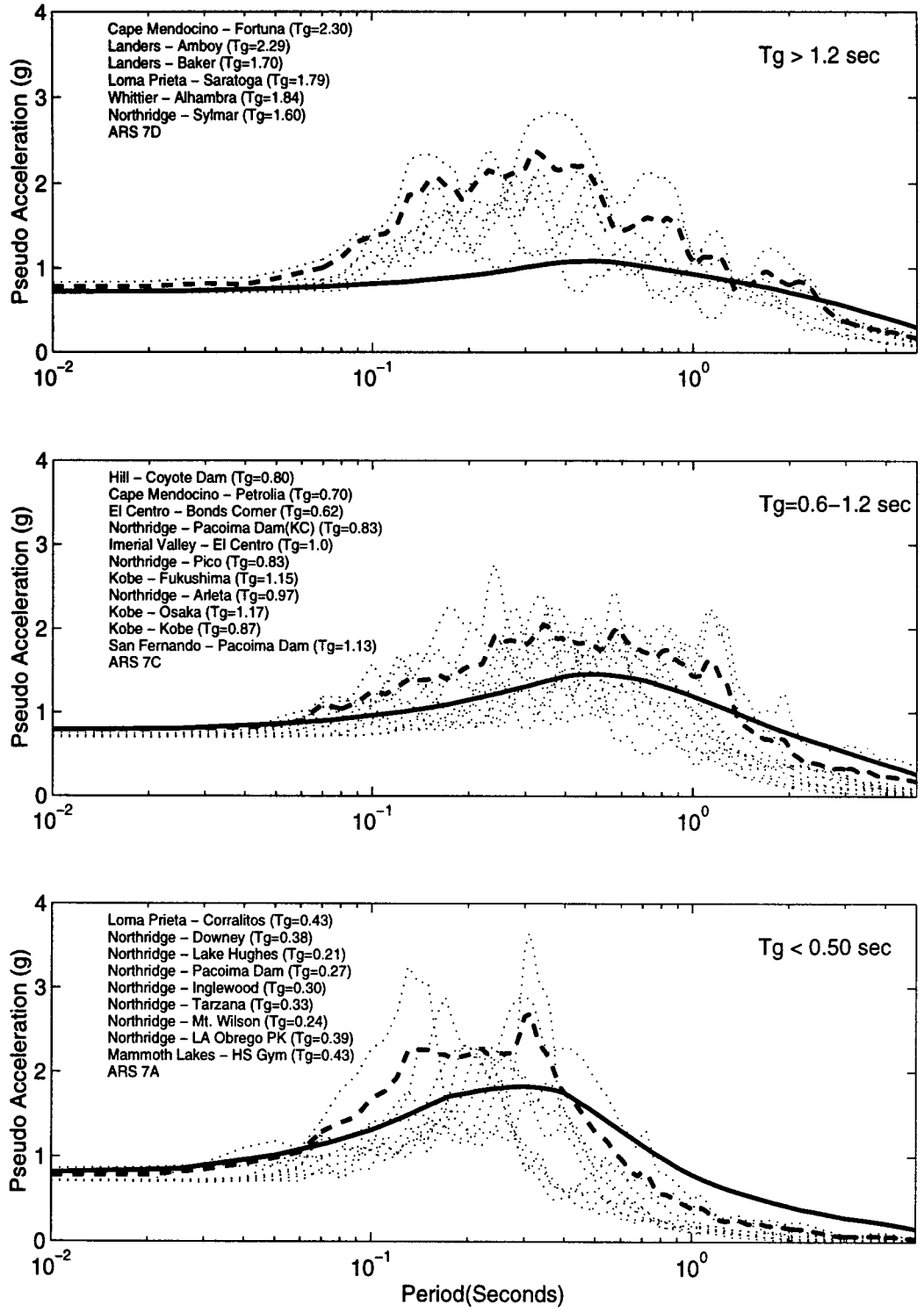

Figure 4.1: Mean Plus One Standard Deviation (- - -) of the Pseudo-Acceleration Spectra (5% Damping) for 26 Ground Motions Compared With Caltrans ARS Spectra (——).

4.3 Parameter Study for Hinge Displacement

A parameter study is conducted to study the effect of the parameters identified in section 4.1 on the relative displacement of the hinge. The parameters studied are the restrainer stiffness ratio ($\kappa = \frac{K_r}{K_{mod}}$), ground motion period ratio ($\frac{T_2}{T_g}$), restrainer slack and hinge gap (s, g_p), friction force (F_f), coefficient of restitution (e), and mass ratio ($\frac{m_1}{m_2}$). Unless otherwise specified, the following values are held constant in the parameter study: $m_1/m_2 = 1.0$, $K_r/K_{mod} = 0.50$, $T_2/T_g = 1.0$, $F_f = 100$ kips (445 kN), and $e = 0.80$. For each parameter, the study is performed for a range of period ratios (T_1/T_2) and target ductility for individual frames (μ). The response is computed for each of the 26 free-field ground motion records, and the mean and mean plus one standard deviation are presented.

4.3.1 Effect of Restrainer Stiffness

The effect of the restrainer stiffness on the hinge displacement is examined by varying the restrainer stiffness ratio, $\kappa = K_r/K_{mod} = (0, 0.5, 1.0, 2.0)$, for a range of frame period ratios and individual frame target ductility ratios. Typical bridges with restrainers have a stiffness ratio in the range of 0.25-0.75. The response is presented for $T_2/T_g = 1.0$. The relative hinge displacement, D_{eq}, is normalized by dividing by the relative hinge displacement for the case without restrainers.

Figure 4.2 shows the results of the parameter study using the 1940 El Centro earthquake (S00E component). The results show that increasing the restrainer stiffness generally decreases the hinge displacement, although there are a few cases where the opposite occurs. For example, for $T_1/T_2 = 0.30$ and $\mu = 1$, the displacement ratio for $\kappa = 1$ is greater than the displacement ratio for $\kappa = 0.50$. This is most likely due to the excitation of a restrained mode, which produces larger hinge responses. Also, the addition of restrainers can promote more impact between frames, which can also increase the relative hinge displacement. The hinge displacement ratio is fairly constant as a function of the period ratio. However, there is considerable variation as a function of the design ductility. As the target ductility increases, the displacement ratio decreases. For example, for $\kappa = 1$ and $T_1/T_2 = 0.70$, the displacement ratio

decreases from 0.75 to 0.25 as μ increases from 1 to 4. Similar reductions are found for other normalized restrainer stiffness and period ratios. As the frame ductility increases, the effective stiffness of the frames decreases, which means the restrainers are more effective.

Figure 4.3 shows the hinge displacement ratio for the 1994 Sylmar Northridge earthquake (Sylmar Hospital free-field record). The results show similar trends for the 1940 El Centro record.

The response of the 2-DOF system was computed for all of the ground motions in table 4.2, and the mean and mean plus one standard deviations of the hinge displacement ratio are shown in figures 4.4 and 4.5. The results from the mean of the input records show similar results to the two previous cases. The effect of the restrainers is fairly uniform as a function of the frame period ratio. As the frame target ductility increases, the hinge displacement decreases. Frames in the entire period ratio range have a hinge displacement ratio of approximately 0.80 for $\kappa = 0.50$ and $\mu = 1$. However, for $\mu = 6$, a value of $\kappa = 0.50$ corresponds to a displacement ratio of approximately 0.50. Similar reductions are found for other values of κ. The study illustrates that restrainers are very effective in limiting the relative hinge displacement of frames in multiple-frame bridges. The effectiveness of restrainers increases for increasing target ductility of frames. A comparison of figures 4.4 and 4.5 shows that there is little variability for the different earthquake records. The standard deviation for the displacement ratio for the 26 earthquake records is approximately 0.05-0.10 for most cases.

Figure 4.5 can also be used as a design tool. Given the relative periods of the frames, relative stiffnesses of the frames, and a design ductility, the approximate required restrainer stiffness to reduce the initial hinge opening to a prescribed value can be obtained.

4.3.2 Effect of Characteristic Period of the Free-Field Ground Motion, T_g

The effect of the characteristic period of the free-field ground motion is examined by plotting the effects of the restrainer stiffness ratio, $\kappa = K_r/K_{mod}$, on the hinge

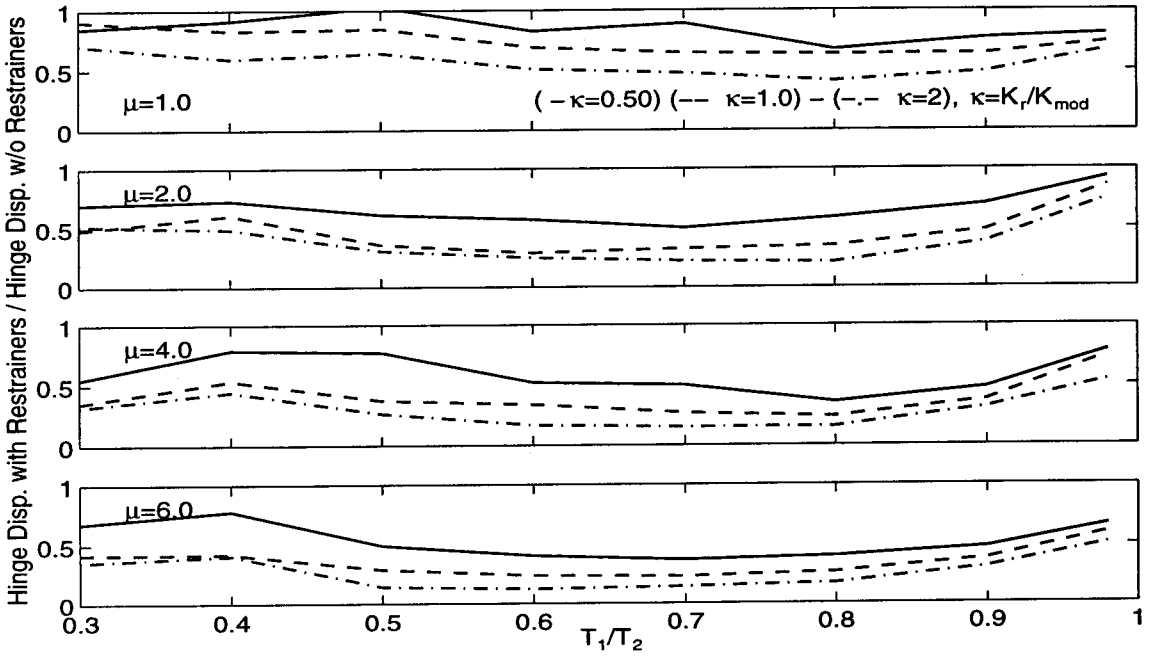

Figure 4.2: Effect of Restrainer Stiffness Ratio on Hinge Displacement Ratio for 1940 El Centro Earthquake (S00E Component), $T_2/T_g = 1.0$.

displacement ratio for T_2/T_g =0.5, 2.0, and 4.0. The results are presented in the same form as the previous section. The results for an input period ratio of 0.50 are very similar to the case with an input period ratio of 1.0, as shown in figure 4.6. This is because, for both cases, T_2 share similar locations near the peak of the pseudo acceleration response spectrum. However, for a larger input period ratio of 2.0, the effectiveness of the restrainers reduces slightly. For T_2/T_g values of 2 and 4, there is approximately a 10% increase in the hinge displacement compared with the cases with T_2/T_g values of 0.50 and 1, as illustrated in figures 4.7 and 4.8. T_2/T_g=2.0 and 4.0 represents cases where the frame periods are to the right of the peak of the acceleration spectrum. As restrainers are added, the modal periods decrease, shifting the response to a location with larger pseudo-acceleration response. This results in a slight decrease in the effectiveness of the restrainers, as evinced in the plot of the hinge displacement ratio.

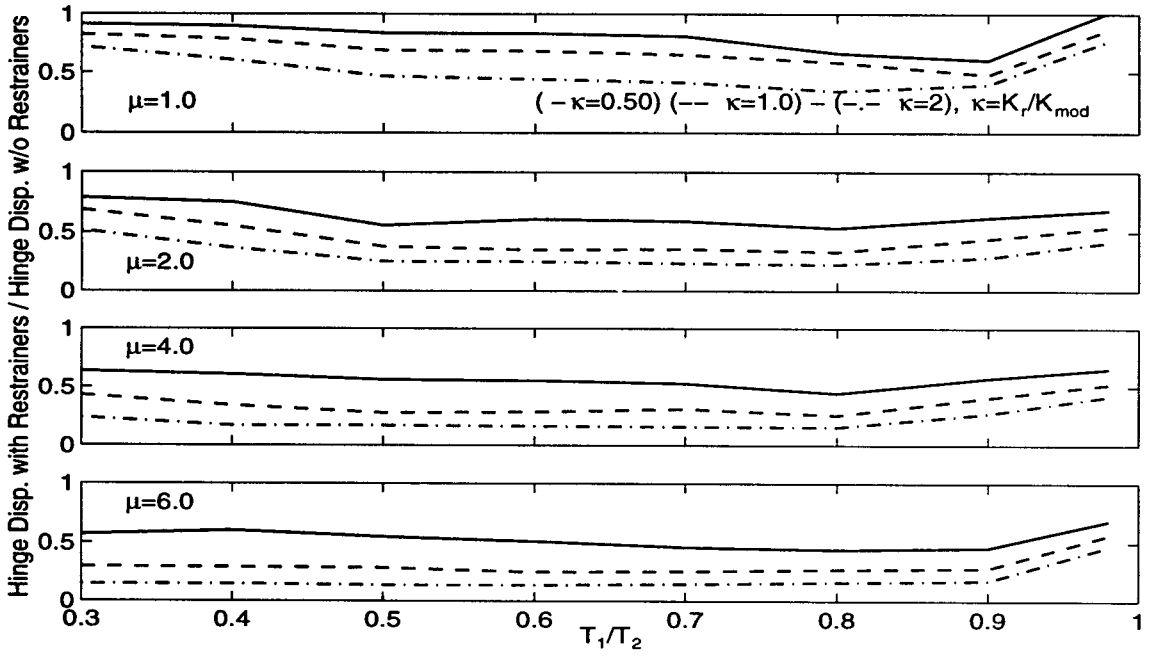

Figure 4.3: Effect of Restrainer Stiffness Ratio on Hinge Displacement Ratio for 1994 Northridge Earthquake (Sylmar Hospital Free-Field Record), $T_2/T_g = 1.0$.

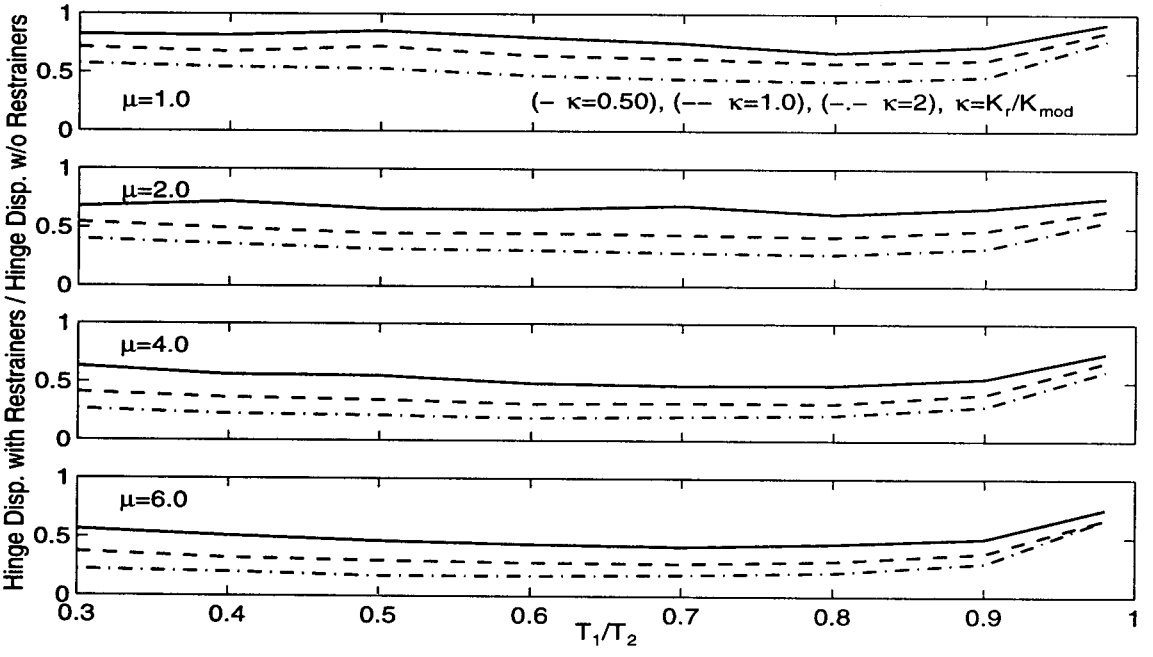

Figure 4.4: Effect of Restrainer Stiffness Ratio on Normalized Hinge Displacement for $T_2/T_g = 1.0$: Mean for 26 Earthquake Records.

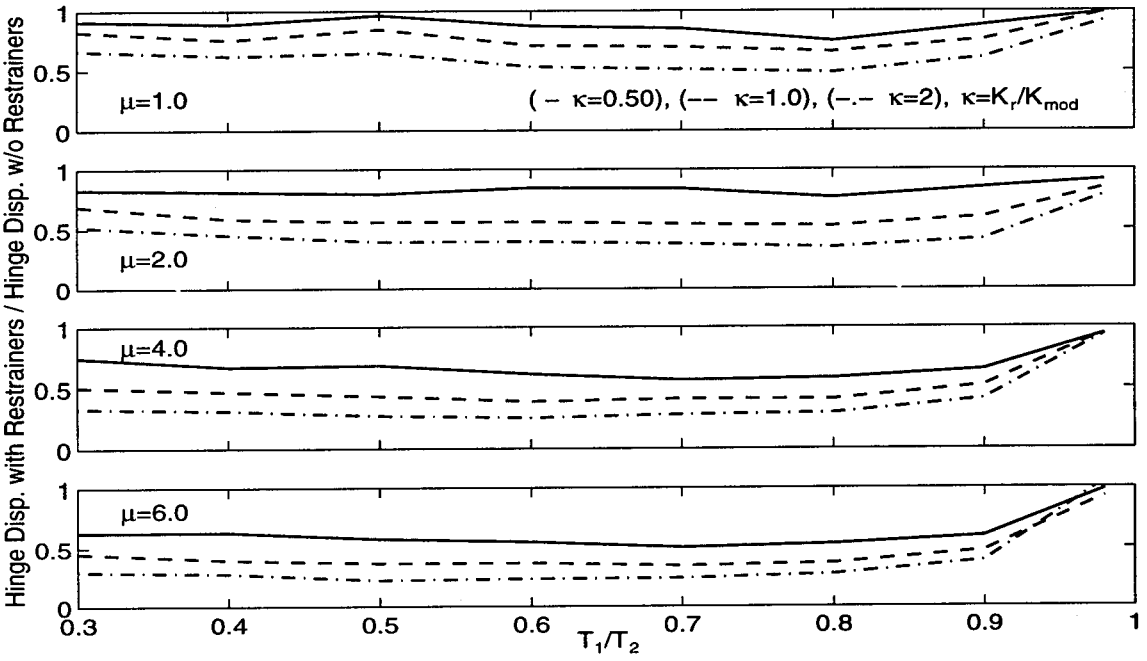

Figure 4.5: Effect of Restrainer Stiffness Ratio on Hinge Displacement Ratio for $T_2/T_g = 1.0$: Mean Plus One Standard Deviation for 26 Earthquake Records.

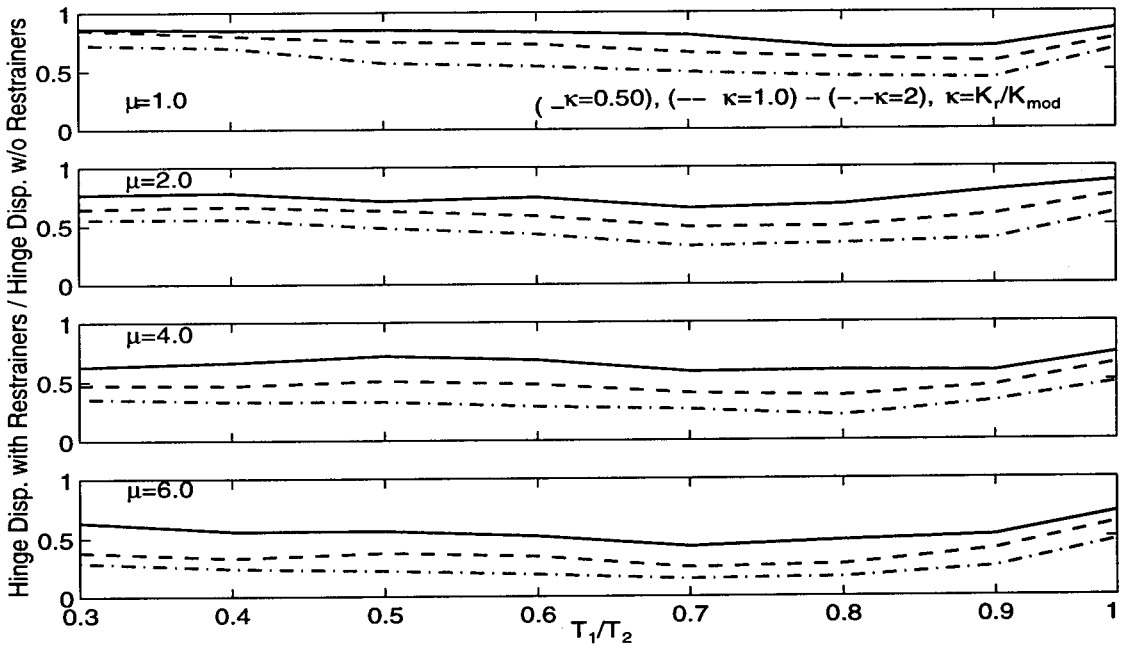

Figure 4.6: Effect of Restrainer Stiffness Ratio on Hinge Displacement Ratio for $T_2/T_g = 0.5$: Mean for 26 Earthquake Records.

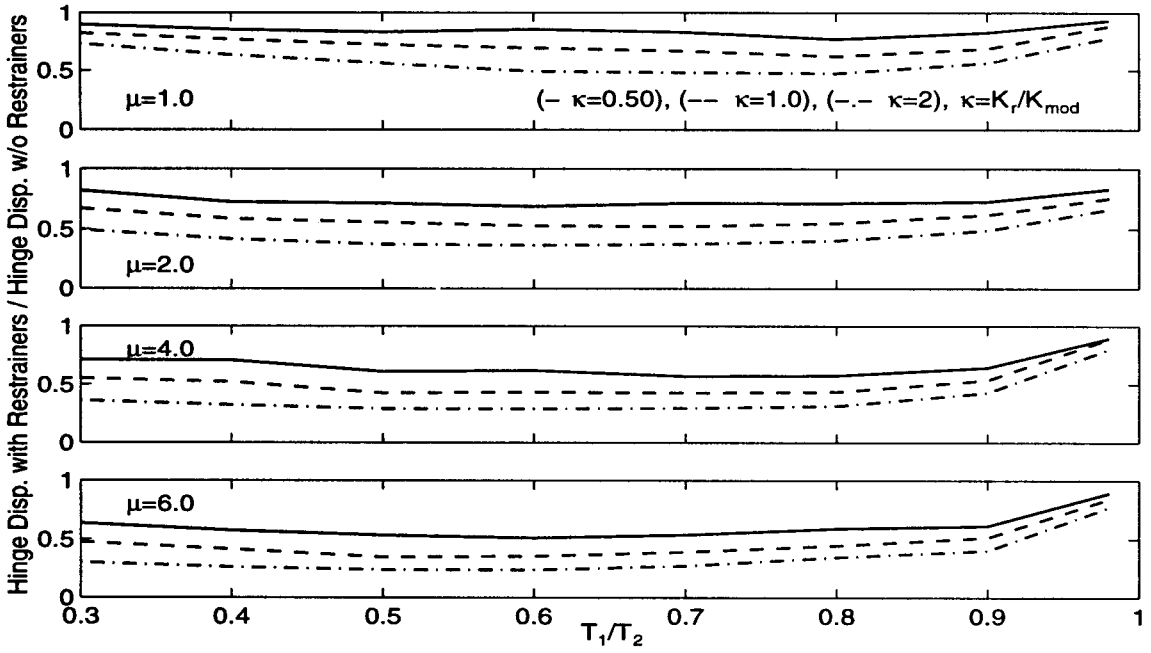

Figure 4.7: Effect of Restrainer Stiffness Ratio on Hinge Displacement Ratio for $T_2/T_g = 2.0$: Mean for 26 Earthquake Records.

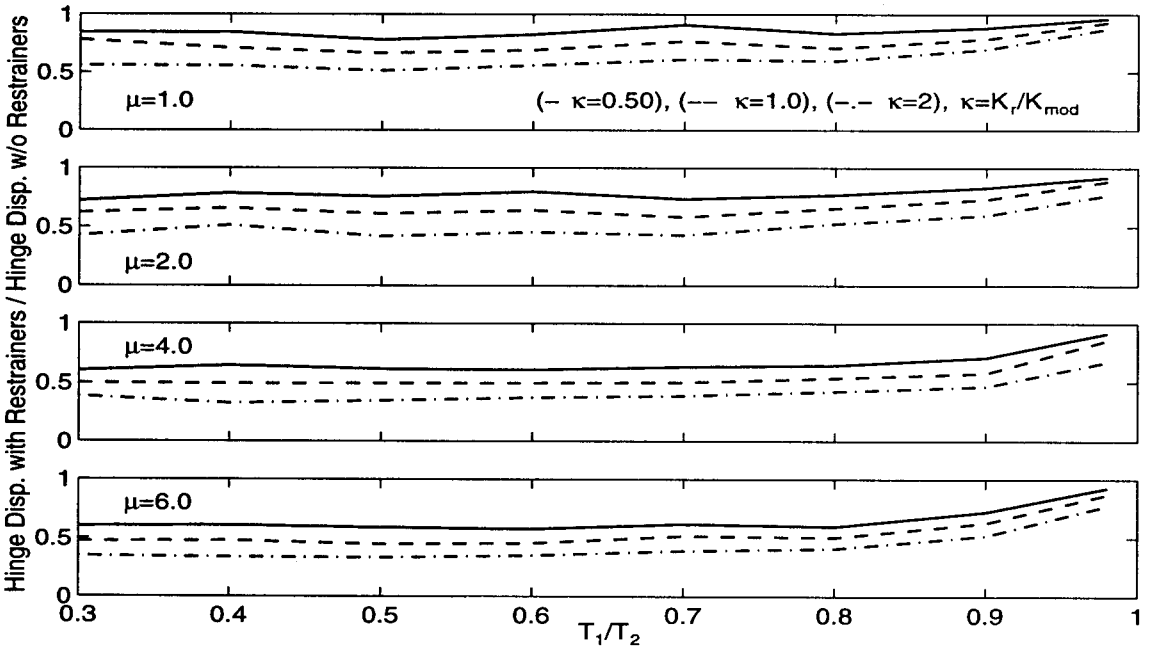

Figure 4.8: Effect of Restrainer Stiffness Ratio on Hinge Displacement Ratio for $T_2/T_g = 4.0$: Mean for 26 Earthquake Records.

4.3.3 Effect of Hinge Gap and Restrainer Slack

The effect of hinge gap and restrainer slack is evaluated by determining the relative hinge displacement for different combinations of slack (s) and gap (g_p) corresponding to high and low ambient temperatures. The following values are used in the parameter study: $m_1/m_2 = 1.0$, $K_r/K_{mod} = 0.50$, $T_2/T_g = 1.0$, $F_f = 100$ kips (445 kN), and $e = 0.80$. During high temperatures, the compression gap decreases and the restrainer slack increases, which is represented by $s = 1$ in. (25.4 mm) and $g_p = 0$. During extreme low temperatures, the compression gap increases and the restrainer slack decreases, which is represented by $s = 0$ and $g_p = 1$ in. (25.4 mm). The hinge displacement is normalized by the hinge displacement for the moderate temperature case ($s = 0.50$ in. (12.7 mm) and $g_p = 0.50$ in. (12.7 mm)). Figure 4.9 shows the results for the 1940 El Centro earthquake (S00E component). In general, the high ambient temperature case produces larger hinge displacements compared with the low temperature case. Several period ratios show a 50% increase in the hinge displacement for the high temperature case compared with the low temperature case. The relative hinge displacement increases because the restrainers are not effective until a hinge displacement of 1.0 in. is surpassed. However, for period ratios near unity, the gap has a significant influence on the response. A decrease in gap results in a decrease in the relative hinge displacement. The results for hinge gap and slack are insensitive to design ductility level.

The evaluation of the hinge gap and slack is shown for the ground motions in table 4.2. The mean of the hinge displacement ratio is shown in figure 4.10. In general, high ambient temperatures increase the hinge displacement by approximately 10-15% compared with moderate ambient temperatures. Similarly low ambient temperatures generally decrease the hinge displacement by approximately 5-10%, except for frames with period ratios near unity. However, individual cases can show differences up to 50%

4.3.4 Effect of Friction Force

The effect of friction in the hinge is examined by varying the friction force from $F_f = 0.0$ (no friction), to $F_f = 200$ kips (890 kN). The results are normalized by

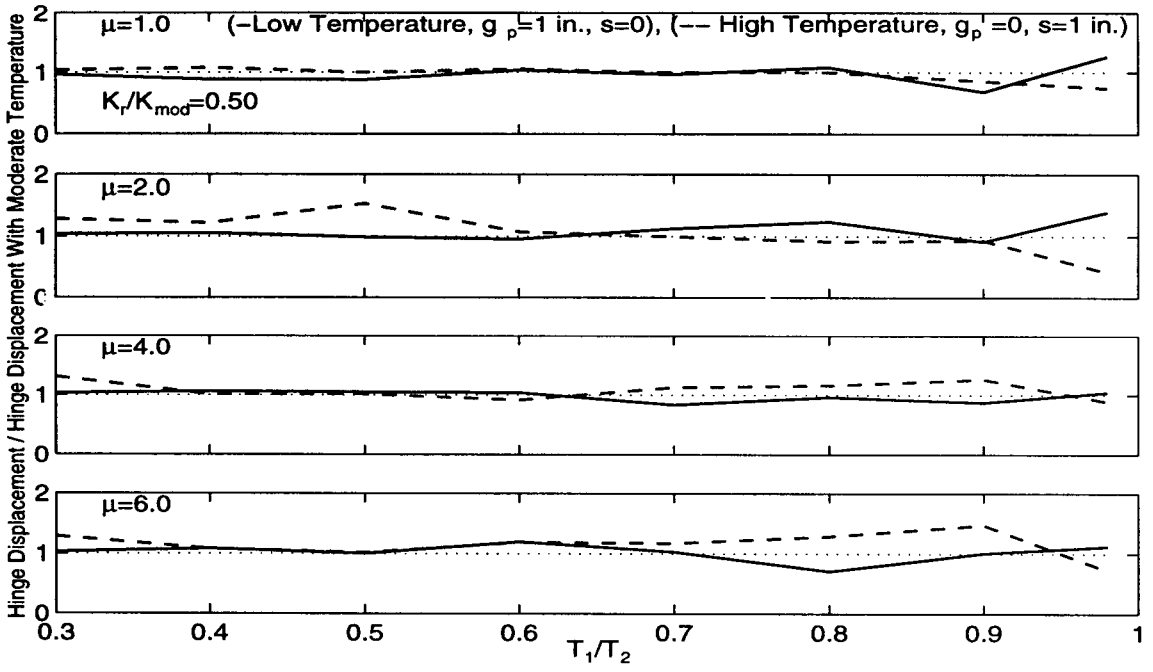

Figure 4.9: Effect of Hinge Gap and Restrainer Slack on Hinge Displacement Ratio for 1940 El Centro Earthquake (S00E Component): $T_2/T_g = 1.0$.

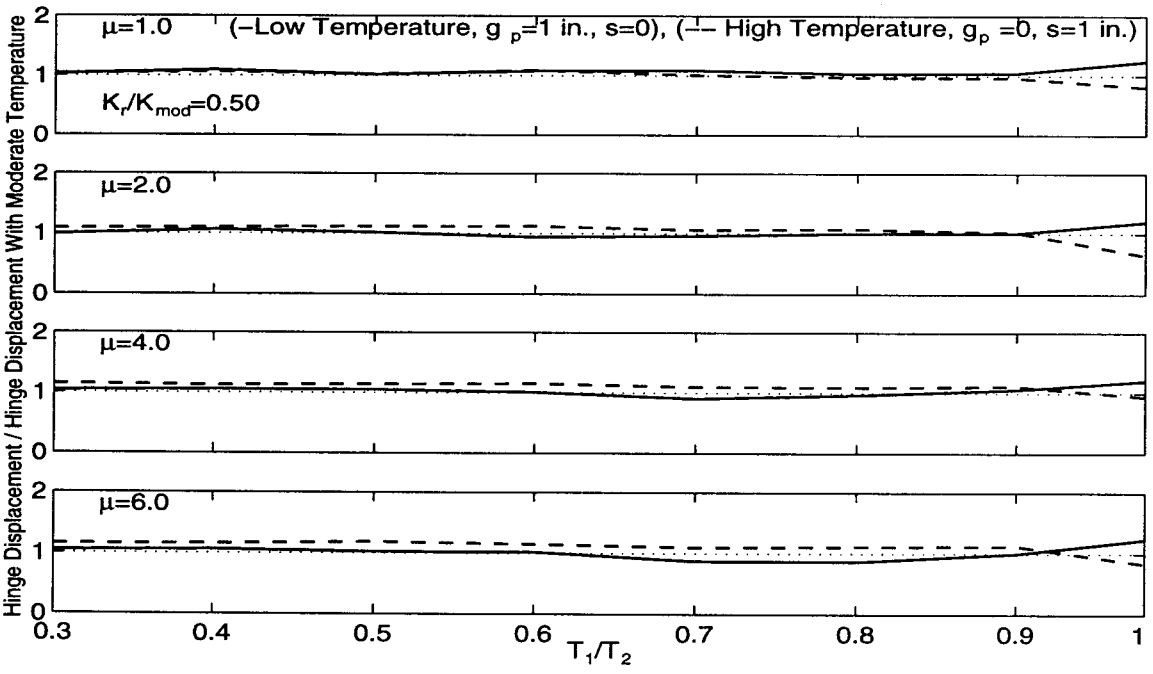

Figure 4.10: Effect of Hinge Gap and Restrainer Slack on Hinge Displacement Ratio for $T_2/T_g = 1.0$: Mean for 26 Earthquake Records.

dividing the hinge displacement for the case with F_f = 100 kips (445 kN). Figure 4.11 shows the hinge displacement for the 1940 El Centro earthquake (S00E component). The effect of friction on limiting hinge displacement is dependent on the frame period ratio and the target ductility. As the period ratio increases, the hinge displacement without friction increases compared with the case with friction. Similarly, as the target ductility increases, the hinge displacement without restrainers increases compared with the case with restrainers. For frames with a target ductility of 4, the hinge displacement without restrainers increases by approximately 5% at T_1/T_2 = 0.30 to greater than 100% at T_1/T_2 approaching unity compared with the case with restrainers. As the frame period ratio increases, the force required to limit hinge displacement decreases. This is due to both a reduction in the modified stiffness, and an increase in in-phase motion of the frames as the frame period ratio approaches unity. Therefore, the friction force as a percentage of the total force across the hinge increases.

For a frame period ratio of 0.80, the hinge displacement without friction increases approximately 10% for elastic frames and approximately 100% for frames with a target ductility of 6 compared to the case with F_f = 100 kips (445 kN). Similar increases occur for other period ranges. The increase in effectiveness of the friction force corresponding to an increase in design ductility is due to the decrease in the effective stiffness of the frames as the frames yield. Previous studies, which did not consider different levels of inelastic response, concluded that the effect of friction on the hinge displacement was minimal (Trochalakis et al., 1997).

A doubling of the friction force has little effect on the hinge displacement. Typical reductions in the hinge displacement ratio are on the order of 5% with a friction force of F_f = 200 kips (890 kN) compared with F_f = 100 kips (445 kN).

The study of the effectiveness of friction is repeated for the list of ground motions in table 4.2. The average displacement ratio for the 26 records is plotted in figure 4.12. In general, the hinge displacement without friction increases by approximately 50-100% from T_1/T_2 = 0.30 to T_1/T_g = 1.0 compared to the case with friction. Also, average hinge displacements for elastic frames without friction increase 10% compared to the case with restrainers. For frames with a target ductility of 6, the

average increase in the hinge displacement without friction compare to the case with $F_f = 100$ kips (445 kN), is 70%.

Figure 4.13 shows the average plus one standard deviation of the displacement ratio for the 26 records. The standard deviation for the hinge displacement ratio increases with both increasing frame period ratio and design ductility.

4.3.5 Effect of Coefficient of Restitution

The effect of the coefficient of restitution on the hinge displacement is examined by comparing the hinge displacement with $e = 0.60$ and $e = 1.0$ with the hinge displacement with $e = 0.80$. Figure 4.14 shows the results for the 1940 El Centro earthquake (S00E component). For the case with elastic frames, the hinge displacement is slightly greater for $e = 1.0$ than for $e = 0.60$. For yielding frames, the hinge displacement is highly variable. There are cases where the hinge displacement is greater for $e = 1.0$ than for $e = 0.60$ and vice versa. Although smaller values of e result in a reduction in the rebound velocity, this does not necessarily result in a reduction in the hinge displacement. The change in the rebound velocity affects the phasing between the frames and therefore affects the rate at which the frames separate. However, for inelastic frames, the effect of e on the hinge displacement is minimal for a wide range of period ratios.

Figure 4.15 shows the same study, except for the 1994 Northridge earthquake (Sylmar Hospital free-field record). The results show that the hinge displacement ratio for both $e = 0.60$ and $e = 1.0$, is approximately the same as for $e = 0.80$.

The study of the coefficient of restitution is repeated for the list of ground motions shown in table 4.2. The average hinge displacement ratio for the 26 input motions is shown in figure 4.16. In general, the coefficient of restitution has little effect on the response of the frames. For both $e = 0.60$ and $e = 1.0$ the hinge displacement is within 5% of hinge displacement with $e = 0.80$. The average plus one standard deviation of the hinge displacement ratio is plotted in figure 4.17. The results are very similar to the average, since the variation in the hinge displacement for different input motions is very small.

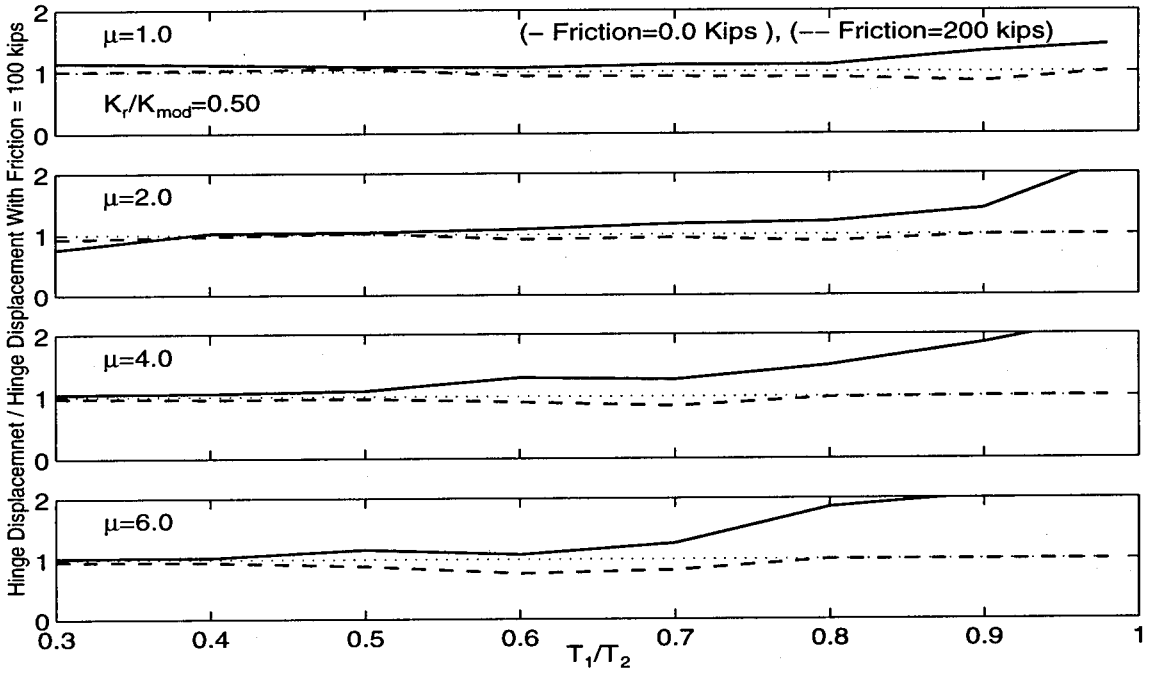

Figure 4.11: Effect of Friction on the Hinge Displacement, $T_2/T_g = 1.0$ for 1940 El Centro Earthquake (S00E Component).

4.3.6 Effect of Frame Mass Ratio

The effect of the frame mass ratio is studied by plotting the effects of the restrainer stiffness ratio, $\kappa = K_r/K_{mod}$, on the hinge displacement for $m_1/m_2 = 2.0$ and 4.0. The hinge displacement, D_{eq}, is normalized by dividing by the hinge displacement for the case without restrainers. Figures 4.18 and 4.19 show the mean of the hinge displacement ratio for mass ratios of 2 and 4, respectively. The hinge displacement ratio for mass ratios of 2 and 4 are very similar to those for a mass ratio of unity. This confirms results from previous studies, which showed that the mass ratio is not an important parameter in the response of multiple-frame bridges (Trochalakis et al., 1997).

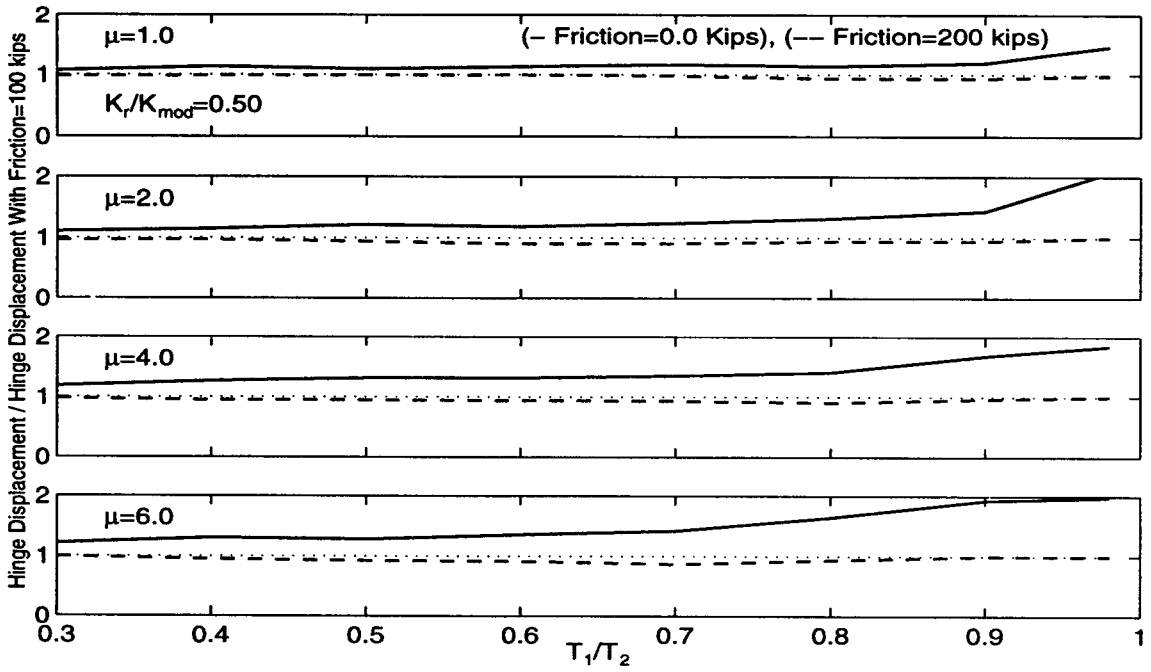

Figure 4.12: Effect of Friction on the Hinge Displacement, $T_2/T_g = 1.0$, Mean for 26 Earthquakes.

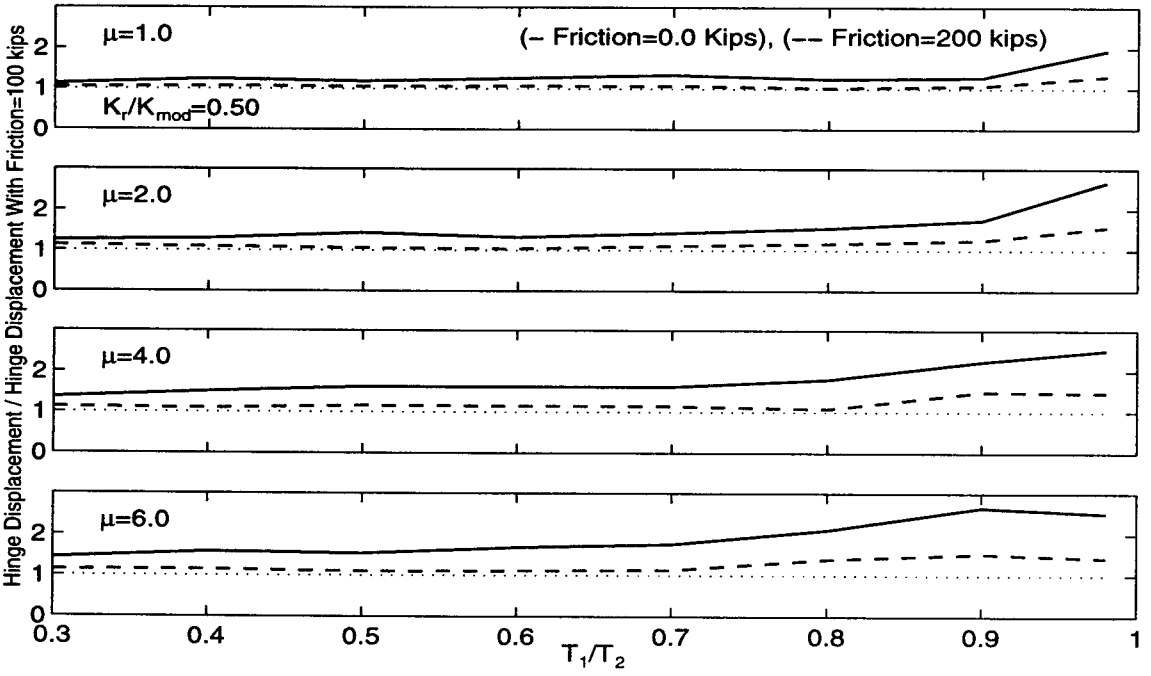

Figure 4.13: Effect of Friction on the Relative Hinge Displacement, $T_2/T_g = 1.0$, Mean Plus One Standard Deviation for 26 Earthquakes.

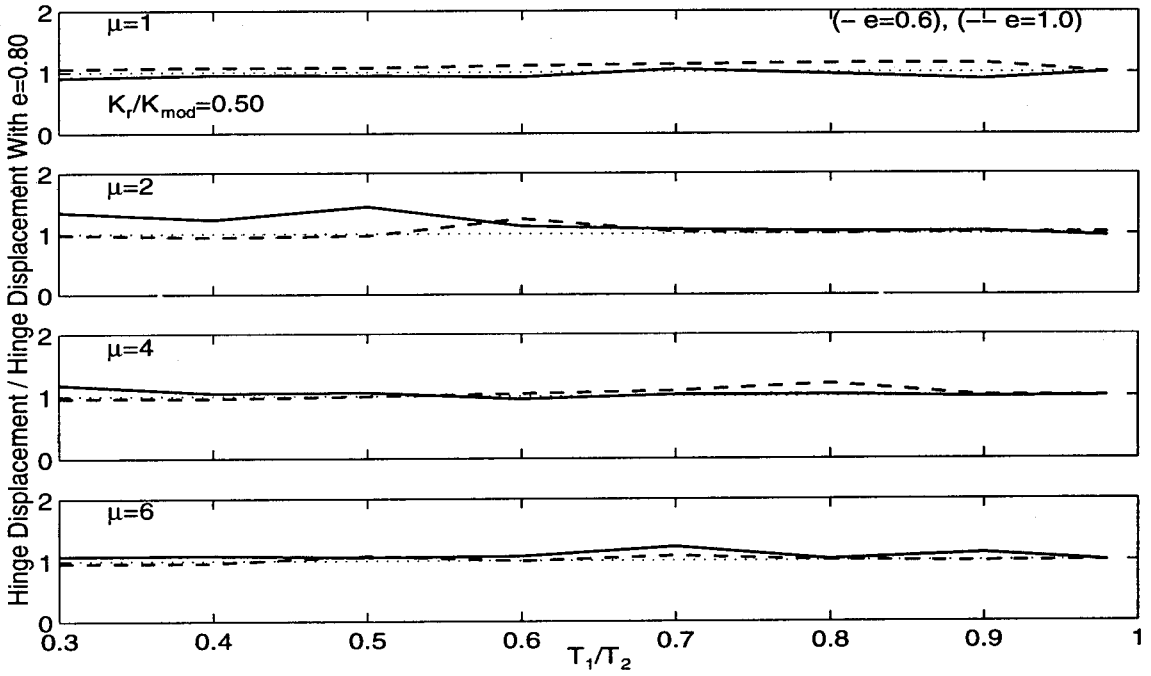

Figure 4.14: Effect of Coefficient of Restitution on the Hinge Displacement, T_2/T_g = 1.0, 1940 El Centro Earthquake (S00E Component).

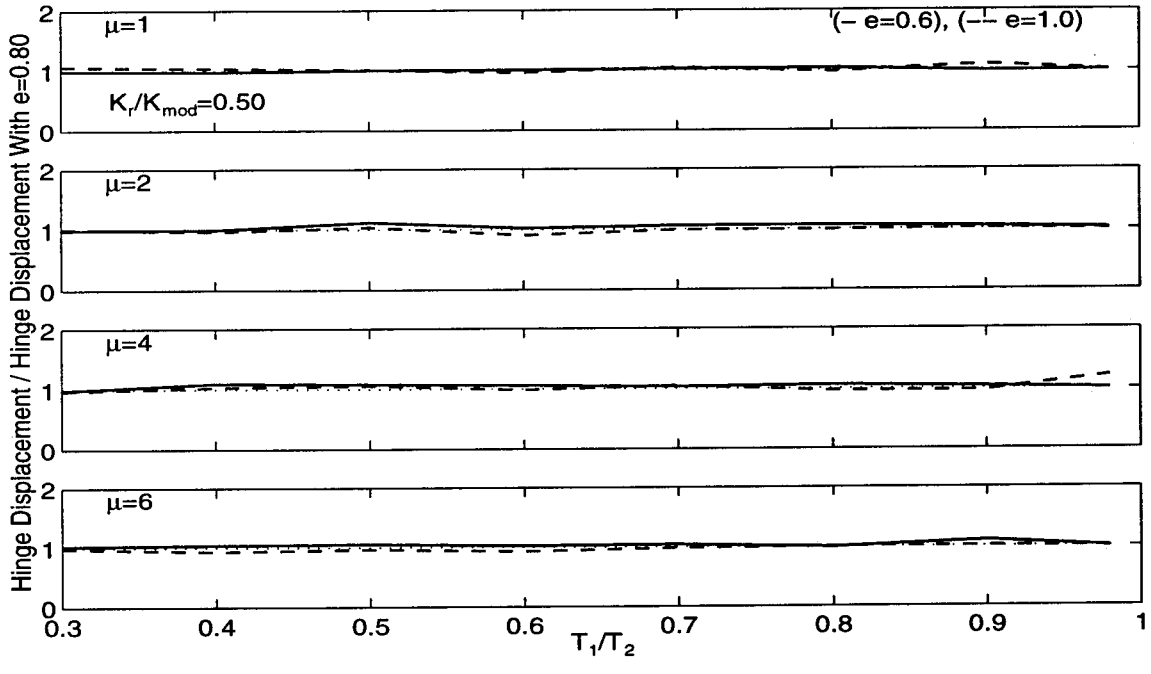

Figure 4.15: Effect of Coefficient of Restitution on Hinge Displacement, $T_2/T_g = 1.0$, 1994 Northridge Earthquake (Sylmar Hospital Free-Field Record).

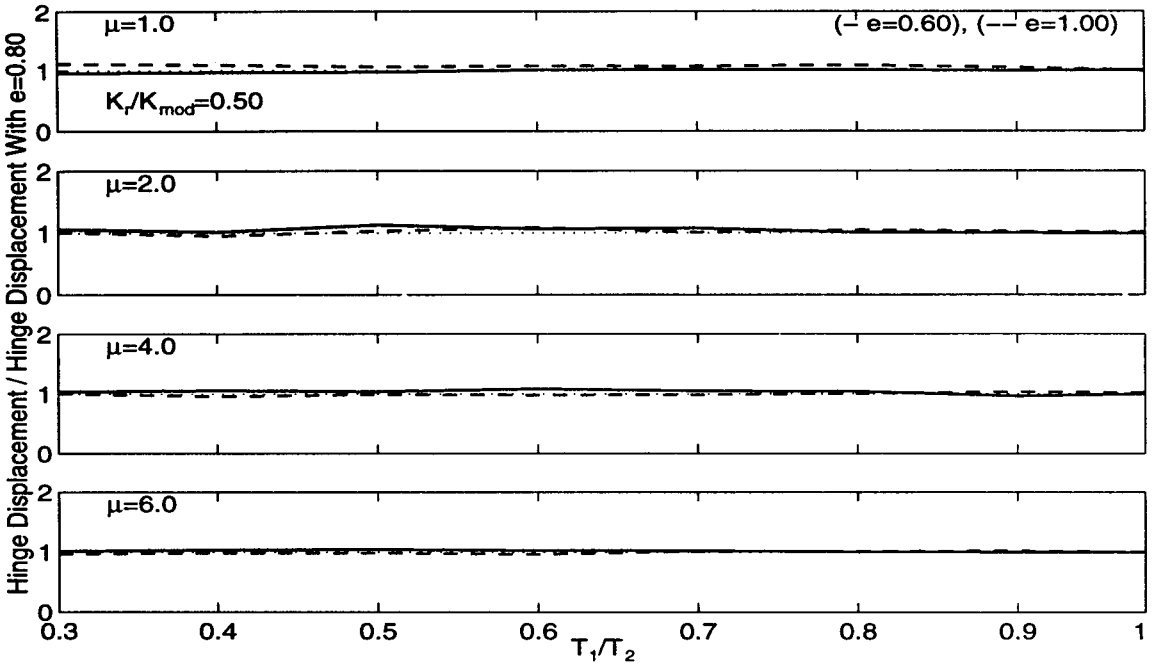

Figure 4.16: Effect of Coefficient of Restitution on Hinge Displacement, $T_2/T_g = 1.0$, Mean for 26 Earthquakes.

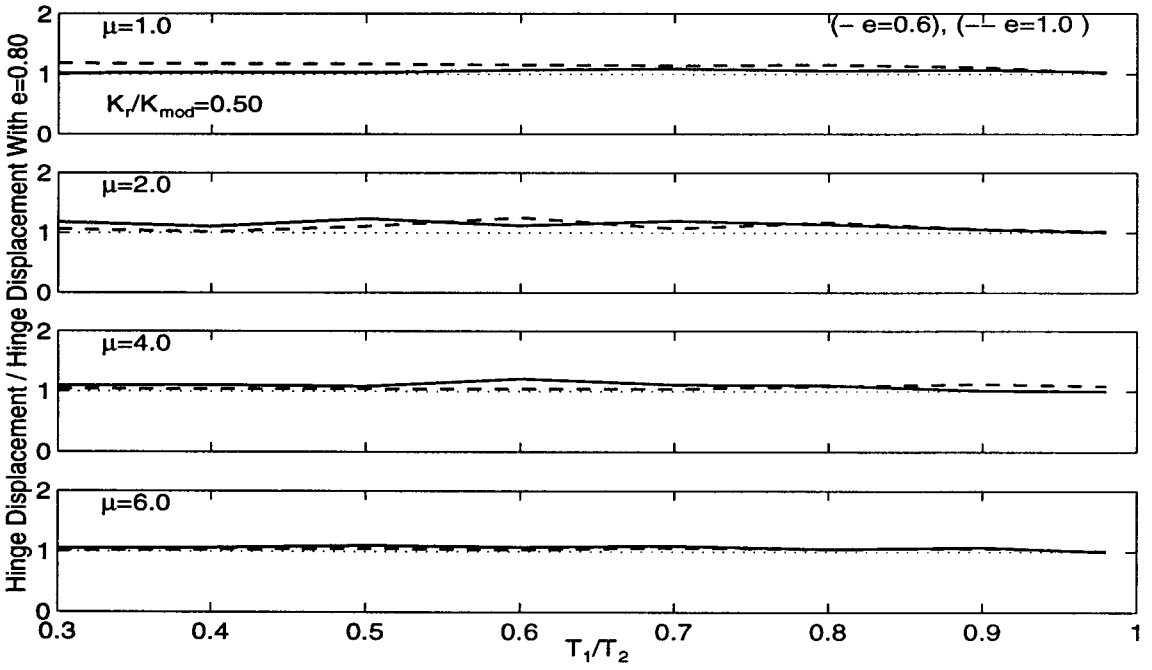

Figure 4.17: Effect of Coefficient of Restitution on Hinge Displacement, $T_2/T_g = 1.0$, Mean Plus One Standard Deviation for 26 Earthquakes.

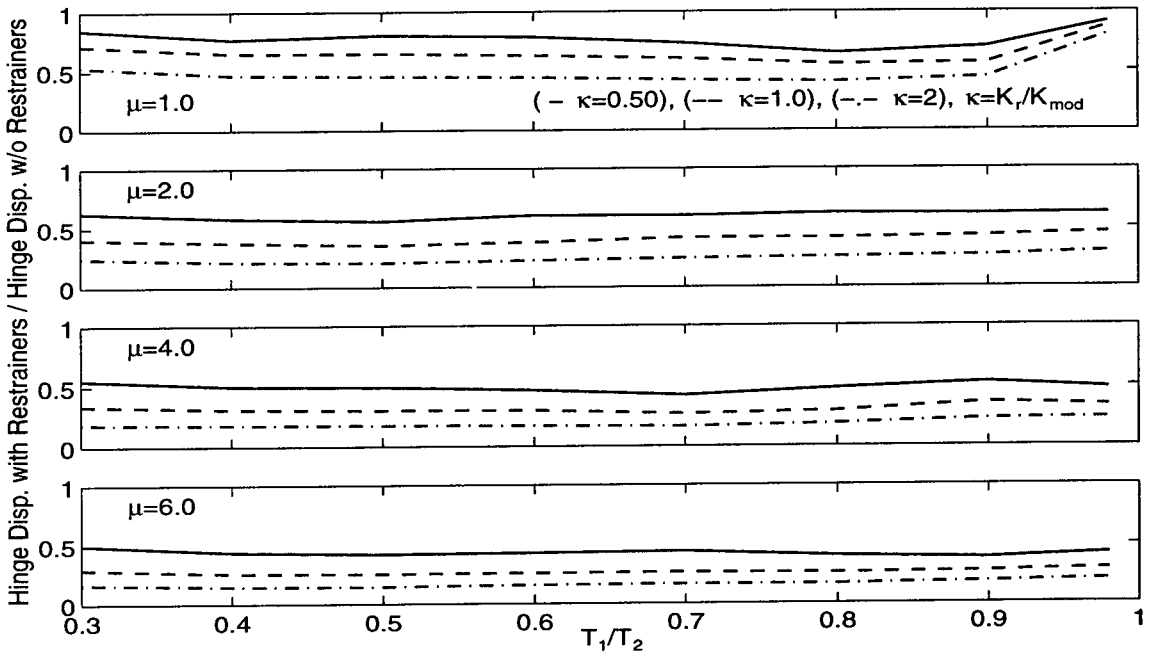

Figure 4.18: Effect of Restrainer Stiffness Ratio on Hinge Displacement for $m_1/m_2 = 2.0$, Mean for 26 Earthquake Records.

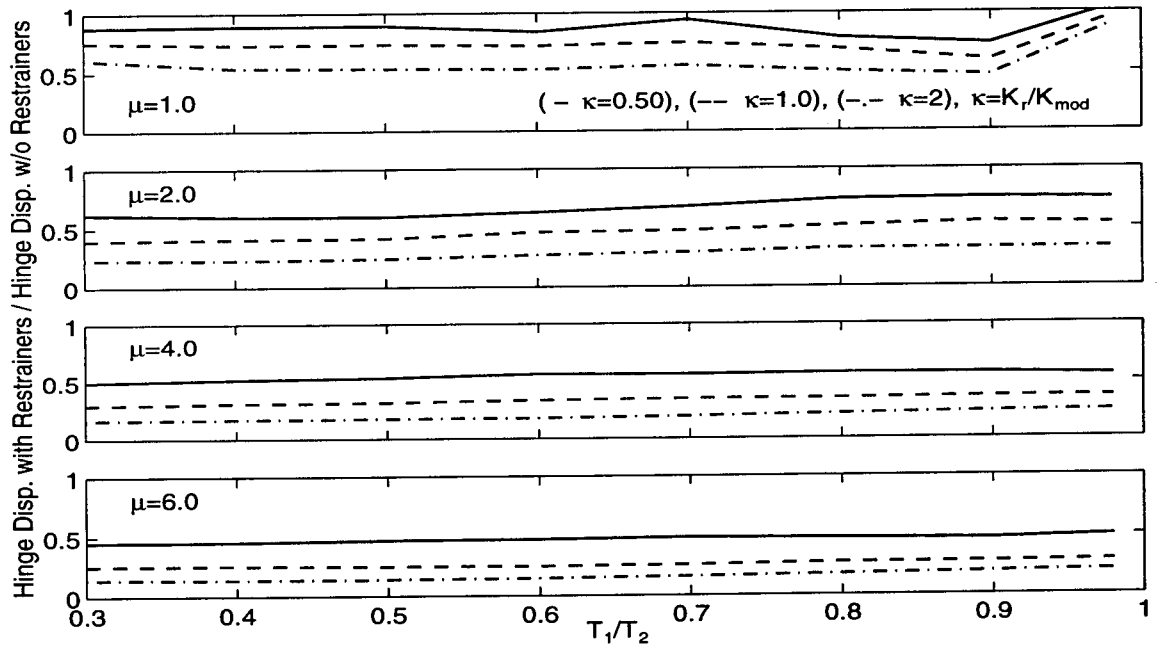

Figure 4.19: Effect of Restrainer Stiffness Ratio on Hinge Displacement for $m_1/m_2 = 4.0$, Mean for 26 Earthquake Records.

Chapter 5

New Design Procedure for Hinge Restrainers

A new restrainer design procedure is developed in this chapter. It is based on a simplified two degree-of-freedom model for the longitudinal earthquake response of two adjacent frames, illustrated in figure 5.1. In a design procedure, a simplified method of representing the restrainers is needed, therefore the nonlinear behavior of the hinge is linearized as illustrated in figure 5.1. Using the linearized model, restrainer design has two parts: (1) estimating the hinge displacement between the frames (D_{eq}), and (2) estimating the restrainer stiffness (K_r) required to reduce the hinge displacement to the designer-specified target displacement (D_r). The maximum relative hinge displacement is achieved by a modal analysis of the 2-DOF linearized system. The restrainer stiffness required to reduce the relative hinge displacement to the target displacement is calculated from a simple sensitivity analysis.

5.1 Theoretical Basis for Design Procedure

5.1.1 Natural Frequencies and Modes

The equations of motion for the linear 2-DOF system shown in figure 5.1 are as follows:

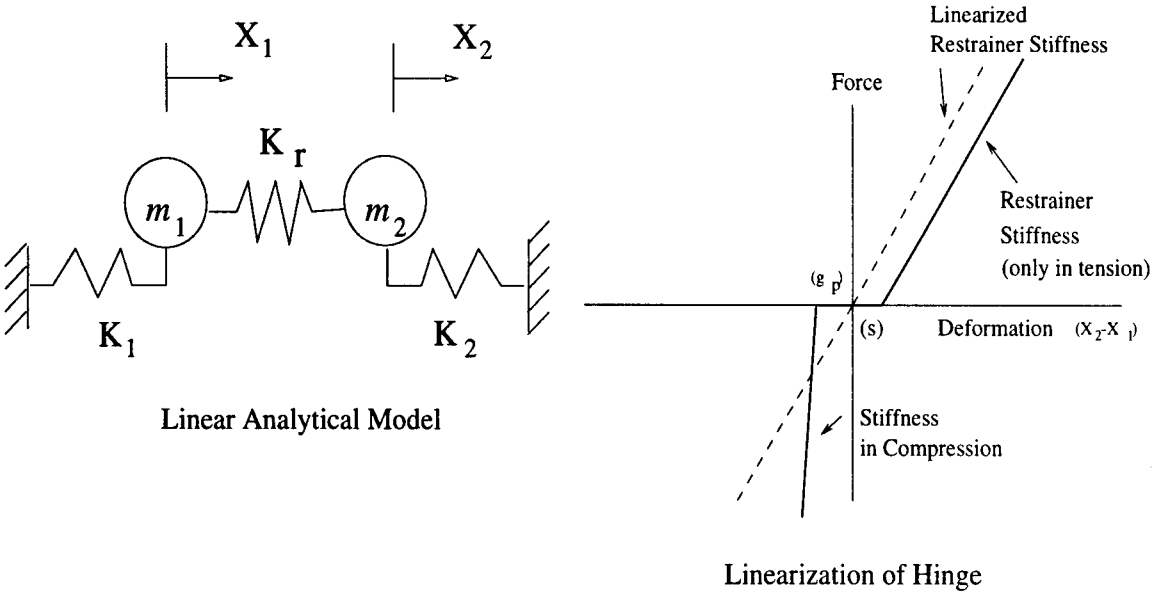

Figure 5.1: Simplified Linear Model for Longitudinal Earthquake Response of Two Adjacent Frames.

$$\mathbf{M}\ddot{\mathbf{x}}(t) + \mathbf{C}\dot{\mathbf{x}}(t) + \mathbf{K}\mathbf{x}(t) = -\mathbf{M}\mathbf{1}\ddot{u}_g(t) \tag{5.1}$$

Because the equations of motion are linearized, they can be solved using modal analysis. The response quantity of interest in this study is the relative hinge displacement, D_{eq}, which is expressed as:

$$D_{eq} = x_2 - x_1 = \mathbf{a}^T\mathbf{x}(t) \tag{5.2}$$

where $\mathbf{a}^T = [-1\ 1]$. The modal response for the relative hinge displacement may be written as:

$$D_{eq_i} = P_i S_{a_i}(T_i, \xi_i) \tag{5.3}$$

where $S_{a_i}(T_i, \xi_i)$ is the pseudo-acceleration response ordinate at the period T_i, and damping ratio ξ_i. The participation factor for relative hinge displacement is

$$P_i = \frac{\phi_i^T \mathbf{M}\mathbf{1}}{\phi_i^T \mathbf{K}\phi_i}(\mathbf{a}^T\phi_i) \tag{5.4}$$

where ϕ_i is the mode shape. The mode shape is determined by solving the following eigenvalue problem

$$\begin{bmatrix} K_1 + K_r & -K_r \\ -K_r & K_2 + K_r \end{bmatrix} \begin{Bmatrix} \phi_{1i} \\ \phi_{2i} \end{Bmatrix} = \omega_i^2 \begin{bmatrix} m_1 & 0 \\ 0 & m_2 \end{bmatrix} \begin{Bmatrix} \phi_{1i} \\ \phi_{2i} \end{Bmatrix} \tag{5.5}$$

Modal Combination

The response $r(t)$ of a structure to earthquake ground motion is the superposition of the modal responses $r_i(t)$. We are interested in estimating the maximum value, r_o, of the total response $r(t)$. In general, modal maxima $(r_i)_o$ do not occur at the same time, so the modal maxima cannot be directly superposed to obtain r_o.

Procedures have been developed to combine modal maxima considering the cross-correlations of modal responses, which is significant for closely spaced frequencies (Der Kiureghian, 1980). The maximum of the total response, r_o, is estimated from a *complete quadratic combination* (CQC) of the modal maxima as follows:

$$r_o = \sqrt{\sum_{i=1}^{N} (r_i)_o^2 + \sum_{\substack{i=1 \\ i \neq j}}^{N} \sum_{j=1}^{N} \rho_{ij} (r_i)_o (r_j)_o} \tag{5.6}$$

where $(r_i)_o$ and $(r_j)_o$ are the maximum values of modal responses $r_i(t)$ and $r_j(t)$. These may be positive or negative depending on the sign of the participation factor. The cross-correlation coefficient, ρ_{ij}, is always positive, and $\rho_{ii} = 1$. The first summation represents the *square root of the sum of the squares* (SRSS) combination rule. The second part, which is a double summation over all pairs of modes, includes the modal cross-correlation terms. The cross-correlation coefficient ρ_{ij} depends on the frequency ratio of the modes ($\beta_{ij} = \frac{\omega_i}{\omega_j}$), and on modal damping ratios ξ_i and ξ_j. The CQC combination method can be used for structures subjected to transient Gaussian wide-band inputs, such as earthquake induced excitations. The method is more accurate when the excitation has a long, stationary phase of strong motion, and the structure is not too lightly damped with a fundamental period, which is several times shorter than the excitation duration. Several expressions, based on random vibration theory, are available for ρ_{ij}. The expression used in this study is from Der Kiureghian (1980):

$$\rho_{ij} = \frac{8\sqrt{\xi_i \xi_j}(\xi_i + \beta\xi_j)\beta^{3/2}}{(1-\beta^2)^2 + 4\xi_i\xi_j\beta(1+\beta^2) + 4(\xi_i^2 + \xi_j^2)\beta^2} \tag{5.7}$$

For the hinge displacement of the 2-DOF model in figure 5.1, the combination rule simplifies to:

$$D_{eq} = \sqrt{D_{eq_1}^2 + D_{eq_2}^2 + 2\rho_{12}D_{eq_1}D_{eq_2}} \tag{5.8}$$

For the case without restrainers, equation 5.6 simplifies to

$$D_{eq_o} = \sqrt{D_1^2 + D_2^2 - 2\rho_{12}D_1D_2} \tag{5.9}$$

where D_i are the individual frame maximum displacements, and D_{eq_o} is the hinge opening without restrainers.

The use of the CQC combination rule is very important for an accurate representation of the relative hinge displacement over a wide range of frame period ratios. The CQC rule accounts for the cross correlation between closely spaced modes, and it represents the reduction in relative hinge displacements due to in-phase motion of frames which have similar periods. Studies of pounding of adjacent buildings have shown that the CQC combination rule provides a good estimate of the relative displacement of adjacent buildings subjected to earthquake ground motions (Kasai et al., 1996).

Effects of Period Ratio and Restrainer Stiffness on Participation Factor and Modal Periods

The first two typical mode shapes for the 2-DOF system are shown in figure 5.2. The first mode has both frames moving in the same direction. The second mode shape is represented with the frames moving in opposite directions. The modal response for the relative hinge displacement is expressed as the product of the participation factor and the pseudo-acceleration. The participation factor for relative displacement is a function of the properties of the system (i.e., mass and stiffness matrices). To understand how the response of the coupled system changes as restrainers are added, the modal periods and the modal participation factors for hinge displacement are plotted as a function of the frame period ratio, and the restrainer stiffness ratio, as

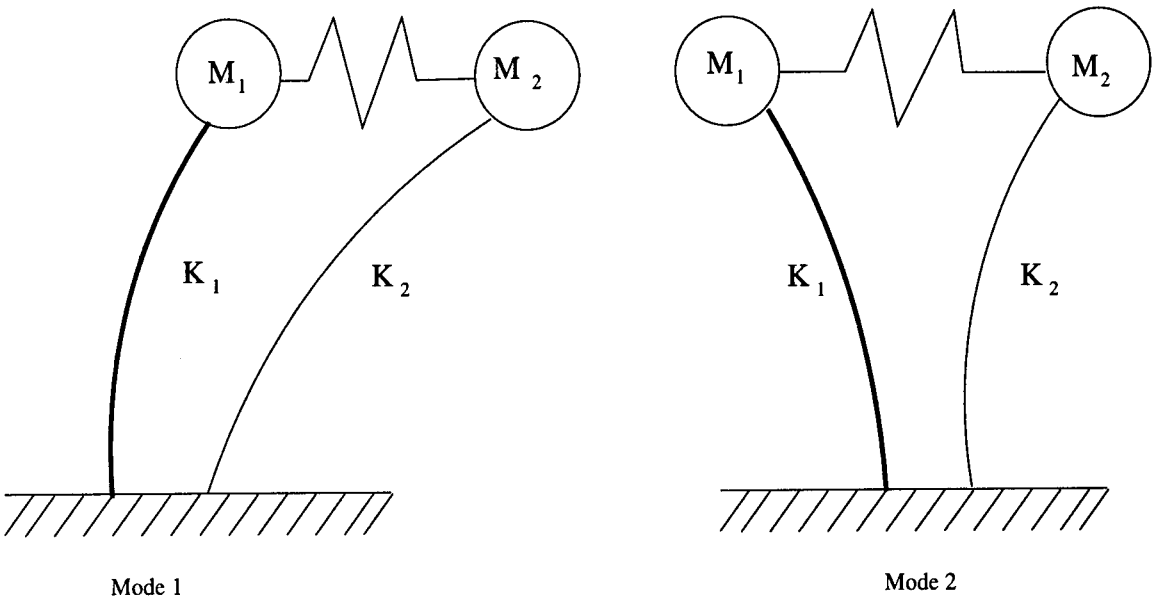

Figure 5.2: Mode Shape For 2-DOF System Representing Bridge Frames with Restrainers

illustrated in figures 5.3 and 5.4. The modal periods, T_{1m} and T_{2m}, are presented in non-dimensional form by dividing them by the independent period of frame 2, T_2. Similarly, the modal participation factor is normalized by dividing by T_2^2.

The normalized modal periods as a function of the frame period ratio and the restrainer stiffness ratio are shown in figure 5.3. The first modal period decreases as the restrainer stiffness ratio increases, particularly for low frame period ratios. Low frame period ratios represent a very stiff frame next to a flexible frame. As the frame period ratio approaches unity, the normalized first mode period approaches unity, regardless of restrainer stiffness ratio. As the frame period ratio approaches unity, the frames move in-phase, and the effect of the restrainers on the period is minimal. The normalized second mode period approaches zero for small frame period ratios. Since the second mode is represented by the frames moving in opposite directions, the small periods are due to the response of frame 1, which is very stiff. As the frame period ratio increases, the normalized second modal period approaches 1 for $K_r/K_{mod} = 0$ and approximately 0.70 for $K_r/K_{mod} = 1.00$. Since the second mode is due to the frames moving in the opposite direction, an increase in the normalized

restrainer stiffness, even for in-phase frames, decreases the normalized second modal period.

For frame period ratios from 0 to 0.60, the normalized modal participation factor varies from 0.025 for $K_r/K_{mod} = 0$ to 0.013 for $K_r/K_{mod} = 1.00$. The addition of restrainers has a significant effect in decreasing the normalized first mode participation factor, since restrainers reduce the displacement of the more flexible frame for the first mode. As the frame period ratio approaches unity, the normalized first mode participation factor approaches zero for all normalized restrainer stiffnesses. The second normalized modal participation factor approaches zero as the frame period ratio approaches zero. The second mode involves the displacement of frame 1, which for low frame period ratios is very small. As the frame period ratio increases, the magnitude of the normalized participation factor increases, reaching a maximum at approximately $T_1/T_2 = 0.80$. Further increases in T_1/T_2 reduce the normalized participation factor until it reaches zero at $T_1/T_2 = 1$. Increasing K_r/K_{mod} reduces the magnitude of the normalized second mode participation factor.

Figures 5.3 and 5.4 show that there are two ways which the participation factor for the relative hinge displacement can be reduced: (1) changing the frame properties such that the individual frames have periods which closely match, and (2) increasing the restrainer stiffness.

5.1.2 Sensitivity Analysis for the Hinge Displacement as a Function of the Restrainer Stiffness

Sensitivity analysis uses the partial derivatives of a structural response function with respect to a design variable to show how a change in a design parameter affects the response. In this case, the response function is the relative hinge displacement and the design variable is the restrainer stiffness. A sensitivity analysis is performed for the 2-DOF system representing the bridge frames with restrainers. The result of the sensitivity analysis is an expression for the change in the hinge displacement as a function of a change in the restrainer stiffness. The formulation is based on the linearization discussed in the previous section. For the linearized model subjected the effective modal earthquake load, P_i, the displacements in mode i are given by

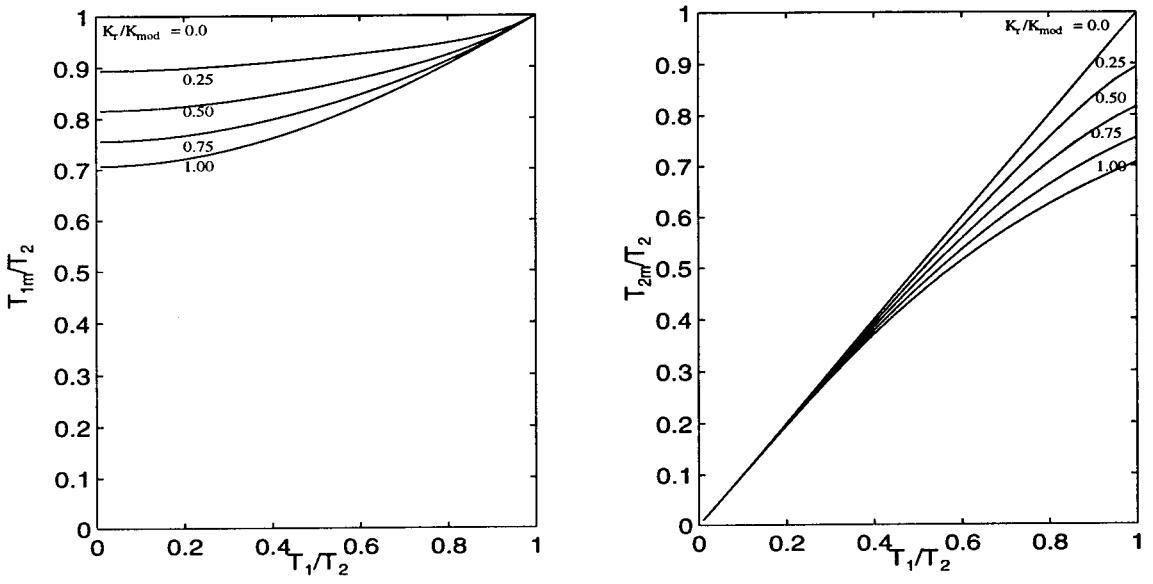

Figure 5.3: Normalized Modal Periods as a Function of Frame Period Ratio and Restrainer Stiffness Ratio.

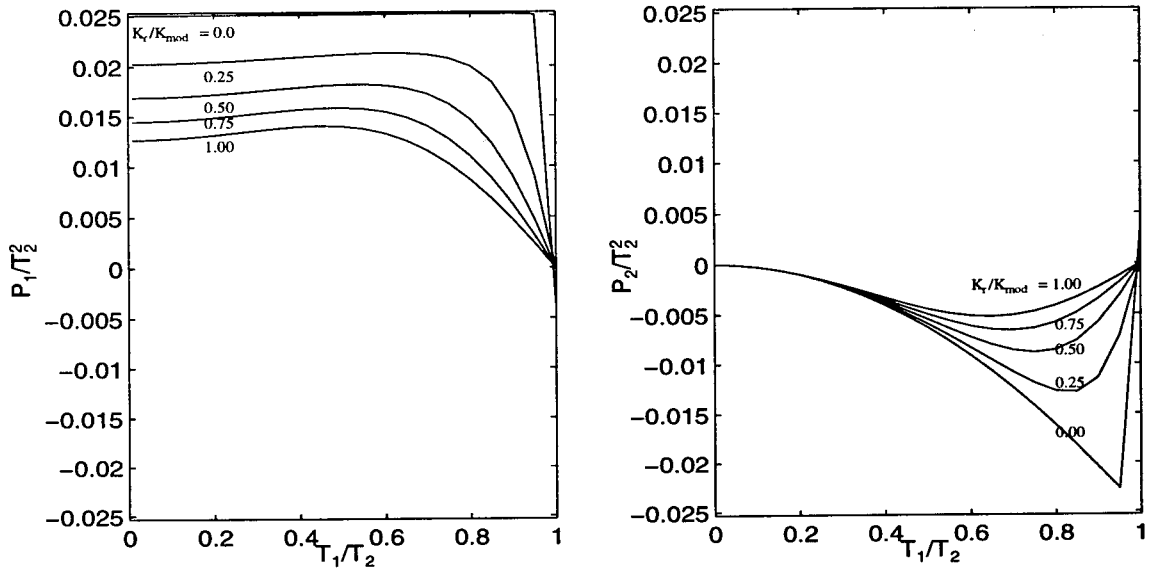

Figure 5.4: Normalized Modal Participation Factors as a Function of Frame Period Ratio and Restrainer Stiffness Ratio.

$$\mathbf{K}\mathbf{x}_i = \mathbf{P}_i \tag{5.10}$$

Taking the partial derivative with respect to the restrainer stiffness, K_r, gives

$$\frac{\partial \mathbf{K}}{\partial K_r}\mathbf{x}_i + \mathbf{K}\frac{\partial \mathbf{x}_i}{\partial K_r} = \mathbf{0} \tag{5.11}$$

where it is assumed that the change in effective modal earthquake load with respect to the change in the restrainer stiffness is zero. In reality the effective earthquake load does depend on K_r, but this change in the earthquake load is accommodated by iterations in the design procedure. It can be shown that performing the sensitivity analysis on the combined hinge displacement, D_{eq}, produces the same result as performing the sensitivity analysis on the individual modes and combining the results with the CQC rule. Therefore sensitivity analysis can be performed on the combined hinge displacement. Expanding equation 5.11 for the 2-DOF model results in

$$\begin{bmatrix} 1 & -1 \\ -1 & 1 \end{bmatrix} \begin{Bmatrix} x_1 \\ x_2 \end{Bmatrix} + \begin{bmatrix} K_1 + K_r & -K_r \\ -K_r & K_2 + K_r \end{bmatrix} \begin{Bmatrix} \frac{\partial x_1}{\partial K_r} \\ \frac{\partial x_2}{\partial K_r} \end{Bmatrix} = \begin{Bmatrix} 0 \\ 0 \end{Bmatrix} \tag{5.12}$$

Equation 5.12 can be re-written as

$$\begin{Bmatrix} -1 \\ 1 \end{Bmatrix} D_{eq} = -\begin{bmatrix} K_1 + K_r & -K_r \\ -K_r & K_2 + K_r \end{bmatrix} \begin{Bmatrix} \frac{\partial x_1}{\partial K_r} \\ \frac{\partial x_2}{\partial K_r} \end{Bmatrix} \tag{5.13}$$

which can also be written as

$$\mathbf{a}D_{eq} = -\mathbf{K}\frac{\partial \mathbf{x}}{\partial K_r} \tag{5.14}$$

and multiplying both sides by $\mathbf{K}^{-1}$ gives

$$\mathbf{K}^{-1}\mathbf{a}D_{eq} = -\frac{\partial \mathbf{x}}{\partial K_r} \tag{5.15}$$

Substituting $D_{eq} = \mathbf{a}^T\mathbf{x}$ we get

$$\frac{\partial D_{eq}}{\partial K_r} = -(\mathbf{a}^T\mathbf{K}^{-1}\mathbf{a})D_{eq} \tag{5.16}$$

$$\frac{\partial D_{eq}}{\partial K_r} = -\frac{K_1 + K_2}{K_1 K_2 + K_r(K_1 + K_2)} D_{eq} \tag{5.17}$$

$$\frac{\partial D_{eq}}{\partial K_r} = -\frac{1}{K_{mod} + K_r} D_{eq} \tag{5.18}$$

where $K_{mod} = \frac{1}{K_1} + \frac{1}{K_2}$ is the sum of the flexibilities of the two frames. A Taylor series expansion about the current solution, D_{eq_j}, can be used to obtain the hinge displacement, $D_{eq_{j+1}}$, due to a change in the restrainer stiffness from K_{r_j} to $K_{r_{j+1}}$:

$$D_{eq_{j+1}} = D_{eq_j} + \frac{\partial D_{eq}}{\partial K_r} |_{D_{eq_j}} (K_{r_{j+1}} - K_{r_j}) \tag{5.19}$$

where $D_{eq_{j+1}}$ is the target relative hinge displacement at the next step. At each step the target displacement is D_r, therefore, setting $D_{eq_{i+1}}$ equal to D_r in equation 5.19 results in the following;

$$D_r = D_{eq_i} + \frac{\partial D_{eq}}{\partial K_r} |_{D_{eq_i}} (K_{r_{i+1}} - K_{r_i}) \tag{5.20}$$

Writing equation 5.20 in terms of K_r and solving for $K_{r_{j+1}}$ gives the next estimate for the restrainer stiffness

$$K_{r_{j+1}} = K_{r_j} + (K_{mod} + K_{r_j}) \frac{(D_{eq_j} - D_r)}{D_{eq_j}} \tag{5.21}$$

as a function of the relative hinge opening D_{eq_j}, and the target hinge displacement, D_r. As shown in the next section, equation 5.21 leads to an iterative procedure that converges to a K_r for $D_{eq} = D_r$. There are important similarities between equation 5.21 and the equivalent static procedure (Caltrans, 1990). In the equivalent static procedure, the restrainer stiffness is determined from the following expression:

$$K_r D_r = max(K_1, K_2)(D_{eq_0} - D_r) \tag{5.22}$$

The right hand side is the force required to displace the stiffest frame an amount $D_{eq_0} - D_r$. Accoring to equation 5.22, the restrainer stiffness K_r is based on developing an equal force over a maximum extension of D_r. For the new procedure, the evaluation of the equation 5.21 for the j=0 iteration is

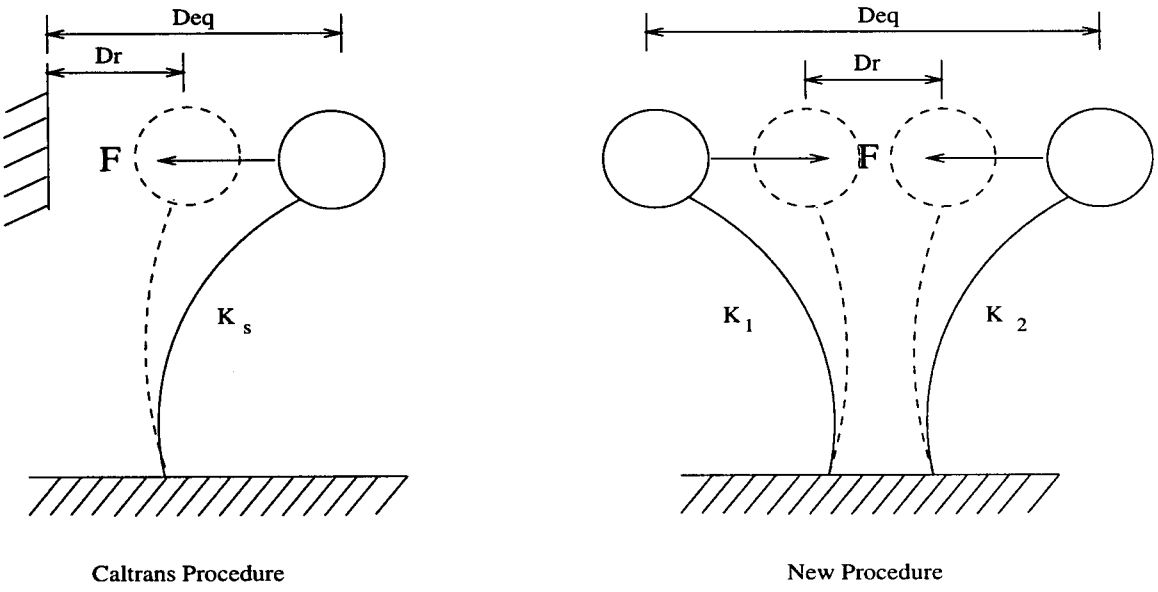

Figure 5.5: Interpretation of the Caltrans and New Procedure For Hinge Restrainers.

$$K_{r_1} D_{eq_0} = K_m (D_{eq_0} - D_r) \tag{5.23}$$

The right hand side of equation 5.23 is the self-equilibrating force required to displace the two frames a relative amount $D_{eq_0} - D_r$. Since $K_m \leq max(K_1, K_2)$, the restrainer force is always less than that given by the equivalent static procedure in equation 5.21. The restrainer stiffness K_r in equation 5.22 is based on the restrainer force acting through the full earthquake displacement D_{eq_0} of the hinge. This results for the first step as a consequence of the sensitivity analysis. Subsequent iterations give increasing K_r until $D_{eq} < D_r$.

5.1.3 Linearization of Yielding Systems

Bridge frames are intended to undergo inelastic deformations during a large earthquake. The results from the parameter study in Chapter 4 showed that yielding frames require significantly fewer restrainers to limit hinge displacement compared with elastic frames. The nonlinearity of frames will be accounted for in the restrainer design procedure by determining equivalent stiffness and damping ratios based on the maxi-

mum displacement of the frames. In this procedure, known as the substitute structure method (Gulkan and Sozen, 1974), the effective stiffness and effective damping ratio are determined such that the displacement of the inelastic system is equal to that of the linear substitute model.

The description of the steady-state response of a nonlinear oscillator by means of an equivalent viscous damping coefficient was first introduced by Jacobsen (1930). Later, Jennings compared several approaches for representing elasto-plastic SDOF oscillators as equivalent linear systems (Jennings, 1968). By assigning prescribed values of stiffness and damping ratio, matching of the resonant amplitude was achieved for steady-state response to sinusoidal loading. However, the closed-form expression for substitute properties could not be stated for earthquake problems due to the random nature of the exciting force.

Later, equivalent viscous damping was viewed on an average rather than cycle-by-cycle basis (Gulkan and Sozen, 1974). This did away with the requirement of steady-state response, leading to the substitute structure method. The values of substitute frequency and damping were determined from results of a series of dynamic tests of SDOF reinforced concrete columns. The substitute frequency was taken as the ratio of measured maximum absolute acceleration to measured maximum displacement response. This is also related to the apparent stiffness observed from the load-displacement relationship. Substitute damping for the yielding system was computed on the premise that the energy input into the system is entirely dissipated by a viscous damper. This may be expressed as follows:

$$\xi_{eff} 2m\omega_{eff} \int_0^{t_f} \dot{x}^2 dt = -m \int_0^{t_f} \ddot{y}\dot{x} dt \tag{5.24}$$

where ξ_{eff} is the substitute damping ratio, m is the mass, ω_{eff} is the substitute circular frequency, $\dot{x}$ is the relative velocity response, $\ddot{y}$ is the base acceleration, and t_f is the duration of shaking. It was shown, for several ground motions, that the displacement response was adequately approximated from a linear spectra with the substitute properties. The substitute damping ratio, ξ_{eff}, was determined as a function of the ductility, μ, for the Takeda hysteresis model (Takeda et al., 1970):

$$\xi_{eff} = 0.02 + 0.2(1 - \frac{1}{\sqrt{\mu}}) \tag{5.25}$$

which was shown to compare well with substitute damping ratios from test measurements.

The two parameters needed for the substitute structure method are effective stiffness, K_{eff}, and effective damping, ξ_{eff}. For idealized elastic-perfectly plastic hysteresis, the effective stiffness decreases with increasing ductility to reach the same displacement as shown in figure 5.6, so that the effective stiffness, K_{eff}, is equal to K/μ. Various relationships of effective damping versus ductility factor have been developed. A recent study modified the relationship in equation 5.25, based on the Takeda hysteresis relationship (MacRae et al., 1993):

$$\xi_{eff} = \xi + \frac{1 - \frac{0.95}{\sqrt{\mu}} - 0.05\sqrt{\mu}}{\pi} \tag{5.26}$$

Experimental studies show that both relationships in equation 5.25 and equation 5.26 may underestimate substitute values for damping (Priestley and Park, 1984). Comparisons of several expressions are shown in figure 5.7. Equation 5.26 is used in this study because the objective is to provide a conservative estimate.

5.2 Restrainer Design Procedure

The frame properties which are used in the new procedure are frame stiffnesses, (K_1 and K_2), frame masses, (m_1 and m_2), and target ductility μ. The properties of the restrainers are the length, L, modulus of elasticity, E, and yield strength, F_y. The restrainer slack is estimated from the ambient temperature. The earthquake characteristics are represented by a pseudo-acceleration response spectrum, $S_a(T_i, \xi_i)$. Given this information, the design procedure for intermediate hinge restrainers is as follows:

Step 1: Calculate Maximum Allowable Hinge Displacement

Restrainers are typically designed to remain elastic. Therefore, the maximum allowable hinge displacement is taken as the sum of the restrainer yield displacement

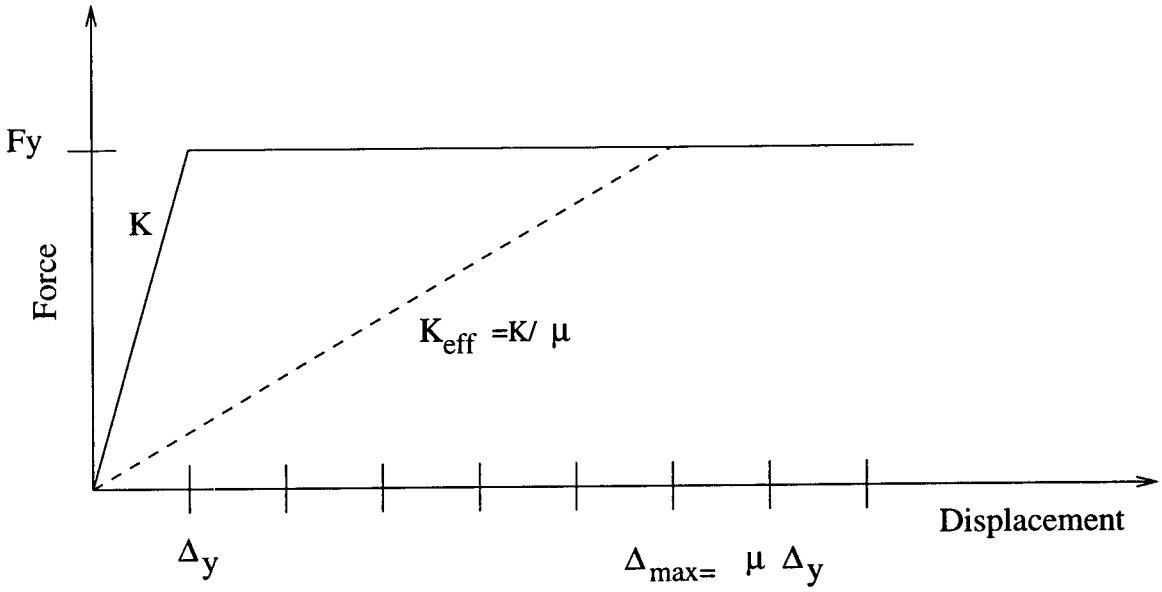

Figure 5.6: Effective Stiffness Values as a Function of Ductility.

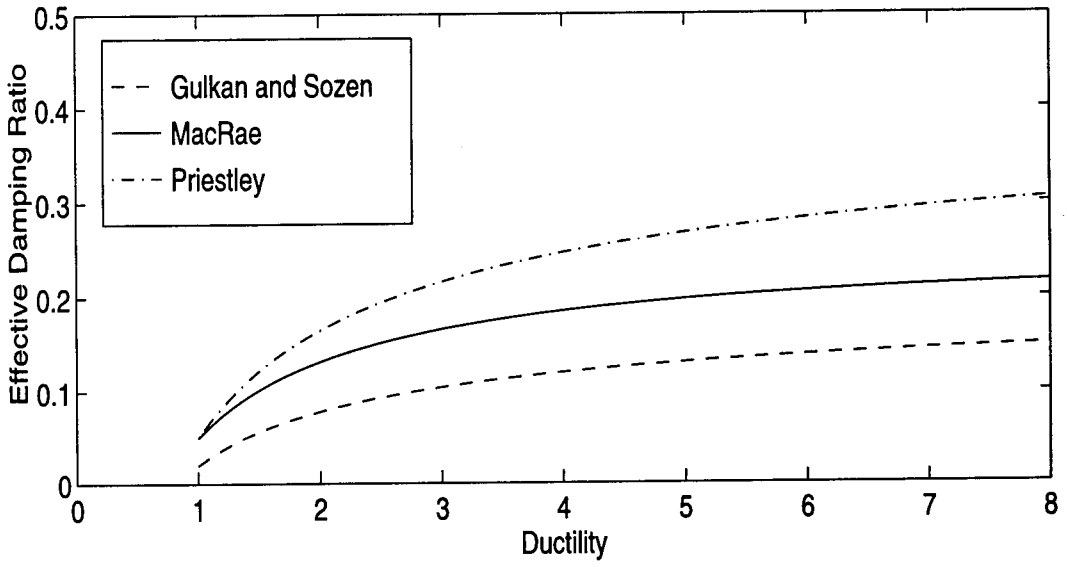

Figure 5.7: Effective Damping Values as a Function of Ductility.

and the slack in the restrainers:

$$D_r = D_y + s$$

where s is the restrainer slack and D_y is the restrainer deflection at yield. The yield displacement of the restrainers, D_y, is:

$$D_y = F_y L/E$$

where F_y=176.1 ksi (1.2 GPa), and E=10,000 ksi (69 GPa) for standard cables.

If the maximum permissible restrainer deformation, D_r, is greater than the available hinge seat width, then the hinge could unseat before the restrainer capacity is reached. In this case, D_r must be reduced by (a) shortening the restrainer length, or (b) decreasing the restrainer gap. Unless otherwise specified, 20 ft restrainers are used at the hinges.

Step 2: Compute the Initial Relative Hinge Displacement

The initial relative hinge displacement can be obtained from equation 5.9:

$$D_{eq_0} = \sqrt{D_1^2 + D_2^2 - 2\rho_{12} D_1 D_2}$$

The frame displacements D_1 and D_2 are determined from a pseudo-acceleration response spectrum as:

$$D_i = (\frac{T_{eff_i}}{2\pi})^2 S_a(T_{eff_i}, \xi_{eff_i})$$

where $T_{eff_i} = 2\pi\sqrt{m_i/K_{eff_i}}$. If $D_{eq_0} < D_r$, use the minimum number of restrainers. If $D_{eq_0} > D_r$, restrainers must be provided according to step 3.

Step 3: Determine Required Restrainer Stiffness

The required restrainer stiffness to limit hinge displacement is obtained from the incremental stiffness expression of equation 5.21 as:

$$K_r = \frac{K_{eff_{mod}}(D_{eq_0} - D_r)}{D_{eq_0}}$$

where

$$K_{eff_{mod}} = \frac{K_1 K_2}{\mu(K_1 + K_2)} \tag{5.27}$$

Step 4: Calculate Relative Hinge Displacement from Modal Analysis

The maximum relative hinge displacement is determined from a 2-DOF modal analysis of the frames with the restrainer stiffness determined in step 3. The relative hinge displacement is obtained from equation 5.8 as follows:

$$D_{eq} = \sqrt{D_{eq_1}^2 + D_{eq_2}^2 + 2\rho_{12} D_{eq_1} D_{eq_2}}$$

where

$$D_{eq_i} = P_i S_{a_i}(T_{eff_i}, \xi_{eff_i})$$

where the participation factor, P_i, is defined as

$$P_i = \frac{\phi_i^T \mathbf{M1}}{\phi_i^T \mathbf{K} \phi_i}(\mathbf{a}^T \phi_i)$$

If $D_{eq} > D_r$, continue to step 5. Otherwise go to step 6 and calculate the required number of restrainers.

Step 5 : Calculate the Incremental Restrainer Stiffness Required to Limit Hinge Displacement

The required restrainer stiffness is given from equation 5.21 as

$$K_{r_{j+1}} = K_{r_j} + (K_{eff_{mod}} + K_{r_j})\frac{(D_{eq_j} - D_r)}{D_{eq_j}} \tag{5.28}$$

Steps 4 and 5 are repeated until $D_{eq} < D_r$.

Step 6 : Calculate the Number of Restrainers

Once the required restrainer stiffness is calculated, the number of restrainers is determined from:

$$N_r = \frac{K_r D_r}{F_y A_r} \tag{5.29}$$

where A_r is the area of one restrainer, which for typical 3/4 in. (19 mm) diameter cables is 0.22 sq in. (143 sq mm).

5.3 Application of New Restrainer Design Procedure

This section demonstrates the use of the new restrainer design procedure. Intermediate hinges in a multiple-frame bridge are designed by isolating the two frames adjacent to the hinge, as shown in figure 1.2. For long span bridges, the effects of abutments are typically negligible. Two earthquake ground motions are used, the 1940 El Centro earthquake (S00E component) and the 1994 Northridge earthquake (Sylmar Hospital free-field record), to represent different source characteristics and soil conditions. The 1940 El Centro earthquake has a broad band spectrum with a characteristic period of $T_g = 1.00$ sec, whereas the Sylmar Hospital free-field record has a near source pulse type motion with $T_g = 1.60$ sec. Both records are scaled to a peak ground acceleration of 0.70g.

For each case, the target hinge displacement, D_r, is 4.7 in. (119 mm), corresponding to a yield displacement for 20 ft (6.10 meters) restrainers of 4.22 in. (107 mm) and a restrainer slack of 0.50 in. (12.7 mm). The frame yield strengths are selected to provide a displacement ductility demand of $\mu = 4$ when responding independently.

The restrainer design procedure is performed for the 1940 El Centro earthquake (S00E component). Figure 5.8 shows detailed step-by-step calculations for the new restrainer design procedure. The displacement response spectrum for 5% and 19% damping are shown in figure 5.9. Nineteen percent damping corresponds to the effective damping for $\mu = 4$. In addition, figure 5.10 graphically illustrates the iterations

in the procedure. The ground motion is applied from right to left and left to right to account for the sign of the ground motion. The frames have a period ratio of 0.50 and an initial hinge opening of approximately 10 in. (254 mm). Since the target displacement is 4.7 in. (119 mm), restrainers are required. The restrainer stiffness determined from the first iteration, based on step 3 of the procedure, is 53.5 kips/in (9.36 kN/mm). The modal analysis gives a relative hinge displacement of $D_{eq} = 7.17$ in. (182 mm). Subsequent iterations result in displacements, D_{eq_j}, of 5.70 in. (145 mm), 4.90 in. (124 mm), and 4.67 in. (119 mm). The final restrainer stiffness required to limit hinge displacement is 154 kips/in (26.9 kN/mm). Eighteen - 20 ft restrainer cables provide this stiffness.

Figure 5.11 shows the response from a nonlinear analysis for the two frames with and without restrainers. Although the restrainers have little effect on the maximum frame displacements, they reduce the relative hinge displacement to the target. The initial hinge opening of approximately 9 in. (229 mm) is reduced to 5.10 in. (130 mm). The initial hinge displacement and the final hinge displacement determined by the new procedure are within 10% of the displacements determined from nonlinear time history analysis.

Figure 5.12 shows the force-deformation relationships for the frames in the example. Although the frames are designed for a ductility of $\mu = 4$, figure 5.12 illustrates the effect of interacting frames on the ductility demands. Without restrainers, frame 1 experiences a reduction of approximately 25% in the frame ductility ($\mu = 3.15$), and frame 2 experiences an increase in ductility of approximately 22% ($\mu = 4.84$). The more flexible frame pounds on the stiffer frame, increasing the demands on the frame beyond its original design. Similarly, the stiffer frame acts to limit the hinge displacement of the more flexible frame. With restrainers, the ductility demand in frame 1 decreases to $\mu = 3.95$ and increases in frame 2 to $\mu = 4.30$, compared to without restrainers, demonstrating that restrainers can balance the ductility demands between frames.

The restrainer design procedure is evaluated for the 1994 Northridge earthquake (Sylmar Hospital free-field record). The displacement response spectrum is shown in figure 5.13. Figure 5.14 illustrates the steps in the design procedure and has the

Example 5.1 - Design Procedure Applied to 1940 El Centro Earthquake (S00E Component), $\mu = 4$

K_1=2040 kips/in (357 kN/mm), K_2 = 510 kips/in (89.3 kN/mm)
$W_1 = W_2$=5000 kips (22.3 MN), μ=4, D_y = 4.20 in., (107 mm), s=0.50 in. (12.7 mm)
Ground Motion = 1940 El Centro Earthquake (S00E Component), Scaled to PGA=0.70g

Step 1 - Calculate Allowable Hinge Displacement
D_r=4.20+0.50=4.7 in. (119 mm)

Step 2 - Compute Hinge Displacement Without Restrainers
K_{eff_1}=2040/4=510 kips/in (89.3 kN/mm), K_{eff_2}=510/4=128 kips/in (22.4) kN/mm
$T_{eff_1} = 2\pi\sqrt{5000/(32.2*12)/510} = 1.0$ sec., $T_{eff_2} = 2\pi\sqrt{5000/(32.2*12)/128} = 2.0$ sec.
$\xi_{eff} = 0.05 + (1 - 0.95/\sqrt{4} - .05\sqrt{4})/\pi = 0.19$
$D_1 = S_d(1.0,0.19)$=4.75 in. (121 mm), $D_2 = S_d(2.0,0.19)$=9.73 in. (247 mm)
$\rho_{12} = \frac{8(0.19)^2(1+2)2^{3/2}}{(1-2^2)^2+4(0.19)^2(2)(1+2)^2} = 0.21$

$D_{eq_0} = \sqrt{4.75^2 + 9.73^2 - (0.21)4.75*9.73} = 9.89$ in. (251 mm)

Step 3 - Determine Required Restrainer Stiffness
$K_{mod_{eff}}$=(510)(128)/(510+128)=102 kips/in (17.9 kN/mm)
$K_r(0)$ = 102*(9.92-4.70)/9.92=53.5 kips/in (9.36 kN/mm)

Step 4 - Calculate Relative Hinge Displacement from Modal Analysis
Solve Modal Equations

$$\begin{bmatrix} 564 & -53.5 \\ -53.5 & 182 \end{bmatrix} \phi_i = \omega^2_{eff_i} \begin{bmatrix} 12.93 & 0 \\ 0 & 12.93 \end{bmatrix} \phi_i$$

$\omega^2_{eff_1} = 13.4\ \frac{1}{sec^2}$, $\omega^2_{eff_2} = 44.2\ \frac{1}{sec^2}$
$T_{eff_1} = 2\pi/\sqrt{13.4} = 1.71$ sec., $T_{eff_2} = 2\pi/\sqrt{44.2} = 0.95$ sec.
$\phi_1 = \begin{Bmatrix} 0.13 \\ 1.00 \end{Bmatrix}$, $\phi_2 = \begin{Bmatrix} 1.00 \\ -0.13 \end{Bmatrix}$

Calculate Participation Factor

$$P_1 = \frac{\{\ 0.13 \quad 1.00\ \} \begin{bmatrix} 12.93 & 0 \\ 0 & 12.93 \end{bmatrix} \begin{Bmatrix} 1 \\ 1 \end{Bmatrix}}{\{\ 0.13 \quad 1.00\ \} \begin{bmatrix} 564 & -53.5 \\ -53.5 & 182 \end{bmatrix} \begin{Bmatrix} 0.13 \\ 1.00 \end{Bmatrix}} (\{\ -1 \quad 1\ \} \begin{Bmatrix} 0.13 \\ 1.00 \end{Bmatrix}) = 0.072\ \frac{1}{sec^2}$$

Similarly, $P_2 = -.022\ \frac{1}{sec^2}$

D_{eq_1}=0.072*96.5=6.94 in. (176 mm), D_{eq_2}=-0.022*203=-4.47 in. (114 mm)
β=1.71/0.95=1.8
$\rho_{12} = \frac{8(0.19)^2(1+1.8)1.8^{3/2}}{(1-1.8^2)^2+4(0.19)^2(1.8)(1+1.8)^2} = 0.27$

$D_{eq} = \sqrt{(6.94)^2 + (-4.47)^2 + 2(0.27)(6.94)(-4.47)}$=7.17 in. (182) mm

$D_{eq} > D_r$, Continue to Step 5

Continue on Next Page $\Longrightarrow$

Continued from Previous Page

Step 5 - Calculate New Restrainer Stiffness
$K_r(1)$ = 53.5 + (102+53.5)(7.17-4.7)/7.17=107 kips/in (18.7 kN/mm)

Step 4 - 2nd Iteration
$\omega^2_{eff_1}$=16.0 $\frac{1}{sec^2}$, $\omega^2_{eff_2}$=49.9 $\frac{1}{sec^2}$

T_{eff_1}=1.57 sec., T_{eff_2}=0 88 sec.
$\phi_1 = \left\{ \begin{array}{c} 0.25 \\ 0.96 \end{array} \right\}$, $\phi_2 = \left\{ \begin{array}{c} 0.96 \\ -0.25 \end{array} \right\}$
P_1=0.055 $\frac{1}{sec^2}$, P_2=-0.018 $\frac{1}{sec^2}$

D_{eq_1}=0.055*97.6=5.37 in. (136 mm), D_{eq_2}=-0.018*219=-3.94 in., (99.6 mm), ρ_{12}=0.28
$D_{eq} = \sqrt{5.37^2 + -3.94^2 + 2(0.28 * 5.37 * -3.94)}$ = 5.70 in (145 mm)
$D_{eq} > D_r$, Continue to Step 5

Step 5 - Calculate Required Restrainer Stiffness
$K_r(2)$=107 + (102+107)(5.70-4.7)/5.70=144 kips/in (25.2 kN/mm)

Step 4 - 3rd Iteration
$\omega^2_{eff_1}$=17.2 $\frac{1}{sec^2}$, $\omega^2_{eff_2}$=54.0 $\frac{1}{sec^2}$

T_{eff_1}=1.51 sec, T_{eff_2}=0.85 sec
$\phi_1 = \left\{ \begin{array}{c} 0.31 \\ 0.95 \end{array} \right\}$, $\phi_2 = \left\{ \begin{array}{c} 0.95 \\ -0.31 \end{array} \right\}$
P_1=0.047 $\frac{1}{sec^2}$, P_2=-0.015 $\frac{1}{sec^2}$

D_{eq_1}=0.047*98.0=4.60 in. (117 mm), D_{eq_2}=-0.015*228=-3.42 in. (86.9 mm), ρ_{12}=0.28
$D_{eq} = \sqrt{4.60^2 + -3.42^2 + 2 * 0.28 * 4.60 * -3.42}$ = 4.90 in. (124 mm)
$D_{eq} > D_r$, Continue to Step 5

Step 5 - Calculate Required Restrainer Stiffness
$K_r(3)$ = 144 + (102+144)(4.90-4.70)/4.90=154 kips/in (27.0 kN/mm)

Step 4 - 4th Iteration
$\omega^2_{eff_1}$=17.5 $\frac{1}{sec^2}$, $\omega^2_{eff_2}$=55.1 $\frac{1}{sec^2}$

T_{eff_1}=1.50 sec., T_{eff_2}=0.85 sec.
$\phi_1 = \left\{ \begin{array}{c} 0.33 \\ 0.95 \end{array} \right\}$, $\phi_2 = \left\{ \begin{array}{c} 0.95 \\ -0.33 \end{array} \right\}$
P_1=0.045 $\frac{1}{sec^2}$, P_2=-0.014 $\frac{1}{sec^2}$

D_{eq_1}=0.045*98.2=4.40 in. (112 mm), D_{eq_2}=-0.014*231=3.23 in. (82 mm), ρ_{12} = 0.28
$D_{eq} = \sqrt{4.40^2 + -3.23^2 + 2 * 4.40 * -3.23}$=4.67 in. (119 mm)
$D_{eq} < D_r$, Goto Step 6

Step 6 - Calculate Number of Restrainers
N_r=(154*4.7)/(176*.222)=18 (20-ft) Restrainer Cables

Figure 5.8: Detailed Example of New Restrainer Design Procedure.

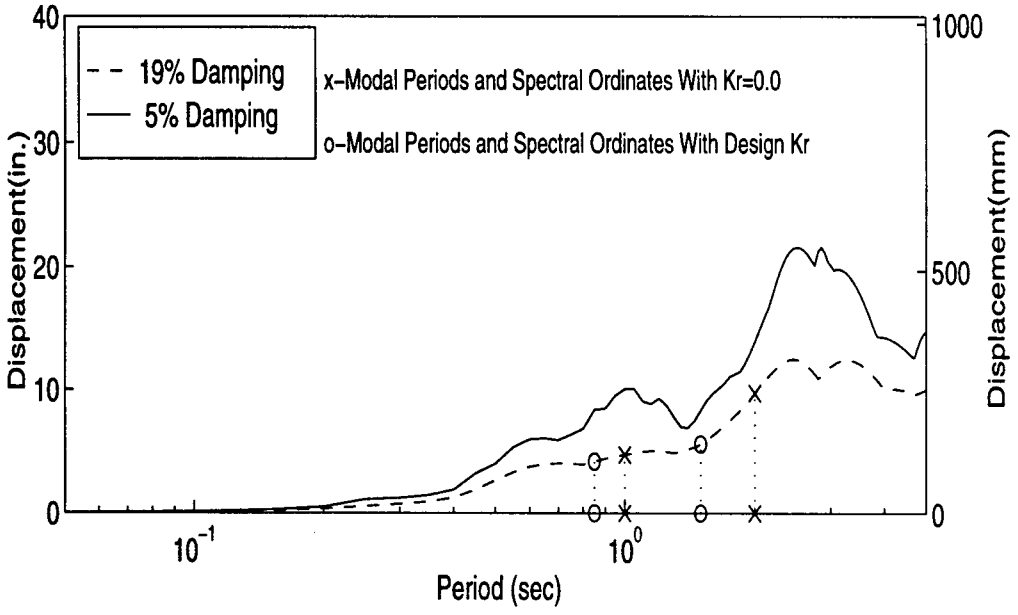

Figure 5.9: Displacement Response Spectrum for 1940 El Centro Earthquake (S00E Component), Showing Spectral Ordinates for First and Last Steps of Example 5.1.

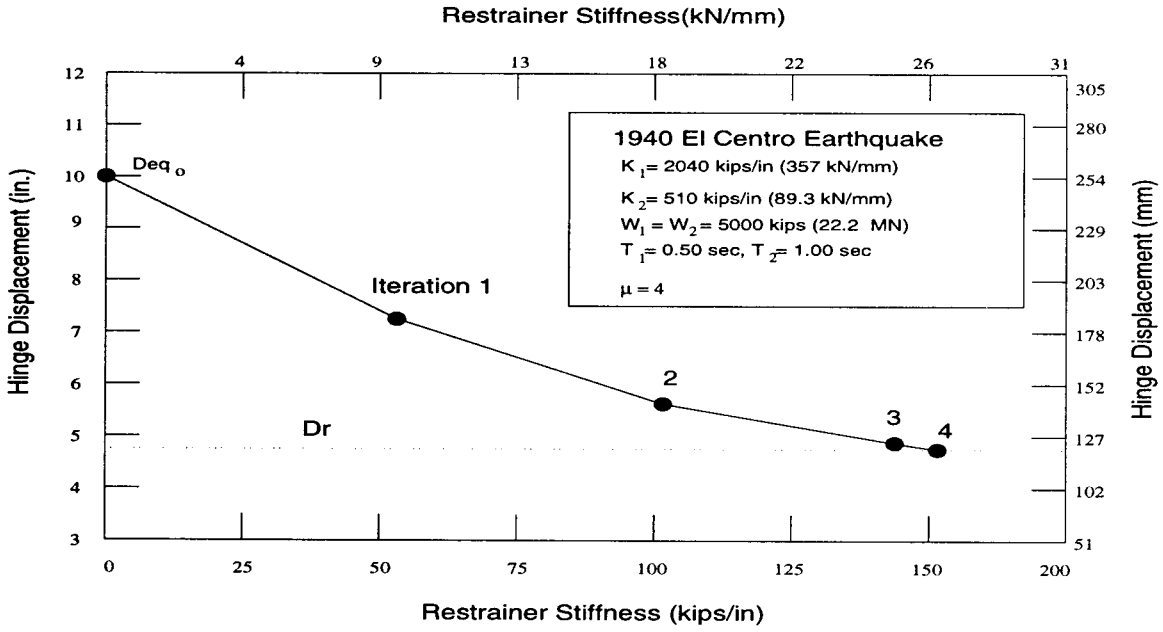

Figure 5.10: Hinge Displacement For Each Iteration of Example 5.1 for 1940 El Centro Earthquake (S00E Component).

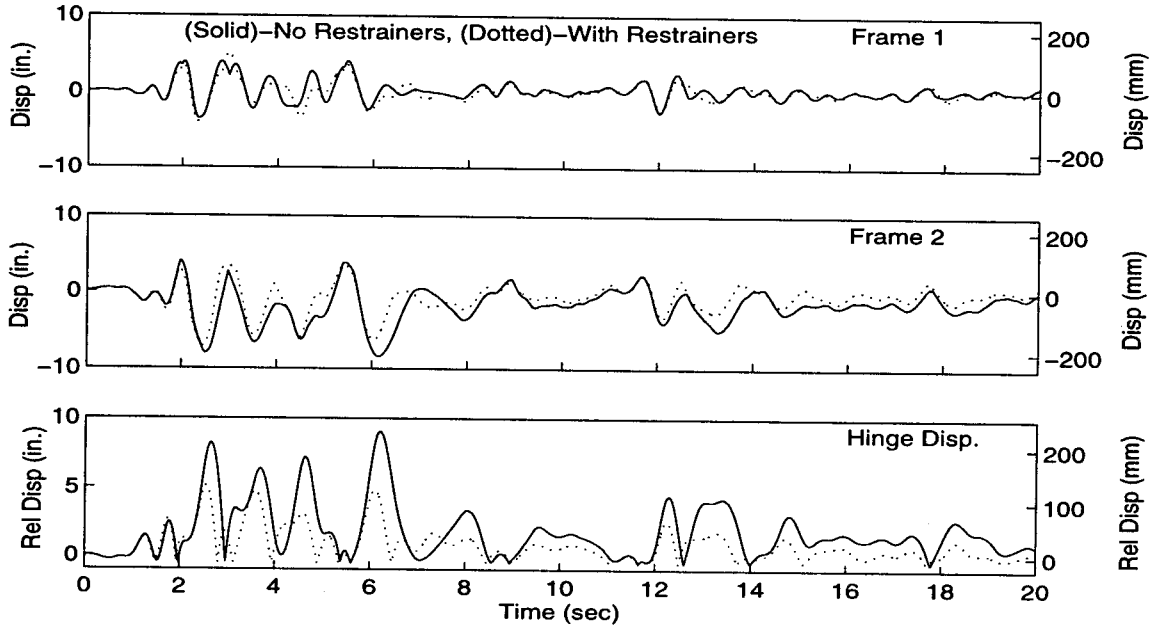

Figure 5.11: Response History for Two Frames Subjected to 1940 El Centro Earthquake (S00E Component) Using Restrainers Determined in Example 5.1.

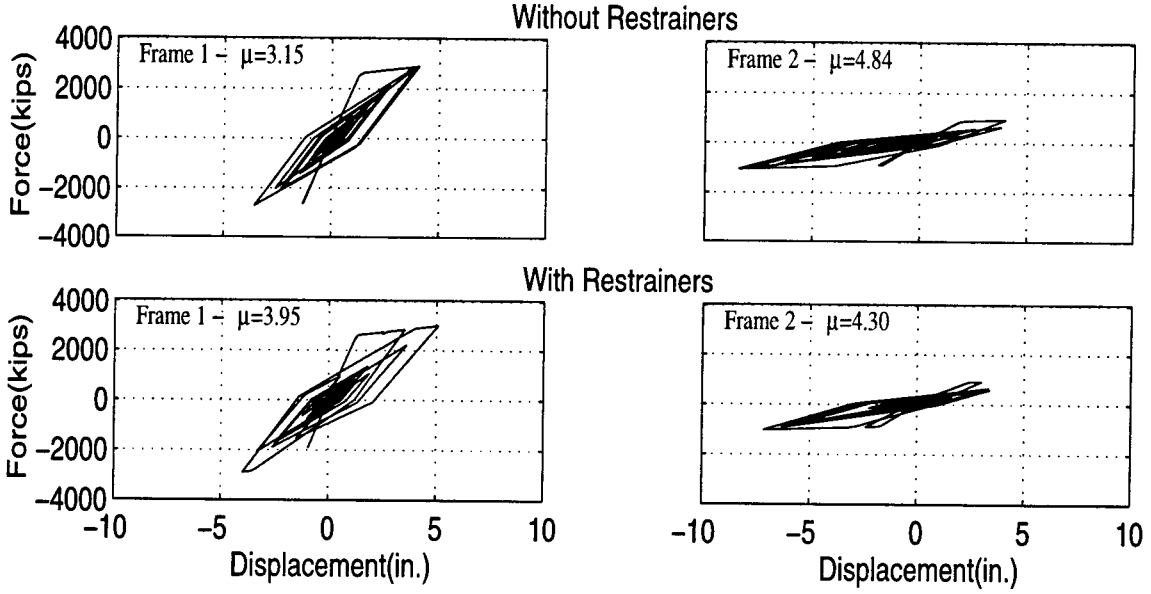

Figure 5.12: Force-Displacement Relationship for Two Frames Subjected to 1940 El Centro Earthquake (S00E Component) Using Restrainers Determined in Example 5.1.

properties of the frames for this analysis. A frame period ratio of 0.40 is evaluated resulting in an initial hinge displacement of 15.0 in. (381 mm). Six iterations are required to limit the hinge displacement to 4.70 in. (119 mm). This corresponds to a restrainer stiffness of 290 kips/in (50.8 kN/mm), approximately 35 restrainers.

Figure 5.15 shows the response history for the two frames from nonlinear analysis. Large relative hinge displacements occur following impact of the frames. The largest displacement, 15.0 in. (381 mm), occurs following impact at approximately 4 seconds into the response. The restrainers are very effective in limiting hinge displacement for this example. Using the restrainers from the design procedure, the relative hinge displacement is reduced to 3.90 in. (100 mm).

Figure 5.16 shows the force-deformation relationship for the frames subjected to the Sylmar record. Without restrainers, the ductility demands are increased by 40% in frame 1 and decreased by 5% in frame 2 relative to the target $\mu = 4$ for the individual frames. With restrainers, the ductility demands increase by 63% in frame 1 and decrease further by 30% in frame 2 from the initial target ductility of 4. The stiffer frame 1 limits the more flexible frame 2, and the more flexible frame 2 pounds and pulls on the stiffer frame 1, increasing it's response.

5.4 Parameter Study for New Restrainer Design Procedure

The effectiveness of the new restrainer design procedure is verified by a parameter study for a range of typical bridge frames. The results in Chapter 4 demonstrate that the important factors are the frame period ratio, frame target ductility, and the T_2/T_g ratio. The ranges of these parameters used to verify the design procedures are shown in table 5.1. The friction force is 100 kips (445 kN), and the coefficient of restitution is e=0.80.

In the evaluation of the design procedure, the restrainer slack and gap are selected to be a function of the hinge displacement without restrainers, D_{eq_o}, determined from a linear model (see equation 5.9). This is useful because it eliminates the amplitude of the ground motion as a factor when examining the effectiveness of the restrainers.

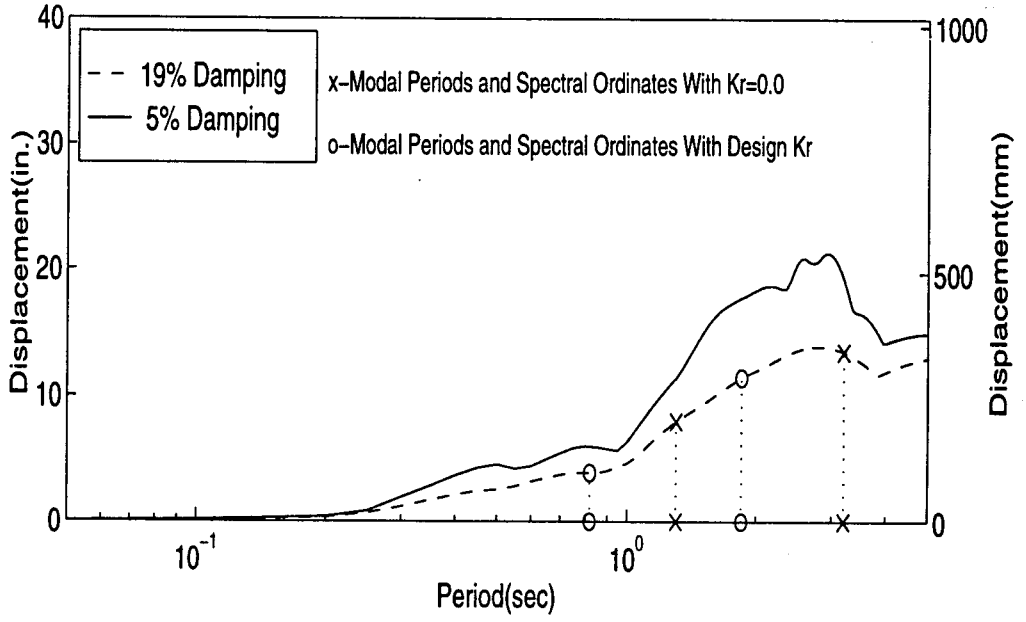

Figure 5.13: Displacement Response Spectrum for 1994 Northridge Earthquake (Sylmar Hospital Free-Field Record) Showing Spectral Ordinates for First and Last Step of Symlar Design Example.

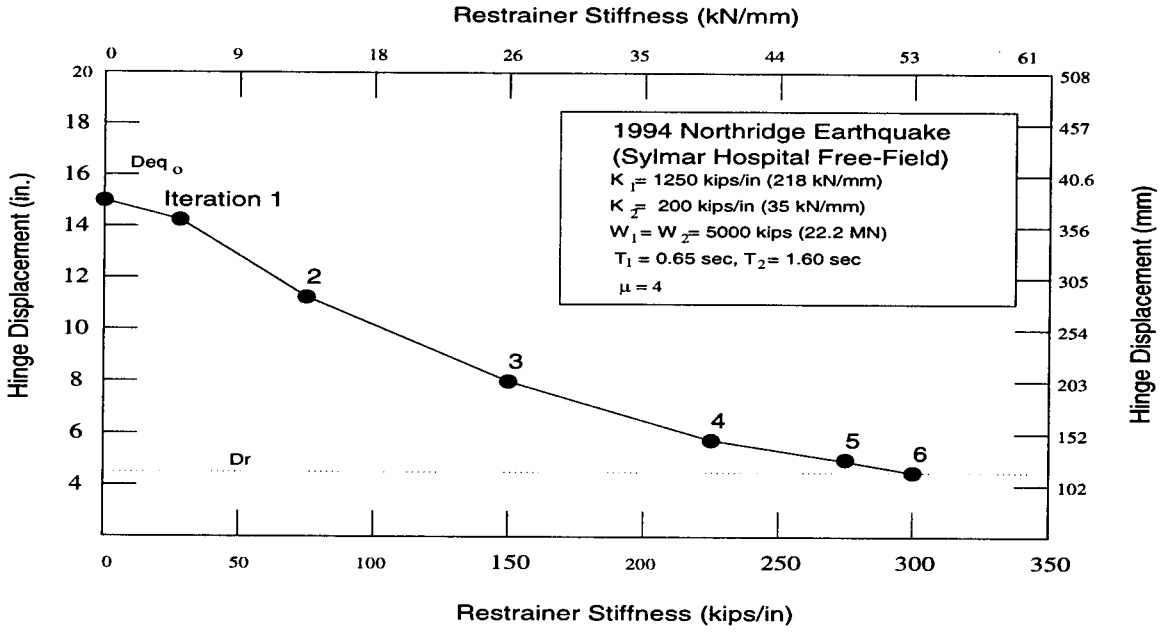

Figure 5.14: Hinge Displacement for Each Iteration of 1994 Northridge Earthquake (Sylmar Hospital Free-Field Record) Design Example.

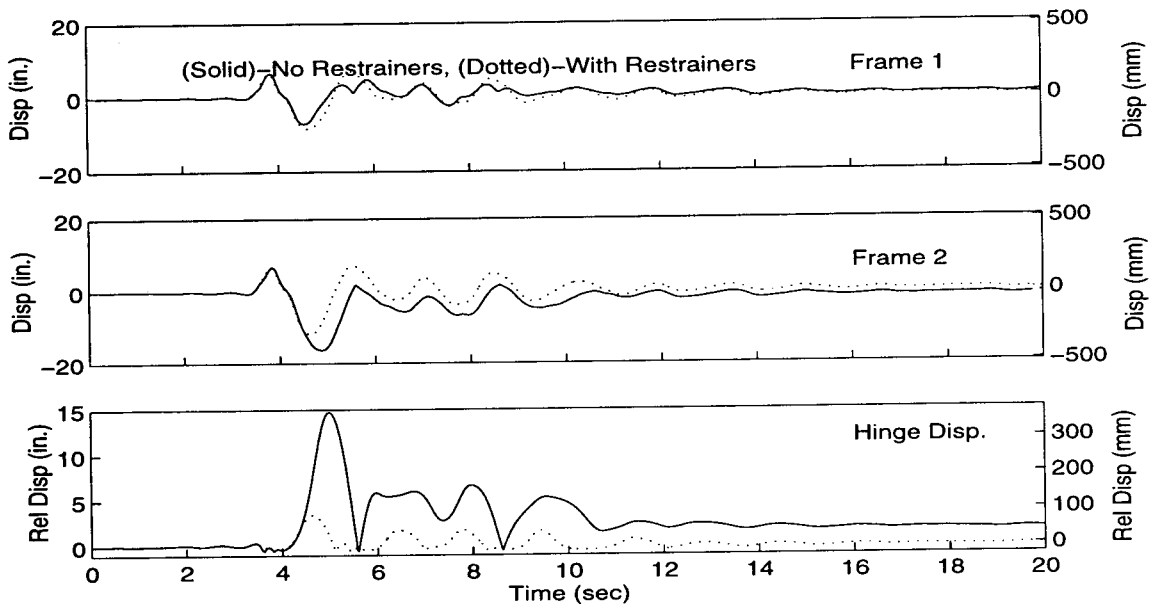

Figure 5.15: Response History for Two Frames Subjected to 1994 Northridge Earthquake (Sylmar Hospital Free-Field Record) Using Restrainers Determined from Design Procedure.

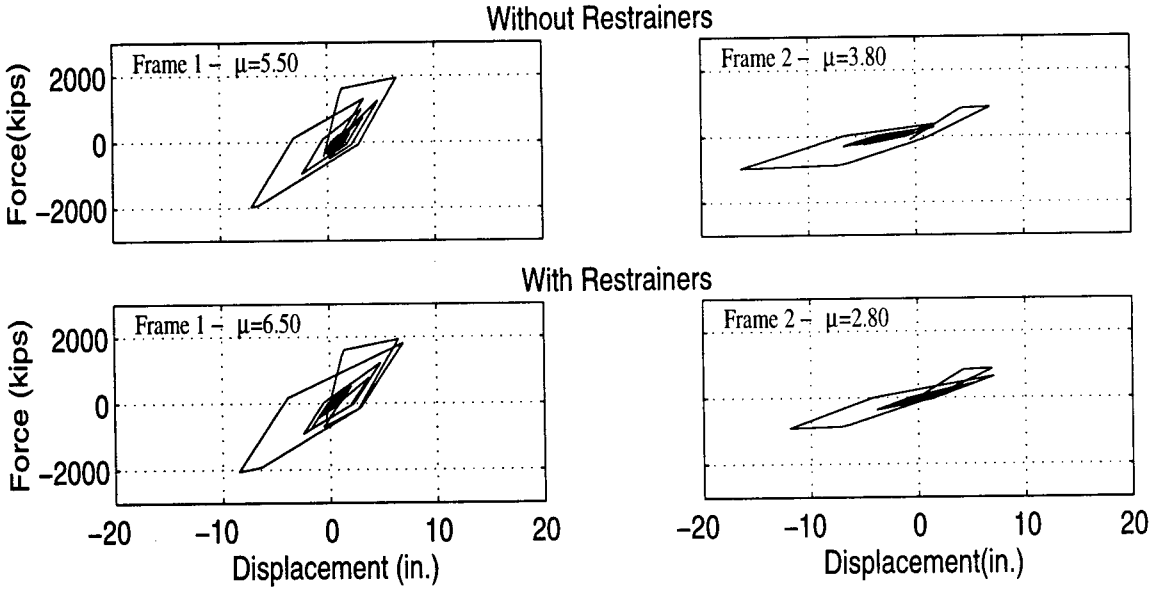

Figure 5.16: Force-Displacement Relationship for Two Frames Subjected to 1994 Northridge Earthquake (Sylmar Hospital Free-Field Record) Using Restrainers Determined from Design Procedure.

Table 5.1: Parameters and Range of Values for Study

Parameter	Values
$\frac{T_1}{T_2}$: Structure Period Ratio	0.3, 0.4, 0.5, 0.6, 0.7, 0.8, 0.9, 0.98
μ_i : Ductility Factor	1, 2, 4, 6
$\frac{T_2}{T_g}$: Input Period Ratio	0.5, 1.0, 2.0, 4.0, 6.0

For example, for low amplitude ground motions, it is possible for the restrainer slack to be greater than the hinge displacement, thereby not engaging the restrainers. By making the restrainer slack and gap a ratio of the initial hinge opening, the restrainers are engaged, and a comparison among different cases is meaningful.

The new restrainer design procedure is used to calculate the required restrainer stiffness to limit hinge displacement to a prescribed value, D_r. The restrainer stiffness predicted by the new procedure is then used in a nonlinear time history analysis to determine the actual maximum hinge displacement. The accuracy of the new procedure is presented in terms of the normalized hinge displacement, which is a ratio of the maximum hinge displacement obtained from the nonlinear analysis to the target hinge displacement. The ground motions are scaled to 0.70g, and applied in both longitudinal directions to account for directionality effects.

5.4.1 Results of Restrainer Design Procedure for 1940 El Centro S00E Earthquake: $T_2/T_g = 1.0$

The new restrainer design procedure is evaluated for the 1940 El Centro Earthquake (S00E component) with D_r/D_{eq_0} values of 0.20 and 0.50. Table 5.2 lists the hinge displacement without restrainers, the target displacement, and the design restrainer stiffness as a function of the frame period ratio. It should be noted that, in general, D_{eq_0} is a function of the design ductility, but in this presentation, D_r, is based on D_{eq_o} for elastic frames.

The restrainer stiffness required to limit hinge displacement ranges from a maximum of 3420 kips/in (595 kN/mm) for elastic frames ($T_1/T_2 = 0.30$) to less than

100 kips/in (17.5 kN/mm) for frames with a target ductility of 6 and $T_1/T_2 > 0.70$. An increase in the target ductility results in a reduction in the required restrainer stiffness. This trend is due to (1) the decrease in the effective stiffness of the frames as they yield, and (2) an increase of in-phase response because of increased energy dissipation of yielding frames. An increase in the target ductility from 1 to 4 results in a decrease in the required restrainer stiffness of approximately 75% for the entire range of frame period ratios. The effect of frame ductility in reducing the relative hinge displacement is highlighted in the parameter study in Chapter 4.

The normalized hinge displacement ranges from a value of 0.30 to 1.30, as illustrated in figure 5.17. For highly out-of-phase frames ($T_1/T_2 < 0.50$), pounding produces large hinge openings, which are not accounted for in the linearized analytical model. For frame period ratios between 0.70 and 1.0, the procedure tends to be slightly conservative. This is primarily due to the effect of pounding and friction. For frames which are nearly in-phase, pounding disrupts the build-up of resonant response. In addition, friction has a larger effect in this period range, because the total force required to limit hinge displacement is smaller. For frames in the moderate frame period ratio range ($0.50 < T_1/T_2 > 0.70$), the procedure works very well.

The case with a larger limiting displacement, $D_r/D_{eq_0} = 0.50$, results in a significant reduction in the required restrainer stiffness compared to the case with $D_r/D_{eq_0} = 0.20$, as illustrated in table 5.3 and figure 5.18. The restrainer stiffness ranges from approximately 1000 kips/in (175 kN/mm) for elastic frames ($T_1/T_2 = 0.30$) to less than 50 kips/in (87.5 kN/mm) for frames with a design ductility of 6 and $T_1/T_2 > 0.70$. The procedure is very effective in limiting hinge displacements as evidenced by the normalized displacement values in the range 0.05-1.15 in figure 5.18.

5.4.2 Results of Restrainer Design Procedure for 1994 Northridge Earthquake (Sylmar Hospital Free-Field Record): $T_2/T_g = 1.0$

As observed in tables 5.4 and 5.5, the hinge displacement without restrainers for the 1994 Sylmar Hospital free-field record is approximately 50-60% greater than the 1940 El Centro record. In general, the results for the 1994 Sylmar record show similar

Table 5.2: Results of Restrainer Design Procedure for 1940 El Centro Earthquake (S00E Component) For $D_r = 0.20 D_{eq_0}$, $T_2/T_g = 1$.

			Restrainer Stiffness, kips/in (kN/mm)			
T_1/T_2	D_{eq_0} (in.)	D_r (in.)	$\mu = 1$	$\mu = 2$	$\mu = 4$	$\mu = 6$
0.30	10.1	2.03	3420 (600)	2590 (454)	1230 (214)	902 (158)
0.40	10.2	2.05	3040 (533)	1430 (249)	785 (137)	546 (95.6)
0.50	10.8	2.16	1730 (303)	926 (162)	479 (83.8)	385 (67.4)
0.60	11.5	2.31	1120 (196)	626 (110)	287 (50.2)	258 (45.1)
0.70	11.3	2.26	909 (159)	372 (65.2)	197 (34.5)	183 (31.9)
0.80	11.2	2.24	536 (93.8)	190 (33.2)	118 (20.8)	108 (18.8)
0.90	9.60	1.92	375 (65.6)	89.4 (15.7)	55.1 (9.64)	47.0 (8.22)
0.98	2.79	0.56	208 (36.4)	20.2 (3.53)	26.1 (4.56)	22.1 (3.86)

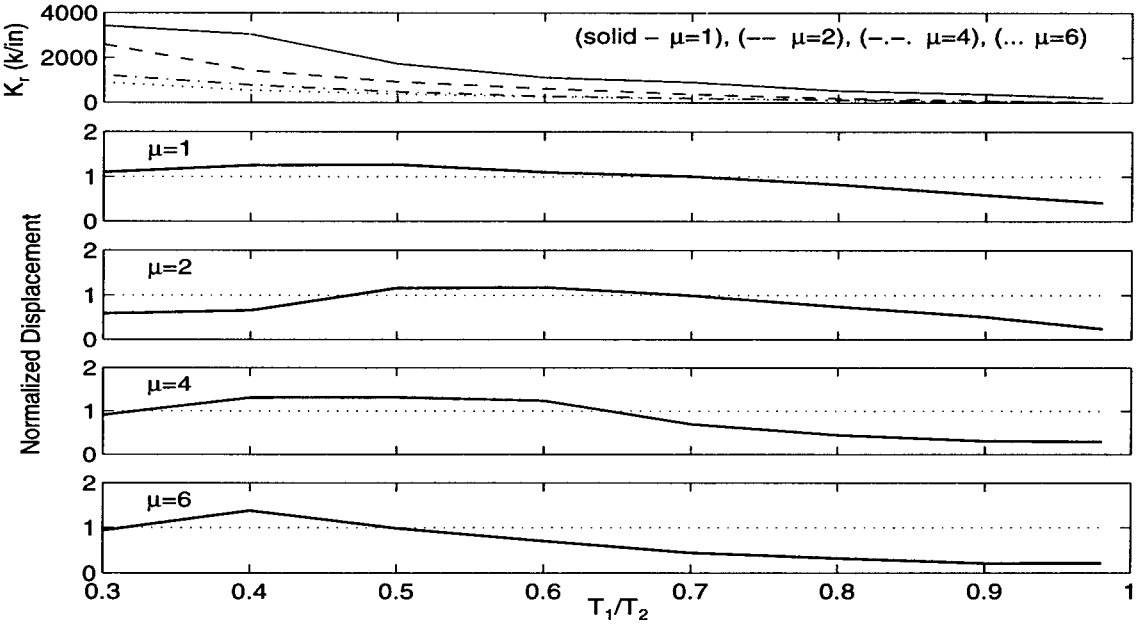

Figure 5.17: Restrainer Design Procedure: 1940 El Centro Earthquake (S00E Component), D_r/D_{eq}=0.20, T_2/T_g=1.0.

Table 5.3: Results of Restrainer Design Procedure for 1940 El Centro Earthquake (S00E Component) For $D_r = 0.50 D_{eq_0}$, $T_2/T_g = 1$.

			Restrainer Stiffness kips/in (kN/mm)			
T_1/T_2	D_{eq_0} (in.)	D_r (in.)	$\mu = 1$	$\mu = 2$	$\mu = 4$	$\mu = 6$
0.30	10.1	5.07	951 (166)	411 (71.9)	204 (35.8)	208 (36.5)
0.40	10.2	5.11	587 (102)	387 (67.8)	162 (28.4)	164 (28.7)
0.50	10.8	5.39	472 (82.6)	265 (46.4)	110 (19.3)	123 (21.7)
0.60	11.5	5.77	420 (73.5)	103 (18.1)	71.8 (12.6)	79.0 (13.8)
0.70	11.3	5.67	333 (58.3)	60.2 (10.5)	42.0 (7.35)	54.1 (9.46)
0.80	11.2	5.60	212 (37.0)	40.0 (7.00)	12.8 (2.23)	22.2 (3.88)
0.90	9.60	4.81	126 (22.1)	20.0 (3.50)	10.1 (1.76)	8.10 (1.42)
0.98	2.79	1.40	111 (19.5)	10.0 (1.75)	5.1 (.89)	3.20 (0.56)

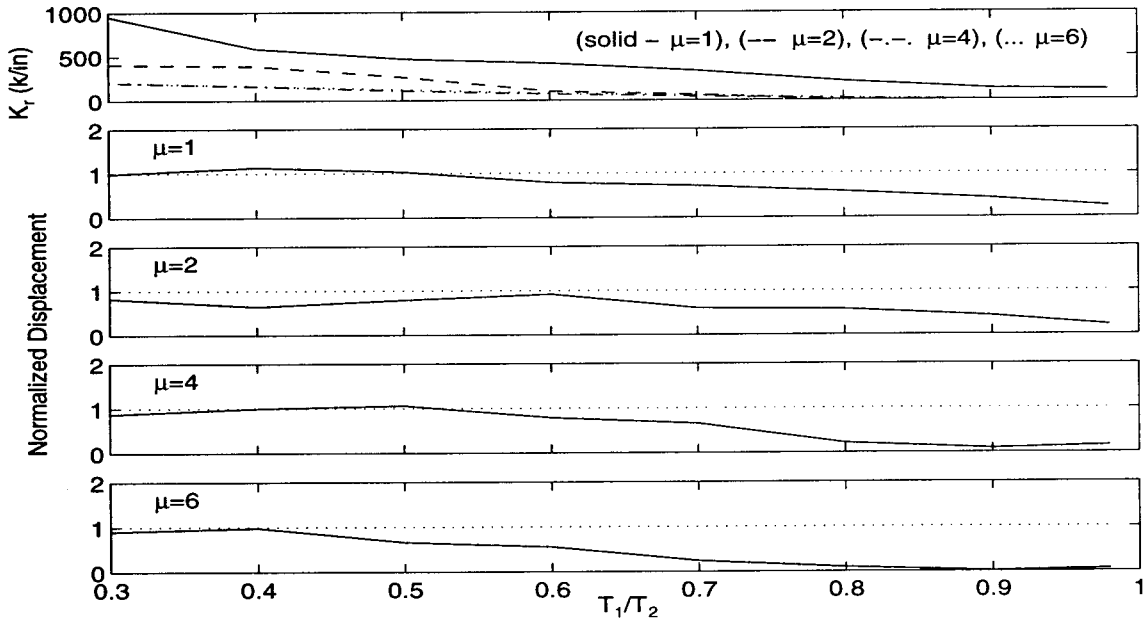

Figure 5.18: Restrainer Design Procedure: 1940 El Centro Earthquake (S00E Component), D_r/D_{eq}=0.50, T_2/T_g=1.0.

trends to the 1940 El Centro record, as shown in figure 5.19 for $D_r/D_{eq_0} = 0.20$. However, for the case with $D_r/D_{eq_o} = 0.50$, the required restrainer stiffness determined from the procedure shows different trends from the previous section. Typically, an increase in the target ductility results in a decrease in the restrainer stiffness. For this earthquake record, however, the required restrainer stiffness is greater for yielding frames than for elastic frames with frame period ratios less than 0.50. This is because the effect of an increased hinge opening, due to an increase in frame displacements (for yielding frames), is greater than the opposing effect of a reduction in the effective frame stiffness when determining the required restrainer stiffness. The procedure works well in predicting the required restrainer stiffness to limit the response, as evidenced by the normalized displacements, which are less than 1.1 for cases in this example, as shown in figure 5.20.

5.4.3 Parameter Study for Restrainer Design Procedure with T_2/T_g=0.5, and 2 for 1940 El Centro Record

The new procedure is evaluated for the 1940 El Centro earthquake (S00E component) with values of T_2/T_g equal to 0.50 and 2.0 as illustrated in figures 5.21 and 5.22. In general, there are no differences between cases with different T_2/T_g ratios. However, the restrainer stiffnesses are significantly different for $T_2/T_g = 0.50$ and $T_2/T_g = 2.0$, which is due to the different frame stiffnesses. The cases for different T_2/T_g show similar trends, and, most importantly, the procedure is effective for all values of T_2/T_g.

5.4.4 Parameter Study for Restrainer Design Procedure: Results for 26 Ground Motion Records

In this section, the effectiveness of the design procedure is evaluated for 26 earthquake records. The normalized hinge displacement is shown for each earthquake, as well as the mean and mean plus and minus one standard deviation of the normalized hinge displacement from the database of earthquake records. The results are shown for the parameters listed in table 5.1. Although 26 earthquake records are used in the

Table 5.4: Results of Restrainer Design Procedure for 1994 Northridge Earthquake (Sylmar Hospital Free-Field Record) For $D_r = 0.20D_{eq_0}$, $T_2/T_g = 1$.

			Restrainer Stiffness kips/in (kN/mm)			
T_1/T_2	D_{eq_0} (in.)	D_r (in.)	$\mu = 1$	$\mu = 2$	$\mu = 4$	$\mu = 6$
0.30	16.8	3.37	1400 (245)	941 (165)	830 (145)	502 (87.8)
0.40	16.9	3.39	844 (148)	663 (116)	497 (86.9)	401 (70.0)
0.50	17.2	3.45	645 (113)	409 (71.6)	298 (52.2)	300 (52.5)
0.60	17.1	3.42	501 (87.6)	273 (47.8)	194 (34.0)	100 (17.5)
0.70	17.9	3.58	335 (58.6)	162 (28.4)	110 (19.3)	50.1 (8.75)
0.80	18.1	3.63	205 (35.8)	86.1 (15.1)	55.9 (9.78)	30.1 (5.25)
0.90	15.6	3.12	140 (24.4)	43.5 (7.61)	27.4 (4.80)	5.00 (0.88)
0.98	4.52	0.90	79.5 (13.9)	22.4 (3.91)	11.3 (1.98)	1.00 (0.18)

Table 5.5: Results of Restrainer Design Procedure for 1994 Northridge Earthquake (Sylmar Hospital Free-Field Record) For $D_r = 0.50D_{eq_0}$, $T_2/T_g = 1$.

			Restrainer Stiffness kips/in (kN/mm)			
T_1/T_2	D_{eq_0} (in.)	D_r (in.)	$\mu = 1$	$\mu = 2$	$\mu = 4$	$\mu = 6$
0.30	16.8	8.40	238 (41.6)	424 (74.3)	374 (65.4)	300 (52.5)
0.40	16.9	8.45	228 (39.9)	342 (59.9)	240 (42.0)	184 (32.2)
0.50	17.2	8.60	207 (36.2)	231 (40.5)	154 (26.9)	112 (19.5)
0.60	17.1	8.55	162 (28.4)	153 (26.9)	106 (18.5)	73.8 (12.9)
0.70	17.9	8.95	109 (19.1)	100 (17.6)	58.8 (10.3)	37.9 (6.63)
0.80	18.1	9.05	79.0 (13.8)	52.7 (9.21)	24.6 (4.29)	13.7 (2.40)
0.90	15.6	7.80	49.0 (8.59)	14.2 (2.49)	10.4 (1.82)	8.40 (1.47)
0.98	4.52	2.26	45.8 (8.02)	5.00 (0.87)	4.3 (0.75)	2.20 (0.38)

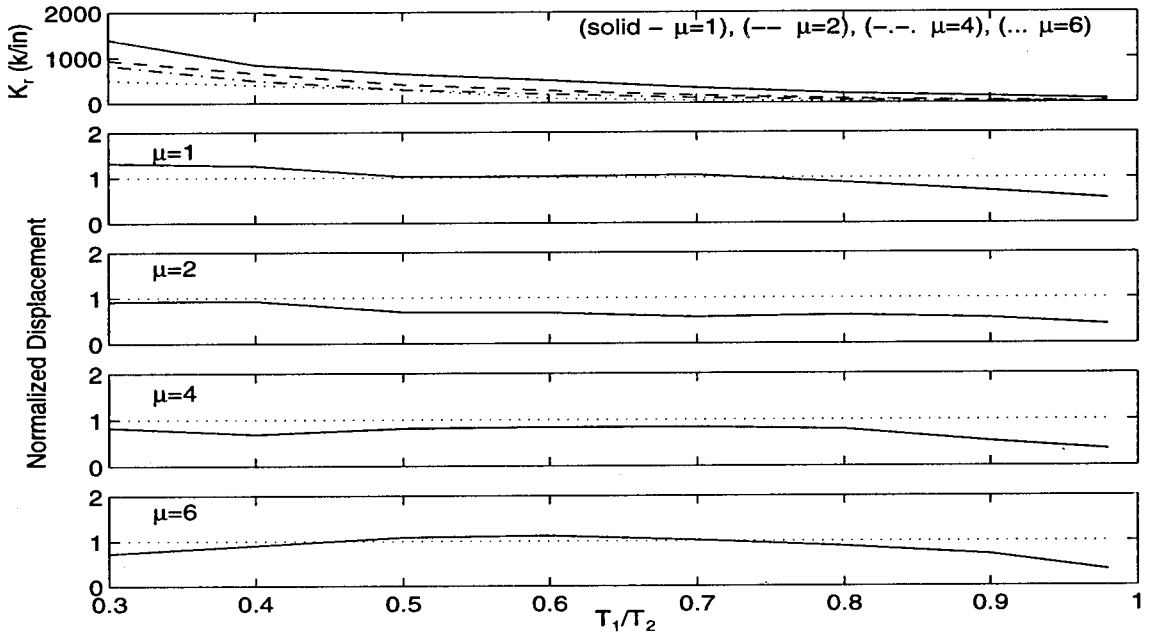

Figure 5.19: Evaluation of Restrainer Design Procedure: 1994 Northridge Earthquake (Sylmar Hospital Free-Field Record), D_r/D_{eq}=0.20, T_2/T_g=1.0.

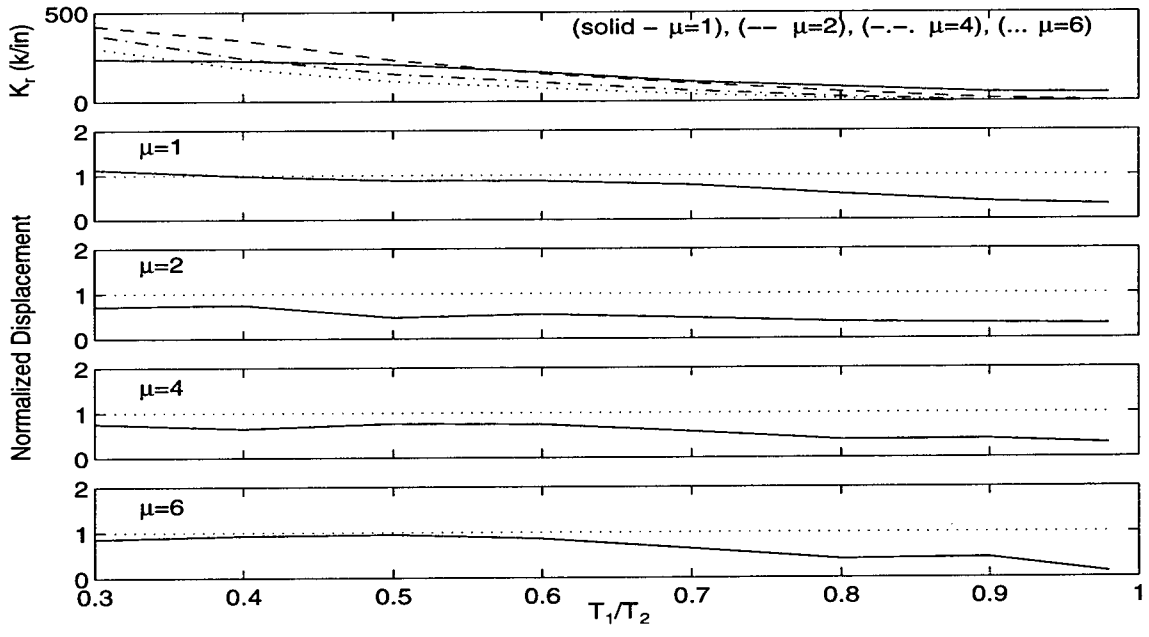

Figure 5.20: Evaluation of Restrainer Design Procedure: 1994 Northridge Earthquake (Sylmar Hospital Free-Field Record), D_r/D_{eq}=0.50, T_2/T_g=1.0.

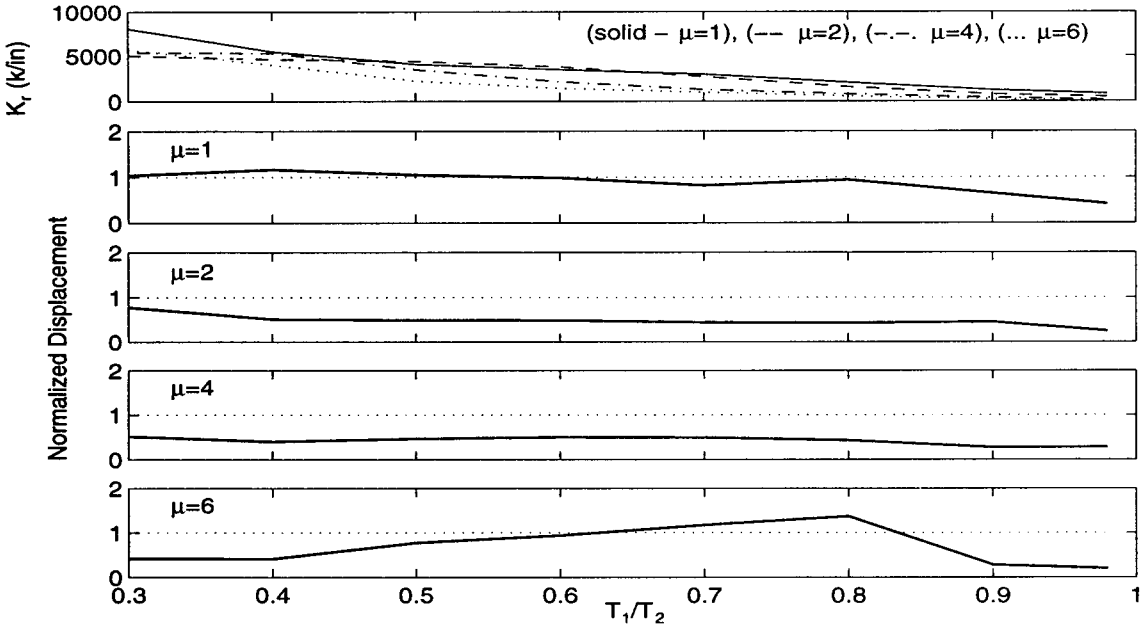

Figure 5.21: Evaluation of Restrainer Design Procedure: 1940 El Centro Earthquake (S00E Component), D_r/D_{eq}=0.20, T_2/T_g=0.50.

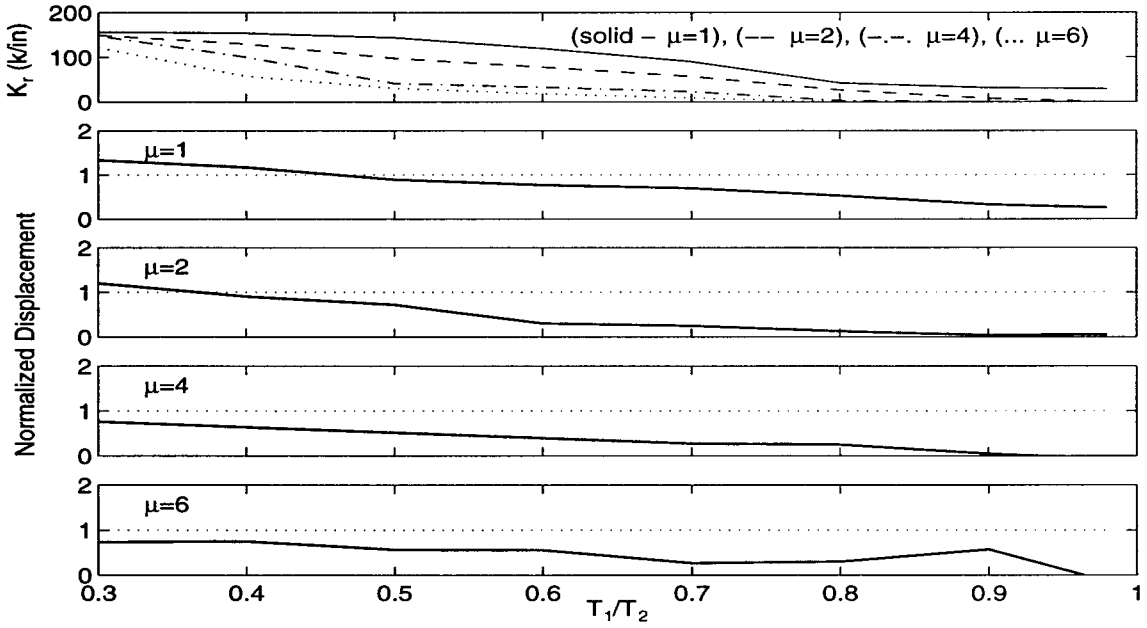

Figure 5.22: Evaluation of Restrainer Design Procedure: 1940 El Centro Earthquake (S00E Component), $D_r/D_{eq} = 0.20$, $T_2/T_g = 2.00$.

study, only a subset are used for each T_2/T_g category. For each value of T_2/T_g, values of T_2 representing realistic frame periods are chosen in the range of 0.20 sec for very stiff frames to 2.30 sec for very flexible frames. Given these values, periods of frame 2 range from 0.60 sec to 2.30 sec for $T_2/T_g = 1.0$. This corresponds to frame 1 periods from 0.18 sec to 2.30 sec. Sixteen ground motions fit this criteria with periods from 0.60 sec to 2.30 sec, and are used in the evaluation. This approach is followed for each value of T_2/T_g.

Figures 5.23 and 5.24 show normalized hinge displacement for $T_2/T_g = 0.50$. The design procedure is slightly unconservative for a few cases with low period ratios, and conservative for frame period ratios approaching unity. As previously mentioned, pounding produces larger displacements for highly out-of-phase frames, particularly for elastic frames. The maximum acceleration in yielding frames is limited by the yield strength of the frames. Therefore, the force transmitted between frames is also limited. The conservative results for the normalized displacement in the period range greater than 0.70 increase for increasing design ductility primarily because of the increased effectiveness of friction.

Figure 5.25 shows the effectiveness of the design procedure for $D_r/D_{eq_0} = 0.20$ and $T_2/T_g = 1.0$. The procedure works well in providing restrainer stiffness to limit hinge displacement. The largest mean and standard deviation are 0.95 and 0.35, respectively, for the case with $\mu = 6.0$ and $T_1/T_2 = 0.50$. For the elastic frames, the procedure is slightly unconservative because of pounding of out-of-phase frames. As the design ductility increases, the scatter between different cases increases, thus producing larger standard deviations. The standard deviation increases from 0.15 for $\mu = 1.0$ to 0.35 for $\mu = 6.0$. The increase in the standard deviation is primarily due to the redistribution of ductility demands as frames pound. Although frames may be designed for a target ductility of 4, the actual ductility can be significantly different as frames pound.

Figure 5.26 shows the results of the parameter study for $D_r/D_{eq_0} = 0.50$ and $T_2/T_g = 1.0$. The results for this study are similar to the case with $D_r/D_{eq_0} = 0.20$, except that the normalized displacements are slightly smaller. The accuracy of the restrainer design procedure is reduced for the case with $D_r/D_{eq_0} = 0.20$. Since the

value of D_r is smaller for $D_r/D_{eq_0} = 0.20$ than for $D_r/D_{eq_0} = 0.50$, a similar error in the value of D_{eq} produces a larger normalized displacement for $D_r/D_{eq_0} = 0.20$.

Figures 5.27 through 5.32 show the results of the parameter study for $T_2/T_g = 2.0$, 4.0, and 6.0. The results show several trends for increasing values of T_2/T_g. As T_2/T_g increases, the normalized displacement of highly out-of-phase frames increases. As T_2/T_g increases, the normalized hinge displacement decreases for frames with period ratios greater than 0.60. Smaller frame stiffnesses require fewer restrainers to limit their displacement. Therefore, the effectiveness of friction is significantly increased leading to smaller normalized hinge displacements.

5.5 Summary of Restrainer Design Procedure

This chapter has presented the new design procedure for hinge restrainers as well as examples and parameter studies to evaluate the effectiveness of the procedure. Overall, the procedure works very well in determining the required number of restrainers to limit hinge displacement to a target value. However, for highly out-of-phase frames ($T_1/T_2 < 0.4$), the procedure is unconservative due to the effects of pounding. Although frames with these characteristics are not common in typical bridges, there are examples of stiff frames near the abutment adjacent to more flexible frames. For cases such as these, a nonlinear analysis may be required to accurately determine the number of restrainers required to limit the hinge displacement.

For nearly in-phase frames ($T_1/T_2 > 0.70$), the new restrainer design procedure is conservative because the effect of friction helps to decrease the hinge displacement, particularly for frames with large target ductilities. However, it is not necessarily recommended that the number of restrainers determined from the procedure for these cases be reduced, since additional restrainers are required to account for uncertainty in the design.

The effect of yielding frames is significant in reducing the required restrainer stiffness to limit hinge displacement. This is very important since for many cases the number of restrainers determined for the case with elastic frames is far more than can realistically be used at a typical hinge. Typical reductions in the number of restrainers for a target ductility of $\mu = 4$ is 50 to 75% compared with elastic frames.

The parameter study illustrated that the procedure is more effective for $D_r/D_{eq0} = 0.50$ than for $D_r/D_{eq0} = 0.20$. It is more difficult to restrain the hinge displacement to smaller values. Typical restrainer design requires limiting the hinge opening to restrainer yield, approximately 4.20 in. (107 mm) for 20 ft restrainers. For these cases, the procedure works very well. For cases where the target displacement is considerably smaller (less than 1.5 in. (38.1 mm)), a small error in the estimate in the number of the restrainers can lead to large normalized hinge displacements.

Given the scatter in the results, it is recommended that the available hinge seat width should be approximately 30% larger than the target hinge displacement. For the typical case with a target displacement of 4.7 in. (119 mm), the available hinge seat width should be approximately 6 in. (152 mm). Given this criteria for the target displacement, there are very few cases in this study in which the maximum hinge displacement would exceed the available hinge seat width.

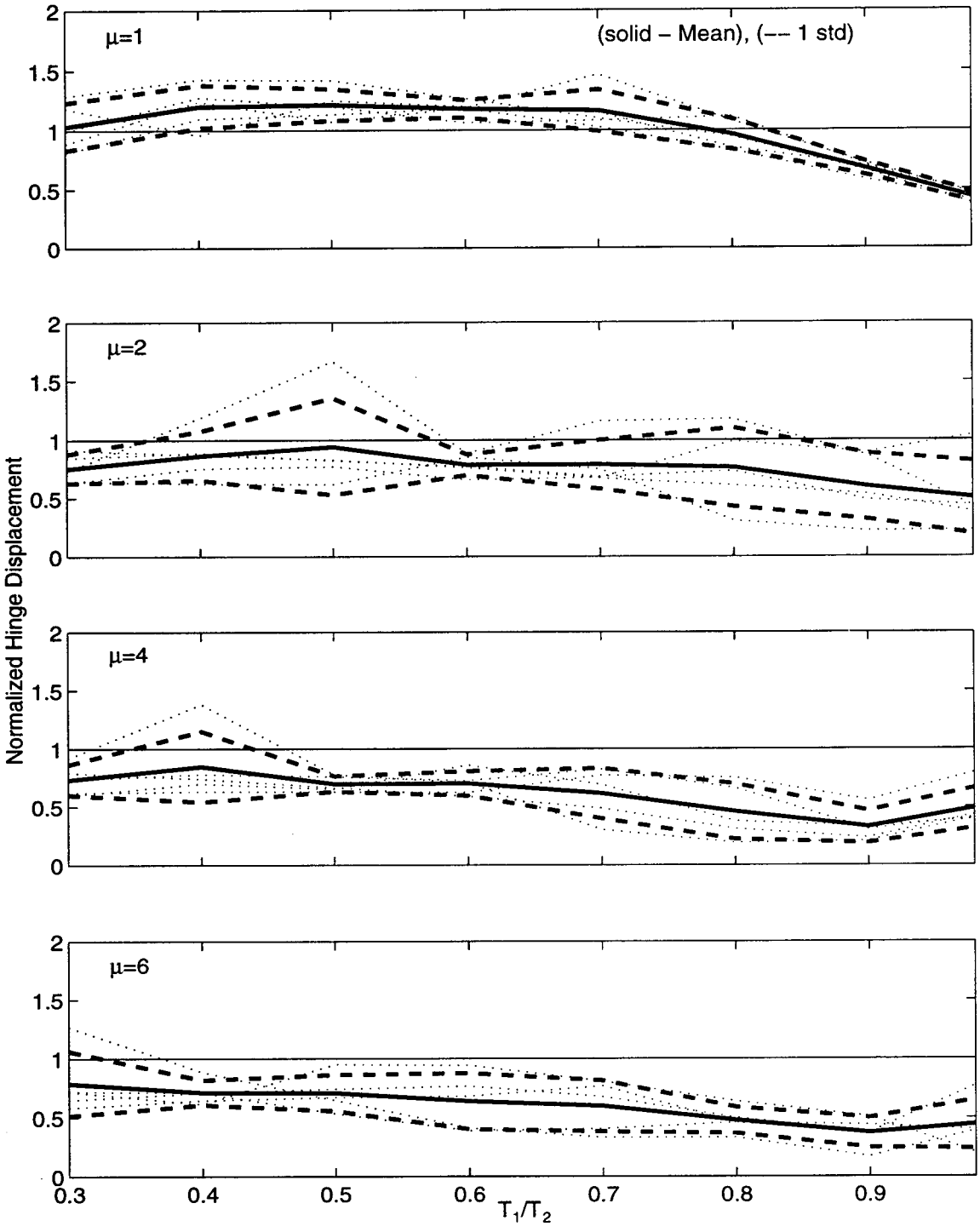

Figure 5.23: Mean ± One Standard Deviation of Normalized Hinge Displacement for Restrainers from Design Procedure (D_r/D_{eq}=0.20, T_2/T_g=0.50).

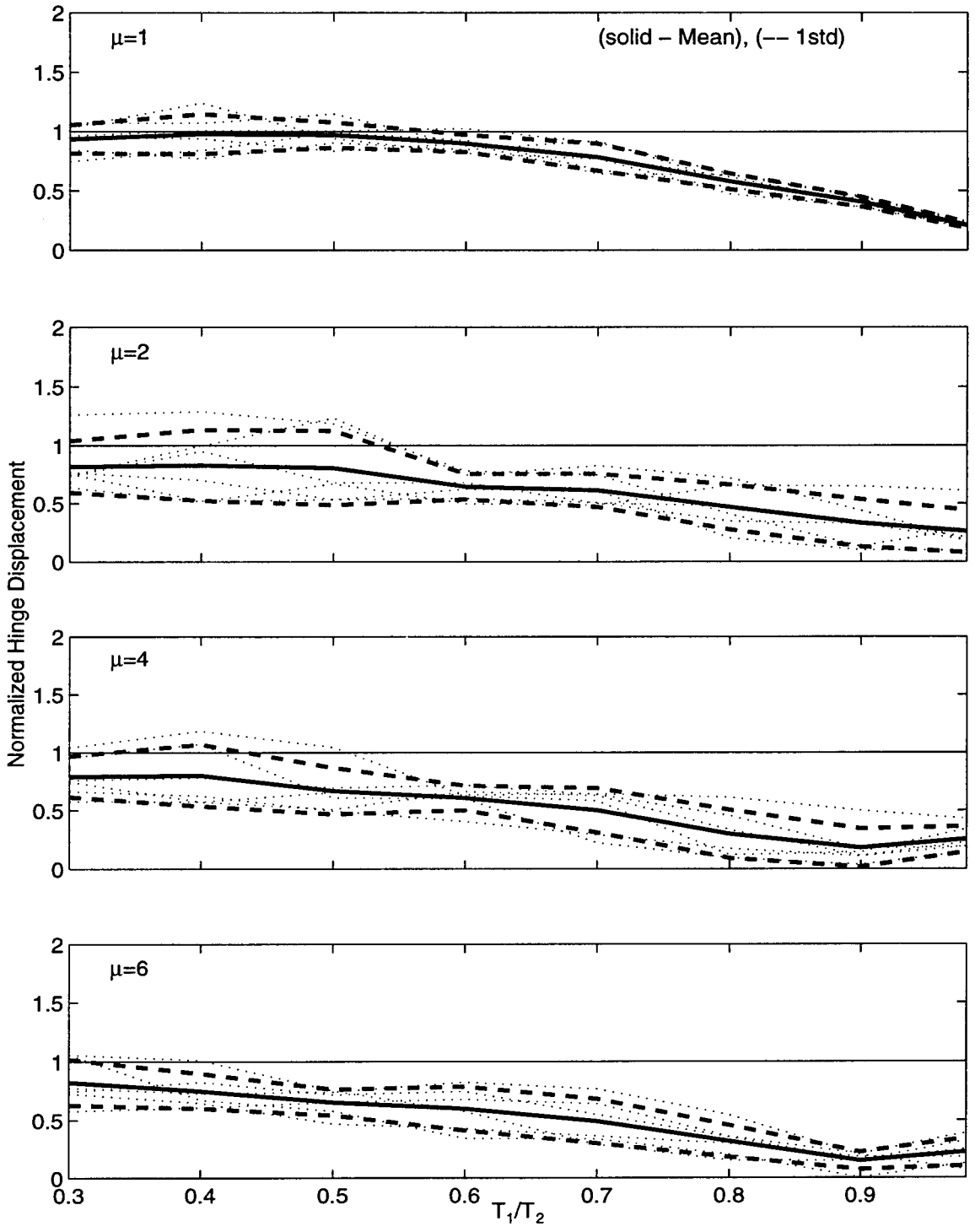

Figure 5.24: Mean ± One Standard Deviation of Normalized Hinge Displacement for Restrainers from Design Procedure (D_r/D_{eq}=0.50, T_2/T_g=0.50).

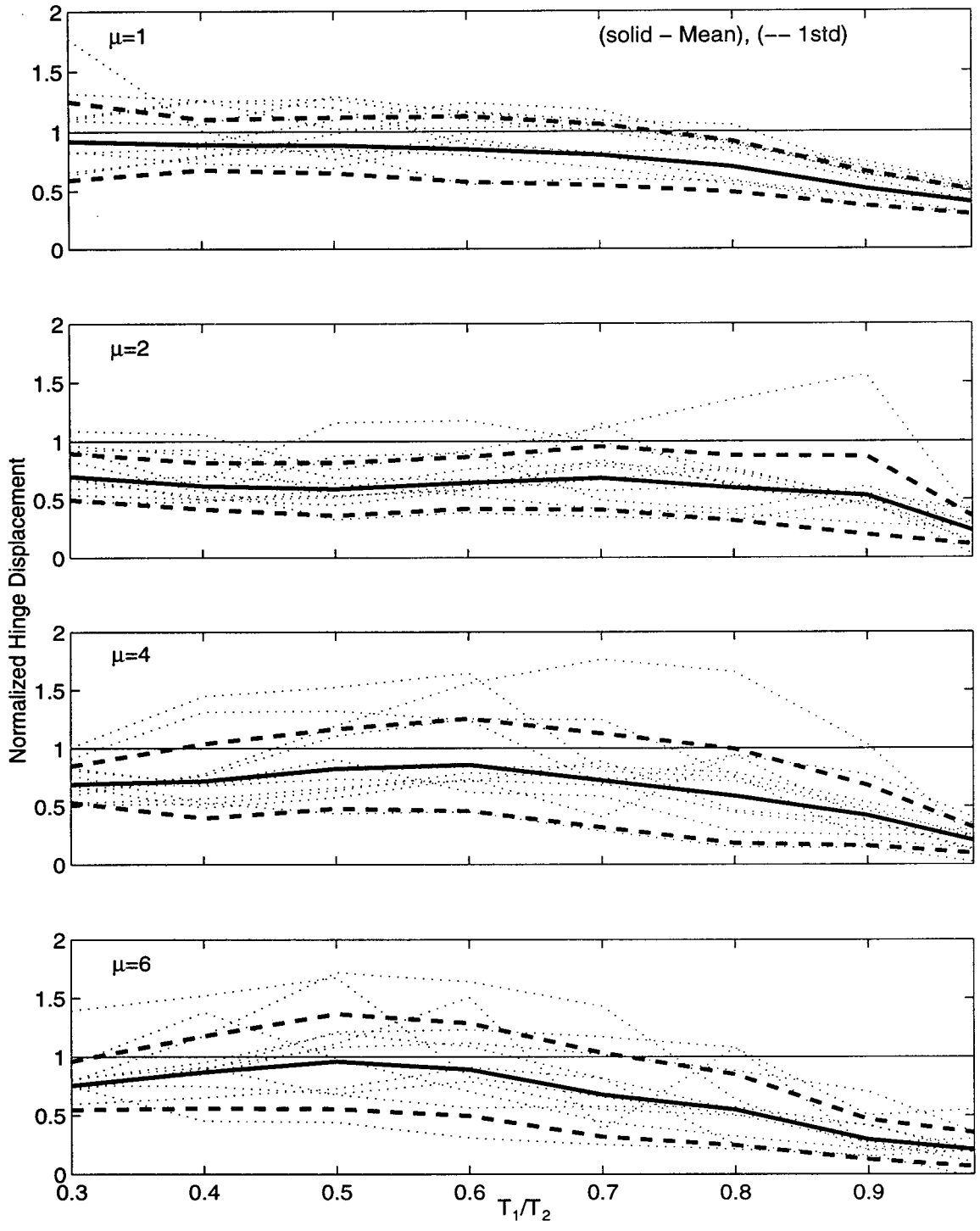

Figure 5.25: Mean ± One Standard Deviation of Normalized Hinge Displacement for Restrainers from Design Procedure (D_r/D_{eq}=0.20, T_2/T_g=1.00).

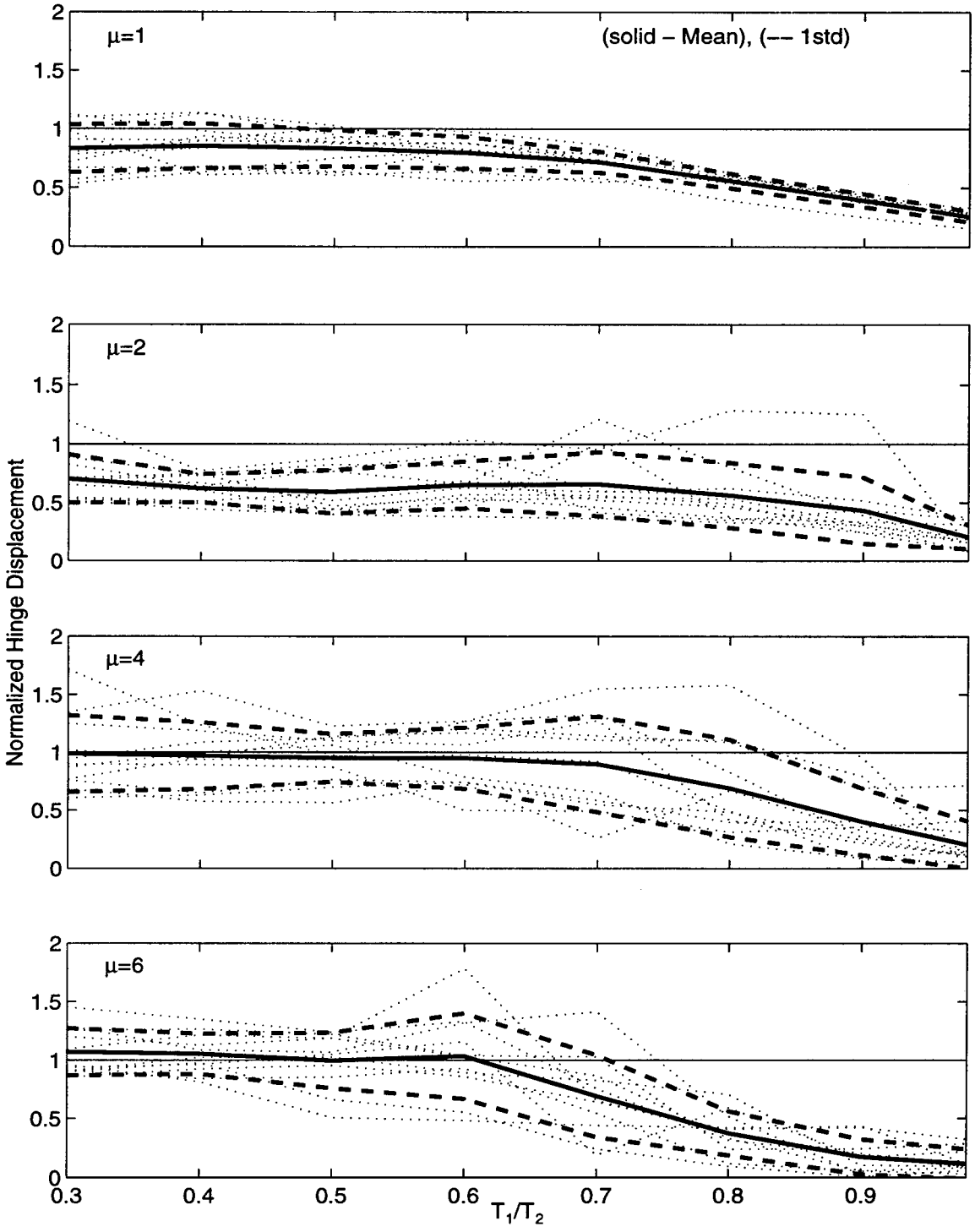

Figure 5.26: Mean ± One Standard Deviation of Normalized Hinge Displacement for Restrainers from Design Procedure (D_r/D_{eq}=0.50, T_2/T_g=1.00).

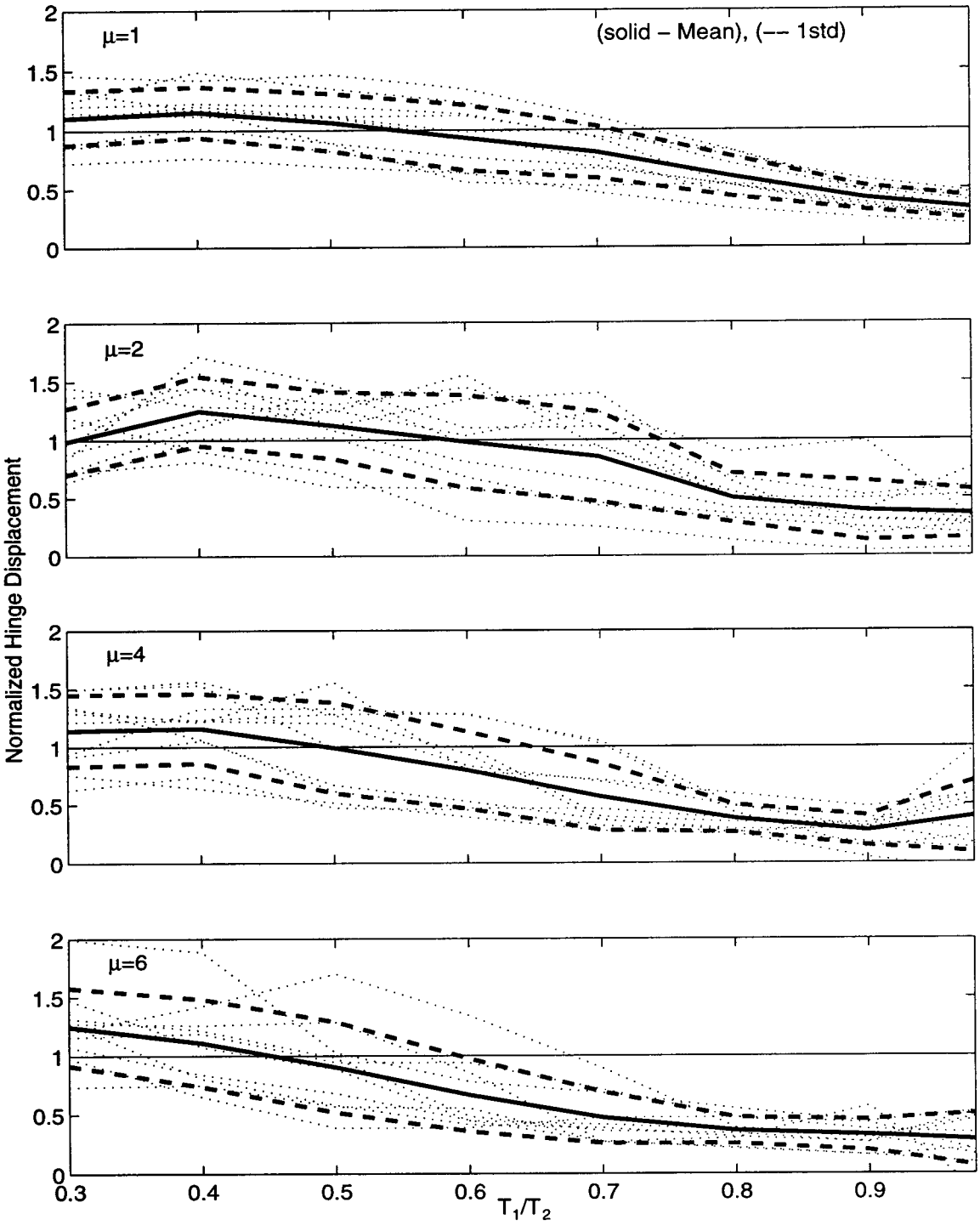

Figure 5.27: Mean ± One Standard Deviation of Normalized Hinge Displacement for Restrainers from Design Procedure (D_r/D_{eq}=0.20, T_2/T_g=2.00).

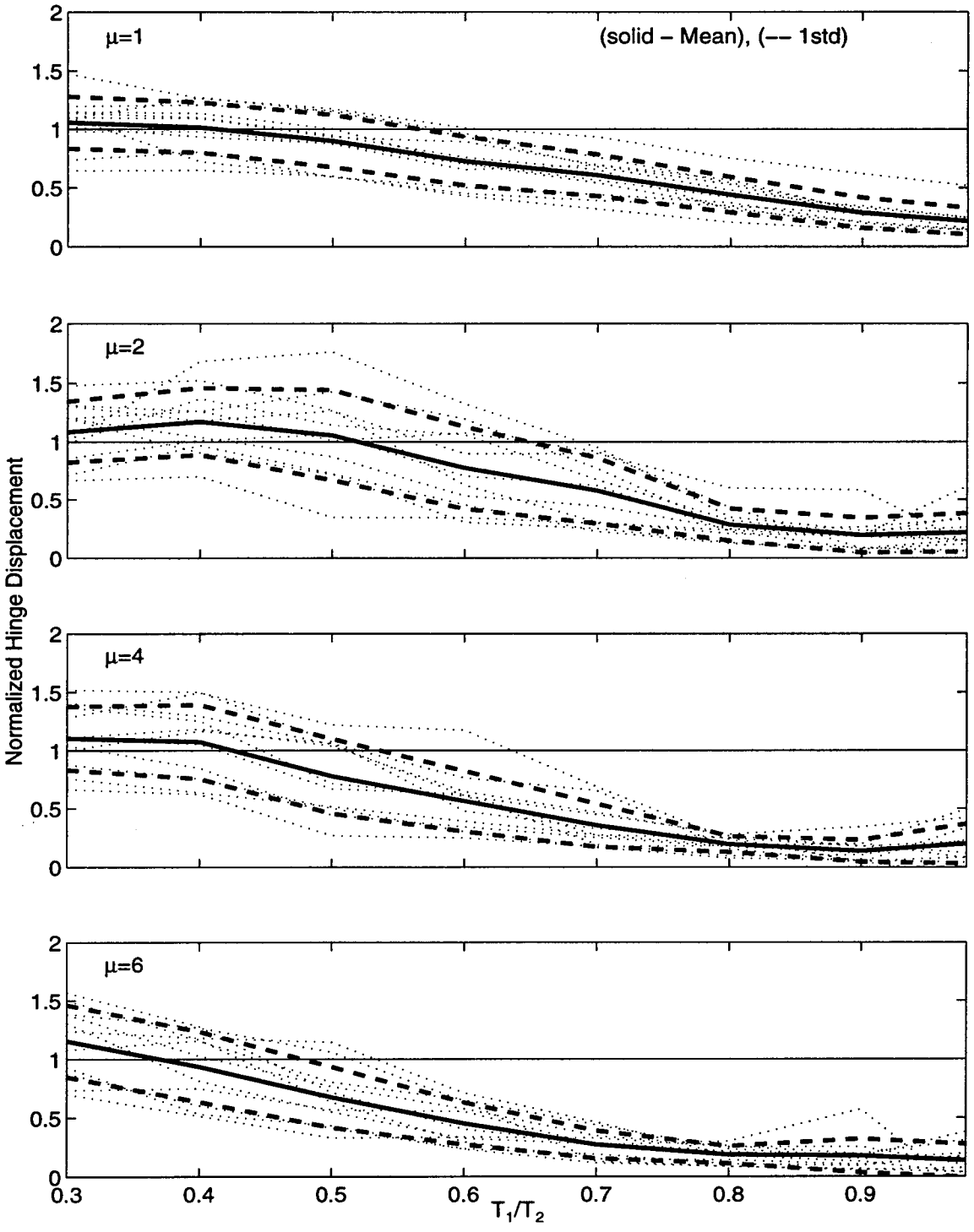

Figure 5.28: Mean ± One Standard Deviation of Normalized Hinge Displacement for Restrainers from Design Procedure (D_r/D_{eq}=0.50, T_2/T_g=2.00).

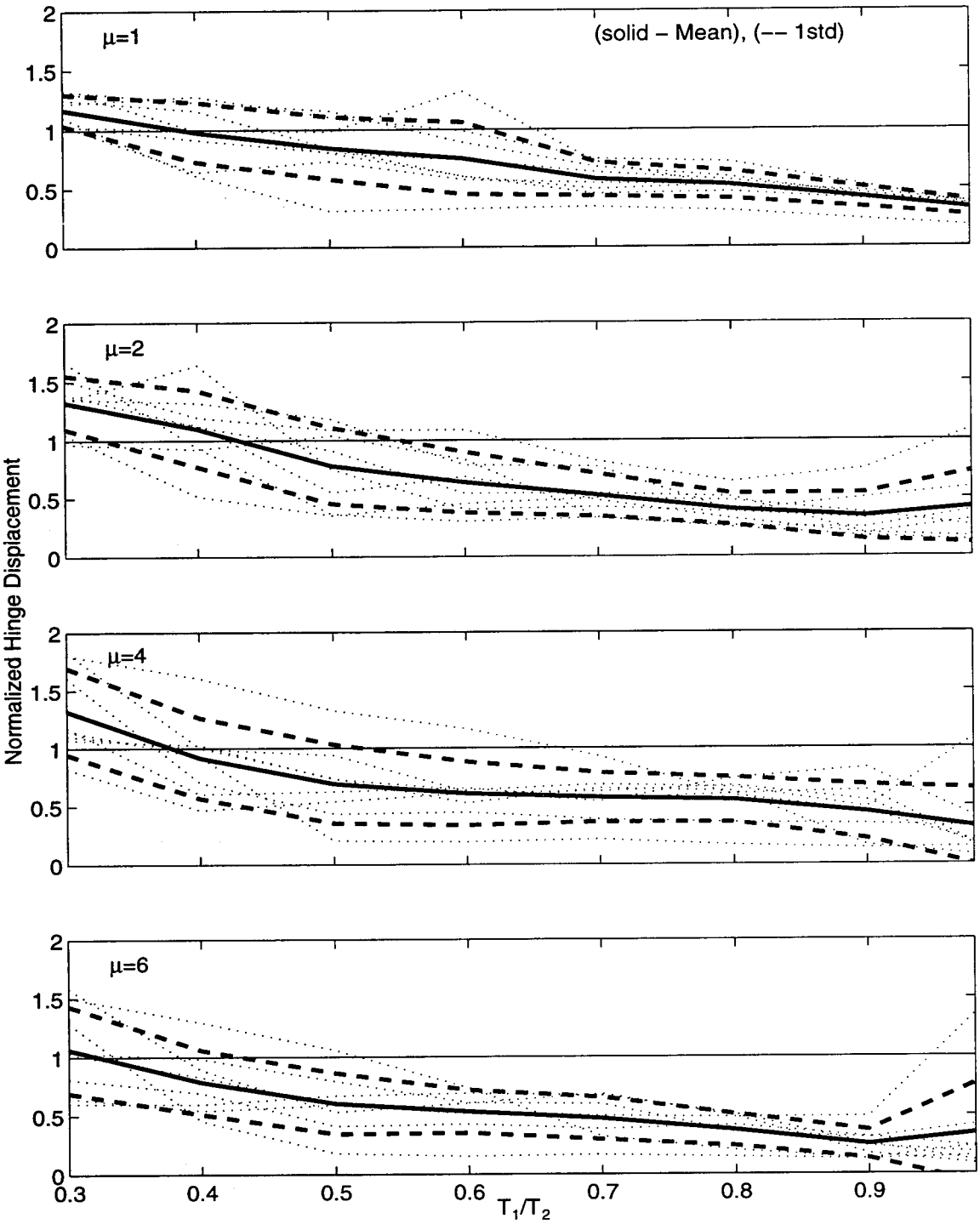

Figure 5.29: Mean ± One Standard Deviation of Normalized Hinge Displacement for Restrainers from Design Procedure (D_r/D_{eq}=0.20, T_2/T_g=4.00).

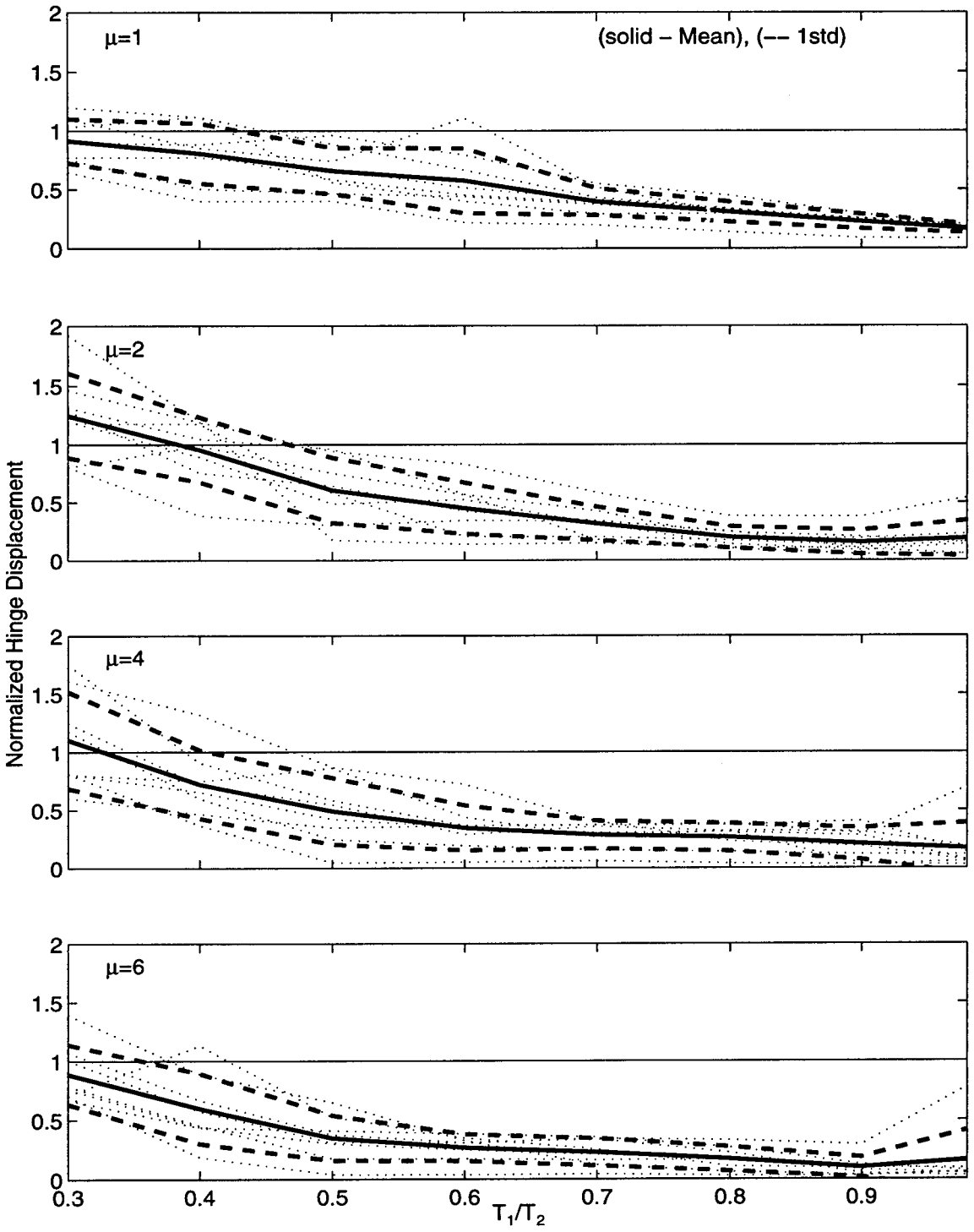

Figure 5.30: Mean ± One Standard Deviation of Normalized Hinge Displacement for Restrainers from Design Procedure (D_r/D_{eq}=0.50, T_2/T_g=4.00).

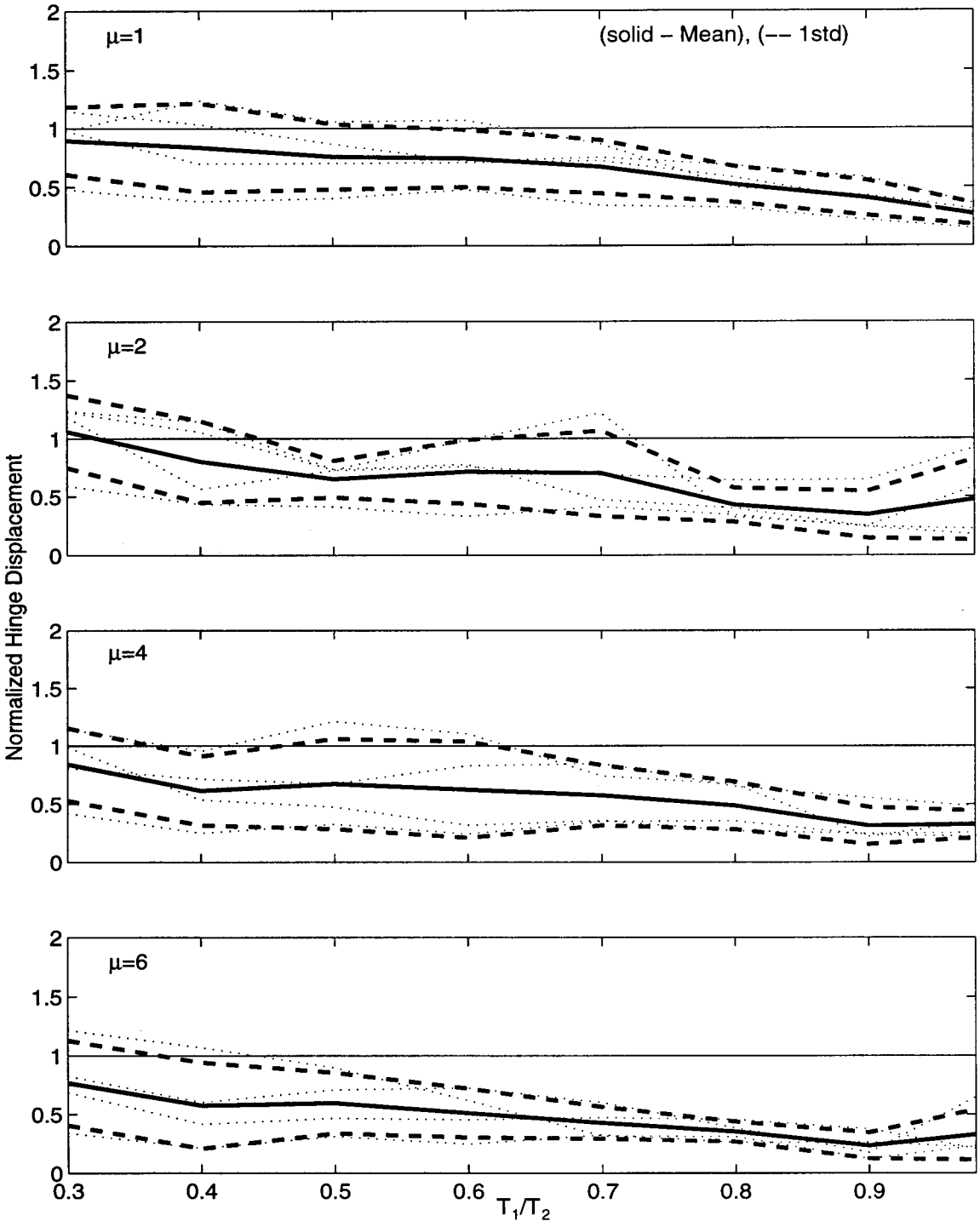

Figure 5.31: Mean ± One Standard Deviation of Normalized Hinge Displacement for Restrainers from Design Procedure (D_r/D_{eq}=0.20, T_2/T_g=6.00).

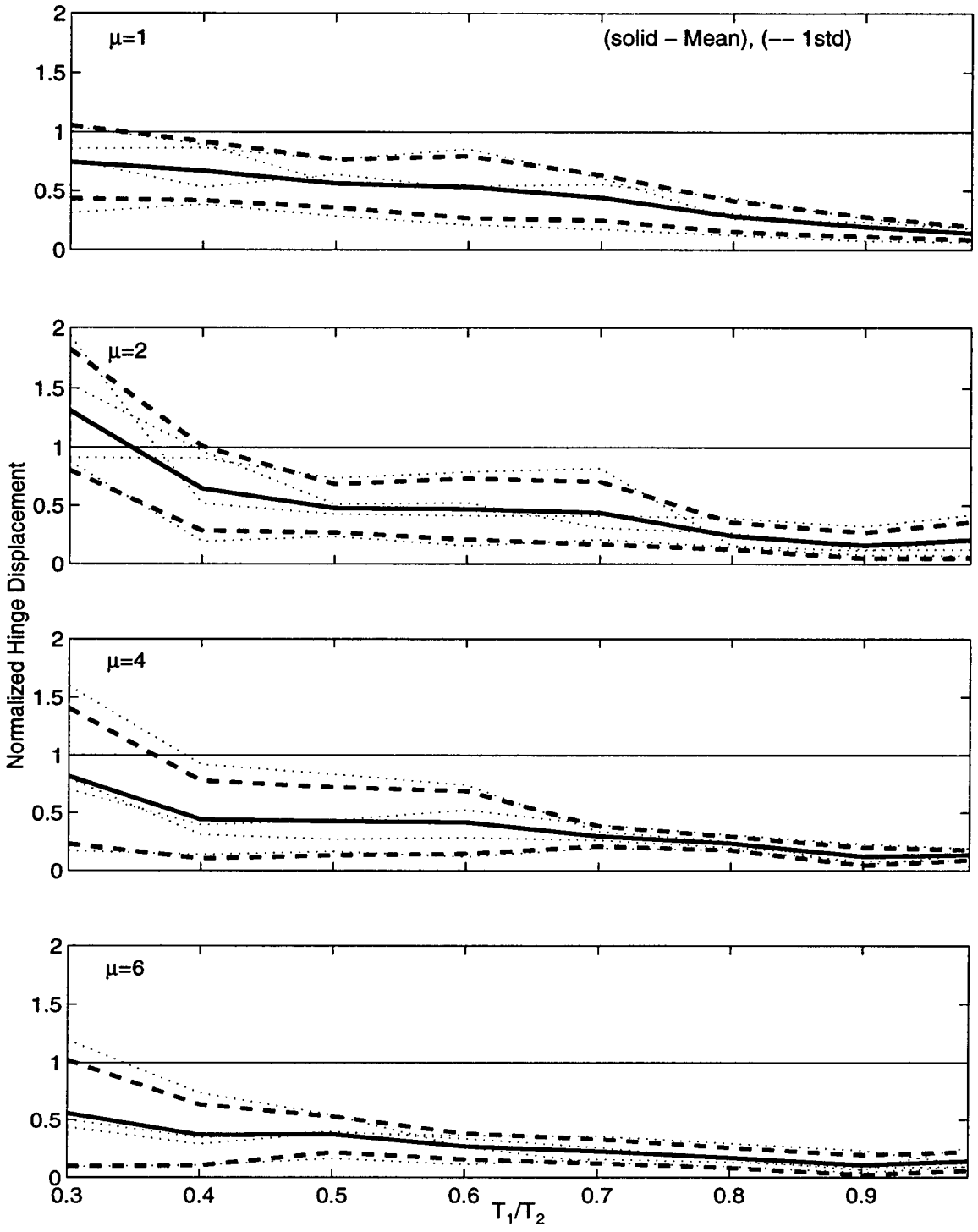

Figure 5.32: Mean ± One Standard Deviation of Normalized Hinge Displacement for Restrainers from Design Procedure (D_r/D_{eq}=0.50, T_2/T_g=6.00).

Chapter 6

Single-Step Design Procedure for Hinge Restrainers

Chapter 5 presented the new restrainer design procedure for long multiple-frame bridges. Although the procedure is simple, several iterations are required to converge to the solution. To simplify the design process for restrainers, a single-step restrainer design procedure is developed in this chapter. As with the multiple-step procedure, the single-step procedure is based on a simplified two-degree-of-freedom linear analytical model for the longitudinal earthquake response of adjacent frames. The single-step procedure is developed by representing the restrainer stiffness in a non-dimensional form, eliminating the need to iterate and perform a modal analysis.

6.1 Definition of Normalized Restrainer Stiffness

There are several ways to represent the restrainer stiffness in non-dimensional form. The non-dimensional form which best reduces the variability of the restrainer stiffness for a wide range of parameters is:

$$\tilde{K}_r = \frac{K_r D_r}{\frac{K_{mod}}{\mu}(D_{eq_o} - D_r)} \tag{6.1}$$

The numerator represents the restrainer force required to limit the hinge displacement to the target displacement, D_r. The denominator represents the force required to

slowly pull the frames together from an initial opening of D_{eq_0} to a final opening of D_r, acting through the effective stiffness, K_{mod}/μ, of the two frames. Equation 6.1 can also be written in the following form:

$$\tilde{K}_r = \frac{K_r}{\frac{K_{mod}}{\mu}(\frac{D_{eq_0}}{D_r} - 1)} \tag{6.2}$$

In this form, $\frac{K_r}{K_{mod}/\mu}$ is an effective restrainer ratio, and $(D_{eq_0}/D_r - 1)$ is a factor representing how much the hinge displacement must be reduced by the restrainers.

The normalized restrainer stiffness is a function of the frame period ratio (T_1/T_2), target ductility (μ), displacement ratio (D_r/D_{eq_0}), and the modified input period ratio $(\tilde{T} = T_{2_{eff}}/T_g)$.

The normalized stiffness definition has the advantage that it accounts for the ground motion amplitude as a factor. For example, a doubling of the ground motion results in a doubling of the hinge displacement without restrainers, D_{eq_0}. However, as long as the target displacement, D_r, doubles, the normalized restrainer stiffness is the same. The normalization accounts for the effects of yielding frames through the effective modified frame stiffness, K_{mod}/μ. Also, the procedure accounts for the effective period of frame 2 relative to the input period of the ground motion by dividing the modified stiffness by the design ductility. As the frames yield, the individual frame periods are modified by a factor of $\sqrt{\mu}$. Therefore, to represent the location of the effective period of the frames with respect to the characteristic period of the input motion, the effective frame period, $T_{2_{eff}} = T_2\sqrt{\mu}$, is divided by the characteristic period of the input motion.

6.1.1 Evaluation of Normalized Restrainer Stiffness

It should be noted that the restrainer stiffness used in the normalization, K_r, is obtained from the multiple-step design procedure. A more accurate method for the restrainer stiffness required to limit the hinge displacement can be obtained from the nonlinear analytical model. The results from the multiple-step procedure, however, showed that the proposed procedure provides a good estimate of the restrainer force compared with a nonlinear analytical model.

The normalized restrainer stiffness is evaluated for the range of parameters in table 6.1. In figures 6.1 through 6.6, the normalized stiffness is plotted as a function of the frame period ratio for fixed values of $\tilde{T}$ and D_r/D_{eq_o}. The 26 earthquake ground motions listed in table 4.2 are used in the study. In the study, only a subset is used for each value of $\tilde{T}$, which gives realistic values of frame periods. For example, for $\tilde{T} = 0.25$, an input ground motion period range of 1.6 sec to 2.3 sec is chosen. This represents elastic periods of frame 2 in the range of 0.16 sec to 0.60 sec. This represents the extreme case of high frequency frames. Moderate frequency and low frequency frames are also investigated.

The mean normalized restrainer stiffness ratio varies from 1.25 at $T_1/T_2 = 0.30$ to 0.50 at $T_1/T_2 = 1.0$ for $D_r/D_{eq_0} = 0.20$ and $\tilde{T} = 0.25$, as illustrated in figure 6.1. In general, the standard deviation decreases as the frame period ratio approaches unity.

Increasing values of $\tilde{T}$ result in increases in $\tilde{K}_r$. The average value of $\tilde{K}_r$ increases from 1.75 for $\tilde{T} = 0.50$ to 7.50 for $\tilde{T} = 6.0$ for low frame period ratios. In general, the variability among earthquakes increases for larger values of D_r/D_{eq_0}. However, the variability decreases with increasing frame period ratio. In fact, for frame period ratios greater than 0.70, $\tilde{K}_r$ has little variation over a range of $\tilde{T}$ and D_r/D_{eq_0}. It is not clear why an increase in the displacement ratio results in the increase in the normalized stiffness and the variability of the normalized stiffness. However, one possible explanation is the sensitivity of the expression for the normalized stiffness to slight changes in the displacement ratio, as shown in equation 6.2. The denominator of equation 6.2 contains the expression $D_{eq_0}/D_r - 1$. As D_{eq_0} approaches D_r, the denominator approaches zero and the expression for the normalized stiffness becomes very large.

Table 6.1: Parameters for Normalized Restrainer Stiffness Calculations.

Parameter	Values
Structure Period Ratio : $\frac{T_1}{T_2}$	0.3, 0.4, 0.5, 0.6, 0.7, 0.8, 0.9, 0.98
Target Frame Ductility : μ	1, 2, 4, 6
Normalized Target Displacement : $\frac{D_r}{D_{eq_0}}$	0.20, 0.50
Modified Normalized Frame : $\tilde{T} = \frac{T_2\sqrt{\mu}}{T_g}$ Period Ratio	0.25, 0.50, 1.0, 2.0, 4.0, 6.0

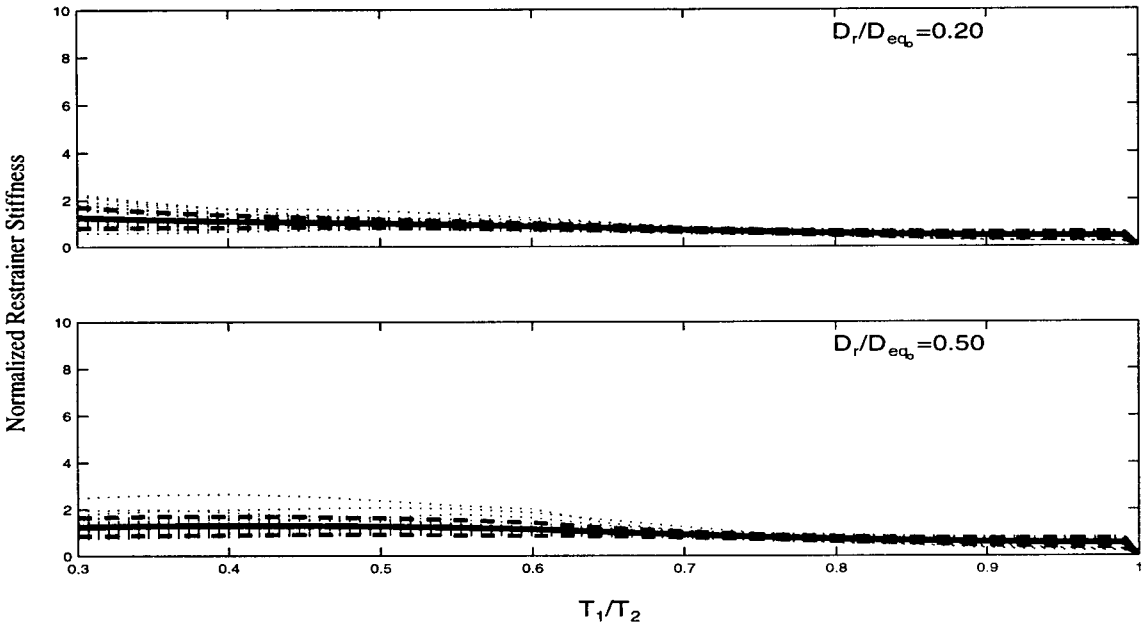

Figure 6.1: Mean ± One Standard Deviation of the Normalized Restrainer Stiffness for $\tilde{T} = 0.25$.

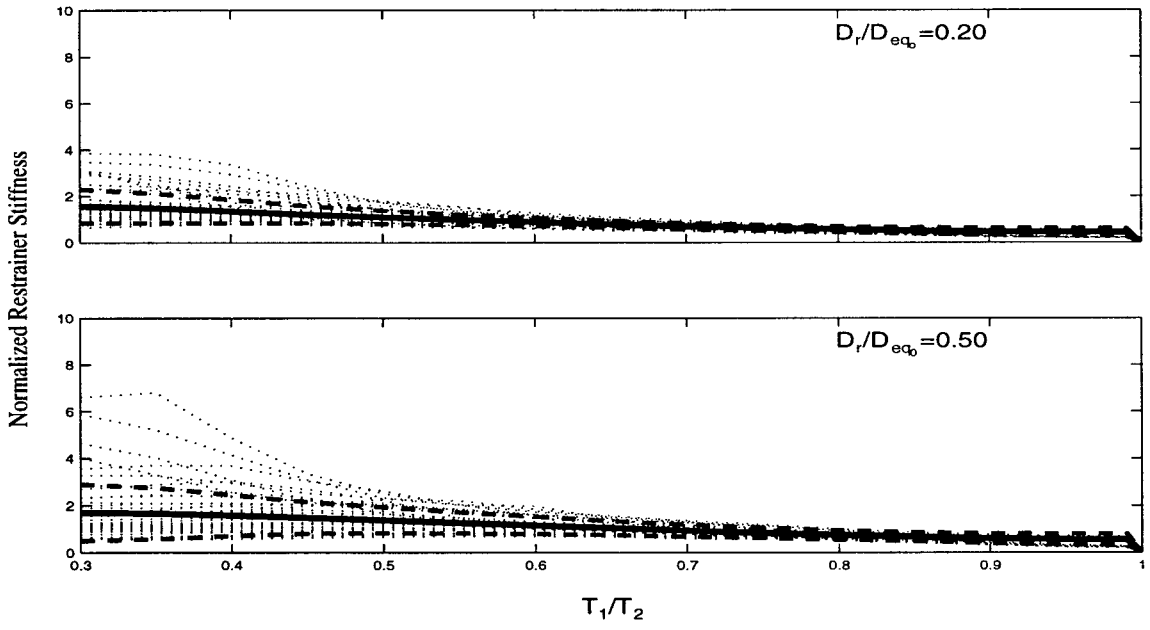

Figure 6.2: Mean ± One Standard Deviation of the Normalized Restrainer Stiffness for $\tilde{T} = 0.50$.

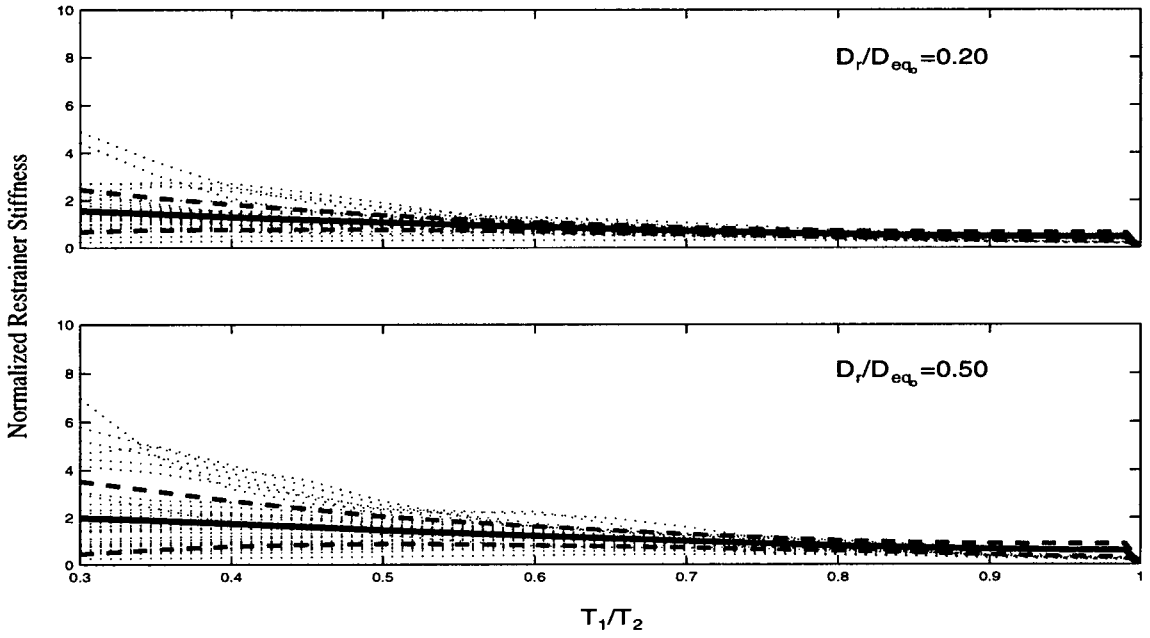

Figure 6.3: Mean ± One Standard Deviation of the Normalized Restrainer Stiffness for $\tilde{T} = 1.00$.

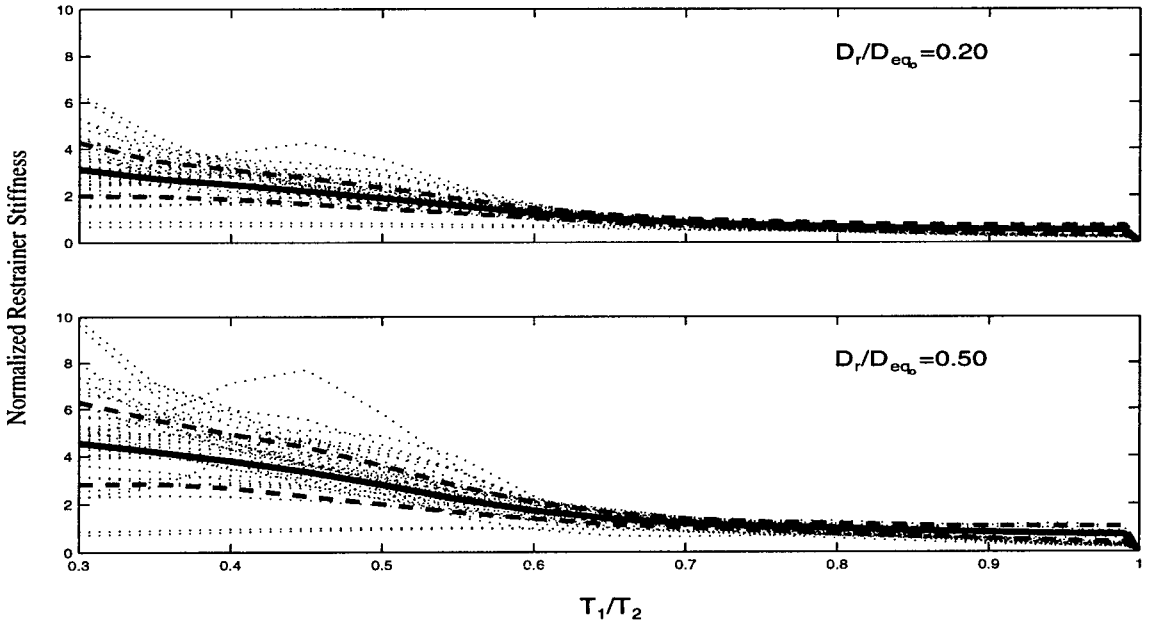

Figure 6.4: Mean ± One Standard Deviation of the Normalized Restrainer Stiffness for $\tilde{T} = 1.50$.

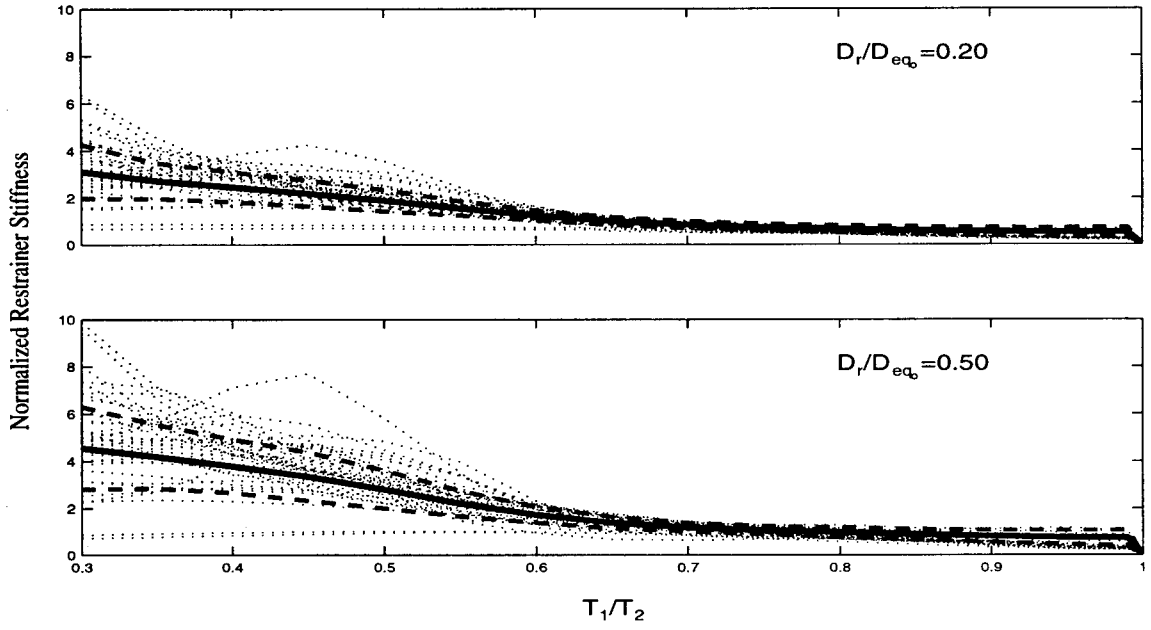

Figure 6.5: Mean ± One Standard Deviation of the Normalized Restrainer Stiffness for $\tilde{T} = 3.00$.

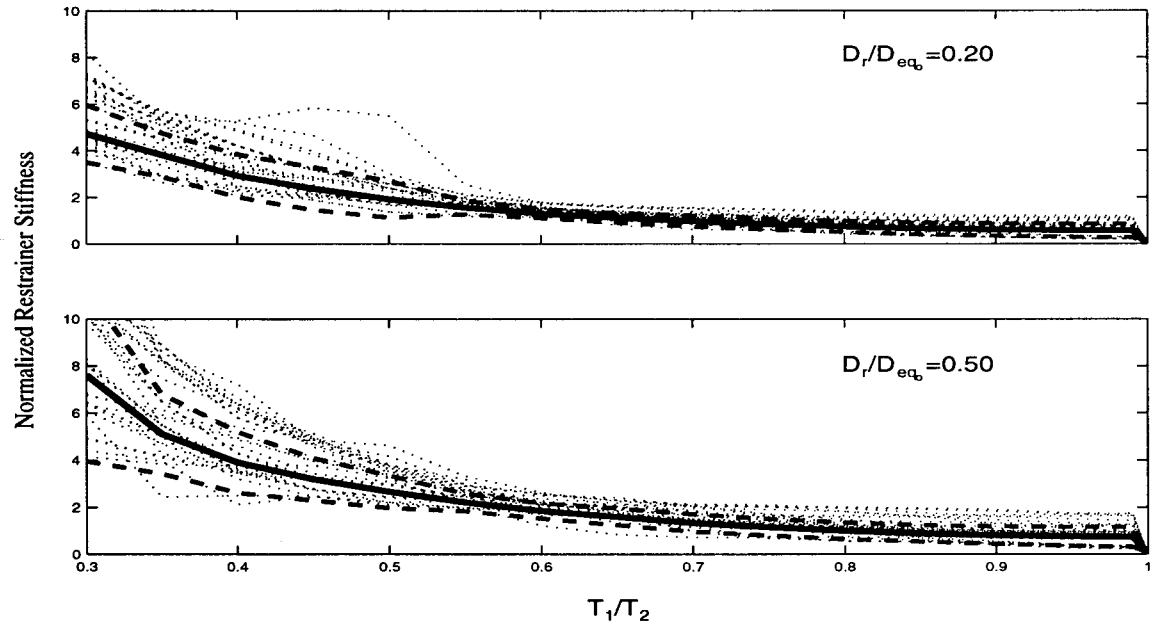

Figure 6.6: Mean ± One Standard Deviation of the Normalized Restrainer Stiffness for $\tilde{T} = 6.00$.

6.2 Regression Analysis for Normalized Restrainer Stiffness

In this section, a closed form expression for $\tilde{K}_r$ in terms of T_1/T_2, $\tilde{T}$, and D_r/D_{eq_o} is obtained from a regression analysis of the normalized restrainer stiffness shown in figures 6.1 to 6.6. A simple function is selected which provides a least squares fit for the mean plus one standard deviation polynomial of the normalized restrainer stiffness. Since $\tilde{K}_r$ is fairly constant for $T_1/T_2 = 0.70$ to T_1/T_2 approaching unity, it can be represented by a constant value in this range. In the range of $T_1/T_2 = 0.30$ to $T_1/T_2 = 0.70$, a best fit linear function is determined for $\tilde{K}_r$. The results of the regression analysis for each value of $\tilde{T}$ and D_r/D_{eq_o} are shown in figures 6.7 and 6.8. For $T_1/T_2 > 0.70$, $\tilde{K}_r$ is fairly constant with a best fit value of 0.75 for $D_r/D_{eq_o} = 0.20$ and 1.10 for $D_r/D_{eq_o} = 0.50$.

To characterize the change in $\tilde{K}_r$ as a function of $\tilde{T}$, regression analysis is performed for the lines in figures 6.7 and 6.8 for $0.30 \leq T_1/T_2 < 0.70$. Since all the lines have approximately the same value at $T_1/T_2 = 0.70$, a linear curve fit can be done at $T_1/T_2 = 0.30$, and subsequently an expression for this line from 0.30 to 0.70 can be obtained. This is performed for both values of D_r/D_{eq_0}.

The regression analysis of the expressions for $\tilde{K}_r$ results in the following expression:

$$\tilde{K}_r = 2 + 0.4\frac{T_2\sqrt{\mu}}{T_g} - (3.3 + \frac{T_2\sqrt{\mu}}{T_g})(\frac{T_1}{T_2} - 0.3) \tag{6.3}$$

for $D_r/D_{eq_0} = 0.20$, and

$$\tilde{K}_r = 3 + 1.0\frac{T_2\sqrt{\mu}}{T_g} - (5.5 - 2\frac{T_2\sqrt{\mu}}{T_g})(\frac{T_1}{T_2} - 0.3) \tag{6.4}$$

for $D_r/D_{eq_0} = 0.50$

Assuming a linear change in $\tilde{K}_r$ as a function of D_r/D_{eq_0}, we get

$$\tilde{K}_r = \tilde{D}[2 - 0.4\frac{T_2\sqrt{\mu}}{T_g} - (3.3 + \frac{T_2\sqrt{\mu}}{T_g})(\frac{T_1}{T_2} - 0.30)] \tag{6.5}$$

where $\tilde{D} = [1 + 1.66(\frac{D_r}{D_{eq_0}} - 0.20)]$

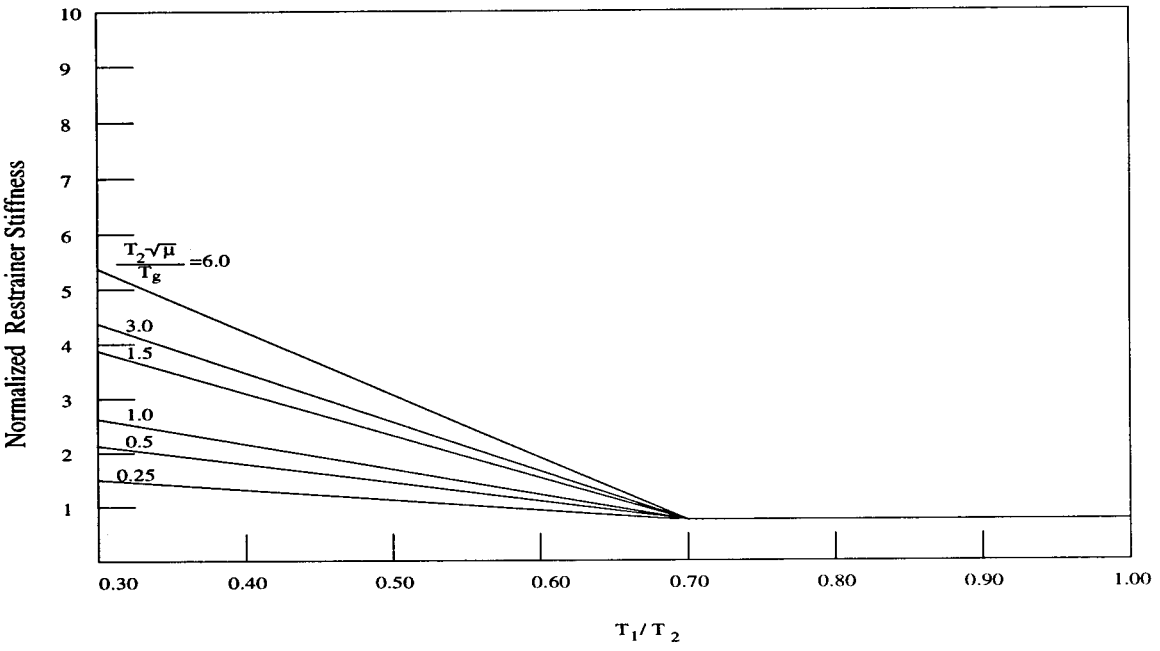

Figure 6.7: Bilinear Curve-Fit for Normalized Restrainer Stiffness for $D_r/D_{eq_o} = 0.20$.

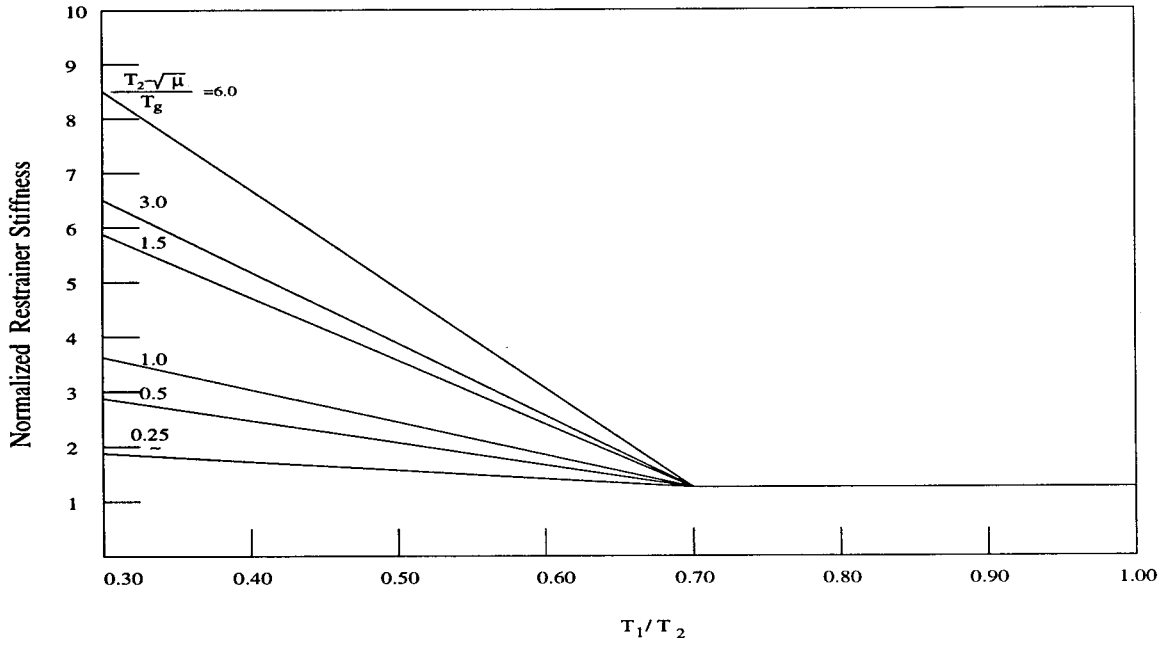

Figure 6.8: Bilinear Curve-Fit for Normalized Restrainer Stiffness for $D_r/D_{eq_o} = 0.50$.

6.3 Single-Step Restrainer Design Procedure

The data required to use the single-step procedure is the same as for the multiple-step procedure. The single-step procedure, however, does not require a modal analysis or iterations to determine the restrainer stiffness. The single-step procedure is outlined below.

(a) Calculate Normalized Restrainer Stiffness

for $T_1/T_2 > 0.70$

$$\tilde{K}_r = D_r/D_{eq_0} + 0.50 \tag{6.6}$$

for $T_1/T_2 \leq 0.70$

$$\tilde{K}_r = \tilde{D}[2 + 0.4(\frac{T_2\sqrt{\mu}}{T_g}) - (3.3 + \frac{T_2\sqrt{\mu}}{T_g})(\frac{T_1}{T_2} - 0.30)] \tag{6.7}$$

where $\tilde{D} = [1 + 1.66(D_r/D_{eq_0})]$

(b) Calculate Required Restrainer Stiffness

$$K_r = \tilde{K}_r \frac{\frac{K_{mod}}{\mu}(D_{eq_0} - D_r)}{D_r} \tag{6.8}$$

(c) Calculate Number of Restrainers

$$N_r = \frac{K_r D_r}{F_y A_r} \tag{6.9}$$

It is observed from equation 6.6 that the normalized restrainer stiffness for $T_1/T_2 > 0.70$ increases as D_r/D_{eq_0} increases. However, this does not lead to increases in the restrainer stiffness. Substituting equation 6.6 into equation 6.8 produces the following expression for the restrainer stiffness as a function of the D_r/D_{eq_0} ratio:

$$K_r = \frac{K_{mod}}{\mu}[0.50 + \frac{0.50 - (\frac{D_r}{D_{eq_0}})^2}{\frac{D_r}{D_{eq_0}}}] \tag{6.10}$$

From equation 6.10, as D_r/D_{eq_0} approaches zero, the restrainer stiffness approaches infinity. This represents the case of limiting the hinge displacement to zero. As D_r/D_{eq_0} approaches unity, the restrainer stiffness approaches zero. This represents the case where the target displacement is equal to the hinge opening without restrainers.

Equation 6.10 confirms the results of the parameter study in chapter 4. In figure 4.4, it was determined that a restrainer stiffness ratio, $K_r/K_{mod} = 0.50$, produces a D_r/D_{eq_0} value of approximately 0.70 for $T_1/T_2 > 0.70$ for elastic frames. Substituting $D_r/D_{eq_0} = 0.70$ into equation 6.10 results in $K_r/K_{mod} = 0.51$. The comparison between figure 4.4 and equation 6.10 can also be made for other values of μ and D_r/D_{eq_0}.

6.3.1 Evaluation of Single-Step Restrainer Design Procedure

As an example, the single-step restrainer design procedure is applied to the same example bridge in section 5.3. The two frames with $T_1 = 0.50$ sec and $T_2 = 1.00$ sec are subjected to the 1940 El Centro earthquake (S00E component), scaled to 0.70g peak ground acceleration. The target frame design ductility is $\mu = 4$, and the target hinge displacement is 4.7 in.(119 mm). The application of the single-step procedure is given in figure 6.9. For the same case, the multiple-step procedure gives a restrainer stiffness of 154 kips/in (27.0 kN/mm) which results in a maximum hinge displacement of 5.10 in.(130 mm).

The single-step procedure gives a restrainer stiffness of 270 kips/in (47.3 kN/mm). This is approximately an 80% greater restrainer stiffness than that given by the multiple-step procedure. A nonlinear response history analysis with $K_r = 270$ kips/in (47.3 kN/mm) results in a hinge displacement of 4.06 in. (103 mm). Although some level of conservatism in the design is appropriate, if the recommendation of the available hinge seat width is followed, it may not be necessary to have a conservative design for hinge restrainers, such as given by the single-step procedure. The single-step procedure gives conservative restrainer stiffnesses because the expression for the normalized restrainer stiffness is based on the mean plus one standard deviation of the normalized restrainer stiffness for the range of earthquakes used in the study.

6.4 Parameter Study for Single Step Design Procedure

A parameter study, similar to that discussed in section 5.3 for the multiple-step procedure, is performed for the single-step procedure. For the range of parameters in table 6.1, the hinge displacement with restrainers from the single-step procedure is compared with results from nonlinear time history analyses. The effectiveness of the procedure is presented in terms of a normalized hinge displacement, similar to that for the multiple-step procedure.

Example 6.1 - Single-Step Design Procedure Applied to 1940 El Centro Earthquake (S00E Component) For Yielding Frames, $\mu = 4$.

K_1=2040 kips/in (357 kN/mm), K_2=510 kips/in (89.3 kN/mm)
$W_1 = W_2$=5000 kips (22.3 MN), μ=4, s=0.50 in. (12.7 mm), D_r=4.2 in. (107 mm)
Ground Motion = 1940 El Centro Earthquake (S00E Component), (Scaled to 0.70g)

(a) - Allowable Hinge Displacement
D_r=4.20+0.50=4.7 in. (120 mm)

(b) - Hinge Displacement Without Restrainers
K_{eff_1}=2041/4=510 kips/in (89.3 kN/mm), K_{eff_2}=510/4=128 kips/in (22.4 kN/mm)
$T_{eff_1} = 2\pi\sqrt{5000/(32.2*12)/510} = 1.0$ sec., $T_{eff_2} = 2\pi\sqrt{5000/(32.2*12)/128} = 2.0$ sec.
$\xi_{eff} = 0.05 + (1 - 0.95/4 - .05\sqrt{4})/\pi = 0.19$
$D_1 = S_d(1.0,0.19)$=4.75 in. (121 mm) $D_2 = S_d(2.0,0.19)$=9.73 in. (247 mm)
$\rho_{12} = \frac{8(0.19)^2(1+2)2^{3/2}}{(1-2^2)^2+4(0.19)^2(2)(1+2)^2} = 0.21$

$D_{eq_0} = \sqrt{4.75^2 + 9.73^2 - (0.21)4.75*9.73} = 9.89$ in. (251 mm)

Normalized Restrainer Stiffness
D_r/D_{eq_0}=4.7/9.92=0.47, T_1/T_2=0.5
T_{eff_2}/T_g=2, $\tilde{D}$=1+1.66(.5-.2)=1.45
$\tilde{K}_r$=1.5[2+.4(2)-(3.25+2)(.5-.3)]=2.6
Restrainer Stiffness and Number of Restrainers
$K_r = 2.6\frac{(2041)(510)/(2041+510)(9.89-4.7)}{4*4.7}$=270 kips/in (47.3 kN/mm)

N_r=270*4.7/(176*.222)=32 Restrainers

Figure 6.9: Example of Single-Step Hinge Restrainer Design Procedure for the 1940 El Centro Earthquake (S00E Component).

6.4.1 Results of Single-Step Restrainer Design Procedure for 1940 El Centro Earthquake S00E: $T_2/T_g = 1.0$

The single-step restrainer design procedure is evaluated for the 1940 El Centro Earthquake (S00E component) for D_r/D_{eq_0} values of 0.20 and 0.50. Tables 6.2 and 6.3 list the normalized restrainer stiffness and the restrainer stiffness for a range of frame period ratios and target frame ductilities. The restrainer stiffness varies from 4000 kips/in for elastic frames ($T_1/T_2 = 0.30$) to less than 100 kips/in for frames with a design ductility of 6, and $T_1/T_2 > 0.70$. Figure 6.10 shows a plot of the restrainer stiffnesses predicted by the single-step procedure along with its associated normalized hinge displacement for the selected restrainers. For a target ductility of $\mu = 1$, the procedure does a fairly good job of limiting hinge displacements, except for a frame period ratio of 0.40, where the normalized displacement ratio is approximately 1.30. For a target ductility of $\mu = 2$, the procedure fails to limit hinge displacement to the target for frame period ratios ranging from 0.50 to 0.70.

Table 6.2: Results of Single-Step Restrainer Design Procedure for 1940 El Centro Earthquake (S00E Component), $D_r = 0.20 D_{eq_0}$, $T_2/T_g = 1.0$.

	Normalized Restrainer Stiff.				Restrainer Stiffness, kips/in (kN/mm)			
$\frac{T_1}{T_2}$	$\mu = 1$	$\mu = 2$	$\mu = 4$	$\mu = 6$	$\mu = 1$	$\mu = 2$	$\mu = 4$	$\mu = 6$
.30	2.40	2.56	2.80	2.98	3980 (697)	2130 (373)	1160 (203)	825 (144)
.40	1.98	2.10	2.28	2.40	3080 (539)	1640 (286)	887 (155)	627 (109)
.50	1.55	1.63	1.75	1.83	2240 (392)	1180 (207)	633 (111)	444 (77.7)
.60	1.13	1.16	1.22	1.27	1500 (261)	776 (136)	408 (71.3)	282 (49.3)
.70	0.70	0.70	0.70	0.70	850 (148)	425 (74.4)	213 (37.2)	142 (24.8)
.80	0.70	0.70	0.70	0.70	773 (135)	386 (67.6)	193 (33.8)	129 (22.5)
.90	0.70	0.70	0.70	0.70	700 (122)	350 (61.2)	175 (30.6)	117 (20.4)
.98	0.70	0.70	0.70	0.70	646 (113)	323 (56.5)	162 (28.3)	108 (18.8)

The normalized displacement ratio in this range varies from 1.50-1.70. The high values of the normalized displacement in this range are most likely due to limitation of the single-step procedure in capturing all the changes in the response of the system as restrainers are added. As restrainers are added to the system, the period and mode shapes change. This in turn alters the response by shifting the periods to different locations on the response spectrum. In the multiple-step procedure, this is taken

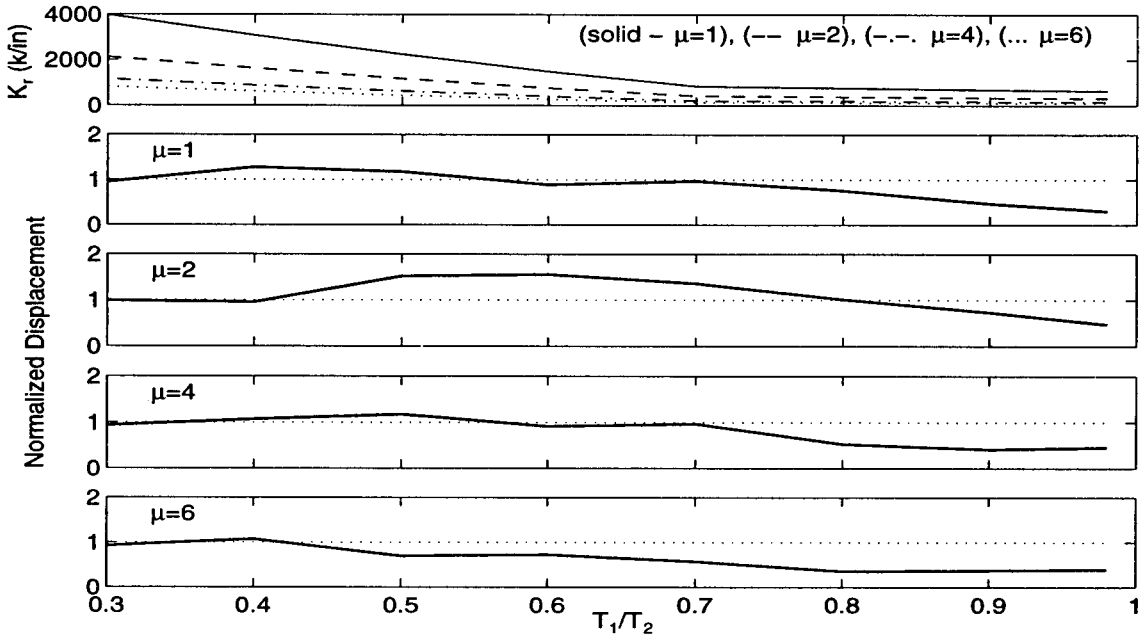

Figure 6.10: Single-Step Restrainer Design Procedure: 1940 El Centro Earthquake (S00E Component) D_r/D_{eq}=0.20, T_2/T_g=1.0.

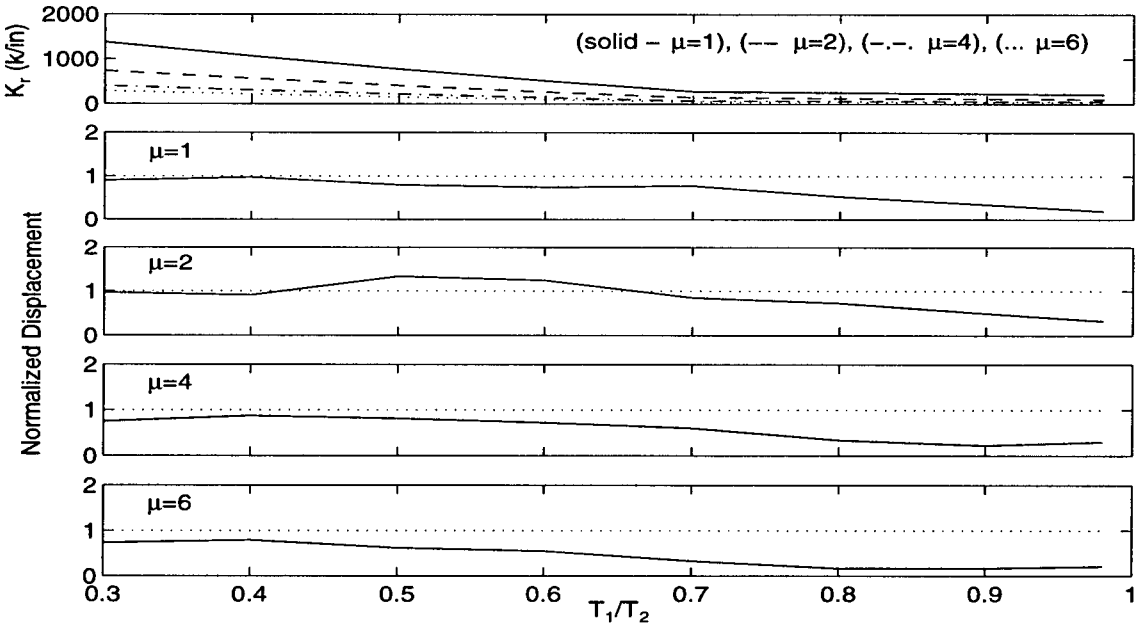

Figure 6.11: Single-Step Restrainer Design Procedure: El Centro Earthquake (S00E Component) D_r/D_{eq}=0.50, T_2/T_g=1.0.

Table 6.3: Results of Single-Step Restrainer Design Procedure for 1940 El Centro Earthquake (S00E Component), $D_r = 0.50D_{eq_0}$, $T_2/T_g = 1.0$.

	Normalized Restrainer Stiff.				Restrainer Stiffness, kips/in (kN/mm)			
$\frac{T_1}{T_2}$	$\mu = 1$	$\mu = 2$	$\mu = 4$	$\mu = 6$	$\mu = 1$	$\mu = 2$	$\mu = 4$	$\mu = 6$
.30	3.60	3.84	4.19	4.46	1380 (241)	736 (129)	402 (70.3)	285 (49.9)
.40	2.96	3.14	3.40	3.61	1070 (186)	566 (99.1)	306 (53.7)	217 (37.9)
.50	2.32	2.44	2.62	2.75	776 (135)	409 (71.5)	219 (38.3)	153 (26.9)
.60	1.68	1.75	1.83	1.90	518 (90.6)	268 (46.9)	141 (24,7)	97.1 (17.0)
.70	1.00	1.00	1.00	1.00	280 (49.1)	147 (25.7)	73.5 (12.9)	49.0 (8.57)
.80	1.00	1.00	1.00	1.00	254 (44.6)	127 (22.3)	63.7 (11.1)	42.4 (7.42)
.90	1.00	1.00	1.00	1.00	230 (40.4)	115 (20.2)	57.7 (10.1)	38.5 (6.73)
.98	1.00	1.00	1.00	1.00	213 (37.3)	106 (18.6)	53.3 (9.32)	35.5 (6.21)

into account by updating the response after restrainers are added in each iteration cycle. The procedure works well for the target ductilities of 4 and 6. The normalized displacement is near unity for most frame period ratios, and slightly exceeds unity in a limited period ratio range. For the target ductility of $\mu = 6$, the procedure is conservative. For frame period ratios larger than 0.40, the normalized displacement ratio averages approximately 0.75.

The procedure similarly works well for $D_r/D_{eq_0} = 0.50$. Large values of normalized displacement ratios are found with $\mu = 2$ for frame period ratios of 0.50 and 0.60. However, the procedure is conservative for all other cases.

6.4.2 Results of Single-Step Restrainer Design Procedure for 1994 Northridge Earthquake (Sylmar Hospital Free-Field Record): $T_2/T_g = 1.0$

A similar application of the single-step design procedure is performed for the 1994 Northridge Earthquake (Sylmar Hospital free-field record) as shown in tables 6.4 and 6.5 and figures 6.12 and 6.13. For $D_r/D_{eq_0} = 0.20$, the procedure works very well for the entire range of frame period ratios and design ductilities except for a target ductility of $\mu = 6$. The entire range of frame period ratios is unconservative for this value of design ductility. The results for the displacement ratio of 0.50 are similar, except that the normalized displacement values for the design ductility of 6 are not

as large.

Table 6.4: Results of Single-Step Restrainer Design Procedure for the 1994 Northridge Earthquake (Sylmar Hospital Free-Field Record), $D_r = 0.20D_{eq_0}$, $T_2/T_g = 1.0$

	Normalized Restrainer Stiff.				Restrainer Stiffness, kips/in (kN/mm)			
$\frac{T_1}{T_2}$	$\mu = 1$	$\mu = 2$	$\mu = 4$	$\mu = 6$	$\mu = 1$	$\mu = 2$	$\mu = 4$	$\mu = 6$
.30	2.20	2.57	2.80	2.98	1560 (272)	832 (146)	454 (79.5)	322 (56.4)
.40	1.83	2.10	2.28	2.41	1200 (210)	639 (112)	346 (60.6)	245 (42.8)
.50	1.45	1.63	1.75	1.84	877 (153)	461 (80.8)	247 (43.3)	173 (30.4)
.60	1.08	1.17	1.22	1.26	585 (102)	303 (53.1)	159 (27.9)	110 (19.3)
.70	0.70	0.70	0.70	0.70	332 (58.1)	166 (29.1)	83.0 (14.5)	55.4 (9.68)
.80	0.70	0.70	0.70	0.70	302 (52.8)	150 (26.4)	75.4 (13.2)	50.3 (8.80)
.90	0.70	0.70	0.70	0.70	273 (47.8)	136 (23.9)	68.4 (12.0)	45.6 (7.97)
.98	0.70	0.70	0.70	0.70	252 (44.2)	126 (22.1)	63.1 (11.0)	42.1 (7.36)

Table 6.5: Results of Single-Step Restrainer Design Procedure for the 1994 Northridge Earthquake (Sylmar Hospital Free-Field Record), $D_r = 0.50D_{eq_0}$, $T_2/T_g = 1.0$.

	Normalized Restrainer Stiff.				Restrainer Stiffness, kips/in (kN/mm)			
$\frac{T_1}{T_2}$	$\mu = 1$	$\mu = 2$	$\mu = 4$	$\mu = 6$	$\mu = 1$	$\mu = 2$	$\mu = 4$	$\mu = 6$
.30	3.29	3.84	4.19	4.46	538 (94.2)	287 (50.3)	157 (27.5)	111 (19.5)
.40	2.73	3.14	3.40	3.61	416 (72.8)	221 (38.7)	119 (20.9)	84.6 (14.8)
.50	2.17	2.44	2.62	2.75	303 (53.0)	159 (27.9)	85.5 (14.9)	59.9 (10.5)
.60	1.61	1.75	1.83	1.90	202 (35.4)	104 (18.3)	55.0 (9.63)	38.0 (6.65)
.70	1.00	1.00	1.00	1.00	109 (19.2)	57.4 (10.0)	28.7 (5.02)	19.1 (3.34)
.80	1.00	1.00	1.00	1.00	99.5 (17.4)	49.7 (8.70)	24.9 (4.35)	16.6 (2.90)
.90	1.00	1.00	1.00	1.00	90.1 (15.8)	45.1 (7.88)	22.5 (3.94)	15.0 (2.60)
.98	1.00	1.00	1.00	1.00	83.2 (14.6)	41.6 (7.28)	20.8 (3.64)	13.8 (2.42)

6.4.3 Parameter Study for Restrainer Design Procedure: Results for 26 Ground Motion Records

In this section, the effectiveness of the single-step procedure is evaluated by examining the normalized hinge displacement for the 26 earthquake records. Figures 6.14 and 6.15 show the results of the mean and mean plus and minus one standard deviation of the normalized hinge displacement for $T_2/T_g = 0.50$. The results show that a few cases are slightly unconservative for low period ratios, and conservative for

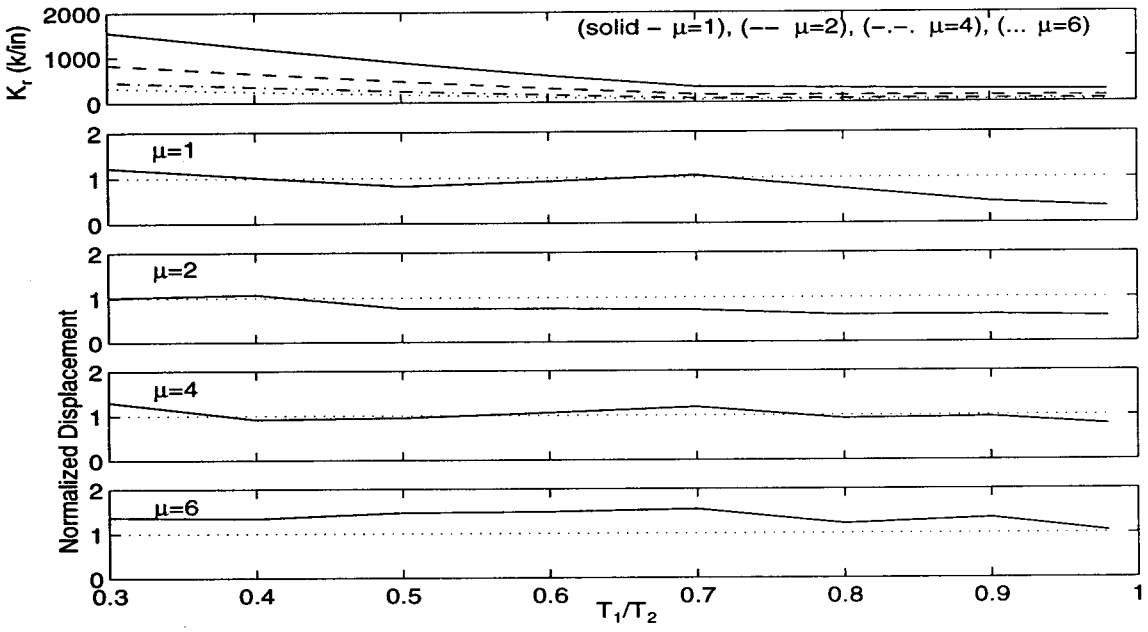

Figure 6.12: Single-Step Restrainer Design Procedure: 1994 Northridge Earthquake (Sylmar Hospital Free-Field Record) D_r/D_{eq}=0.20, T_2/T_g=1.0.

frame period ratios approaching unity. As previously mentioned, pounding produces larger displacements for highly out-of-phase frames, which is particularly important for elastic frames. The results for the single-step procedure, shown in figures 6.14 and 6.15 for $T_2/T_g = 0.50$, are similar to those for the multiple-step procedure, although the standard deviation for the single-step procedure is slightly greater than that for the multiple-step procedure.

Figures 6.16 and 6.17 show the normalized hinge displacement for D_r/D_{eq_0}=0.20 and D_r/D_{eq_0}=0.50 for $T_2/T_g = 1.0$. The procedure works well in providing the restrainer stiffness to limit hinge displacement. The mean plus one standard deviation of the normalized hinge displacement ranges from approximately 0.90 for elastic frames to 1.2 for a target ductility of 6. This is slightly less than the normalized hinge displacements for the multiple-step procedure for the same case. However, in general the standard deviation is greater for the single-step procedure than the multiple-step procedure. As the design ductility increases, the scatter between different cases increases, thus producing larger standard deviations.

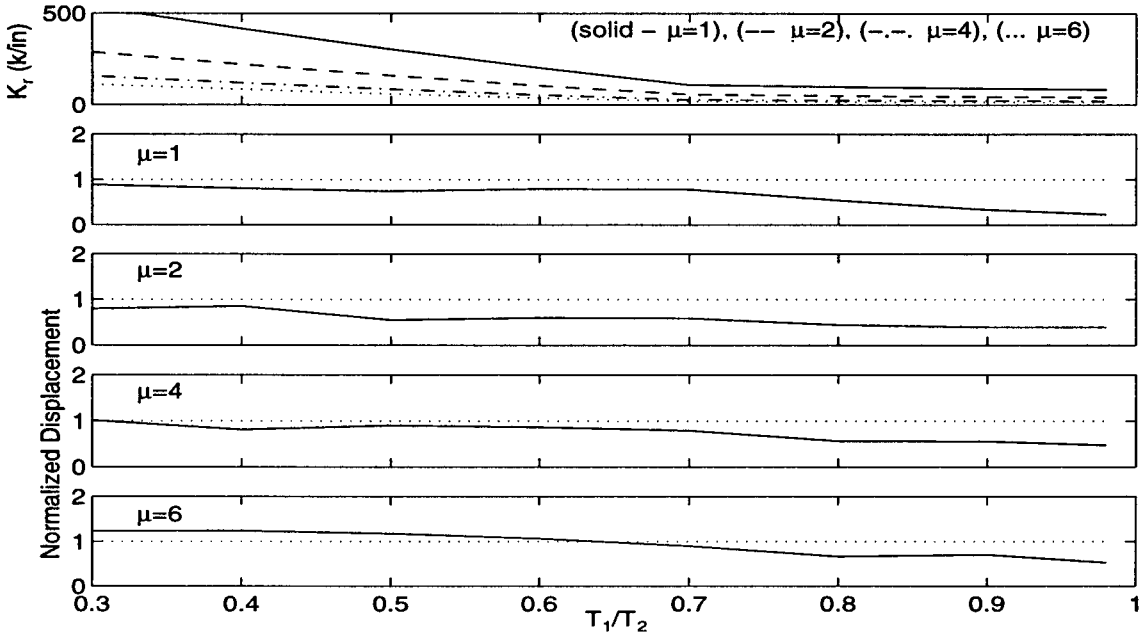

Figure 6.13: Single-Step Restrainer Design Procedure: 1994 Northridge Earthquake (Sylmar Hospital Free-Field Record) D_r/D_{eq}=0.50, T_2/T_g=1.0.

Figures 6.18 and 6.19 show the results of the parameter study for T_2/T_g=2.0 and D_r/D_{eq_0}=0.20 and D_r/D_{eq_0}=0.50. For D_r/D_{eq_0}=0.20, the procedure is unconservative, represented by a mean plus one standard deviation of the normalized displacement in the range of 1.25-2.30 for frame period ratios less than 0.70 for elastic frames. Yielding frames have values for the mean plus one standard deviation of the normalized hinge displacement in the range of 1.2 to 2.1 for frame period ratios less than 0.70. This is partly due to the effect of pounding. However, it may also be caused by an inadequate representation of the change in normalized displacement as a function of $T_{2_{eff}}/T_g$. The results are much better for $D_r/D_{eq_0} = 0.50$.

Figures 6.20 and 6.21 show the results for $T_2/T_g = 4.0$ and $T_2/T_g = 6.0$ with $D_r/D_{eq_0} = 0.50$. For most of the cases, the normalized displacement is less than unity. There is more variability in the results for T_2/T_g=4.0 and T_2/T_g=6.0 for the single-step procedure than for the multiple-step procedure. The standard deviations are approximately 0.50 for most ductilities and frame period ratios for the single-step procedure compared with 0.15 for the multiple-step procedure.

6.4.4 Summary of Single-Step Restrainer Design Procedure

This chapter presented the single-step design procedure for hinge restrainers as well as parameter studies to verify the effectiveness of the procedure. It is shown that the procedure is much less accurate than the multiple-step procedure, particularly for low frame period ratios. The procedure is typically conservative for $T_2/T_g < 1$ and unconservative for cases with $T_2/T_g > 2$. However, the single-step procedure has certain limitations. The study is based on regression analysis for D_r/D_{eq_o} in the range of 0.20-0.50. For values outside this range, it is recommended that the multiple-step procedure be used to design hinge restrainers. Also, to obtain the best results, it is recommended that for the single-step procedure, the frame period ratios be limited to 0.70. In this range, the restrainer stiffness can be determined from a simple expression, which is only a function of the system properties, initial hinge displacement, and the target displacement.

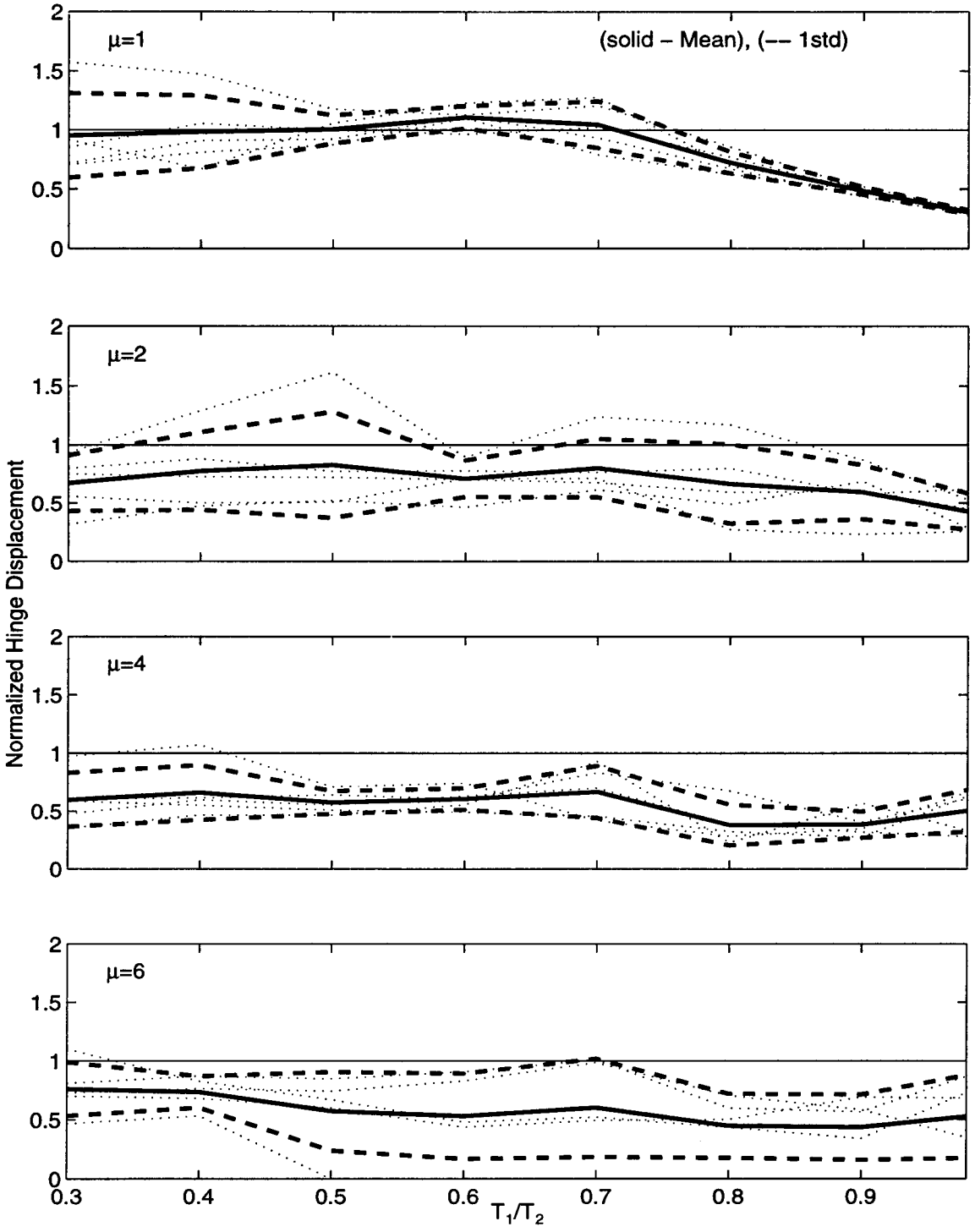

Figure 6.14: Mean ± One Standard Deviation of the Normalized Hinge Displacement from Single-Step Design Procedure for D_r/D_{eq}=0.20, T_2/T_g=0.5.

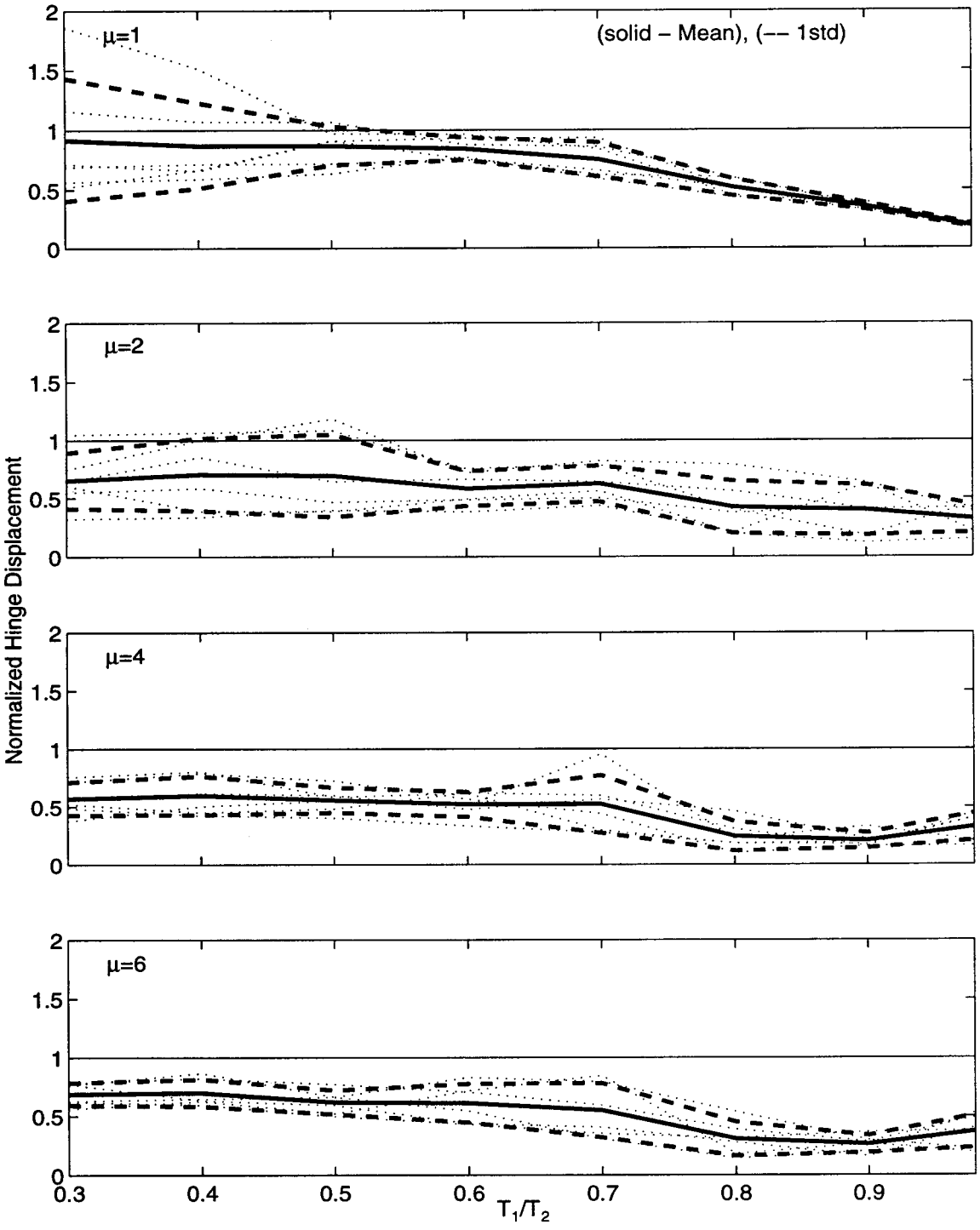

Figure 6.15: Mean ± One Standard Deviation of the Normalized Hinge Displacement from Single-Step Design Procedure for D_r/D_{eq}=0.50, T_2/T_g=0.5.

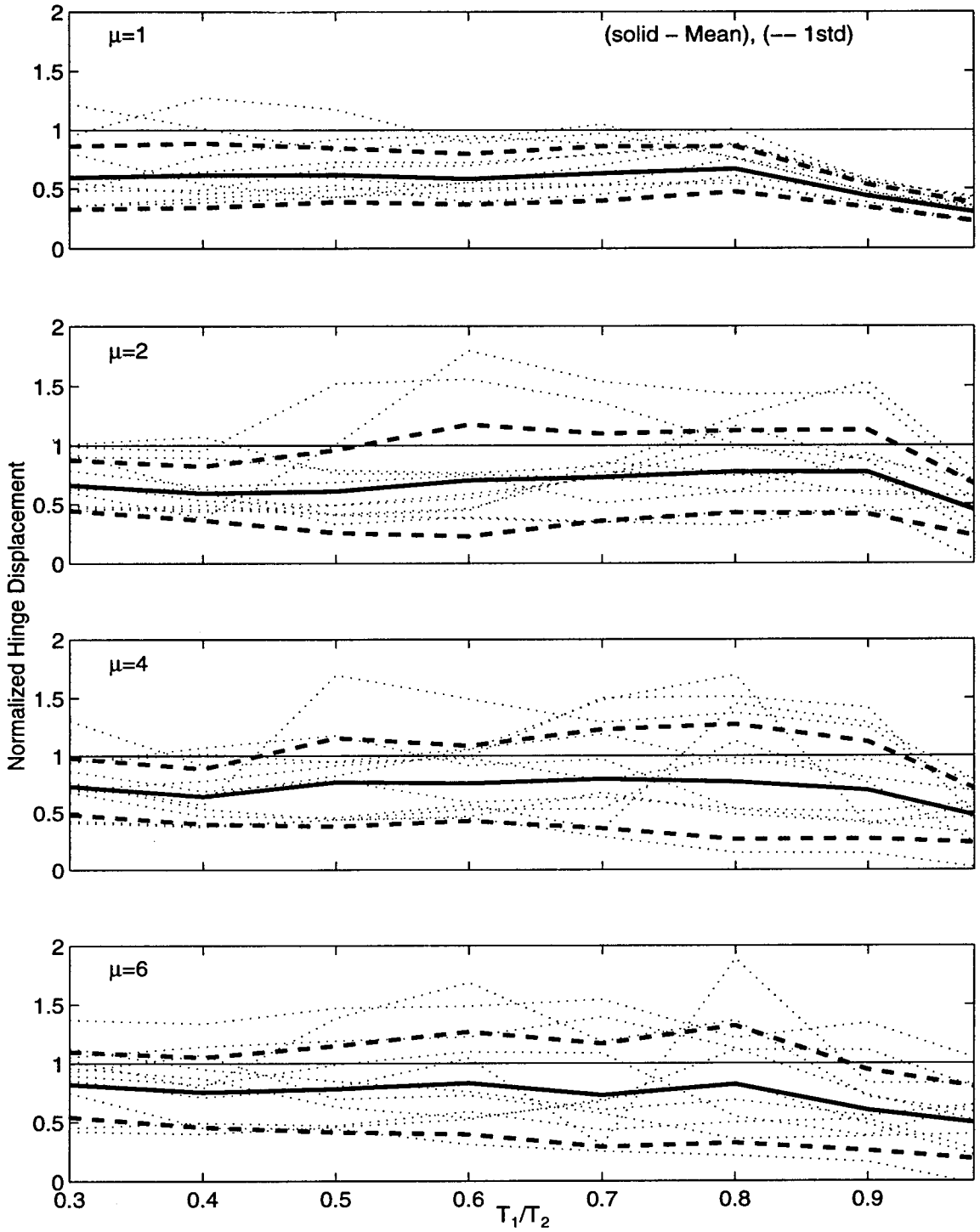

Figure 6.16: Mean ± One Standard Deviation of the Normalized Hinge Displacement from Single-Step Design Procedure for D_r/D_{eq}=0.20, T_2/T_g=1.0.

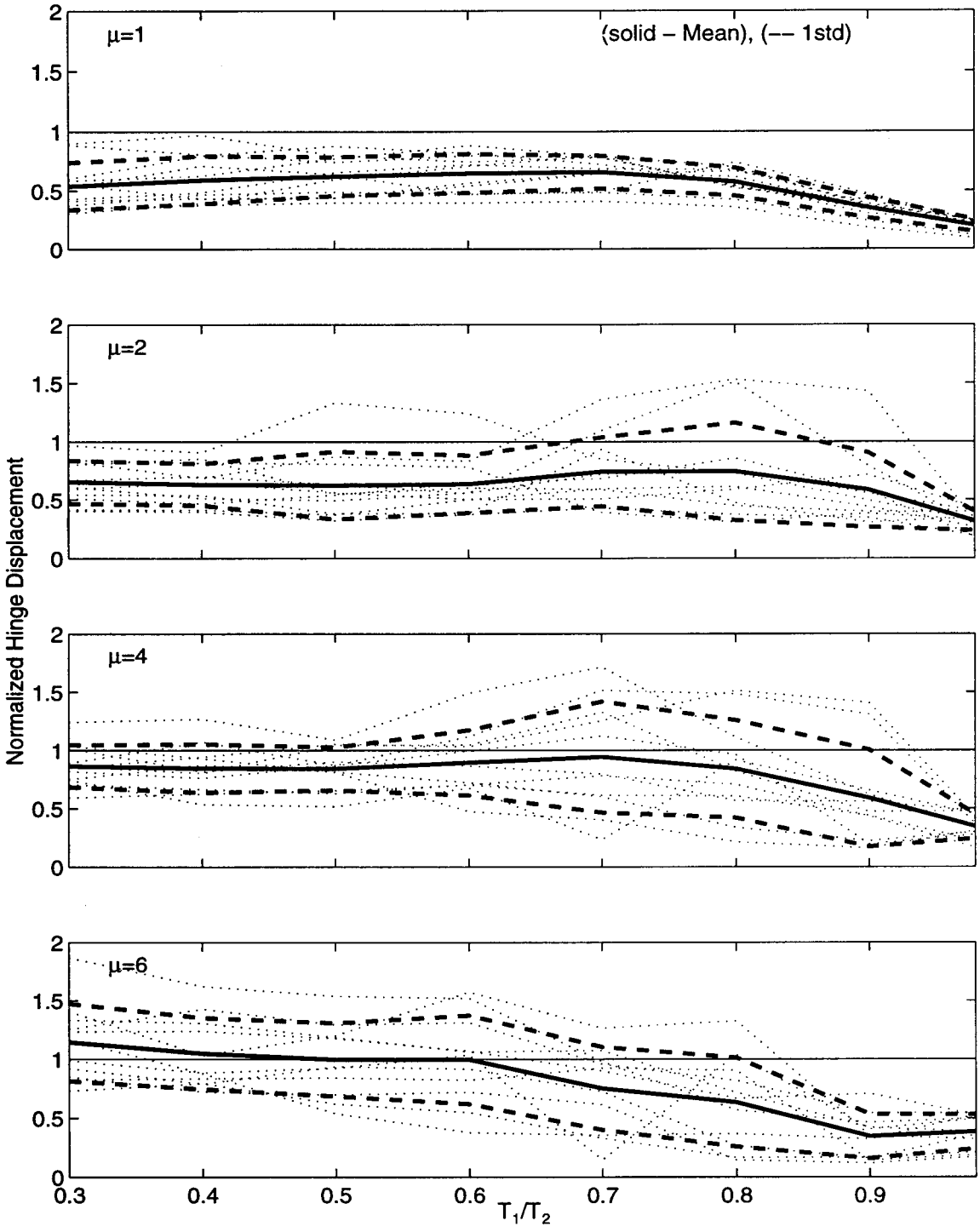

Figure 6.17: Mean ± One Standard Deviation of the Normalized Hinge Displacement from Single-Step Design Procedure for D_r/D_{eq}=0.50, T_2/T_g=1.0.

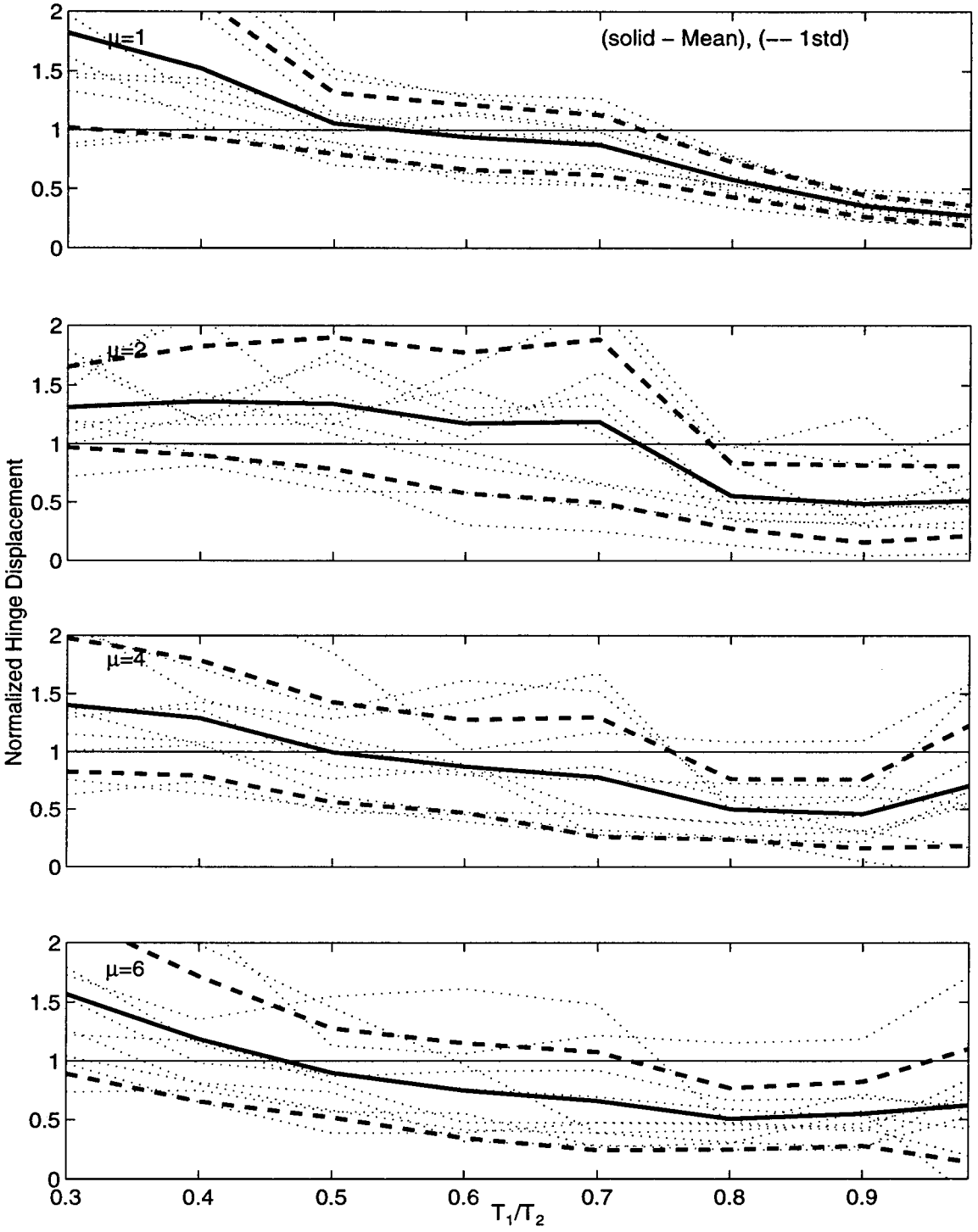

Figure 6.18: Mean ± One Standard Deviation of the Normalized Hinge Displacement from Single-Step Design Procedure for D_r/D_{eq}=0.20, T_2/T_g=2.0.

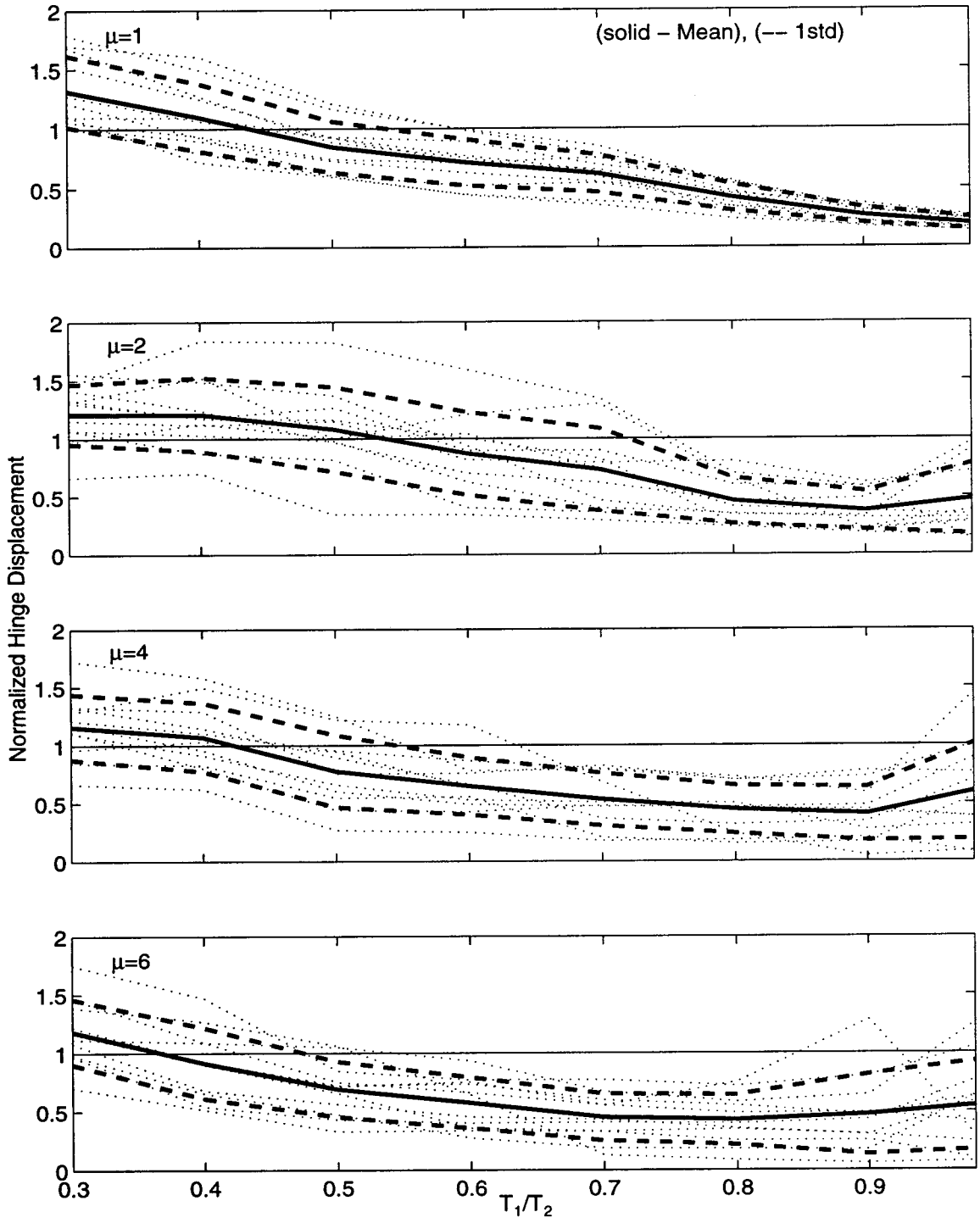

Figure 6.19: Mean ± One Standard Deviation of Normalized Hinge Displacement from Single-Step Design Procedure for D_r/D_{eq}=0.50, T_2/T_g=2.0.

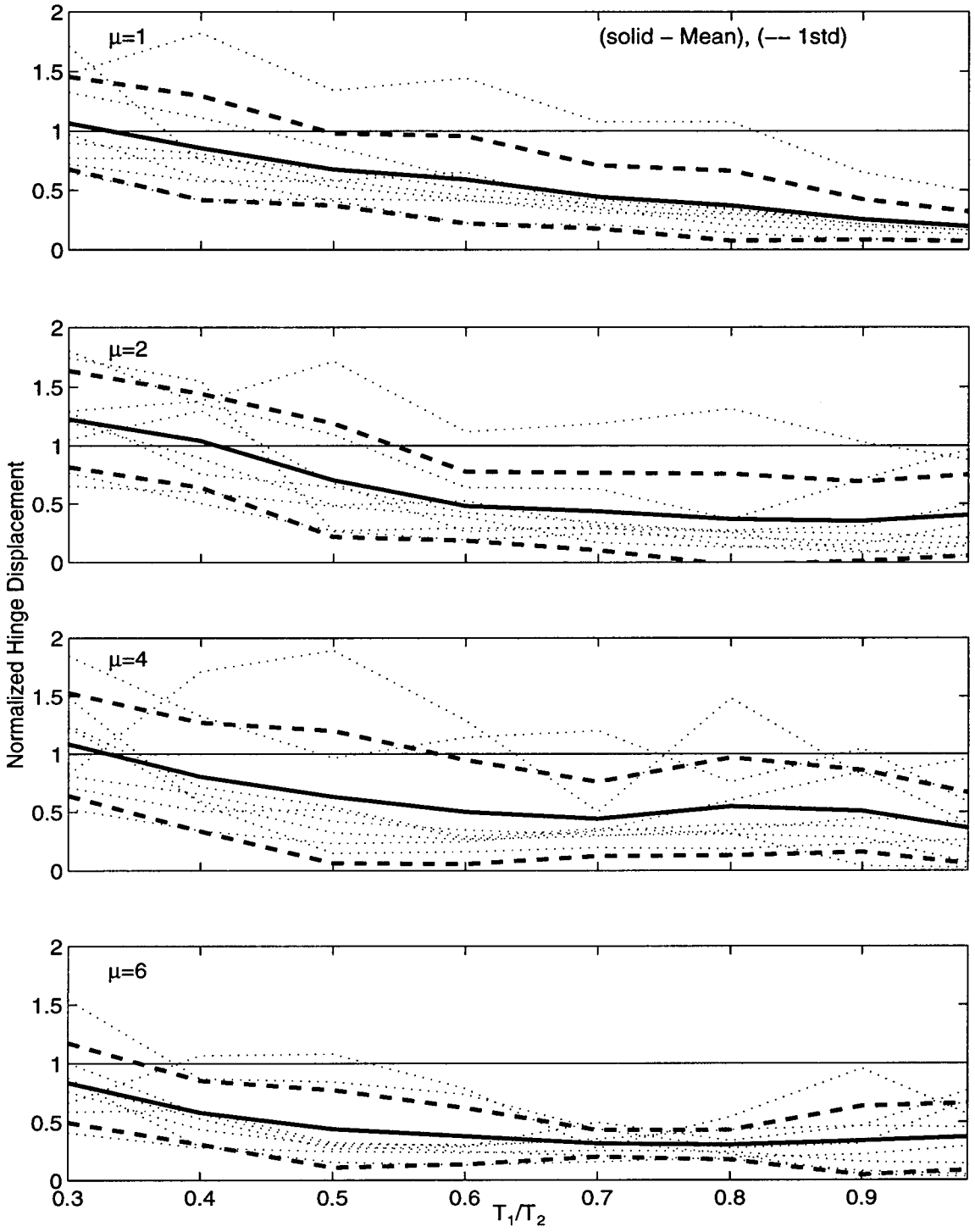

Figure 6.20: Mean ± One Standard Deviation of the Normalized Hinge Displacement from Single-Step Design Procedure for D_r/D_{eq}=0.50, T_2/T_g=4.0.

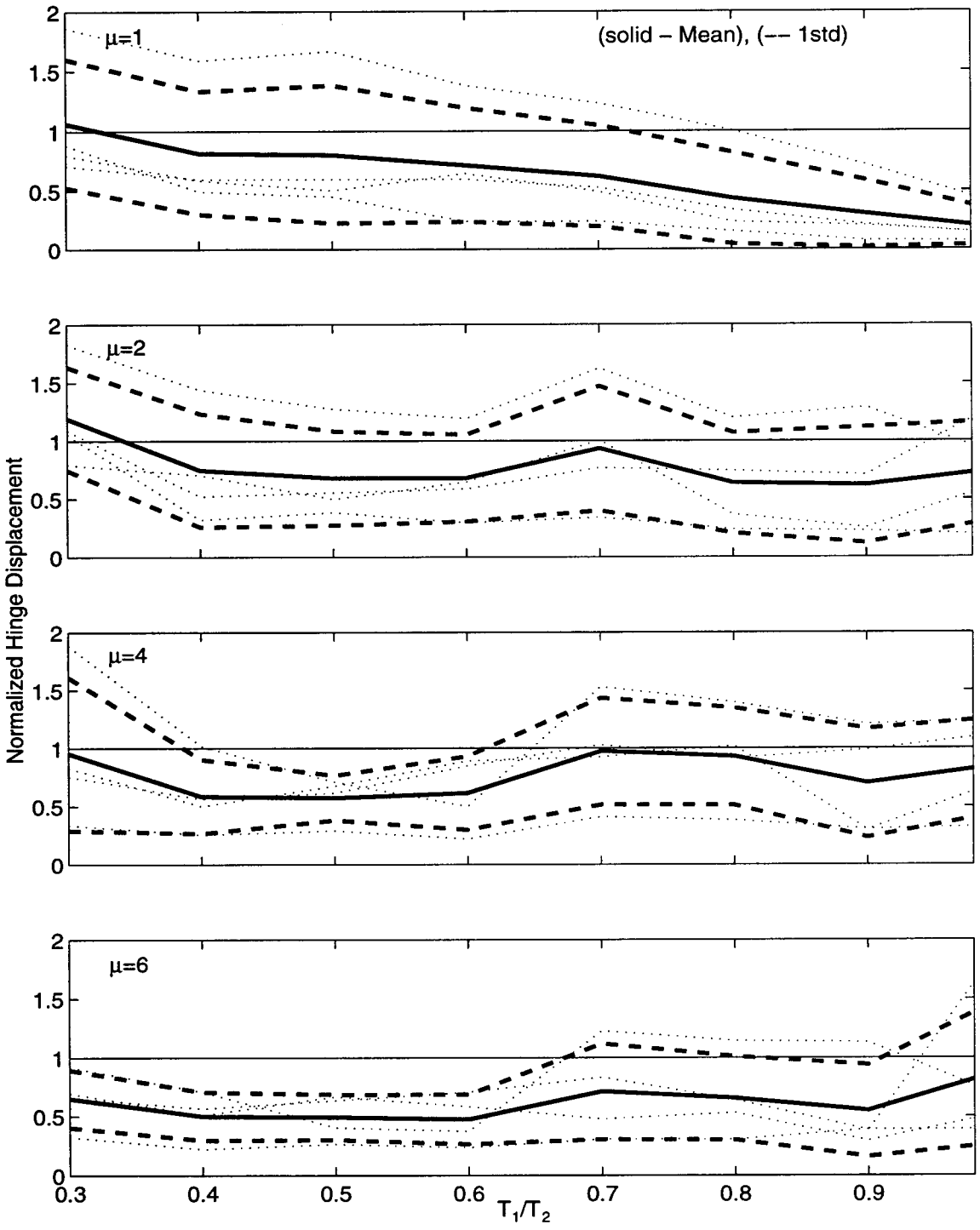

Figure 6.21: Mean ± One Standard Deviation of the Normalized Hinge Displacement from Single-Step Design Procedure for D_r/D_{eq}=0.50, T_2/T_g=6.0.

Chapter 7

Comparison of Design Procedures for Hinge Restrainers and Hinge Seat Widths

The previous chapters evaluated the effectiveness of the new multiple-step and single-step restrainer design procedures. Chapter 2 summarized the restrainer design procedures currently used and those which have recently been proposed, including the Caltrans, AASHTO, Japan, New Zealand, Trochalakis, and capacity design procedures. This chapter compares the effectiveness of the current restrainer design procedures in determining the required restrainer stiffness to limit hinge displacements to a prescribed value. The Japan and New Zealand codes are based on hinge restriction devices which typically do not allow any relative displacement between frames, so they are not included in the comparisons.

None of the referred procedures explicitly accounts for yielding frames with the exception of the capacity design approach. This is a major drawback, since yielding frames require significantly fewer restrainers than elastic frames to limit them to a target displacement, as was shown in Chapter 5 and Chapter 6.

7.1 Case Studies for Hinge Restrainer Design Procedures for 2-DOF Elastic Frames

The multiple-step, single-step, Caltrans, modified Caltrans, AASHTO, and Trokalakis procedures are compared for a 2-DOF system representing a 2-frame bridge. The procedures are compared for the 1940 El Centro earthquake (S00E component) and 1994 Northridge earthquake (Sylmar Hospital free-field record), scaled to 0.70g peak ground acceleration. The frame properties are the same as the example presented in section 5.2, except that the frames are elastic. The frames have stiffnesses of K_1=2040 kips/in (357 kN/mm) and K_2=510 kips/in (89 kN/mm). The weight of each frame is 5000 kips (22.3 MN). This results in a frame period ratio of 0.50. The target hinge displacement is 4.7 in. (119 mm). Detailed calculations are provided for the case with the 1940 El Centro earthquake (S00E component) in the examples below.

7.1.1 Multiple-Step Restrainer Design Procedure

The multiple-step restrainer design procedure is applied to a 2-frame bridge subjected to the 1940 El Centro S00E ground motion. The calculations for this example are shown in figure 7.1. The multiple-step procedure determines a required restrainer stiffness of 740 kips/in (130 kN/mm). The resulting maximum hinge displacement is 4.96 in. (126 mm). A nonlinear analysis determines that a restrainer stiffness of 800 kips/in (140 kN/mm) is required to limit the hinge displacement to 4.7 in. (119 mm). Although slightly unconservative, the multiple-step procedure reasonably provides the required restrainer stiffness to limit the hinge displacement.

7.1.2 Single-Step Restrainer Design Procedure

The single-step design procedure is evaluated for the same example, as shown in figure 7.2. The single-step procedure gives a restrainer stiffness of 1150 kips/in (201 kN/mm). This is much larger than the required restrainer stiffness of 800 kips/in (140 kN/mm) determined from the nonlinear analysis. This results in a maximum hinge displacement of 4.02 in. (102 mm). Chapter 6 illustrated that the single-step

Example 7.1 : Multiple-Step Design Procedure For 1940 El Centro Earthquake (S00E Component), Elastic Frames

K_1=2040 kips/in (357 kN/mm), K_2=510 kips/in (89 kN/mm)
$W_1 = W_2$=5000 kips (22.3 MN), Elastic Frames, D_y=4.20 in., s=0.50 in.
Ground Motion = 1940 El Centro Earthquake (S00E Component), Scaled to PGA=0.70g

Step 1 - Calculate Allowable Hinge Displacement
D_r=4.20+0.50=4.7 in. (119 mm)

Step 2 - Compute Hinge Displacement Without Restrainers
K_1=2041 kips/in (357 kN/mm), K_2=510 kips/in (89 kN/mm)
$T_1 = 2\pi\sqrt{5000/(32.2*12)/2041} = 0.50$ sec., $T_2 = 2\pi\sqrt{5000/(32.2*12)/510} = 1.0$ sec.
ξ=0.05
$D_1 = S_d(0.5,0.05)$=4.0 in. (102 mm) $D_2 = S_d(1.0,0.05)$=10.1 in. (257 mm)
$\rho_{12} = \frac{8(0.05)^2(1+2)2^{3/2}}{(-2^2)^2+4(0.05)^2(2)(1+2)^2} = 0.019$

$D_{eq_0} = \sqrt{4.00^2 + 10.1^2 - (0.019)4.00(10.1)} = 10.8$ in. (275 mm)

Step 3 - Determine Initial Required Restrainer Stiffness
$K_{mod_{eff}}$=(510)(128)/(510+128)=408 kips/in (71.4 kN/mm)
$K_r(0)$ = 408(10.8-4.70)/10.8=230 kips/in (40.4 kN/mm)

Step 4 - Calculate Relative Hinge Displacement from Modal Analysis
From Modal Analysis of 2-DOF system, the following information is obtained:
For More Detail, see Example 1 in Section 5.2
Modal Periods : T_1=0.85 sec., T_2=0.47 sec.
Modal Spectral Ordinates : S_{d1}=8.39 in. (213 mm), S_{d2}=3.57 in. (90.7 mm)
Modal Participation Factors : P_1=0.017 $\frac{1}{sec^2}$, P_2=-0.005 $\frac{1}{sec^2}$
Modal Hinge Displacement :
$D_{eq_1} = 0.017(8.39*7.39^2)$=7.79 in. (198 mm), $D_{eq_2} = -0.005(3.44*13.4^2)$=-3.09 in. (78.5 mm)
β=.85/0.47=1.8
$\rho_{12} = \frac{8(0.05)^2(1+1.8)1.8^{3/2}}{(1-1.8^2)^2+4(0.05)^2(1.8)(1+1.8)^2} = 0.026$

$D_{eq} = \sqrt{(7.79)^2 + (-3.09)^2 + 2(0.026)(7.79)(-3.09)} = 8.35$ in. (212 mm)
$D_{eq} > D_r$, Continue to Step 5

Step 5 - Calculate New Restrainer Stiffness
$K_r(1)$ = 230 + (408+230)(8.65-4.7)/8.65=509 kips/in (89.1 kN/mm)
After four iterations of steps 4 and 5, the procedure converges to a solution
(See example 1 in section 5.2 for details)
K_r= 740 kips/in (130 kN/mm)
D_{eq} = 4.69 in. (120 mm)
$D_{eq} < D_r$, Goto Step 6

Step 6 - Calculate Number of Restrainers
N_r=(740*4.7)/(176*.222)=89 Restrainers

Figure 7.1: Detailed Example of Multiple-Step Restrainer Design Procedure for the 1940 El Centro Earthquake (S00E Component), $\mu = 1$.

procedure is conservative for many cases. However, the procedure is very simple to use.

Example 7.2 : Single-Step Design Procedure for El Centro Earthquake (S00E Component), Elastic Frames

K_1=2040 kips/in (357 kN/mm), K_2=510 kips/in (89 kN/mm)
$W_1 = W_2$=5000 kips (22.3 MN), Elastic Frames, D_y=4.20 in., s=0.50 in.
Ground Motion = 1940 El Centro Earthquake (S00E Component), Scaled to PGA=0.70g

Calculate Allowable Hinge Displacement

D_r=4.20+0.50=4.7 in. (119 mm)

Compute Hinge Displacement Without Restrainers

K_1=2041 kips/in (357 kN/mm), K_2=510 kips/in (89 kN/mm)

$T_1 = 2\pi\sqrt{5000/(32.2*12)/2041} = 0.50$ sec., $T_2 = 2\pi\sqrt{5000/(32.2*12)/510} = 1.0$ sec.

ξ=0.05
$D_1 = S_d(0.5,0.05)$=4.0 in. (102 mm) $D_2 = S_d(1.0,0.05)$=10.1 in. (257 mm)

$\rho_{12} = \frac{8(0.05)^2(1+2)2^{3/2}}{(-2^2)^2+4(0.05)^2(2)(1+2)^2} = 0.019$

$D_{eq_0} = \sqrt{4.00^2 + 10.1^2 - (0.019)4.00*10.1} = 10.8$ in. (275 mm)

Calculate Restrainer Stiffness

$D_r/D_{eq_0} = 4.7/10.8 = 0.44$, $T_1/T_2 = 0.5$

$T_{eff_2}/T_g = 1$, $\tilde{D}$=1+1.66(.44-.2)=1.40

$\tilde{K_r} = 1.4[2 + .4(1) - (3.25 + 1)(.5 - .3)] = 2.17$

$K_r = 2.17\frac{(2041)(510)/(2041+510)*(10.8-4.7)}{1*4.7} = 1150$ kips/in (201 kN/mm)

N_r=(1150*4.7)/(176*.222)=138 Restrainers

Figure 7.2: Detailed Example of the Single-Step Restrainer Design Procedure for 1940 El Centro Earthquake (S00E Component), $\mu = 1$.

7.1.3 Caltrans Restrainer Design Procedure

The Caltrans restrainer design procedure separates the coupled 2-DOF system into two single-degree-of-freedom oscillators. Assuming the frame with the smaller displacement controls the response, restrainers are added until the frame displacement is less than the target. More detail about the procedure can be found in section 2.3.

For this case, the Caltrans procedure predicts that no restrainers are needed to limit hinge displacement. This results in a hinge displacement, determined from nonlinear analysis, of 9.26 in. (235 mm). The initial hinge displacement is the minimum of the individual frame displacements without restrainers. In this case, the minimum frame displacement, D_1, is 4.0 in. (102 mm), which is less than the target displacement. The use of the frame with the smallest displacement is a major shortcoming in the Caltrans procedure. In most cases, the frame with the largest displacement controls the response of the system. In the next section, the modified Caltrans procedure looks at the effect of using the frame with the largest displacement. The calculations for the Caltrans restrainer design procedure are shown in figure 7.3.

7.1.4 Modified Caltrans Restrainer Design Procedure

The modified Caltrans restrainer design procedure is similar to the Caltrans procedure, except that the frame with the largest displacement is used as the controlling case. The modified Caltrans procedure predicts a required restrainer stiffness of 1350 kips/in (230 kN/mm), as shown in figure 7.4. This is almost twice the actual required restrainer stiffness determined from a nonlinear response history analysis. Although the initial hinge displacement is close to that determined from a nonlinear analysis, the calculation of the required restrainer stiffness to limit hinge displacement is not represented correctly. The required restrainer stiffness is determined from the stiffness of frame 2, but the restrainer stiffness should be based on the stiffness of both frames. As restrainers are added, the dynamic properties (periods, mode shapes, and participation factors) change. In the calculations for the multiple-step procedure, the first mode participation factor for relative hinge displacement decreases as restrainers are added. These changes, which help to reduce the hinge displacement, are not recognized in this procedure.

7.1.5 Trochalakis Restrainer Design Procedure

The Trochalakis procedure (1997) is similar to the Caltrans procedure in that it separates the coupled 2-DOF system into two SDOF uncoupled oscillators. However, instead of obtaining the relative displacement from the displacement of frame 1 or

Example 7.3 : Caltrans Design Procedure for 1940 El Centro Earthquake (S00E Component), Scaled to 0.70g.

K_1=2040 kips/in (357 kN/mm), K_2=510 kips/in (89 kN/mm)
$W_1 = W_2$=5000 kips (22.3 MN), Elastic Frames, D_y=4.20 in., s=0.50 in.
Ground Motion = 1940 El Centro Earthquake (S00E Component), Scaled to PGA=0.70g

Step 1 - Calculate Allowable Hinge Displacement
D_r=4.20+0.50=4.7 in. (119 mm)

Step 2 - Compute Hinge Displacement Without Restrainers
K_1=2041 kips/in (357 kN/mm), K_2=510 kips/in (89 kN/mm)
$T_1 = 2\pi\sqrt{5000/(32.2*12)/2041} = 0.50$ sec., $T_2 = 2\pi\sqrt{5000/(32.2*12)/510} = 1.0$ sec.
ξ=0.05
$D_1 = S_d(0.5,0.05)$=4.0 in. (102 mm), $D_2 = S_d(1.0,0.05)$=10.1 in. (257 mm)
D_{eq_0}=minimum(D_1, D_2)=4.0 in., (102 mm)
Since 4.0 < 4.7, NO RESTRAINERS ARE REQUIRED, K_r=0.0, N_r=0.

Figure 7.3: Detailed Example of Caltrans Restrainer Design Procedure for 1940 El Centro Earthquake (S00E Component), μ=1.0.

Example 7.4 : Modified Caltrans Design Procedure for El Centro Earthquake (S00E Component), Scaled to 0.70g.

K_1=2040 kips/in (357 kN/mm), K_2=510 kips/in (89 kN/mm)
$W_1 = W_2$=5000 kips (22.3 MN), Elastic Frames, D_y=4.20 in., s=0.50 in.
Ground Motion = 1940 El Centro Earthquake (S00E Component), Scaled to PGA=0.70g.

Step 1 - Calculate Allowable Hinge Displacement
D_r=4.20+0.50=4.7 in. (119 mm)

Step 2 - Compute Hinge Displacement Without Restrainers
K_1=2041 kips/in (357 kN/mm), K_2=510 kips/in (89 kN/mm)
$T_1 = 2\pi\sqrt{5000/(32.2*12)/2041} = 0.50$ sec., $T_2 = 2\pi\sqrt{5000/(32.2*12)/510} = 1.0$ sec.
ξ=0.05
$D_1 = S_d(0.5,0.05)$=4.0 in. (102 mm) $D_2 = S_d(1.0,0.05)$=10.1 in. (257 mm)
D_{eq_0}=maximum(D_1, D_2)=10.1 in. (257 mm)
Since 10.1>4.7, Add restrainers

Step 3 - Calculate Required Restrainer Stiffness to Limit Hinge Displacement
$K_r = K_2\frac{(D_{eq_0}-D_r)}{D_r} = 510(10.1-4.7)/4.7 = 586$ kips/in (103 kN/mm)

Step 2 - 2nd Iteration
$T_2 = 2\pi\sqrt{5000/(32.2*12)/(510+586)} = 0.68$ sec.
$D_{eq_0} = D_2 = S_d(0.68, 0.05) = 6.08$ in., 154 mm

Step 3 - 2nd Iteration
K_r=586+(510+586)(6.08-4.7)/4.7=909 kips/in (159 kN/mm)

After 8 Iterations of Steps 2 and 3 we obtain
K_r=1350 kips/in (236 kN/mm), N_r=162 Restrainers

Figure 7.4: Detailed Example of Modified Caltrans Restrainer Design Procedure for 1940 El Centro Earthquake (S00E Component), $\mu = 1$.

frame 2, the relative hinge displacement is obtained from an empirical equation for the relative hinge displacement (see equation 2.1). Although the Trochalakis procedure is based on a model with yielding frames, the level of inelastic response is not explicitly accounted for in the expression for the relative hinge displacement. The Trochalakis procedure predicts a restrainer stiffness of 255 kips/in (44.6 kN/mm), as shown in figure 7.5. This is much less than the required restrainer stiffness determined from nonlinear analysis. The initial hinge displacement calculated from this procedure is 30% less than the actual initial hinge displacement. After the first iteration, the displacements for frames 1 and 2 determined by the Trochalakis procedure are 7.36 in. (187 mm) and 3.59 in. (91.2 mm), respectively. Using these values in the expression for the relative hinge displacement produces a hinge displacement of 4.77 in. (121 mm). In fact, the actual hinge displacement from a nonlinear time history analysis is approximately 8 in. (203 mm). This example highlights that the simplified expression for the hinge displacement does not adequately represent the hinge displacement for the elastic system considered in this example. The next section will look at the effectiveness of the procedure for yielding frames.

7.1.6 AASHTO Restrainer Design Procedure

The AASHTO procedure specifies using a restrainer force equal to the acceleration coefficient multiplied by the weight of the lighter frame. This is the simplest procedure, because it only uses two parameters. For this case, the AASHTO procedure gives a restrainer stiffness of 745 kips/in (130 kN/mm), which is very close to the restrainer stiffness determined from nonlinear analysis, as shown in figure 7.6. Although the AASHTO procedure works well in this case, it is not accurate for all cases. In fact, the procedure would give the same restrainer stiffness regardless of the frame period ratio. The next section evaluates the effectiveness of the procedure over a wide range of parameters.

Example 7.5 : Trochalakis Design Procedure (1997) for 1940 El Centro Earthquake (S00E Component), scaled to 0.70g.

K_1=2040 kips/in (357 kN/mm), K_2=510 kips/in (89 kN/mm)
$W_1 = W_2$=5000 kips (22.3 MN), Elastic Frames, D_y=4.20 in., s=0.50 in.
Ground Motion = 1940 El Centro Earthquake (S00E Component), Scaled to PGA=0.70g

Step 1 - Calculate Allowable Hinge Displacement
D_r=4.20+0.50=4.7 in. (119 mm)

Step 2 - Compute Hinge Displacement Without Restrainers
K_1=2041 kips/in (357 kN/mm), K_2=510 kips/in (89 kN/mm)
$T_1 = 2\pi\sqrt{5000/(32.2*12)/2041} = 0.50$ sec., $T_2 = 2\pi\sqrt{5000/(32.2*12)/510} = 1.0$ sec.
$\xi = 0.05$
$D_1 = S_d(0.5,0.05)$=4.0 in. (102 mm) $D_2 = S_d(1.0,0.05)$=10.1 in. (257 mm)
$D_{eq_0} = \frac{D_1+D_2}{4}\frac{T_1}{T_2} = \frac{10.1+4}{4}\frac{1.0}{0.5} = 7.05$ in. (179 mm)

Since 7.05>4.7, Add restrainers
Step 3 - Calculate Required Restrainer Stiffness to Limit Hinge Displacement
$K_r = K_2\frac{(D_{eq_0}-D_r)}{D_r}$=510(7.05-4.7)/4.7=255 kips/in (44.6 kN/mm)
Step 2 - 2nd Iteration
$T_1 = 2\pi\sqrt{5000/(32.2*12)/(2040+255)} = .47$ sec.,
$T_2 = 2\pi\sqrt{5000/(32.2*12)/(510+255)} = .82$ sec.
D_1=3.59 in., D_2=7.36 in. (187 mm)
$D_{eq_0} = \frac{7.36+3.59}{4}\frac{0.82}{0.47} = 4.77$ in. (120 mm)
K_r=255 kips/in (44.6 kN/m), N_r=29 Restrainers

Figure 7.5: Detailed Example of the Trochalakis Restrainer Design Procedure for 1940 El Centro Earthquake (S00E Component), $\mu = 1$.

Example 7.6 : AASHTO Design Procedure for El Centro Earthquake (S00E Component), Scaled to 0.70g.

K_1=2040 kips/in (357 kN/mm), K_2=510 kips/in (89 kN/mm)
$W_1 = W_2$=5000 kips (22.3 MN), Elastic Frames, D_y=4.20 in., s=0.50 in.
Ground Motion = 1940 El Centro Earthquake (S00E Component), Scaled to PGA=0.70g

Step 1 - Calculate Allowable Hinge Displacement
D_r=4.20+0.50=4.7 in. (119 mm)

Step 2 - Calculate Required Restrainer Force
F_r=0.70*W_1=0.70*5000=3500 kips (15.6 MN)
Step 3 - Calculate Required Restrainer Stiffness and Number of Restrainers
$K_r = F_r/D_r$=3500/4.7=745 kips/in (130 kN/mm)
N_r=85 Restrainers

Figure 7.6: Detailed Example of the AASHTO Restrainer Design Procedure For 1940 El Centro Earthquake (S00E Component), $\mu = 1$.

7.2 Case Study for Yielding Frames

The multiple-step, single-step, Trochalakis and capacity design procedures are compared for yielding frames, which were evaluated for the new procedures in sections 5.2 and 6.3. The Caltrans and AASHTO procedures are not compared because they do not account for yielding frames. The frames have a period ratio of 0.50, and are designed for a target ductility of μ=4 for the 1940 El Centro earthquake (S00E Component). The multiple-step and single-step procedures give restrainer stiffnesses of 154 kips/in (27.0 kN/mm) and 270 kips/in (47.3 kN/mm), respectively, to limit hinge displacement to 4.7 in. (119 mm). A nonlinear time history analysis determines that the actual restrainer stiffness required to limit hinge displacement is 180 kips/in (31.5 kN/mm). A nonlinear analysis using the results from the multiple-step and single-step procedure results in a maximum hinge displacement of 5.10 in. (130 mm) and 4.06 in. (103 mm), respectively. Below, the Trochalakis and capacity design procedures are used to determine the number of restrainers for this example.

Since the above example is the same as the example in the previous section, except with yielding frames, the Trochalakis procedure gives the same restrainer stiffness as was determined for elastic frames, K_r=255 kips/in (44.6 kN/mm). As previously mentioned, the Trochalakis procedure does not explicitly account for different levels of inelastic demand. For this example, the Trochalakis procedure is slightly conservative. The procedure predicts approximately 40% more restrainers than determined from nonlinear time history analysis. The maximum hinge displacement obtained from nonlinear time history analysis using the restrainer stiffness from the Trochalakis procedure is 4.10 in. (104 mm).

In the capacity design procedure, the restrainer force is equal to the difference between the frame longitudinal shear force capacities (Priestley et al., 1995). After the allowable hinge displacement is calculated, the next step is to calculate the absolute maximum displacement of the frames. The procedure does not specify how this is done, but for consistency, the frame displacements are determined from the substitute structure method. The required restrainer force, based on the difference in the frame capacities, is 1620 kips (7.21 MN), as shown in figure 7.7. The stiffness of the restrainers is determined by dividing the required restrainer force by the relative

absolute displacements of the frames, resulting in a restrainer stiffness of 325 kips/in (57 kN/mm). This is nearly twice the actual restrainer stiffness determined from nonlinear analysis. The maximum hinge displacement from nonlinear analysis using the stiffness determined from the capacity design procedure is 3.80 in. (96.5 mm).

Example 7.7 : Capacity Design Procedure For El Centro Earthquake (S00E Component), For Yielding Frames ($\mu = 4$).

K_1=2040 kips/in (357 kN/mm), K_2=510 kips/in (89.3 kN/mm)
$W_1 = W_2$=5000 kips (22.3 MN), μ =4, D_y=4.20 in., s=0.50 in
F_{y_1}=2500 kips (11.1 MN), F_{y_2}=880 kips (3.92 MN)
Ground Motion = 1940 El Centro Earthquake (S00E Component), Scaled to PGA=0.70g.

Step 1 - Calculate Allowable Hinge Displacement
D_r=4.20+0.50=4.7 in. (119 mm)

Step 2 - Compute Frame Displacements Without Restrainers
K_{eff_1}=2041/4=510 kips/in (89.3 kN/mm), K_{eff_2}=510/4=128 kips/in (22.4 kN/mm)

$T_{eff_1} = 2\pi\sqrt{5000/(32.2*12)/510} = 1.0$ sec.,
$T_{eff_2} = 2\pi\sqrt{5000/(32.2*12)/128} = 2.0$ sec.

$\xi_{eff} = 0.05 + (1 - 0.95/\sqrt{4} - .05\sqrt{4})/\pi = 0.19$
$D_1 = S_d(1.0,0.19)$=4.75 in. (121 mm)
$D_2 = S_d(2.0,0.19)$=9.73 in. (247 mm)

Calculate the Required Restrainer Stiffness to Limit Hinge Displacement
$F_R = F_{y_1} - F_{y_2}$=2500-880=1620 kips (7.21 MN)
$D_{eq_0} = \mid D_2 \mid - \mid D_1 \mid$ = 9.73-4.75=4.98 in. (126 mm)
$K_r = F_R/D_{eq_0}$=1620/4.98=325 kips/in (1.45 MN)

N_r=38 Restrainers

Figure 7.7: Detailed Example of the Capacity Design Procedure For Restrainers With Yielding Frames for El Centro Earthquake (S00E Component), $\mu = 4$.

This capacity design procedure, which suffers from ignoring dynamics, has several shortcomings, as discussed in section 2.4.4. First, calculating the required force as the difference of the overstrengths in the frames assumes that the frames are moving in phase and have reached their maximum displacements when the maximum opening occurs. This may not necessarily be the case, and is dependent on the properties of the frames and the ground motion. Second, equilibrium of a free body diagram of the system illustrates that the frame inertia forces must be included to adequately determine the restrainer force. The third problem with this procedure is the calcu-

lation of the restrainer stiffness. The procedure specifies adjusting the yield strength of the restrainers until the yield displacement is equal to the relative displacement of the frames. This seems to defeat the purpose of the restrainer design procedure. The goal of the procedure should be to limit the displacement to a value less than the initial hinge opening.

The results from the design procedures for hinge restrainers are summarized in tables 7.1 and 7.2. The next section compares the procedures over a range of frame period ratios.

Table 7.1: Maximum Hinge Displacement for Various Hinge Restrainer Design Procedures for 1940 El Centro Earthquake (S00E Component): $T_1 = 0.50$ sec., $T_2 = 1.00$ sec., $D_r = 4.7$ in. (119 mm), and $\mu = 1$.

	Restrainer Stiffness	No. of Restrainers	Hinge Displacement
Method	K_r, kips/in (kN/mm)	N_r	D_{eq}, in. (mm)
Nonlinear Anal.	800 (140)	97	4.70 (119)
Multi-Step	740 (130)	90	4.96 (126)
Single-Step	1150 (201)	138	4.02 (102)
Caltrans	0 (0)	0	9.26 (235)
Mod. Caltrans	1350 (236)	162	3.90 (99.0)
Trochalakis	255 (44.6)	29	8.11 (206)
AASHTO	745 (130)	85	4.90 (124)

Table 7.2: Maximum Hinge Displacement for Various Hinge Restrainer Design Procedures for 1940 El Centro Earthquake (S00E Component): $T_1 = 0.50$ sec., $T_2 = 1.00$ sec., $D_r = 4.7$ in. (119 mm), and $\mu = 4$.

	Restrainer Stiffness	No. of Restrainers	Hinge Displacement
Method	K_r, kips/in (kN/mm)	N_r	D_{eq}, in. (mm)
Nonlinear Anal.	180 (31.5)	21	4.70 (119)
Multi-Step	154 (27.0)	18	5.10 (130)
Single-Step	270 (47.3)	32	4.06 (103)
Trochalakis	255 (44.6)	29	4.10 (104)
Capacity Design	325 (56.9)	39	3.80 (96.5)

7.3 Evaluation of Hinge Restrainer Design Procedures for 2-DOF Elastic Frames

The effectiveness of the restrainer design procedures is examined for a range of frame period ratios. Only elastic frames are explicitly considered because yielding is not considered in most of the procedures discussed in section 7.1. For each frame period ratio, a nonlinear analysis is performed to determine the restrainer stiffness required to limit hinge displacement. The restrainer design procedures are evaluated for the 1940 El Centro earthquake (S00E component) and 1994 Sylmar Hospital free-field record for T_1/T_2=0.30 to 1.00, and D_r = 4.7 in. (119 mm). The results, discussed below, are shown in figures 7.8 and 7.9.

For the 1940 El Centro record, the nonlinear time history analysis shows that restrainer stiffnesses ranging from K_r = 1550 kips/in (182 MN/m) for highly out-of-phase frames and no restrainers for frames with period ratios greater than 0.80 are needed to limit hinge displacement to 4.7 in. (119 mm). For the Sylmar record, the nonlinear analysis shows restrainer stiffnesses ranging from K_r = 1400 kips/in (245 MN/m) are needed for highly out-of-phase frames and no restrainers for are needed frames with period ratios greater than 0.90. Since the nonlinear analysis accounts for pounding and friction, it provides the most realistic estimate of the required number of restrainers to limit hinge displacement.

For the 1940 El Centro record, the multiple-step procedure gives restrainer stiffnesses less than those determined from nonlinear analysis for frame period ratios less than 0.50 and greater than those determined from nonlinear analysis for frame period ratios greater than 0.50. For the 1994 Sylmar Hospital free-field record, the multiple-step procedure is unconservative for frame period ratios less than 0.50, and compares well with nonlinear analysis for frame period ratios greater than 0.50. The previous chapters showed that, for highly out-of-phase frames, the multiple-step procedure is slightly unconservative, and for in-phase frames the procedure is conservative. Overall, however, the multiple-step procedure does a good job of determining the restrainer stiffnesses to limit hinge displacements to yield.

For both the 1940 El Centro record and 1994 Sylmar Hospital free-field records, the

single-step procedure compares well with the restrainer stiffnesses determined from nonlinear analyses. For the entire frame period ratio range, the single-step procedure is within 20% of the stiffness determined from nonlinear analyses.

The Caltrans procedure does not perform adequately in predicting the required restrainer stiffness to limit hinge displacement for the 1940 El Centro and 1994 Sylmar Hospital free-field records, as is evident in figures 7.8 and 7.9. For low frame period ratios, the Caltrans procedure determines that restrainers are not required. By using the smallest frame displacement as the hinge displacement, the Caltrans procedure significantly underestimates the response of frames. As the frame period ratio approaches unity, the procedure does not account for the reduction in the required restrainer stiffness due to the in-phase motion of the frames. Overall, the procedure is unconservative for out-of-phase frames and conservative for frames that are in-phase.

The modified Caltrans procedure performs much better than the Caltrans procedure in predicting the required restrainer stiffness to limit hinge displacement. For low to moderate frame period ratios, the modified Caltrans procedure gives a restrainer stiffness which is similar to the multiple-step procedure. For out-of-phase frames, the hinge displacement is typically controlled by the response of the most flexible frame, so the modified Caltrans procedure works well for these cases. For frame period ratios greater than 0.50, however, the modified Caltrans procedure gives over twice as many restrainers as determined from nonlinear analysis.

For the 1940 El Centro record, the Trochalakis procedure is unconservative in determining the required restrainer stiffness to limit hinge displacement. For the frame period range between 0.30 and 0.60, the Trochalakis procedure predicts 50% fewer restrainers than that determined from nonlinear analysis. For the 1994 Sylmar Hospital free-field record, the Trochalakis procedure is also unconservative. For out-of-phase frames, the Trochalakis procedure does not accurately determine the required restrainer stiffness to limit hinge displacement.

For the 1940 El Centro record, the AASHTO procedure is unconservative for highly out-of-phase frames. However, for frame period ratios greater than 0.50, the AASHTO procedure is too conservative. The AASHTO procedure predicts over twice

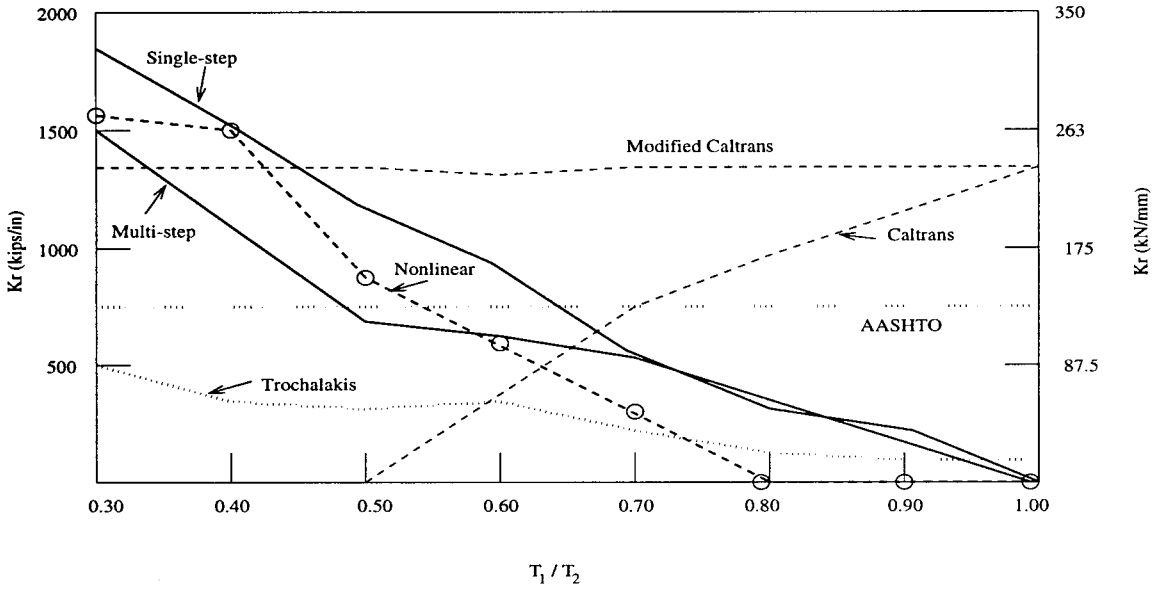

Figure 7.8: Comparison of Required Restrainer Stiffness for 1940 El Centro Earthquake (S00E Component), $D_r = 4.7$ in. (119 mm), $\mu = 1$.

as many restrainers as the nonlinear analysis in this range. Similarly, for the 1994 Sylmar Hospital free-field record, the AASHTO procedure is unconservative for low frame period ratios and conservative for frame period ratios larger than 0.40. Since the AASHTO procedure is only based on the peak ground acceleration and the weight of the frames, it does not account for the relative phasing of the frames.

7.4 Application of Restrainer Design Procedures to Four-Frame Bridge

In this section, the design procedures are compared for a typical four-frame bridge. The properties of the bridge are shown in figure 7.10. The hinges have a restrainer slack and gap of 0.50 in. (12.7 mm), and a target hinge displacement of 4.7 in. (119 mm), corresponding to the yield displacement of 20 ft (6.10 m) restrainers plus the restrainer slack. The procedures are compared for the 1940 El Centro earthquake (S00E component) and the 1994 Northridge earthquake (Sylmar Hospital free-field record). The procedures are first compared for elastic frames.

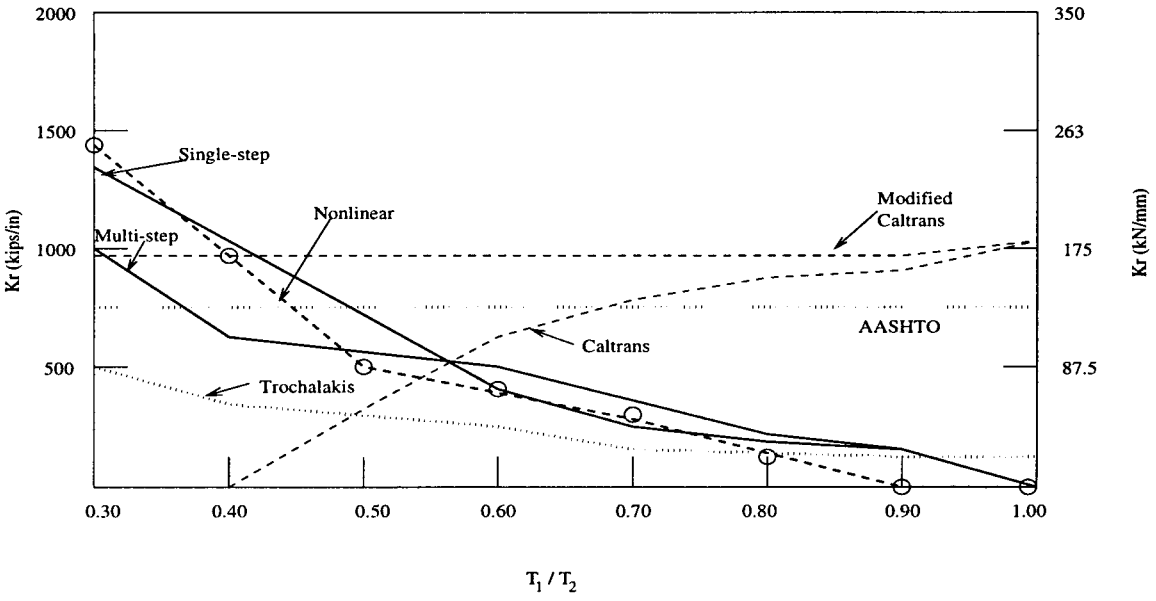

Figure 7.9: Comparison of Restrainer Stiffness for 1994 Northridge Earthquake (Sylmar Hospital Free-Field Record), $D_r = 4.7$ in. (119 mm), $\mu = 1$.

The design procedure is applied to hinges 1 and 2 because the bridge is symmetric about the center. The response of hinges in a multiple-frame bridge is highly nonlinear. During an earthquake, the condition of the intermediate hinge alternates between the closed and open positions. In the open position, the frames vibrate independently if the restrainers have not engaged. In the closed position, the frames are in contact and vibrate together. To achieve a conservative hinge restrainer design, all possible hinge conditions are considered. The design at each hinge is accomplished by considering several cases of frame movement. For hinge 1, case 1 evaluates frame 1 moving left and frame 2 moving right (hinge 2 open). Case 2 evaluates frame 1 moving left and frame 2 & 3 moving right (hinge 2 closed). Similarly, the cases considered for hinge 2 are frame 2 moving left and frame 3 moving right (hinges 1 and 3 open), frames 1 & 2 moving left and frame 3 moving right (hinge 1 closed, hinge 3 open), frames 1 & 2 moving left and frames 3 & 4 moving right (hinges 1 and 3 closed). The case which produces the largest number of restrainers controls the design for each hinge.

The restrainer stiffness determined from each procedure is used in a nonlinear

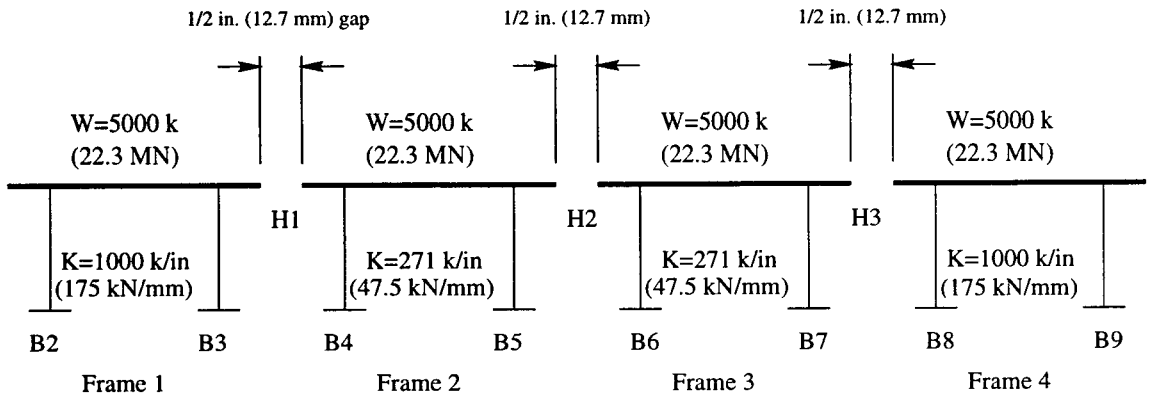

Figure 7.10: Four-Frame Bridge Used for Example Case.

time history analysis of the four frame bridge to determined the hinge displacement, D_{eq}. Table 7.3 shows the restrainer stiffness predicted by each procedure, and the corresponding hinge displacement for the frames subjected to the 1940 El Centro record. The multiple-step procedure does a good job of determining the required number of restrainers to limit hinge displacement to 4.7 in. (119 mm). The procedure gives 89 and 75 restrainers for hinges 1(3) and 2, respectively. The corresponding hinge displacements are 3.86 in. (98.0 mm) and 2.92 in. (74.2 mm). The single-step procedure gives a similar number for hinge 1(3) and 40% fewer restrainers for hinge 2. However, the hinge displacements are within 0.25 in. (35 mm) of the target displacement.

The Caltrans procedure gives results similar to the multiple-step procedure for hinge 1(3); however, the procedure requires 2.5 times more restrainers for hinge 2. The resulting hinge displacements show an interesting phenomenon. Although the Caltrans procedure requires slightly more restrainers at hinge 1(3) than the multiple-step procedure, the hinge displacement is 50% greater. The large number of restrainers at hinge 2 effectively locks that hinge. This introduces a mode where frames 2 and 3 are moving in unison and pounding against frames 1 and 4. This example highlights the importance of balancing the restrainer stiffnesses to distribute hinge displacements. The modified Caltrans procedure gives four times the number of restrainers as the multiple-step procedure for hinges 1(3) and 2. The small hinge displacements are a

result of the large number of restrainers used at the hinges. The Trochalakis procedure does a good job of providing the required number of restrainers to limit hinge displacement. The restrainers for hinges 1(3) and 2 produce displacements of 4.70 in. (119 mm) and 3.90 in. (99.0 mm), respectively. The AASHTO design procedure for hinge restrainers also does an adequate job of limiting hinge displacement.

Table 7.3: Results of Restrainer Design Procedure for Elastic Four-Frame Bridge for the 1940 El Centro Earthquake (S00E Component), $D_r = 4.7$ in. (119 mm)

	Restrainer Stiffness kips/in (kN/mm) [N_r]		Hinge Displacement in. (mm)	
Method	H1, H3	H2	D_{eq} (H1)	D_{eq} (H2)
Multi-Step	775 (136) [89]	647 (113) [75]	3.86 (98.0)	2.92 (74.2)
Single-Step	765 (133) [88]	400 (70.0) [46]	4.88 (124)	4.43 (113)
Caltrans	850 (149) [98]	1569 (275) [181]	5.70 (144)	2.50 (64.0)
Mod. Caltrans	3140 (550) [360]	2411 (421) [278]	1.93 (49.0)	0.84 (21.3)
Trochalakis	947 (165) [109]	264 (46.2) [30]	4.70 (120)	3.90 (99.0)
AASHTO	745 (130) [86]	745 (130) [86]	3.60 (91.4)	2.75 (69.9)

The study is repeated for the bridge subjected to the 1994 Northridge earthquake (Sylmar Hospital free-field record), as shown in table 7.4. In general, all the procedures are conservative in the estimate of the required number of restrainers. The procedures which require the largest number of restrainers are the modified Caltrans and the single-step procedure. The multiple-step and Trochalakis procedures require the fewest restrainers, and the maximum hinge displacements for both cases are less than the target.

The multiple-step, single-step, and Trochalakis procedures are compared for yielding frames subjected to the 1940 El Centro earthquake (S00E Component), as shown in table 7.5. The yield strength of the frames is determined such that the individual frames have a target ductility of $\mu = 4$. The multiple-step procedure requires 26 and 15 restrainers for hinges 1(3) and 2, respectively, approximately one-quarter of the restrainers for the elastic frames. The hinge displacements, 4.01 in. (102 mm) for hinge 1(3) and 3.54 in. (90 mm) for hinge 2, are less than the target displacement of 4.7 in. (119 mm). The single-step procedure predicts more restrainers for hinge 1(3) and fewer restrainers for hinge 2. The hinge displacements, however, are less than

the target. The Trochalakis procedure provides the same number of restrainers as for the elastic case, which is four times the number from the multiple-step procedure for hinge 1 and two times the number from hinge 2. The resulting hinge displacements are small because of the large number of restrainers.

Table 7.4: Results of Restrainer Design Procedure for Elastic Four-Frame Bridge for the 1994 Northridge Earthquake (Sylmar Hospital Free-Field Record), D_r=4.7 in. (119 mm)

	Restrainer Stiffness kips/in (kN/mm) [N_r]		Hinge Displacement in. (mm)	
Method	H1, H3	H2	D_{eq} (H1)	D_{eq} (H2)
Multi-Step	667 (117) [77]	502 (87.8) [58]	2.60 (66.0)	2.40 (61.0)
One-Step	1000 (175) [115]	900 (158) [104]	2.20 (55.9)	1.17 (29.7)
Caltrans	307 (53.7) [35]	1335 (233) [154]	3.80 (96.5)	2.20 (54.0)
Mod. Caltrans	2065 (361) [237]	1031 (180) [119]	1.19 (30.5)	1.30 (33.0)
Trochalakis	473 (82.7) [54]	138 (24.2) [16]	3.40 (86.4)	3.00 (76.2)
AASHTO	745 (130) [86]	745 (130) [86]	2.70 (68.6)	2.30 (58.4)

Table 7.5: Results of Restrainer Design Procedure for a Four-Frame Bridge for the 1940 El Centro Earthquake (S00E Component), $\mu = 4$, D_r=4.7 in. (119 mm)

	Restrainer Stiffness kips/in (kN/mm) [N_r]		Hinge Displacement in. (mm)	
Method	H1, H3	H2	D_{eq} (H1)	D_{eq} (H2)
Multi-Step	226 (39.5) [26]	134 (23.5) [15]	4.01 (102)	3.54 (90.0)
Single-Step	320 (56.0) [36]	101 (17.6) [12]	3.21 (81.5)	2.12 (53.8)
Trochalakis	947 (165) [109]	264 (46.2) [30]	1.96 (49.8)	2.34 (59.4)

7.5 Comparison of Procedures for Curved Multiple-Frame Bridge

In this section, the new procedure is compared with the AASHTO and Caltrans procedures for the Northwest Connector bridge at the I10/215 interchange in Colton, California. The Northwest Connector is a 2540 ft long, curved, concrete box girder

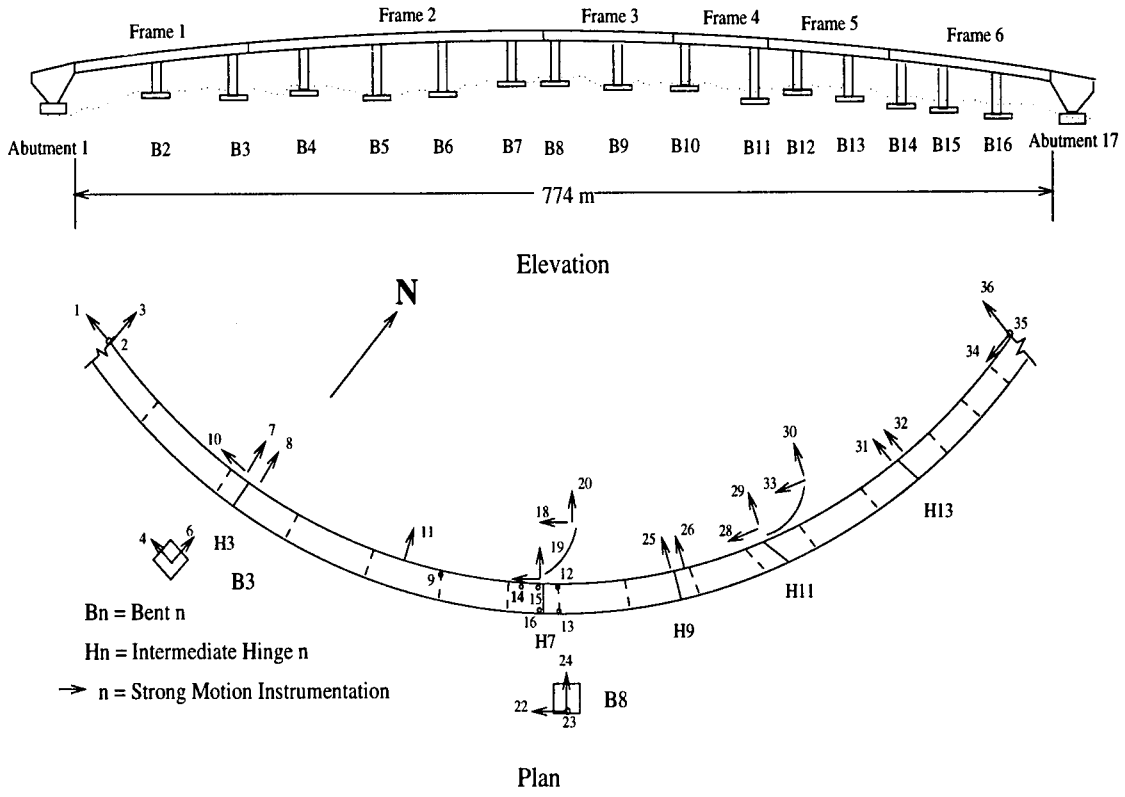

Figure 7.11: General Plan and Strong Motion Instrumentation of the Northwest Connector at the Interstate 10/215 Interchange in Colton, California.

bridge with sixteen spans supported by single column bents and diaphragm abutments as shown in Figure 7.11. Extensive instrumentation of the bridge prior to the 1992 Landers and Big Bear earthquakes has led to studies on the response of the curved bridge as well as the response of the intermediate hinges (DesRoches and Fenves, 1997). For this study, frame elements modeled as elastic and nonlinear compression-only and tension-only elements are used at the intermediate hinges.

The multiple-step procedure is applied to the Northwest Connector subjected to the Landers earthquake, scaled to 0.30g. This level of ground motion correlates well with the previous study by DesRoches and Fenves (1997). The procedure is applied by rotating the the input ground motion into two components at each hinge: one longitudinal to the hinge and one perpendicular to the hinge. The ground motion longitudinal to the hinge is used for the design of the hinge restrainers. The target

hinge displacement is 4.7 in. (119 mm), representing the yield displacement of 20 ft. (6.10 m) restrainers plus a gap of 0.50 in. (12.7 mm).

The results from Caltrans, AASHTO, and multiple-step procedures are shown in table 7.6. The results for the required restrainer stiffness vary greatly between the three procedures. The Caltrans procedure determines that restrainers are not required at any of the hinges. According to the Caltrans procedure, the stiff frame has a displacement less than the permissible hinge opening, resulting in the use of no restrainers. A three-dimensional nonlinear time history analysis shows that the lack of restrainers at hinges 3 and 7 results in hinge displacements which exceed the target displacement.

The restrainer stiffnesses determined from the AASHTO procedure are shown in table 7.6. The results from a nonlinear time history analysis using the stiffness from the AASHTO procedure show that the displacements at hinges 3, 7 and 9 are greater than the target displacement, and the displacements at hinges 11 and 13 are below the target.

The restrainer stiffness determined by the multiple-step results in displacements from a nonlinear analysis which are close to the target. The multiple-step procedure predicts twice as many restrainers as the AASHTO for hinge seven, resulting in displacements close to the target. In addition, the procedure determines that restrainers are not required at hinges 9 and 13, because the hinge displacement without restrainers is smaller than the target displacement of 4.7 in. (119 mm).

Overall, the multiple-step procedure is the most effective procedure for determining the required restrainer stiffness to limit hinge displacement for the case considered. The procedure provides a large number of restrainers in hinges where the frames are highly out-of-phase (H3 and H7), and a low number of restrainers where the frames are in-phase (H9 and H13). The result of a nonlinear time history analysis confirms that the restrainer stiffnesses predicted by the procedure correlate well with those determined from nonlinear time history analysis.

Table 7.6: Comparison of Restrainer Design Procedures for a Curved Connector Bridge Subjected to Landers Earthquake, Scaled to 0.30g, $D_r = 4.7$ in. (119 mm).

Hinge	Caltrans Procedure		AASHTO Procedure		Multi-Step Procedure	
	K_r (kips/in) (N_r) *K_r (kN/mm)*	D_{eq} (in) *D_{eq} (mm)*	K_r (kips/in) (N_r) *K_r (kN/mm)*	D_{eq} (in) *D_{eq} (mm)*	K_r (kips/in) (N_r) *K_r (kN/mm)*	D_{eq} (in) *D_{eq} (mm)*
H3	0 (0) *0*	7.32 *185*	230 (28) *40.2*	6.36 *162*	533 (64) *93.3*	4.56 *116*
H7	0 (0) *0*	7.80 *198*	209 (25) *36.6*	4.80 *121*	260 (31) *45.5*	3.90 *99.0*
H9	0 (0) *0*	0.60 *15.3*	181 (22) *31.6*	5.28 *134*	0 (0) *0*	4.02 *102*
H11	0 (0) *0*	2.16 *54.9*	181 (22) *31.6*	1.80 *45.7*	70 (8) *12.3*	1.56 *39.6*
H13	0 (0) *0*	3.12 *79.3*	228 (7) *39.9*	1.80 *45.7*	0 (0) *0*	2.52 *64.0*

7.6 Comparisons of Hinge Seat Width Recommendations for Bridges

The current hinge seat width recommendations and procedures were discussed in section 2.3. The current procedures are based on expressions which account for hinge displacement due to thermal expansion of the deck, drift of the frame, and skew angle of the hinge. The minimum hinge seat width from the Caltrans, AASHTO, and New Zealand procedures is 12 in. (508 mm). The minimum hinge seat width from the Japanese code is 28 in. (711 mm). Although these are the minimum hinge seat widths specified in the current codes, new bridge construction in California has minimum hinge seat widths of 24-36 in. (610-914 mm).

Priestley et al. (1996) recommends a simplified procedure for determining the hinge seat width. According to this procedure, the relative hinge displacement can be determined from the difference between the absolute maximum peak of longitudinal displacement calculated for the two frames, where each frame is considered as independent. The procedure does not recommend methods to determine the dis-

placement of yielding frames. However, for consistency, the displacements can be estimated using the substitute structure approach.

The proposed procedure for the hinge seat width is based on a performance level of collapse prevention. Previous earthquakes have shown that unseating of bridge spans can lead to collapse of bridges. Therefore, the design ground motion should be based on the maximum credible earthquake for the site.

The proposed procedure for hinge seat widths is determined from a condition that the hinge does not have restrainers. If the hinge seat recommendation is followed, restrainers are not necessary to limit hinge displacement. However, restrainers may be used to achieve higher performance levels. Based on this, the recommendation for hinge seat widths is:

$$N = 1.3D_{eq_0} \tag{7.1}$$

where D_{eq_0} is the maximum relative hinge displacement without restrainers and is obtained from the first step of the multiple-step procedure from section 5.1 as follows:

$$D_{eq_0} = \sqrt{D_1^2 + D_2^2 - 2\rho_{12}D_1D_2}$$

The frame maximum displacements, D_i, are obtained from a response spectrum analysis as discussed in section 5.1. The factor of 1.3 increases the displacement, D_{eq_0}, to allow for uncertainties in the system and the input ground motion. A similar expression has been proposed to determine the minimum separation between buildings to avoid pounding (Kasai et al., 1996).

Relative hinge displacements are affected by the frame period ratio, frame ductility demand, and the characteristics of the ground motion, as was shown in Chapter 4. A parameter study is conducted to compare equation 7.1 and current hinge seat width recommendations with the maximum hinge displacement (without restrainers) from nonlinear time history analysis. The parameter study is performed over a range of frame period ratios, and frame target ductilities. The frame period ratio is varied from 0.30 to 1.00, and the frame target ductilities are μ=1, 2, and 4. The study is performed without restrainers, since current procedures assume no restrainers at the hinge. The procedure is applied for the 1940 El Centro earthquake (S00E component) and 1994 Northridge earthquake (Sylmar Hospital free-field record), scaled to 0.70g.

Figure 7.12 shows the maximum relative hinge displacement for the 1940 El Centro record. For elastic frames, the maximum relative hinge displacement from nonlinear time history analysis is approximately 8 in. (203 mm) for out-of-phase frames, and decreases to zero as T_1/T_2 approaches unity. The recommended hinge seat widths from the Japan, Caltrans, AASHTO, and New Zealand codes are all greater than the maximum hinge displacement from the nonlinear time history analysis. The proposed hinge seat width is approximately 30% greater than results from nonlinear time history analysis for low frame period ratios, and is approximately 40-60% larger for frame period ratios greater than 0.50. The results from the Priestley procedure is unconservative for frame period ratios from 0.40-0.90. The hinge seat width from this procedure is approximately 30% less than the maximum relative hinge displacements determined from nonlinear time history analysis.

For $\mu = 2$, the hinge displacement determined from the nonlinear time history analysis is approximately 30% less than the displacement from elastic analysis, except for $T_1/T_2 = 0.30$, where the proposed hinge seat width is approximately the same as determined from nonlinear analysis. The results from the Priestley procedure are unconservative by approximately 50-75% in the entire range of frame period ratios. The hinge displacement for $\mu = 4$ shows similar results. However, the Priestley procedure shows much better correlation with the results from nonlinear time history analysis for this case.

The hinge displacements from the 1994 Northridge earthquake (Sylmar Hospital free-field record), shown in figure 7.13, show similar trends. However, the hinge displacements determined from nonlinear time history analysis exceed the proposed minimum hinge seat width from the AASHTO and New Zealand codes (12 in.). However, they are well below the minimum hinge seat widths for Japan and Caltrans. The Priestley recommendation is unconservative for the entire range of frame period ratios.

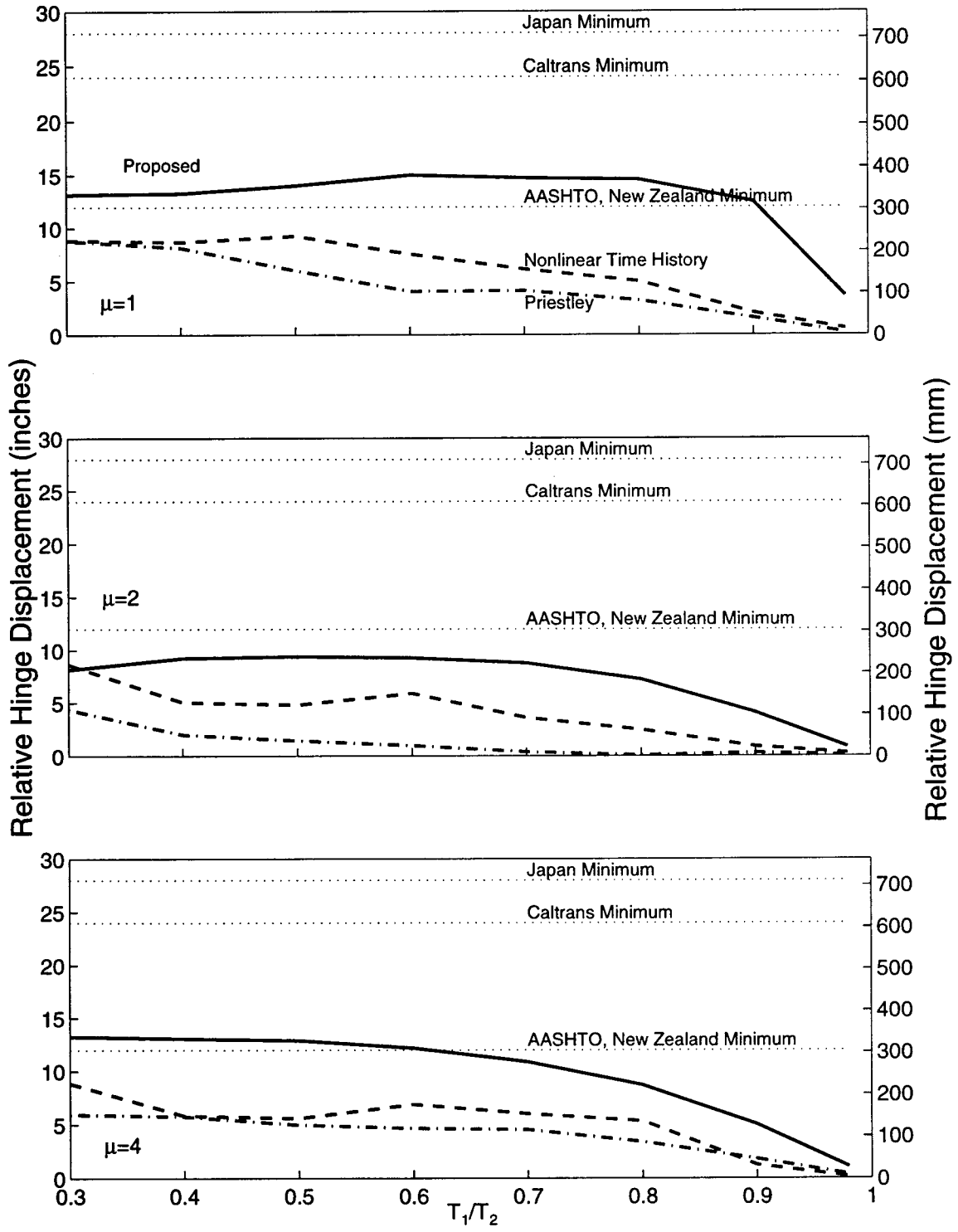

Figure 7.12: Comparison of Hinge Seat Widths with Nonlinear Time History Analysis for 1940 El Centro Earthquake (S00E Component), $T_2/T_g = 1.0$.

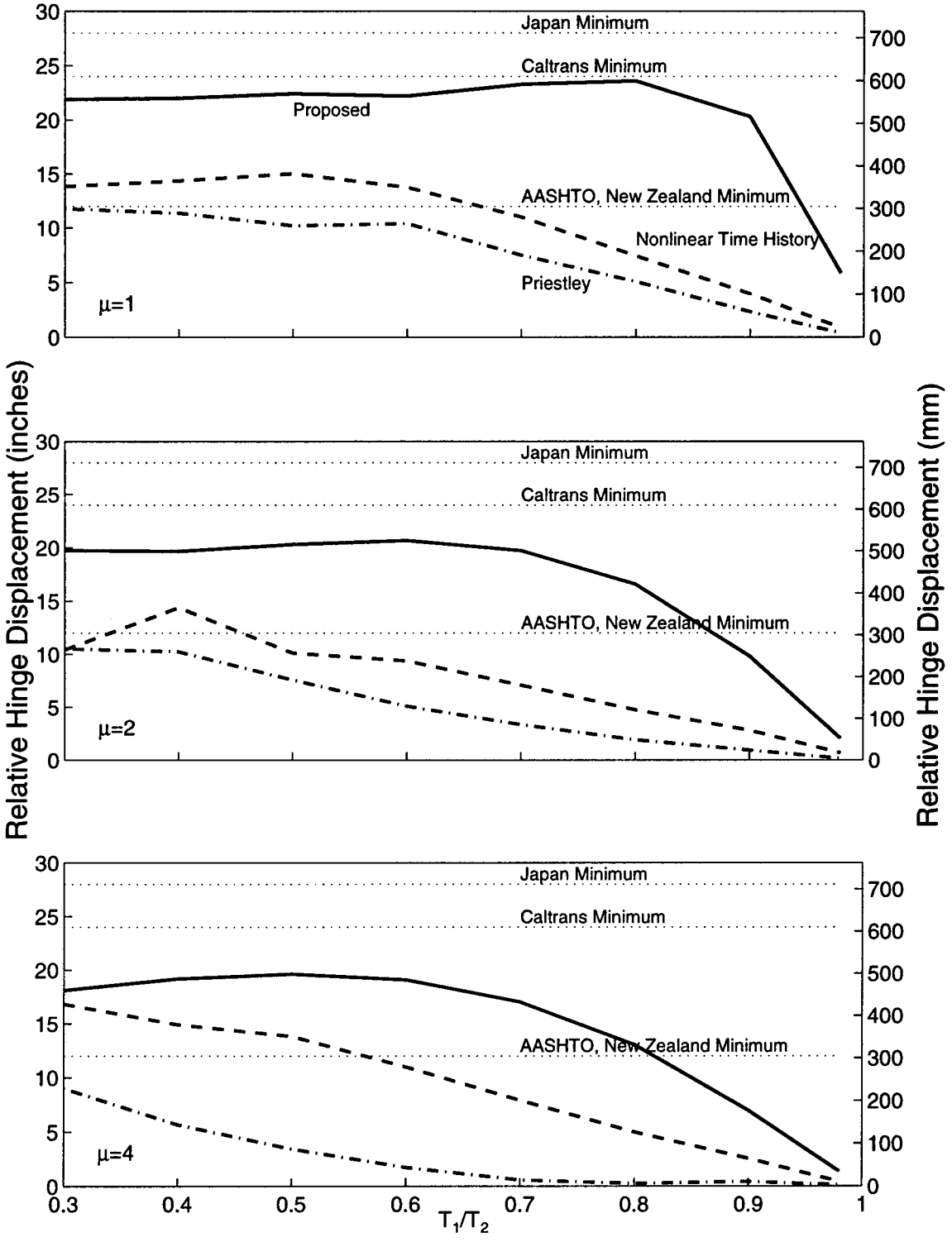

Figure 7.13: Comparison of Proposed Hinge Seat Widths with Nonlinear Time History Analysis for 1994 Northridge Earthquake (Sylmar Hospital Free-Field Record), $T_2/T_g = 1.0$.

7.7 Summary of Comparison of Restrainer and Hinge Seat Width Design Procedures

This chapter has shown that the current procedures cannot adequately determine the restrainer stiffness to limit hinge displacement to a prescribed value. Several procedures are reasonable for either small frame period ratios or frame period ratios near unity. However, none are adequate for a wide range of frame period ratios. The multiple-step and single-step procedures correlate best with the solutions obtained from nonlinear analysis. The Caltrans procedure is unconservative for low frame period ratios and conservative for frame period ratios approaching unity. The modified Caltrans procedure is adequate for highly out-of-phase frames, however, it is very conservative for frames which are in-phase. For elastic frames, the Trochalakis procedure is unconservative for low to moderate frame period ratios. The procedure gives less than half of the restrainers required to limit hinge displacement in this range. The AASHTO procedure is unconservative for low frame period ratios and conservative for frame period ratios greater than 0.50.

Comparisons are made between the multiple-step, single-step, Trochalakis, and capacity design procedure for yielding frames with $\mu = 4$. For the case examined, the Trochalakis procedure is slightly conservative. The capacity design procedure is unrealistic in its estimate of the restrainer stiffness. However, as discussed in section 7.2, the procedure makes several assumptions which lead to inconsistent and unreliable results.

The procedures are applied to a typical four-frame bridge to determine their effectiveness for multiple-frame bridges. In general, the procedures are conservative in determining the number of restrainers to limit hinge displacement. The importance of distributing restrainer stiffnesses to balance the hinge displacement is highlighted in the study. A large number of restrainers at one hinge can "lock" that hinge, which causes a large hinge displacement at another hinge.

As previously shown in Chapter 5, yielding frames require significantly fewer restrainers to limit their hinge displacement. A four-frame bridge example confirms this observation.

The multiple-step procedure, applied to a curved connector bridge, shows results which compare well with nonlinear time history analysis.

In summary, the new proposed seat widths show good correlation with maximum relative hinge displacements determined from nonlinear time history analysis. The proposed hinge seat width matches well with nonlinear time history analysis for low frame period ratios, and is conservative at frame period ratios approaching unity. Based on this study, the recommended minimum hinge seat width is the maximum of the displacement determined from equation 7.1 and 24 in. (610 mm). For the earthquake records investigated in this study, the maximum hinge displacement is controlled by the later criteria.

The displacements determined from nonlinear analysis are well below the Caltrans and Japan minimum hinge seat width recommendations. However, the minimum for the AASHTO and New Zealand codes are exceeded for the case with the Sylmar record. The Priestley et al. (1996) recommendation is generally unconservative for the cases examined.

The parameter study shows that the relative hinge displacement for yielding frames is similar to or slightly less than that for frames which are elastic. Although yielding frames may have larger individual frame displacements, there is more in-phase motion, resulting in smaller relative hinge displacements.

Chapter 8

Effects of Pounding and Restrainers on Ductility Demands in Multiple-Frame Bridges

Thus far, it has been shown that cable restrainers are effective in limiting intermediate hinge displacements in multiple-frame bridges subjected to earthquake ground motion. However, the pounding of adjacent frames at the hinge and the engaging of restrainers have a significant effect on the distribution of ductility demands on the frames. This chapter investigates the effect of pounding and engaging of restrainers on the ductility demand in frames, as schematically represented in figure 8.1. Through a parameter study, the factors affecting the distribution of deformation in frames are investigated. Various methods of limiting the system are investigated as a basis for developing a new displacement-based design procedure for determining frame yield strengths to ensure frame ductilities in multiple-frame bridges are less than a target design level.

In section 5.3, it was shown that the response of two frames subjected to the 1994 Northridge earthquake (Sylmar Hospital Free-Field record) is modified due to pounding and engaging of restrainers. The frames are designed to have individual frame ductilities of $\mu = 4$. Without restrainers, the stiffer frame experienced a 40% increase in the ductility demand from it's target design ductility. The more flexible frame had a 5% decrease in the demand compared with the case without pounding.

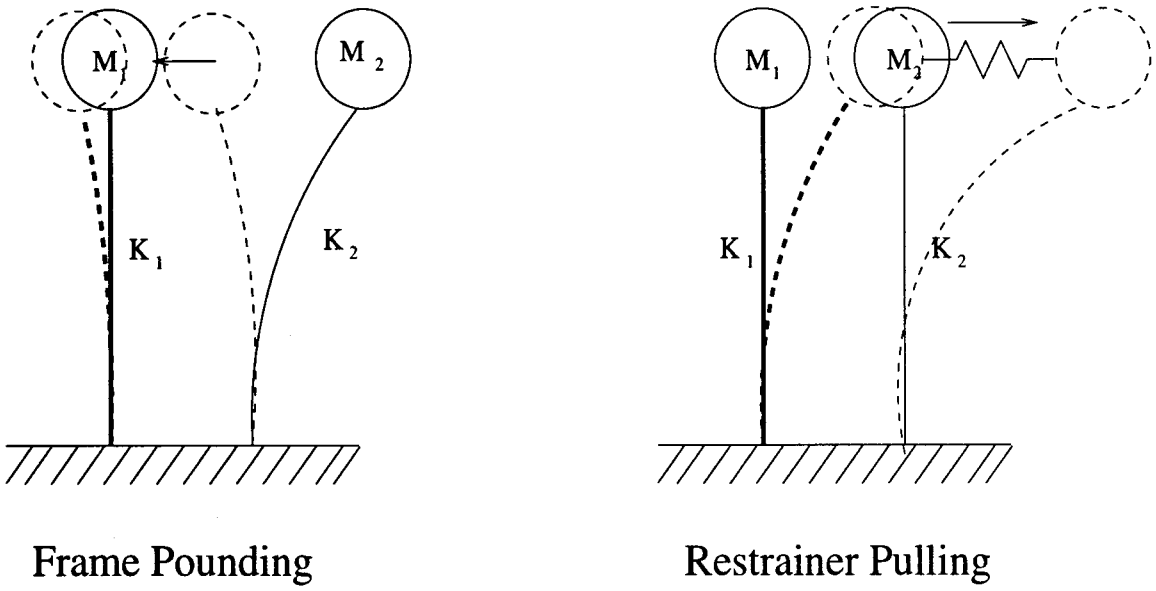

Figure 8.1: Schematic Representation of Frame Pounding and Restrainer Pulling in Adjacent Frames With Different Frame Properties.

The more flexible frame, which has a larger displacement, pounds the stiffer frame, increasing its demand. Likewise, the stiffer frame provides an "obstacle" for the more flexible frame, thereby limiting its displacement. The ground motion is characterized by a large velocity pulse, which makes the effect of pounding more pronounced. The response of the same system with restrainers produces even larger imbalances of the ductilities. The more flexible frame pulls on the stiffer frame increasing its demand. With restrainers, the stiffer frame has a 60% increase in the ductility demand and the more flexible frame has a 45% decrease in the ductility demand.

8.1 Factors Affecting Ductility Distribution in Multiple-Frame Bridges

In this section, a parameter study is conducted to investigate the factors affecting the frame ductility demands. In Chapter 4, it is demonstrated that the important factors in the response of intermediate hinges are frame period ratio, design ductilities, and restrainer stiffness. To examine the effects on frame ductility, the frame period

ratio is varied from 0.30 to 0.98, and three design ductilities are evaluated: $\mu = 2, 4,$ and 6. The frame yield strengths are determined using a constant ductility spectrum to provide the required ductility for individual frames. The effect of restrainer stiffness is determined by looking at three levels of hinge restraint: $D_r/D_{eq_0} = 0.20$, $D_r/D_{eq_0} = 0.50$, and $D_r/D_{eq_0} = 1.00$. These represent the cases with a large number of restrainers, moderate number of restrainers, and the case without restrainers.

Figure 8.2 shows the results for the frames subjected to the 1940 El Centro earthquake (S00E component). Frame 2 has a period of 1.0 sec corresponding to $T_2/T_g = 1.0$. For a target $\mu = 2$, the ductility of frame 2 without restrainers is approximately unity for $T_1/T_2 < 0.50$, and approaches 2 as T_1/T_2 approaches unity. As previously shown, the more flexible frame typically has a reduced ductility demand since it is restrained by impact with the stiffer frame. As restrainers are added, the ductility demand for low period ratios is approximately 1.5, which indicates that, for this case, restrainers are effective in balancing the ductilities of the more flexible frame. The ductility demand for frame 1 remains approximately constant at the design ductility for the case without restrainers for the entire frame period ratio. The addition of restrainers significantly increases the ductility of frame 1. The ductility of frame 1 for highly out-of-phase frames increases as much as 200% for the case with restrainers. The flexible frame 2 is pulling on the stiffer frame 1, producing larger displacements of frame 1 than if it was unrestrained.

The results for target $\mu = 4$ and $\mu = 6$ for the case without restrainers in figure 8.2 are similar to results for the case with $\mu = 2$. Without restrainers, however, frame 1 has an increase in the ductility demand for frame period ratios less than 0.70. This indicates that the pounding of frames increases the displacement of the stiffer frame.

Figure 8.3 shows the same study for the frames subjected to the 1994 Northridge earthquake (Sylmar Hospital free-field record). Frame 2 has a period of 1.6 sec, corresponding to $T_2/T_g = 1.0$. For a target $\mu = 2$, frame 2 has a ductility of 1.5 for $T_1/T_2 = 0.30$ and approaches 2 as T_1/T_2 approaches unity. For the cases with restrainers, the ductility varies from approximately 0.50 at $T_1/T_2 = 0.30$ to 2 as T_1/T_2 approaches unity. The ductility demand of frame 1 increases because of pounding of frames and pulling of restrainers. As the restrainer stiffness increases, the ductility

demand on frame 1 increases; however, this is not necessarily the case for the 1994 Sylmar Hospital free-field record. For $T_1/T_2 = 0.30$, there is a 75% increase in the ductility demands for the case without restrainers, a 50% increase for the case with $D_r/D_{eq_0} = 0.50$, and a 25% increase for $D_r/D_{eq_0} = 0.50$.

For a target $\mu = 4$, the ductility demand on frame 2 without restrainers is approximately constant at $\mu = 4$. However, with restrainers, the frame ductility reduces approximately 50% for low frame period ratios. Frame 1 experiences a 50-75% increase in the ductility for frame period ratios less than 0.50, regardless of the restrainer stiffness. This may indicate that the increase in demand is primarily due to pounding of frames.

For a target $\mu = 6$, the ductility demand on frame 2 without restrainers changes from 7.5 at $T_1/T_2 = 0.30$ to 6 at $T_1/T_2 = 1.0$ without restrainers. The ductility demand is reduced with the addition of restrainers, similar to the cases for target $\mu = 2$ and $\mu = 4$. Frame 1 experiences a significant increase in the ductility demand for low frame period ratios. Increases of approximately 50%, 100%, and 150% are seen for D_r/D_{eq_o} values of 1.0, 0.50, and 0.20, respectively.

Frame pounding and engaging of restrainers can have a significant effect on the ductility demands on the frames. In general, the more flexible frame experiences a reduction in the ductility demand, and the stiffer frame has an increase in the demand. The changes in ductility are most prevalent for out-of-phase frames and decrease as the frames become more in-phase.

8.2 Bounding Models for Multiple-Frame Bridges

A nonlinear model of a bridge including opening and closing of the intermediate hinge and inelastic behavior of the frames is not typically used in bridge design. To account for the nonlinear hinge behavior, it is common to bound the response by two linear models: a tension model and a compression model (Caltrans, 1990). The tension model is intended to capture the response of the bridge when all the hinges are open. In the tension model, there is no longitudinal restraint at the hinges except that provided by the cable restrainers. The restrainers are represented by a linear truss element which can resist both compression and tension. The compression model

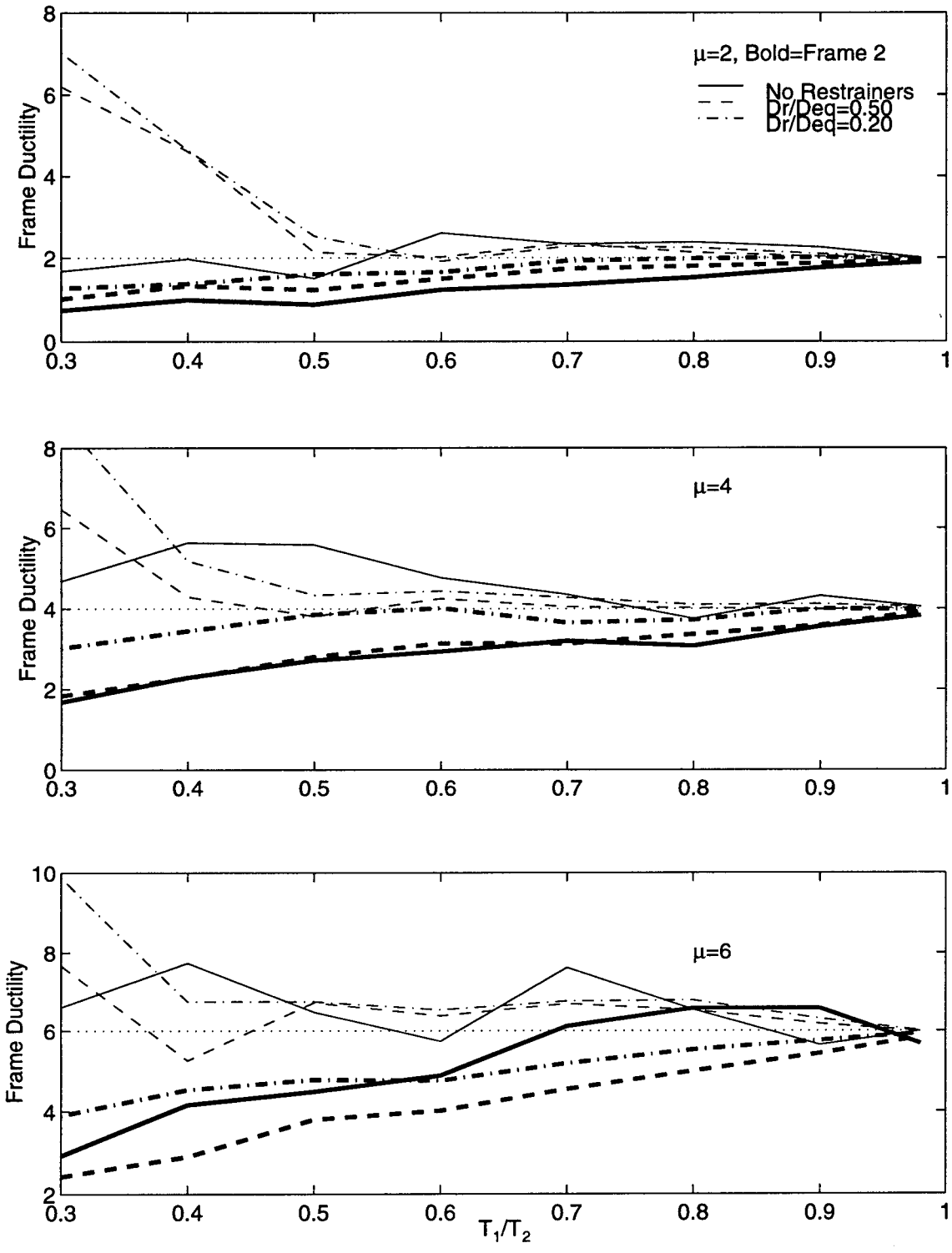

Figure 8.2: Frame Ductilities for Bridge Subjected to 1940 El Centro earthquake (S00E component), $T_2/T_g = 1.0$.

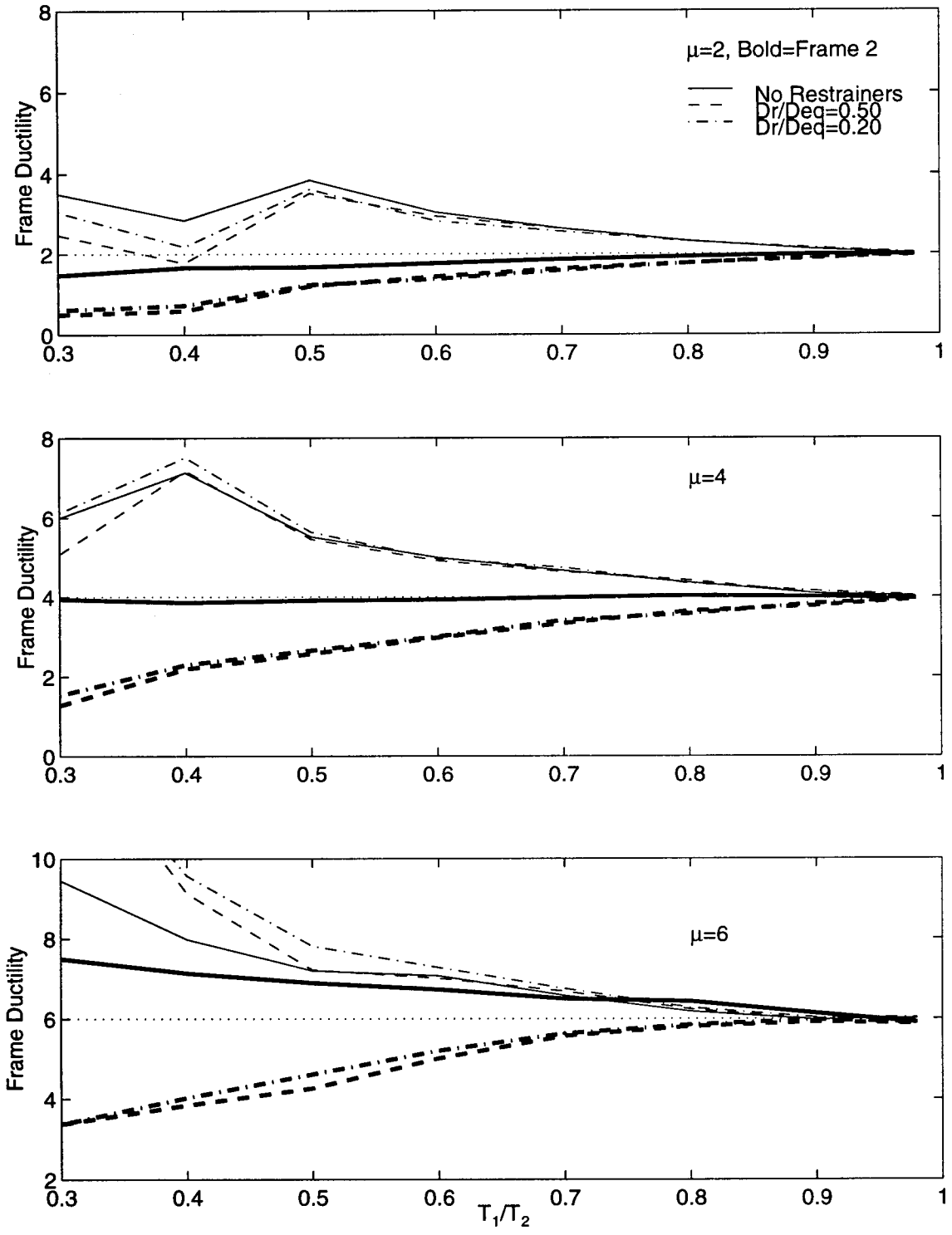

Figure 8.3: Frame Ductilities for Bridge Subjected to 1994 Northridge Earthquake (Sylmar Hospital Free-Field Record), $T_2/T_g = 1.0$.

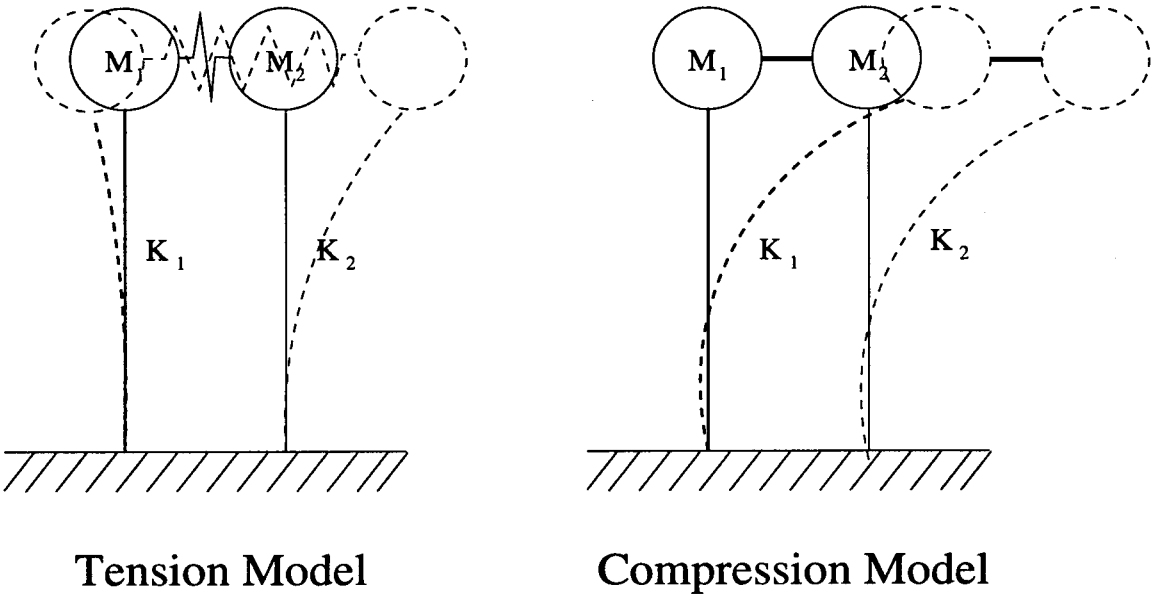

Figure 8.4: Schematic Representation of Tension and Compression Bounding Models

represents the response of the bridge when all the hinges are closed. The relative displacement at the hinge is constrained to be zero. Figure 8.4 shows a graphical representation of the tension and compression models.

For a force-based design, the maximum of the forces obtained from the two models is typically taken as the bounding force for the nonlinear model. A previous study of a multiple-frame curved bridge showed that the tension and compression model works well in bounding column forces (DesRoches and Fenves, 1997). A nonlinear elastic time history analysis compared with the results of the linear bounding model found that only 1 of the 16 column moments was not bounded by the tension and compression models.

The previous study focused on forces from elastic frames. However, typically, frames are designed to yield under strong earthquake ground motion. Although forces may be bounded by the tension and compression model, this does not necessarily imply that the ductility demands can be reliably estimated by this procedure.

8.2.1 Application of Tension and Compression Models

As an example, the bounding models are applied to the two-frame bridge studied in section 5.3, subjected to the 1940 El Centro earthquake (S00E component), scaled to 0.70g. The bounding models are evaluated to determine if they bound: (1) forces in the frames, and (2) ductility demands in the frames. Frame properties and calculations for the example are shown in figure 8.5.

The maximum of the forces from the tension and compression models for frames 1 and 2 are 12,400 kips (55.2 MN), and 5130 kips (22.8 MN), respectively. The elastic forces for frames 1 and 2 obtained from a nonlinear time history analysis, including hinge opening and pounding, are 9800 kips (43.6 MN), and 4700 kips (20.9 MN), respectively. The tension and compression models provide a good bound for the frame forces in this case.

The bounding of frame ductility demands is evaluated by the following procedure:

Step 1: Determine the maximum force from the tension and compression models.

Step 2: Determine the frame yield force by applying a force reduction factor to the elastic frame forces determined from step 1. The force reduction factor is selected such that the frame would have the specified target ductility if responding independently of other frames.

In example 8.1, shown in figure 8.5, the bounding models are evaluated for a design ductility of $\mu = 4$. Using the forces determined from the elastic bounding models, the yield strengths of the frames are determined. A nonlinear analysis of the system results in frame ductility demands which are significantly different than the target $\mu = 4$. Frame 1 has a frame ductility of $\mu_1 = 2.63$, and frame 2 has a frame ductility of $\mu_2 = 7.21$. It is clear from this example that, although the bounding models are adequate in bounding forces, they are not adequate for bounding frame design ductilities, using a force reduction factor based on independent frame response.

Example 8.1 : Example of Bounding Models for Bounding Force and Frame Ductility
K_1=2040 kips/in (357 kN/mm), K_2=510 kips/in (89.3 kN/mm)
$W_1 = W_2$=5000 kips (22.3 MN), $\mu = 4$, $s = 0.50$ in. $g = 0.50$ in.
Ground Motion = 1940 El Centro Earthquake (S00E Component), Scaled to 0.70g.
Calculate Force From Compression Model
F_{1c}=12400 kips= (55.2 MN), F_{2c}=3100 kips (13.8 MN)
Calculate Force From Tension Model
F_{1t}=8250 kips (36.7 MN), F_{2c}=5130 kips (22.8 MN)
Calculate Maximum Force from Tension and Compression Models
F_{1max}=maximum(12400,8250)=12400 kips (55.2 MN),
F_{2max}=maximum(3100,5130)=5130 kips (22.8 MN)
Calculate Force Reduction Factors - Using Constant Ductility Spectrum
Z_1=3.17, Z_2=5.80
F_{y1}=12400/3.17=3900 kips (17.4 MN), F_{y2}=5130/5.80=890 kips (3.96 MN)
Perform Nonlinear Time History Analysis With Properties from Bounding Model
U_{1max}=5.02 in. (128 mm), U_{2max}=12.5 in. (316 mm)
μ_1=2.63, μ_2=7.21

Figure 8.5: Detailed Example of Application of Bounding Models for Four-Frame Bridge for the 1940 El Centro Earthquake (S00E Component).

8.2.2 Parameter Study to Evaluate Tension and Compression Models

The methodology in example 8.1 is applied over a range of frame period ratios, and target ductilities. Figure 8.6 shows the frame elastic forces determined from the tension and compression models compared with the force from nonlinear analysis for elastic frames. The tension and compression models provide a good bound for the frame forces except for highly out-of-phase frames. For $T_1/T_2 = 0.30$, the force determined from the nonlinear analysis for frame 1 without restrainers is 30% greater than that determined from the bounding models. For highly out-of-phase frames, pounding of the stiff frame by the more flexible frame can produce displacements which cannot be captured by the linear bounding models. For the other frame period ratios, the bounding models work well.

Figure 8.7 shows the frame ductility demands using the bounding models. The bounding models are evaluated for target ductilities of $\mu = 2$, 4, 6 for cases with and without restrainers. For $\mu = 2$, the ductility demands in frames 1 and 2 without restrainers are close to the target ductility. With restrainers, the ductility demands on frame 2 increase by 50% compared with the target for $T_1/T_2 = 0.40$. Similarly,

frame 1 ductility increases 50% for $T_1/T_2 = 0.30$.

For target $\mu = 4$, the ductility demand for frame 1 without restrainers is less than the target for the entire frame period ratio range. With restrainers, the ductility demand of frame 1 at $T_1/T_2 = 0.30$ is 25% greater than the target. Frame 2 ductility demands are approximately 50% greater than the target for $T_1/T_2 < 0.70$. The addition of restrainers tends to decrease the ductility demand, except for $T_1/T_2 = 0.40$. The trends for target $\mu = 6$ are similar to those for $\mu = 4$.

Repeating the analysis for the 1994 Northridge earthquake (Sylmar Hospital free-field record) for elastic frames in figures 8.8 and 8.9, the tension and compression models provide an upper bound on the forces in the frames for the entire range of frame period ratios. The bounding models for yielding frames show similar trends as observed from the El Centro record.

In general, the bounding models work well for frame period ratios greater than 0.70. However, for $T_1/T_2 < 0.70$, there are several trends observed from the examples above. For low frame period ratios, the ductility demand in frame 1 without restrainers is near or below the target ductility. With restrainers, there is not much change in the frame ductility compared with the case without restrainers, except for highly out-of-phase frames ($T_1/T_2 = 0.30$). Several cases for both the El Centro and Sylmar records showed increases in design ductilities of 50 to 100% compared to the case with no restrainers.

For $T_1/T_2 < 0.70$, frame 2 ductility demands without restrainers are generally 25 to 75% greater than the target ductility. The addition of restrainers tends to slightly reduce the ductility demands in the frame.

There may be several reasons why the tension and compression models do not bound the ductility demands in the frames. First, for highly out-of-phase frames, the effect of pounding cannot be represented by linear bounding models. Second, the reduction factors which are applied to obtain the frame yield strengths are based on the period of an individual frame. However, the maximum forces are determined from the tension and compression models. If the forces are determined from the compression model, the force reduction factor should be determined from the period of the frame from the compression model.

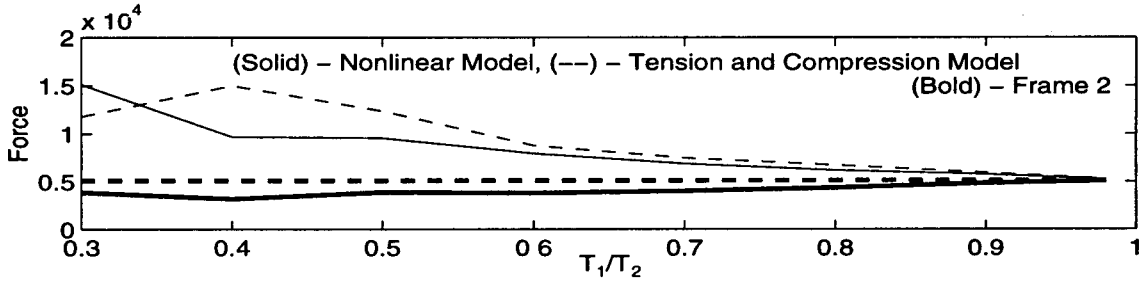

Figure 8.6: Frame Forces from Bounding Models for Frames Subjected to 1940 El Centro Earthquake (S00E Component), $T_2/T_g = 1.0$.

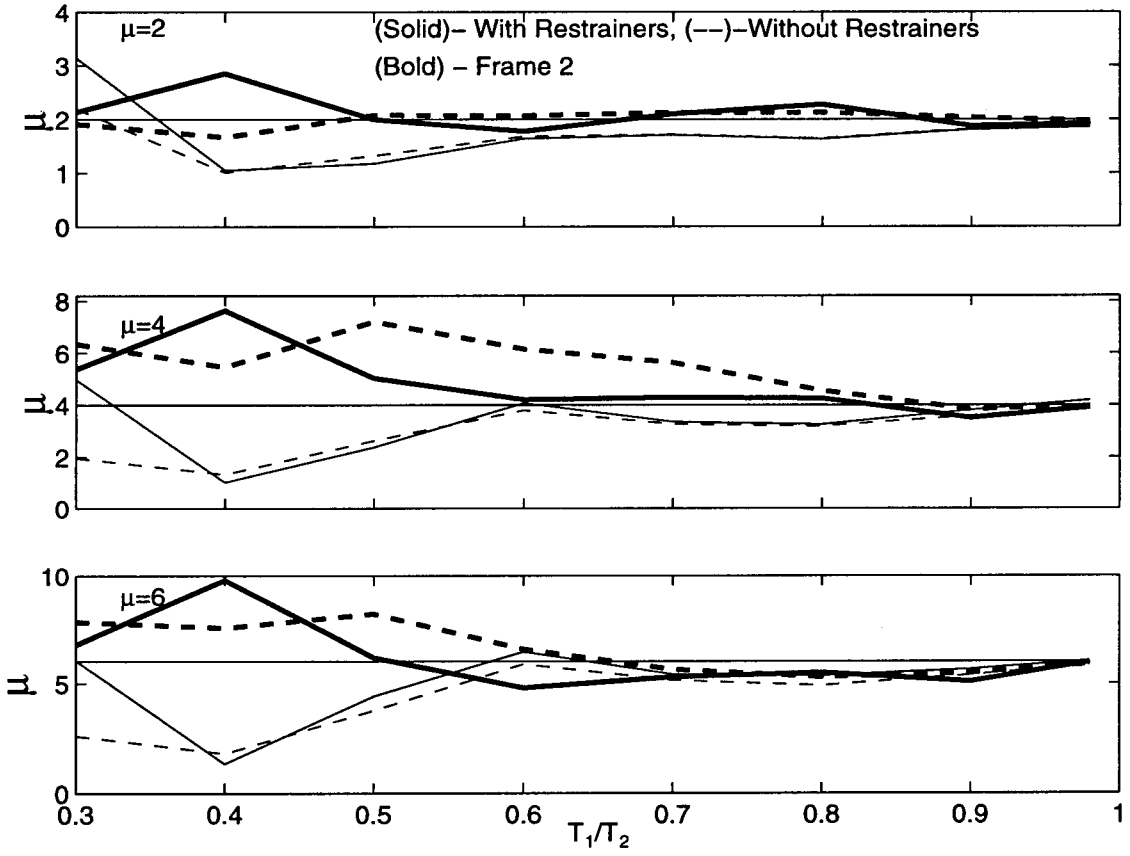

Figure 8.7: Frame Ductility Demands Using Tension and Compression Bounding Models for Frames Subjected to 1940 El Centro Earthquake (S00E Component), $T_2/T_g = 1.0$.

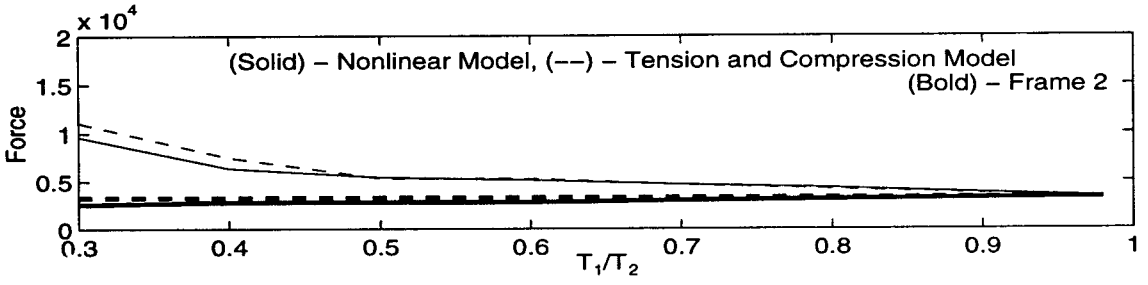

Figure 8.8: Frame Forces from Bounding Models for Frames Subjected to 1994 Northridge Earthquake (Sylmar Hospital Free-Field), $T_2/T_g = 1.0$.

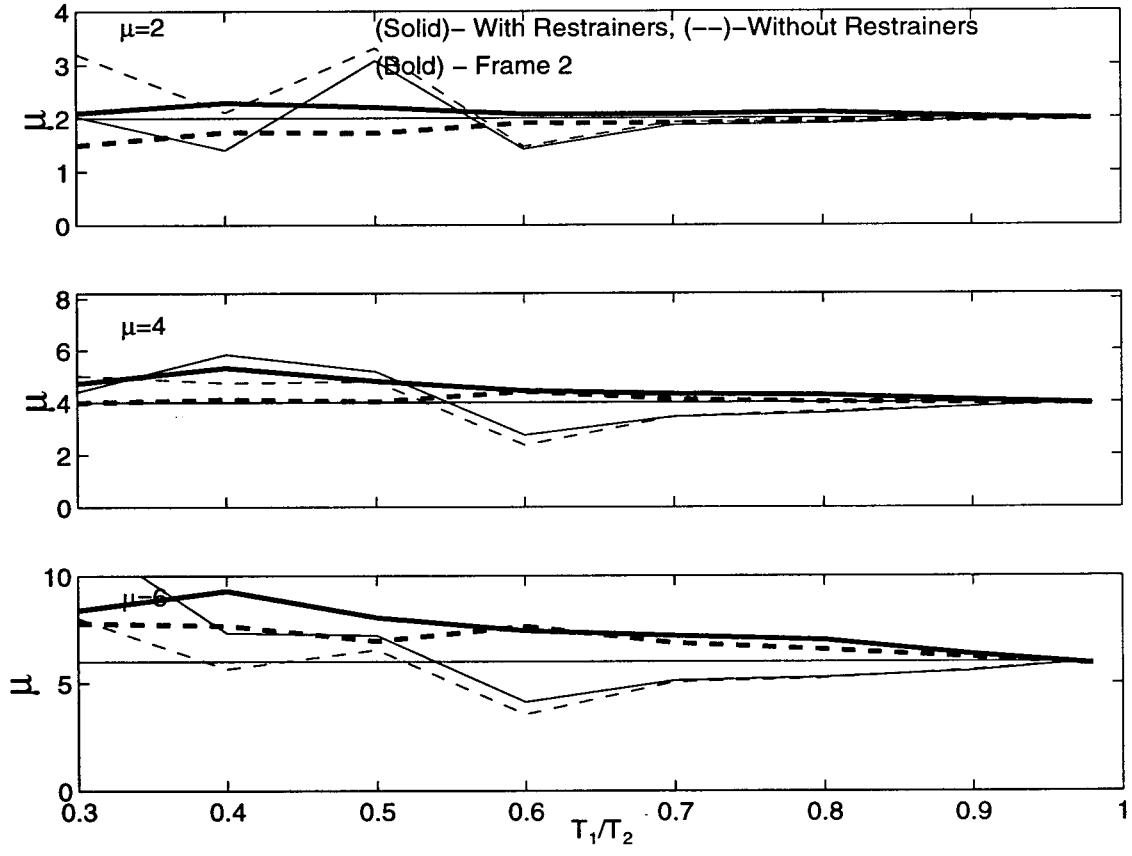

Figure 8.9: Frame Ductility Demands Using Tension and Compression Bounding Models for Frames Subjected to Northridge Earthquake (S00E Component), $T_2/T_g = 1.0$.

Chapter 9

Design Recommendations

9.1 Retrofit of Hinges

9.1.1 Performance Criteria

The goal of bridge retrofit using restrainers is to prevent unseating, which can lead to collapse. Therefore, the performance criteria for the design procedure for hinge restrainers is collapse prevention. The retrofit design should prevent collapse under the maximum credible ground motion.

9.1.2 Maximum Displacement and Restrainer Length

The maximum hinge displacement, D_r, is recommended to be 0.70 % of the available seat width,

$$D_r = 0.70 N_{available} \tag{9.1}$$

where $N_{available}$ is the available hinge seat width accounting for the minimum bearing length and initial gap (which is temperature dependent), and other conditions which may affect the loss of support. Seat extenders may be necessary to increase $N_{available}$. From D_r, the yield displacement, D_y, and the length of restrainers, L_r, may be calculated from

$$D_r = D_y + s \tag{9.2}$$

and

$$L_r = \frac{D_y E}{F_y} \tag{9.3}$$

where s is the slack, $E = 10,0000$ ksi (69 GPa), and $F_y = 176.1$ ksi (1.2 GPa).

9.1.3 Restrainer Design

There are three options for designing hinge restrainers for multiple-frame bridges: (1) the multiple-step procedure, (2) the single-step procedure, and (3) nonlinear time history analysis. The third option should only be used when options 1 and 2 are not applicable.

Multiple-Step Restrainer Design Procedure

The multiple-step restrainer design procedure is an iterative procedure which uses modal analysis to determine the maximum relative hinge displacement, and an incremental stiffness expression to determine the required restrainer stiffness to limit hinge displacement to target. Section 5.2 details the steps in the procedure, and example 5.1 (Figure 5.8) gives detailed calculations for an application of the procedure for highly out-of-phase frames.

The multiple-step procedure is restricted to frames with period ratios greater than 0.30. This represents a stiffness ratio of approximately 10. The response of highly out-of-phase frames is controlled by the pounding of frames. The results from parameter studies in section 5.4 found that nonlinear analysis, which includes pounding, can yield relative hinge displacements which are 25-50% greater than analyses which do not account for pounding.

Single-Step Restrainer Design Procedure

The single-step procedure is a simplified method for determining the required number of restrainers to limit hinge displacement. The single-step procedure does not require modal analysis or iterations to converge to a solution. The only information required for the single-step procedure is the hinge displacement without

restrainers, D_{eq_0}, and the target displacement, D_r. The steps in the procedure and sample calculations are shown in section 6.3.

Since the procedure is based on empirical methods, the range of applicability is more limited than the multiple-step procedure. Although the method was evaluated for T_1/T_2 between 0.30 and 1.00, the variability in the results for $T_1/T_2 < 0.70$ is too large for design. The frame period ratio should therefore be greater than 0.70 for application of the single-step procedure. This represents frame stiffness ratios less than 2. Another limitation for this procedure is the value of the target hinge displacement, D_r. For best results, D_r should be between $0.20D_{eq_0}$ and $0.50D_{eq_0}$. For values outside this range, the multiple-step procedure should be used.

Nonlinear Time History Analysis

Nonlinear time history analysis can be effectively used to design hinge restrainers. Nonlinear time history analysis will provide the most accurate results compared with the other methods since it accounts for all the nonlinearities in the system, including pounding, tension-only restrainers, and friction. However, the complexities and cost of nonlinear time history diminish its practicality. Time history analysis should only be used for cases in which the multiple-step and single-step procedures are not applicable. Chapter 4 discusses the models and numerical methods for nonlinear time history analysis.

Minimum Restrainer Stiffness

There may be cases where the procedures above determine that very few or no restrainers are required to limit hinge displacement (i.e. in-phase frames). However, to provide a level of safety, a minimum stiffness of $K_r = 0.50K_{eff_{mod}}$, where

$$K_{eff_{mod}} = \frac{K_1 K_2}{\mu(K_1+K_2)}$$

should be used in the design of restrainers. For example, for the case with two frames with same stiffness, $K_1 = K_2 = 510$ kips/in (89.3 kN/mm), designed for a target ductility of $\mu = 4$, the minimum recommended restrainer stiffness is 63.8 kips/in (11.2 kN/mm), or $N_r = 8$ restrainers (20-ft length).

Application to Multiple-Frame Bridges

The restrainer design procedure is developed by the analysis of two frames connected at a hinge. In a multiple-frame bridge, the design at each hinge is accomplished by considering the hinge condition at least one hinge away from the hinge which is being designed. Restrainer design calculations consider cases with adjacent hinges (1) open, and (2) completely closed. The case which results in the largest number of restrainers controls the design. It may be necessary to evaluate the overall restrainer design for the system to ensure that there is a balanced design. Section 7.5 illustrated that cases in which one hinge has a large number of restrainers compared with another may lead to an undesirable response of the system.

Application to Curved Bridges

Although the proposed multiple-step restrainer design procedure is developed for straight bridges subjected to longitudinal motion, section 7.6 shows its applicability to curved bridges subjected to longitudinal and transverse motion. The multiple-step procedure is applied by considering only the component of ground motion along the longitudinal axis of each hinge. Although the procedure worked adequately for the example case considered, more studies may be necessary to account for curved bridges and transverse motion in the response of bridges.

Skew Hinges

Although the restrainer design procedure was successfully applied to a curved bridge with slightly skewed hinges, the procedure should be limited to bridges with skew less than 20 degrees. Further investigation is needed to determine applications to bridges with heavy skew. A nonlinear analysis should be used for cases with large skew.

Abutments

The effect of abutments is not explicitly accounted for in the proposed restrainer design procedures. However, for long, multiple-framed bridges, the effect of abutments

in the relative hinge displacement is minimal. In addition, previous studies of 2-frame bridges have shown that abutments have little effect on the maximum relative hinge displacement (Trochalakis et al., 1997). The use of the procedure, as presented in this report, should be limited to long multiple-frame bridges. For cases where the abutments may have a significant effect on the relative hinge displacement, it may be necessary to incorporate the abutment into the design by linearizing the abutment stiffness.

9.2 Design of New Hinges

9.2.1 Performance Criteria

For new bridge design, the performance criteria for hinge seat width is collapse prevention similar to that for retrofit.

9.2.2 Hinge Seat Width

The hinge seat width for new bridges can be obtained from the following equation:

$$N = 1.3D_{eq_0}, > 24\ in.(610\ mm) \tag{9.4}$$

where D_{eq_0} is the hinge displacement without restrainers determined from equation 5.9. The hinge displacement is based on the maximum credible earthquake. The procedure is limited to frames with $T_1/T_2 > 0.30$. For other cases, a nonlinear analysis may be necessary to account for the effects of pounding.

9.2.3 Restrainer Design

Restrainers are not necessary in new bridges if the hinge seat recommendations above are followed and the primary concern is prevention of collapse. However, restrainers may be beneficial in balancing the force distribution between frames. Further studies may be needed to confirm the effectiveness of restrainers in balancing forces in frames.

9.2.4 Bounding Models

The tension and compression bounding models perform adequately in bounding elastic forces in frames, however, they do not adequately bound frame design ductilities. This study shows that, for frame period ratios less than 0.70, the tension and compression bounding models may not provide an adequate bound for frame ductilities. For cases with $T_1/T_2 < 0.70$, nonlinear time history analyses may be necessary to bound the target design ductilities for multiple-frame bridges.

Chapter 10

Conclusions and Future Work

10.1 Summary and Conclusions

The collapse of bridges due to unseating at the hinges in recent earthquakes emphasized the vulnerability of bridges with short seats at intermediate hinges. Although there are no earthquake observations which show failure of restrainers designed by current practice, analytical observations show that the current hinge restrainer design procedures do not adequately determine the required number of restrainers to limit hinge displacement.

The main objective of this research was to develop a reliable procedure to design hinge restrainers for multiple-frame bridges. A simplified nonlinear numerical model is developed to capture the nonlinear behavior of interacting frames subjected to ground motion in the longitudinal direction. The model includes tension-only restrainers, pounding of frames, yielding of frames, and friction.

Using the numerical model and a database of 26 strong motion records, a parameter study is conducted to determine the important system parameters which affect the opening displacement at the hinge. The results show that the most important parameters are the frame period ratio, the restrainer stiffness, and the frame target ductility. As the frame period ratio approaches unity, the relative hinge displacement approaches zero. Frames with low period ratios (highly out-of-phase frames) typically have the largest hinge displacement. The restrainer stiffness is a very important factor in limiting the hinge displacement.

Using the parameter study as a framework, a new multiple-step restrainer design procedure is developed. The procedure is based on a linearized model, which allows the use of modal analysis and optimization theory. Since yielding of frames was found to be very important, it is incorporated into the procedure by means of the substitute structure method. The new design procedure is evaluated by comparing results determined from the new procedure with those from nonlinear time history analysis. The comparison over a range of frame properties and ground motion input records shows that the new design procedure for hinge restrainers is effective in limiting hinge displacement. For highly out-of-phase frames, the procedure is slightly unconservative due to pounding of frames. For these cases, the hinge displacements from the nonlinear analysis compared with the proposed procedure are approximately 25% greater. For frames with a period ratio between 0.50-0.80, the procedure works well. The hinge displacement determined from the proposed procedure is generally within 10% of that determined from the nonlinear analysis. For frame period ratios near unity, the procedure is conservative.

The frame target ductility has a significant influence on the number of restrainers required to limit hinge displacement. Typically, an increase in the frame target ductility from 1 to 4 decreases the required restrainer stiffness approximately 50-75%. This occurs because of the decrease in the effective stiffness of the frames as they yield, and because yielding frames tend to vibrate more in-phase due to greater hysteretic energy dissipation.

Although the multiple-step procedure is fairly simple to use, it does require a modal analysis and several iterations to converge to a solution. Therefore, an alternative to the multiple-step procedure is developed. The single-step procedure is based on a non-dimensional value which is determined by performing a larger number of designs over a range of non-dimensional parameters and earthquake ground motions.

The single-step procedure is evaluated in a similar manner as the multiple-step procedure. The results show that the single-step results correlate well with nonlinear time history analysis. The accuracy of the procedure, however, depends on the frame period ratio. For highly out-of-phase frames, the single-step procedure tends to be conservative. The procedure works best for frame period ratios in the range of 0.70-

1.00.

The multiple-step procedure is applied to a multiple-frame, curved connector bridge. Although the procedure is based on a straight bridge subjected to longitudinal ground motion, proper orientation of the ground motion allows for adequate representation of the longitudinal hinge response. The maximum hinge displacement obtained from nonlinear time history analysis corresponds well with results from the multiple-step procedure, showing that the effects of transverse motion, slightly skewed hinges (less than 30 degrees), and abutments are not important for this typical case.

The results from the multiple-step and single-step procedure are compared with current restrainer design procedures including the Caltrans (1990), AASHTO (1992), Trochalakis (1997), and capacity design procedures (Priestley et al., 1995). None of the procedures perform as well as the multiple-step procedure for the entire range of frame period ratios. The Caltrans procedure is unconservative for low frame period ratios and conservative for high frame period ratios. Similarly the AASHTO procedure is unconservative for low frame period ratios and conservative for high frame period ratios. For frame period ratios greater than 0.50, the procedures predict two to three times the restrainer stiffness determined from nonlinear time history analysis. For elastic frames, the Trochalakis (1997) procedure is slightly unconservative for the entire range of frame period ratios. However, for yielding frames, the procedure is conservative. The capacity design procedure can be either unconservative or conservative depending on the case.

An important aspect of the earthquake response of multiple-frame bridges is pounding of frames at the hinges. When the distance between frames decreases (eventually reaching zero), dynamic impact (pounding) of frames occurs. This can lead to design forces and displacements greater than those typically assumed in design. A parameter study is conducted to determine the factors affecting the distribution of ductility demands between pounding frames in a multiple-frame bridge. Although frames may be designed for a specific target ductility, the actual frame ductility demand can be significantly different. It is shown that highly out-of-phase frames may have ductility demands up to twice the target ductility. Typically, the more flexible frame pounds against the stiff frame, increasing the demands on the stiff frame

beyond the design demand. Similarly, the stiff frame provides an "obstacle" for the more flexible frame, thereby reducing the flexible frame's response. For frame period ratios greater than 0.70, the ductility demands are generally within 25% of the target.

Tension and compression linear models are evaluated to see if they can bound the elastic forces and ductility demands of interacting frames in a multiple-frame bridge. Although they provide a bound for the forces, these models do not represent the ductility in the frames caused by pounding. The ductility demands in multiple-frame bridges designed using the bounding models can have ductilities 1.5-2.0 times the target design ductility.

10.2 Recommendations for Further Research

This study achieved its main objective of developing rational design procedures for hinge restrainers. In the process, areas of future research have been identified. These areas are listed below:

- The current procedures do not account for the effects of abutments. Although the effects of abutments for long-span bridges may be neglected; for shorter bridges they may help limit the hinge displacement. The new procedures need to be modified to account for abutments.

- The current study only accounts for longitudinal earthquake response of straight hinges subjected to longitudinal ground motion. Although an example of a curved bridge shows that the procedures may be applicable to transverse motion and slightly skewed hinges (less than 30 degrees), bridge damage in earthquakes have demonstrated the problems with highly skewed hinges. The current design procedures need to be modified to account for longitudinal and transverse motion for skewed hinges.

- The current procedures do not account for non-uniform input motion due to different soil conditions and the wave passage effects. Previous studies have shown that non-uniform input motion may have an effect on the recommended hinge seat width, and restrainer design. Methods, such as the CQC method for

non-uniform input motion, have been developed, and can be easily implemented into the current procedure.

- Although the current study included the response of intermediate hinges for a large set of earthquake ground motions, further studies are needed to better understand the characteristics of earthquake ground motions which make multiple-frame bridges most susceptible to collapse, particularly the effects of large velocity pulses in forward-directivity near-source ground motions.

- It was shown that force-based design does not provide adequate bounds for the displacement of frames in a multiple-frame bridge. Other methods, such as energy-based method need to be developed to better account for the interaction between frames.

- The relative motion between frames at a hinge provides an opportunity to study the effect of using energy dissipation devices at intermediate hinges. These devices can be used to decrease both relative hinge displacement and overall frame displacements.

- There are no experimental dynamic tests of multiple-frame bridges with hinges and restrainers. An experimental test can be performed to study the effect of frame pounding, friction, and tension-only restrainers on the response of intermediate hinges subjected to strong earthquake ground motion. The test can also investigate the efficacy of energy dissipation devices in limiting relative hinge displacement and overall frame displacements. The experimental studies would provide an opportunity to validate the effectiveness of current numerical models for intermediate hinges.

References

AASHTO (1992). "Standard Specifications for Highway Bridges," American Association of State Highway and Transportation Officials.

Athanassiadou, C. J., Penelis, G. G., and Kappos, A. J. (1994). "Seismic Response of Adjacent Buildings with Similar or Different Characteristics," *Earthquake Spectra*, Vol. 10(No. 2):pp. 293–317.

Bjornsson, S., Stanton, J., and Eberhard, M. (1997). "Seismic Behavior of Skew Bridges," *Report No. SGEM–97/1*, Structural and Geotechnical Engineering and Mechanics, University of Washington, Seattle, January.

Caltrans (1990). "Bridge Design Specifications Manual," California Department of Transportation.

Clough, R. W. and Penzien, J. (1993). *Dynamics of Structures*, 2nd Edition, McGraw-Hill, New York, New York.

Comartin, C., Green, M., and Tubbesing, S. (1995). "The Hyogo-Ken Nanbu Earthquake," *Preliminary Reconnaissance Report*, Earthquake Engineering Research Institute, Oakland, CA., February.

Der Kiureghian, A. (1980). "A Response Spectrum Method for Random Vibrations," *Report No. UBC/EERC–80/15*, Earthquake Engineering Research Center, University of California, Berkeley, December.

DesRoches, R. and Fenves, G. L. (1997). "Earthquake Response and Analysis of a Curved Highway Bridge," *Earthquake Spectra*, Vol. 13(No. 3):pp. 363-386.

Goldsmith, W. (1960). *Impact: the Theory and Physical Behavior of Colliding Solids*, Edward Arnold, London, England.

Gulkan, J. and Sozen, M. (1974). "Inelastic Response of Reinforced Concrete Structures to Earthquake Motion," *ACI Structural Journal*, Vol. 71(No. 12):pp. 604–610.

Jacobsen, L. (1930). "Steady Forced Vibration as Influenced by Damping," *ASME Transactions*, Vol. 52(No. 1):pp. 169–181.

Jennings, P. C. (1968). "Equivalent Viscous Damping for Yielding Structures," *Journal of the Engineering Mechanics Division, ASCE*, Vol. 94(No. 1):pp. 163–113.

Jennings, P. C. (1971). "Engineering Features of the San Fernando Earthquake of February 9, 1971," *Report No. EERL–71–02*, Earthquake Engineering Research Laboratory, California Institute of Technology, Pasadena, December.

Kasai, K., Jagiasi, A., and Jeng, V. (1996). "Inelastic Vibration Phase Theory for Seismic Pounding Mitigation," *Journal of Structural Engineering, ASCE*, Vol. 122(No. 10):pp. 1136–1146.

Kubo, T. and Penzien, J. (1979). "Analysis of Three-Dimensional Strong Motions Along Principle Axes, San Fernando Earthquake," *Earthquake Engineering and Structural Dynamics*, Vol. 7(No. 1):pp. 265–278.

MacRae, G., Priestley, N. M. J., and Tao, J. (1993). "P-Delta Designs in Seismic Regions," *Report No. UCSD/SSRP–93/05*, Structural Systems Research Project, University of California, San Diego, La Jolla, May.

Miranda, E. and Bertero, V. V. (1994). "Evaluation of Strength Reduction Factors for Earthquake-Resistant Design," *Earthquake Spectra*, Vol. 10(No. 2):pp. 357–379.

Moehle, J. P. (1995). "Northridge Earthquake of January 17, 1994: Reconnaissance Report, Volume 1 – Highway Bridges and Traffic Management," *Earthquake Spectra*, Vol. 11(No. 3):pp. 287–372.

Naeim, F., Anderson, J. C., and Jain, S. (1994). "A Database of Earthquake Records for Design," *Proceedings of the Fifth U.S. National Conference on Earthquake Engineering*, volume 2, pp. 263–272, Oakland, CA.

New Zealand Transit (1990). "New Zealand Transit Bridge Specifications," New Zealand Society of Bridge Officials.

Prakash, V., Powell, G. H., and Filippou, F. C. (1992). "DRAIN-3DX: Base Program User Guide," *Report No. UCB/SEMM-92/30*, Structural Engineering, Mechanics and Materials, University of California, Berkeley.

Priestley, M. J. N. and Park, R. (1984). "Strength and Ductility of Bridge Structures," *National Roads Board, RRU Bulletin 71*, volume 1, p. 1, Wellington, New Zealand.

Priestley, M. J. N., Seible, F., and Uang, C. M. (1994). "The Northridge Earthquake of January 17, 1994: Damage Analysis of Selected Freeway Bridges," *Report No. UCSD/SSRP-94/06*, Structural Systems Research Project, University of California, San Diego, La Jolla.

Priestley, M. J. N., Seible, F., and Calvi, G. M. (1995). *Seismic Design and Retrofit of Bridges*, Wiley-Interscience, New York, NY.

Saiidi, M. and Sozen, M. A. (1979). "Simple and Complex Models for Nonlinear Seismic Response of Reinforced Concrete Structures," *Report No. UILU-ENG-79-2013*, Structural Research Series No. 465, University of Illinois, Urbana, Il.

Saiidi, M., Maragakis, E., Abdel-Ghaffar, S., Feng, S., and O' Connor, D. (1993). "Response of Bridge Hinge Restrainers During Earthquakes-Field Performance, Analysis, and Design," *Report No. CCEER 93/06*, Center for Civil Engineering Earthquake Research, University of Nevada, Reno, June.

Saiidi, M., Maragakis, E., and Feng, S. (1996). "Parameters in Bridge Restrainer Design for Seismic Retrofit," *Journal of Structural Engineering, ASCE*, Vol. 122(No. 1):pp. 55–61.

Selna, L. G., Malvar, L., and Zelinski, R. (1989). "Bridge Retrofit Testing: Hinge Cable Restrainers," *Journal of Structural Engineering, ASCE*, Vol. 115(No. 4):pp. 920–933.

Singh, S. and Fenves, G. L. (1994). "Earthquake Analysis and Response of Two-level Viaducts," *Report No. UCB/EERC 94-11*, Earthquake Engineering Research Center, University of California, Berkeley, November.

Takahashi, H. (1990). "Specifications for Highway Bridges Part 5 : Seismic Design," Japan Society of Civil Engineers.

Takeda, T., Sozen, M., and Nielsen, N. (1970). "Reinforced Concrete Response to Simulated Earthquake," *Journal of the Structural Division, ASCE*, Vol. 96(No. 12):pp. 55–61.

Trochalakis, P., Eberhard, M., and Stanton, J. (1997). "Evaluation and Design of Seismic Restrainers for In-Span Hinges," *Journal of Structural Engineering, ASCE*, Vol. 123(No. 4):pp. 103–113.

Uang, C. M. and Bertero, V. V. (1990). "Evaluation of Seismic Energy in Structures," *Earthquake Engineering and Structural Dynamics*, Vol. 19(No. 1):pp. 77–90.

Yang, Y. S., Priestley, M. J. N., and Ricles, J. (1994). "Longitudinal Seismic Response of Bridge Frames Connected By Restrainers," *Report No. UCSD/SSRP-94/09*, Structural Systems Research Project, University of California, San Diego, La Jolla, September.

Yashinsky, M. (1992). "Caltrans Bridge Restrainer Retrofit Program," California Department of Transportation.

Yashinsky, M. (1995). "Seismic Design and Retrofit Procedures for Highway Bridges in Japan," California's office of Earthquake Engineering, California Department of Transportation.

EERC REPORTS

EERC reports are available from the National Information Service for Earthquake Engineering (NISEE) and from the National Technical Information Service (NTIS). To order EERC Reports, please contact the Earthquake Engineering Research Center, 1301 S. 46th Street, Richmond, California 94804-4698, ph 510-231-9468.

UCB/EERC-97/16 Evaluation of Seismic Code Provisions Using Strong-Motion Building Records from the 1994 Northridge Earthquake, by De la Llera, J.C. and Chopra, A.K., May 1998. $33

UCB/EERC-97/15 FEQDrain: A Finite Element Computer Program for the Analysis of the Earthquake Generation and Dissipation of Pore Water Pressure in Layered Sand Deposits with Vertical Drains, by Pestana, J.M., Hunt, C.E., and Goughnour, R.R., December 1997. $15

UCB/EERC-97/14 Vibration Properties of Buildings Determined from Recorded Earthquake Motions, by Goel, R.K. and Chopra, A., December 1997. $26

UCB/EERC-97/13: Fatigue Life Evaluation of Changeable Message Sign Structures -- Volume 2: Retrofitted Specimens, by Chavez, J.W., Gilani, A.S., and Whittaker, A.S., December, 1997. $20

UCB/EERC-97/12: New Design and Analysis Procedures for Intermediate Hinges in Multiple-Frame Bridges, by DesRoches, R. and Fenves, G.L., December, 1997. $26

UCB/EERC-97/11: Viscous Heating of Fluid Dampers During Seismic and Wind Excitations--Analytical Solutions and Design Formulae, by Makris, N., Roussos, Y., Whittaker, A.S., and Kelly, J.M., November, 1997. $15

UCB/EERC-97/10: Fatigue Life Evaluation of Changeable Message Sign Structures -- Volume 1: As-Built Specimens, by Gilani, A.M., Chavez, J.W., and Whittaker, A.S., November, 1997. $20

UCB/EERC-97/09: Second U.S.-Japan Workshop on Seismic Retrofit of Bridges, edited by Kawashima, K. and Mahin, S.A., September, 1997. $57

UCB/EERC-97/08: Implications of the Landers and Big Bear Earthquakes on Earthquake Resistant Design of Structures, by Anderson, J.C. and Bertero, V.V., July 1997. $20

UCB/EERC-97/07: Analysis of the Nonlinear Response of Structures Supported on Pile Foundations, by Badoni, D. and Makris, N., July 1997. $20

UCB/EERC-97/06: Executive Summary on: Phase 3: Evaluation and Retrofitting of Multilevel and Multiple-Column Structures -- An Analytical, Experimental, and Conceptual Study of Retrofitting Needs and Methods, by Mahin, S.A., Fenves, G.L., Filippou, F.C., Moehle, J.P., Thewalt, C.R., May, 1997. $20

UCB/EERC-97/05: The EERC-CUREe Symposium to Honor Vitelmo V. Bertero, February 1997. $26

UCB/EERC-97/04: Design and Evaluation of Reinforced Concrete Bridges for Seismic Resistance, by Aschheim, M., Moehle, J.P. and Mahin, S.A., March 1997. $26

UCB/EERC-97/03: U.S.-Japan Workshop on Cooperative Research for Mitigation of Urban Earthquake Disasters: Learning from Kobe and Northridge -- Recommendations and Resolutions, by Mahin, S., Okada, T., Shinozuka, M. and Toki, K., February 1997. $15

UCB/EERC-97/02: Multiple Support Response Spectrum Analysis of Bridges Including the Site-Response Effect & MSRS Code, by Der Kiureghian, A., Keshishian, P. and Hakobian, A., February 1997. $20

UCB/EERC-97/01: Analysis of Soil-Structure Interaction Effects on Building Response from Earthquake Strong Motion Recordings at 58 Sites, by Stewart, J.P. and Stewart, A.F., February 1997. $57

UCB/EERC-96/05: Application of Dog Bones for Improvement of Seismic Behavior of Steel Connections, by Popov, E.P., Blondet, M. and Stepanov, L., June 1996. $13

UCB/EERC-96/04: Experimental and Analytical Studies of Base Isolation Applications for Low-Cost Housing, by Taniwangsa, W. and Kelly, J.M., July 1996. $20

UCB/EERC-96/03: Experimental and Analytical Evaluation of a Retrofit Double-Deck Viaduct Structure: Part I of II, by Zayati, F., Mahin, S. A. and Moehle, J. P., June 1996. $33

UCB/EERC-96/02: Field Testing of Bridge Design and Retrofit Concepts. Part 2 of 2: Experimental and

Analytical Studies of the Mt. Diablo Blvd. Bridge, by Gilani, A.S., Chavez, J.W. and Fenves, G.L., June 1996. $20

UCB/EERC-96/01: Earthquake Engineering Research at Berkeley -- 1996: Papers Presented at the 11th World Conference on Earthquake Engineering, by EERC, May 1996. $26

UCB/EERC-95/14: Field Testing of Bridge Design and Retrofit Concepts. Part 1 of 2: Field Testing and Dynamic Analysis of a Four-Span Seismically Isolated Viaduct in Walnut Creek, California, by Gilani, A.S., Mahin, S.A., Fenves, G.L., Aiken, I.D. and Chavez, J.W., December 1995. $26

UCB/EERC-95/13: Experimental and Analytical Studies of Steel Connections and Energy Dissipators, by Yang, T.-S. and Popov, E.P., December 1995. $26

UCB/EERC-95/12: Natural Rubber Isolation Systems for Earthquake Protection of Low-Cost Buildings, by Taniwangsa, W., Clark, P. and Kelly, J.M., June 1996. $20

UCB/EERC-95/11: Studies in Steel Moment Resisting Beam-to-Column Connections for Seismic-Resistant Design, by Blackman, B. and Popov, E.P., October 1995. $20

UCB/EERC-95/10: Seismological and Engineering Aspects of the 1995 Hyogoken-Nanbu (Kobe) Earthquake, by EERC, November 1995. $26

UCB/EERC-95/09: Seismic Behavior and Retrofit of Older Reinforced Concrete Bridge T-Joints, by Lowes, L.N. and Moehle, J.P., September 1995. $20

UCB/EERC-95/08: Behavior of Pre-Northridge Moment Resisting Steel Connections, by Yang, T.-S. and Popov, E.P., August 1995. $15

UCB/EERC-95/07: Earthquake Analysis and Response of Concrete Arch Dams, by Tan, H. and Chopra, A.K., August 1995. $20

UCB/EERC-95/06: Seismic Rehabilitation of Framed Buildings Infilled with Unreinforced Masonry Walls Using Post-Tensioned Steel Braces, by Teran-Gilmore, A., Bertero, V.V. and Youssef, N., June 1995. $26

UCB/EERC-95/05: Final Report on the International Workshop on the Use of Rubber-Based Bearings for the Earthquake Protection of Buildings, by Kelly, J.M., May 1995. $20

UCB/EERC-95/04: Earthquake Hazard Reduction in Historical Buildings Using Seismic Isolation, by Garevski, M., June 1995. $15

UCB/EERC-95/03: Upgrading Bridge Outrigger Knee Joint Systems, by Stojadinovic, B. and Thewalt, C.R., June 1995. $20

UCB/EERC-95/02: The Attenuation of Strong Ground Motion Displacements, by Gregor, N.J., June 1995. $26

UCB/EERC-95/01: Geotechnical Reconnaissance of the Effects of the January 17, 1995, Hyogoken-Nanbu Earthquake, Japan, August 1995. $26

UCB/EERC-94/12: Response of the Northwest Connector in the Landers and Big Bear Earthquakes, by Fenves, G.L. and Desroches, R., December 1994. $20

UCB/EERC-94/11: Earthquake Analysis and Response of Two-Level Viaducts, by Singh, S.P. and Fenves, G.L., October 1994. $20

UCB/EERC-94/10: Manual for Menshin Design of Highway Bridges: Ministry of Construction, Japan, by Sugita, H. and Mahin, S., August 1994. $20

UCB/EERC-94/09: Performance of Steel Building Structures During the Northridge Earthquake, by Bertero, V.V., Anderson, J.C. and Krawinkler, H., August 1994. $26

UCB/EERC-94/08: Preliminary Report on the Principal Geotechnical Aspects of the January 17, 1994 Northridge Earthquake, by Stewart, J.P., Bray, J.D., Seed, R.B. and Sitar, N., June 1994. $26

UCB/EERC-94/07: Accidental and Natural Torsion in Earthquake Response and Design of Buildings, by De la Llera, J.C. and Chopra, A.K., June 1994. $33

UCB/EERC-94/05: Seismic Response of Steep Natural Slopes, by Sitar, N. and Ashford, S.A., May 1994. $26

UCB/EERC-94/04: Insitu Test Results from Four Loma Prieta Earthquake Liquefaction Sites: SPT, CPT, DMT and Shear Wave Velocity, by Mitchell, J.K., Lodge, A.L., Coutinho, R.Q., Kayen, R.E., Seed, R.B., Nishio, S. and Stokoe II, K.H., April 1994. $20

UCB/EERC-94/03: The Influence of Plate Flexibility on the Buckling Load of Elastomeric Isolators, by Kelly, J.M., March 1994. $15

UCB/EERC-94/02: Energy Dissipation with Slotted Bolted Connections, by Grigorian, C.E. and Popov, E.P., February 1994. $26

UCB/EERC-94/01: Preliminary Report on the Seismological and Engineering Aspects of the January 17, 1994 Northridge Earthquake, by EERC, January 1994. $15

UCB/EERC-93/13: On the Analysis of Structures with Energy Dissipating Restraints, by Inaudi, J.A., Nims, D.K. and Kelly, J.M., December 1993. $20

UCB/EERC-93/12: Synthesized Strong Ground Motions for the Seismic Condition Assessment of the Eastern Portion of the San Francisco Bay Bridge, by Bolt, B.A. and Gregor, N.J., December 1993. $26

UCB/EERC-93/11: Nonlinear Homogeneous Dynamical Systems, by Inaudi, J.A. and Kelly, J.M., October 1995. $20

UCB/EERC-93/09: A Methodology for Design of Viscoelastic Dampers in Earthquake-Resistant Structures, by Abbas, H. and Kelly, J.M., November 1993. $26

UCB/EERC-93/08: Model for Anchored Reinforcing Bars under Seismic Excitations, by Monti, G., Spacone, E. and Filippou, F.C., December 1993. $15

UCB/EERC-93/07: Earthquake Analysis and Response of Concrete Gravity Dams Including Base Sliding, by Chavez, J.W. and Fenves, G.L., December 1993. $26

UCB/EERC-93/06: On the Analysis of Structures with Viscoelastic Dampers, by Inaudi, J.A., Zambrano, A. and Kelly, J.M., August 1993. $20

UCB/EERC-93/05: Multiple-Support Response Spectrum Analysis of the Golden Gate Bridge, by Nakamura, Y., Der Kiureghian, A. and Liu, D., May 1993. $15

UCB/EERC-93/04: Seismic Performance of a 30-Story Building Located on Soft Soil and Designed According to UBC 1991, by Teran-Gilmore, A. and Bertero, V.V., 1993. $33

UCB/EERC-93/03: An Experimental Study of Flat-Plate Structures under Vertical and Lateral Loads, by Hwang, S.-H. and Moehle, J.P., February 1993. $26

UCB/EERC-93/02: Evaluation of an Active Variable-Damping-Structure, by Polak, E., Meeker, G., Yamada, K. and Kurata, N., 1993. $15

UCB/EERC-92/18: Dynamic Analysis of Nonlinear Structures using State-Space Formulation and Partitioned Integration Schemes, by Inaudi, J.A. and De la Llera, J.C., December 1992. $15

UCB/EERC-92/17: Performance of Tall Buildings During the 1985 Mexico Earthquakes, by Teran-Gilmore, A. and Bertero, V.V., December 1992. $26

UCB/EERC-92/16: Tall Reinforced Concrete Buildings: Conceptual Earthquake-Resistant Design Methodology, by Bertero, R.D. and Bertero, V.V., December 1992. $26

UCB/EERC-92/15: A Friction Mass Damper for Vibration Control, by Inaudi, J.A. and Kelly, J.M., October 1992. $15

UCB/EERC-92/14: Earthquake Risk and Insurance, by Brillinger, D.R., October 1992. $13

UCB/EERC-92/13: Earthquake Engineering Research at Berkeley - 1992, by EERC, October 1992. $13

UCB/EERC-92/12: Application of a Mass Damping System to Bridge Structures, by Hasegawa, K. and Kelly, J.M., August 1992. $26

UCB/EERC-92/11: Mechanical Characteristics of Neoprene Isolation Bearings, by Kelly, J.M. and Quiroz, E., August 1992. $20

UCB/EERC-92/10: Slotted Bolted Connection Energy Dissipators, by Grigorian, C.E., Yang, T.-S. and Popov, E.P., July 1992. $20

UCB/EERC-92/09: Evaluation of Code Accidental-Torsion Provisions Using Earthquake Records from Three Nominally Symmetric-Plan Buildings, by De la Llera, J.C. and Chopra, A.K., September 1992. $13

UCB/EERC-92/08: Nonlinear Static and Dynamic Analysis of Reinforced Concrete Subassemblages, by Filippou, F.C., D'Ambrisi, A. and Issa, A., August, 1992. $20

UCB/EERC-92/07: A Beam Element for Seismic Damage Analysis, by Spacone, E., Ciampi, V. and Filippou, F.C., August 1992. $20

UCB/EERC-92/06: Seismic Behavior and Design of Semi-Rigid Steel Frames, by Nader, M.N. and Astaneh-Asl, A., May 1992. $33

UCB/EERC-92/05: Parameter Study of Joint Opening Effects on Earthquake Response of Arch Dams, by Fenves, G.L., Mojtahedi, S. and Reimer, R.B., April 1992. $15

UCB/EERC-92/04: Shear Strength and Deformability of RC Bridge Columns Subjected to Inelastic Cyclic Displacements, by Aschheim, M. and Moehle, J.P., March 1992. $20

UCB/EERC-92/03: Models for Nonlinear Earthquake Analysis of Brick Masonry Buildings, by Mengi, Y., McNiven, H.D. and Tanrikulu, A.K., March 1992. $20

UCB/EERC-92/02: Response of the Dumbarton Bridge in the Loma Prieta Earthquake, by Fenves, G.L., Filippou, F.C. and Sze, D.T., January 1992. $20

UCB/EERC-92/01: Studies of a 49-Story Instrumented Steel Structure Shaken During the Loma Prieta Earthquake, by Chen, C.-C., Bonowitz, D. and Astaneh-Asl, A., February 1992. $20

UCB/EERC-91/18: Investigation of the Seismic Response of a Lightly-Damped Torsionally-Coupled Building, by Boroschek, R. and Mahin, S.A., December 1991. $26

UCB/EERC-91/17: A Fiber Beam-Column Element for Seismic Response Analysis of Reinforced Concrete Structures, by Taucer, F., Spacone, E. and Filippou, F.C., December 1991. $20

UCB/EERC-91/16: Evaluation of the Seismic Performance of a Thirty-Story RC Building, by Anderson, J.C., Miranda, E., Bertero, V.V. and The Kajima Project Research Team, July 1991. $26

UCB/EERC-91/15: Design Guidelines for Ductility and Drift Limits: Review of State-of-the-Practice and State-of-the-Art in Ductility and Drift-Based Earthquake-Resistant Design of Buildings, by Bertero, V.V., Anderson, J.C., Krawinkler, H., Miranda, E. and The CUREe and The Kajima Research Teams, July 1991. $20

UCB/EERC-91/14: Cyclic Response of RC Beam-Column Knee Joints: Test and Retrofit, by Mazzoni, S., Moehle, J.P. and Thewalt, C.R., October 1991. $13

UCB/EERC-91/13: Shaking Table - Structure Interaction, by Rinawi, A.M. and Clough, R.W., October 1991. $26

UCB/EERC-91/12: Performance of Improved Ground During the Loma Prieta Earthquake, by Mitchell, J.K. and Wentz, Jr., F.J., October 1991. $20

UCB/EERC-91/11: Seismic Performance of an Instrumented Six-Story Steel Building, by Anderson, J.C. and Bertero, V.V., November 1991. $20

UCB/EERC-91/10: Evaluation of Seismic Performance of a Ten-Story RC Building During the Whittier Narrows Earthquake, by Miranda, E. and Bertero, V.V., October 1991. $20

UCB/EERC-91/09: A Preliminary Study on Energy Dissipating Cladding-to-Frame Connections, by Cohen, J.M. and Powell, G.H., September 1991. $15

UCB/EERC-91/08: A Response Spectrum Method for Multiple-Support Seismic Excitations, by Der Kiureghian, A. and Neuenhofer, A., August 1991. $15

UCB/EERC-91/07: Estimation of Seismic Source Processes Using Strong Motion Array Data, by Chiou, S.-J., July 1991. $20

UCB/EERC-91/06: Computation of Spatially Varying Ground Motion and Foundation-Rock Impedance Matrices for Seismic Analysis of Arch Dams, by Zhang, L. and Chopra, A.K., May 1991. $20

UCB/EERC-91/05: Base Sliding Response of Concrete Gravity Dams to Earthquakes, by Chopra, A.K. and Zhang, L., May 1991. $15

UCB/EERC-91/04: Dynamic and Failure Characteristics of Bridgestone Isolation Bearings, by Kelly, J.M., April 1991. $15

UCB/EERC-91/03: A Long-Period Isolation System Using Low-Modulus High-Damping Isolators for Nuclear Facilities at Soft-Soil Sites, by Kelly, J.M., March 1991. $26

UCB/EERC-91/02: Displacement Design Approach for Reinforced Concrete Structures Subjected to Earthquakes, by Qi, X. and Moehle, J.P., January 1991. $20

UCB/EERC-90/21: Observations and Implications of Tests on the Cypress Street Viaduct Test Structure, by Bollo, M., Mahin, S.A., Moehle, J.P., Stephen, R.M. and Qi, X., December 1990. $26

UCB/EERC-90/20: Seismic Response Evaluation of an Instrumented Six Story Steel Building, by Shen, J.-H. and Astaneh-Asl, A., December 1990. $15

UCB/EERC-90/19: Cyclic Behavior of Steel Top-and-Bottom Plate Moment Connections, by Harriott, J.D. and Astaneh-Asl, A., August 1990. $15

UCB/EERC-90/18: Material Characterization of Elastomers used in Earthquake Base Isolation, by Papoulia, K.D. and Kelly, J.M., 1990. $15

UCB/EERC-90/17: Behavior of Peak Values and Spectral Ordinates of Near-Source Strong Ground-Motion over a Dense Array, by Niazi, M., June 1990. $20

UCB/EERC-90/14: Inelastic Seismic Response of One-Story, Asymmetric-Plan Systems, by Goel, R.K. and Chopra, A.K., October 1990. $26

UCB/EERC-90/13: The Effects of Tectonic Movements on Stresses and Deformations in Earth Embankments, by Bray, J. D., Seed, R. B. and Seed, H. B., September 1989. $39

UCB/EERC-90/12: Effects of Torsion on the Linear and Nonlinear Seismic Response of Structures, by Sedarat, H. and Bertero, V.V., September 1989. $33

UCB/EERC-90/11: Seismic Hazard Analysis: Improved Models, Uncertainties and Sensitivities, by Araya, R. and Der Kiureghian, A., March 1988. $20

UCB/EERC-90/10: Experimental Testing of the Resilient-Friction Base Isolation System, by Clark, P.W. and Kelly, J.M., July 1990. $20

UCB/EERC-90/09: Influence of the Earthquake Ground Motion Process and Structural Properties on Response Characteristics of Simple Structures, by Conte, J.P., Pister, K.S. and Mahin, S.A., July 1990. $33

UCB/EERC-90/08: Soil Conditions and Earthquake Hazard Mitigation in the Marina District of San Francisco, by Mitchell, J.K., Masood, T., Kayen, R.E. and Seed, R.B., May 1990. $15

UCB/EERC-90/07: A Unified Earthquake-Resistant Design Method for Steel Frames Using ARMA Models, by Takewaki, I., Conte, J.P., Mahin, S.A. and Pister, K.S., June 1990. $15

UCB/EERC-90/05: Preliminary Report on the Principal Geotechnical Aspects of the October 17, 1989 Loma Prieta Earthquake, by Seed, R.B., Dickenson, S.E., Riemer, M.F., Bray, J.D., Sitar, N., Mitchell, J.K., Idriss, I.M., Kayen, R.E., Kropp, A., Harder, L.F., Jr. and Power, M.S., April 1990. $20

UCB/EERC-90/03: Earthquake Simulator Testing and Analytical Studies of Two Energy-Absorbing Systems for Multistory Structures, by Aiken, I.D. and Kelly, J.M., October 1990. $26

UCB/EERC-90/02: Javid's Paradox: The Influence of Preform on the Modes of Vibrating Beams, by Kelly, J.M., Sackman, J.L. and Javid, A., May 1990. $13

UCB/EERC-89/16: Collapse of the Cypress Street Viaduct as a Result of the Loma Prieta Earthquake, by Nims, D.K., Miranda, E., Aiken, I.D., Whittaker, A.S. and Bertero, V.V., November 1989. $15

UCB/EERC-89/15: Experimental Studies of a Single Story Steel Structure Tested with Fixed, Semi-Rigid and Flexible Connections, by Nader, M.N. and Astaneh-Asl, A., August 1989. $26

UCB/EERC-89/14: Preliminary Report on the Seismological and Engineering Aspects of the October 17, 1989 Santa Cruz (Loma Prieta) Earthquake, by EERC, October 1989. $15

UCB/EERC-89/13: Mechanics of Low Shape Factor Elastomeric Seismic Isolation Bearings, by Aiken, I.D., Kelly, J.M. and Tajirian, F.F., November 1989. $20

UCB/EERC-89/12: ADAP-88: A Computer Program for Nonlinear Earthquake Analysis of Concrete Arch Dams, by Fenves, G.L., Mojtahedi, S. and Reimer, R.B., September 1989. $20

UCB/EERC-89/11: Static Tilt Behavior of Unanchored Cylindrical Tanks, by Lau, D.T. and Clough, R.W., September 1989. $26

UCB/EERC-89/10: Measurement and Elimination of Membrane Compliance Effects in Undrained Triaxial Testing, by Nicholson, P.G., Seed, R.B. and Anwar, H., September 1989. $26

UCB/EERC-89/09: Feasibility and Performance Studies on Improving the Earthquake Resistance of New and Existing Buildings Using the Friction Pendulum System, by Zayas, V., Low, S., Mahin, S.A. and Bozzo, L., July 1989. $33

UCB/EERC-89/08: Seismic Performance of Steel Moment Frames Plastically Designed by Least Squares Stress Fields, by Ohi, K. and Mahin, S.A., August 1989. $15

UCB/EERC-89/07: EADAP - Enhanced Arch Dam Analysis Program: Users's Manual, by Ghanaat, Y. and Clough, R.W., August 1989. $20

UCB/EERC-89/06: Effects of Spatial Variation of Ground Motions on Large Multiply-Supported Structures, by Hao, H., July 1989. $20

UCB/EERC-89/05: The 1985 Chile Earthquake: An Evaluation of Structural Requirements for Bearing Wall Buildings, by Wallace, J.W. and Moehle, J.P., July 1989. $26

UCB/EERC-89/04: Earthquake Analysis and Response of Intake-Outlet Towers, by Goyal, A. and Chopra, A.K., July 1989. $39

UCB/EERC-89/03: Implications of Site Effects in the Mexico City Earthquake of Sept. 19, 1985 for Earthquake-Resistant Design Criteria in the San Francisco Bay Area of California, by Seed, H.B. and Sun, J.I., March 1989. $20

UCB/EERC-89/02: Earthquake Simulator Testing of Steel Plate Added Damping and Stiffness Elements, by Whittaker, A., Bertero, V.V., Alonso, J. and Thompson, C., January 1989. $26

UCB/EERC-89/01: Behavior of Long Links in Eccentrically Braced Frames, by Engelhardt, M.D. and Popov, E.P., January 1989. $39

UCB/EERC-88/20: Base Isolation in Japan, 1988, by Kelly, J.M., December 1988. $15

UCB/EERC-88/19: Steel Beam-Column Joints in Seismic Moment Resisting Frames, by Tsai, K.-C. and Popov, E.P., November 1988. $39

UCB/EERC-88/18: Use of Energy as a Design Criterion in Earthquake-Resistant Design, by Uang, C.-M. and Bertero, V.V., November 1988. $15

UCB/EERC-88/17: Earthquake Engineering Research at Berkeley - 1988, by EERC, November 1988. $26

UCB/EERC-88/16: Reinforced Concrete Flat Plates Under Lateral Load: An Experimental Study Including Biaxial Effects, by Pan, A. and Moehle, J.P., October 1988. $26

UCB/EERC-88/15: Dynamic Moduli and Damping Ratios for Cohesive Soils, by Sun, J.I., Golesorkhi, R. and Seed, H.B., August 1988. $15

UCB/EERC-88/14: An Experimental Study of the Behavior of Dual Steel Systems, by Whittaker, A.S., Uang, C.-M. and Bertero, V.V., September 1988. $33

UCB/EERC-88/13: Implications of Recorded Earthquake Ground Motions on Seismic Design of Building Structures, by Uang, C.-M. and Bertero, V.V., November 1988. $20

UCB/EERC-88/12: Nonlinear Analysis of Reinforced Concrete Frames Under Cyclic Load Reversals, by Filippou, F.C. and Issa, A., September 1988. $20

UCB/EERC-88/11: Liquefaction Potential of Sand Deposits Under Low Levels of Excitation, by Carter, D.P. and Seed, H.B., August 1988. $33

UCB/EERC-88/10: The Landslide at the Port of Nice on October 16, 1979, by Seed, H.B., Seed, R.B., Schlosser, F., Blondeau, F. and Juran, I., June 1988. $15

UCB/EERC-88/09: Alternatives to Standard Mode Superposition for Analysis of Non-Classically Damped Systems, by Kusainov, A.A. and Clough, R.W., June 1988. $15

UCB/EERC-88/08: Analysis of Near-Source Waves: Separation of Wave Types Using Strong Motion Array Recordings, by Darragh, R.B., June 1988 $20

UCB/EERC-88/07: Theoretical and Experimental Studies of Cylindrical Water Tanks in Base-Isolated Structures, by Chalhoub, M.S. and Kelly, J.M., April 1988. $15

UCB/EERC-88/06: DRAIN-2DX User Guide, by Allahabadi, R. and Powell, G.H., March 1988. $26

UCB/EERC-88/05: Experimental Evaluation of Seismic Isolation of a Nine-Story Braced Steel Frame Subject to Uplift, by Griffith, M.C., Kelly, J.M. and Aiken, I.D., May 1988. $20

UCB/EERC-88/04: Re-evaluation of the Slide in the Lower San Fernando Dam in the Earthquake of Feb. 9, 1971, by Seed, H.B., Seed, R.B., Harder, L.F. and Jong, H.-L., April 1988. $20

UCB/EERC-88/03: Cyclic Behavior of Steel Double Angle Connections, by Astaneh-Asl, A. and Nader, M.N., January 1988. $15

UCB/EERC-88/02: Experimental Evaluation of Seismic Isolation of Medium-Rise Structures Subject to Uplift, by Griffith, M.C., Kelly, J.M., Coveney, V.A. and Koh, C.G., January 1988. $20

UCB/EERC-88/01: Seismic Behavior of Concentrically Braced Steel Frames, by Khatib, I., Mahin, S.A. and Pister, K.S., January 1988. $26